Regulation and Pathophysiology of H2B Serine 6 Phosphorylation

Dissertation

zur Erlangung des Doktorgrades der Naturwissenschaften
– Dr. rer. nat. –

angefertigt am
Biochemischen Institut des Fachbereichs Medizin
und dem Fachbereich Biologie und Chemie
der Justus-Liebig-Universität Gießen

vorgelegt von

Maximilian Pfisterer

Gießen, Februar 2024

Dekan: **Prof. Dr. Thomas Wilke**
Institut für Allgemeine und Spezielle Zoologie
Fachbereich Biologie und Chemie
Justus-Liebig-Universität Gießen

1. Gutachter: **Prof. Dr. Sandra B. Hake**
Institut für Genetik
Fachbereich Biologie und Chemie
Justus-Liebig-Universität Gießen

2. Gutachter: **Prof. Dr. M. Lienhard Schmitz**
Institut für Biochemie
Fachbereich Medizin
Justus-Liebig-Universität Gießen

Eidesstattliche Erklärung

Ich erkläre: Ich habe die vorgelegte Dissertation selbstständig und ohne unerlaubte fremde Hilfe und nur mit den Hilfen angefertigt, die ich in der Dissertation angegeben habe. Alle Textstellen, die wörtlich oder sinngemäß aus veröffentlichten Schriften entnommen sind, und alle Angaben, die auf mündlichen Auskünften beruhen, sind als solche kenntlich gemacht. Ich stimme einer evtl. Überprüfung meiner Dissertation durch eine Antiplagiat-Software zu. Bei den von mir durchgeführten und in der Dissertation erwähnten Untersuchungen habe ich die Grundsätze guter wissenschaftlicher Praxis, wie sie in der "Satzung der Justus-Liebig-Universität Gießen zur Sicherung guter wissenschaftlicher Praxis" niedergelegt sind, eingehalten.

Maximilian Pfisterer
Gießen, 14.02.2024

Contents

1 Introduction

The human body consists of approximately 36 trillion (3.6×10^{13}) cells (Hatton et al., 2023) and yet they all have one single progenitor cell, the zygote. This cell, formed by the combination of the male and female gametes, divides into two daughter cells, which in turn divide and give rise to the astonishing number of cells in the human organism with a wide variety of functions. This necessitates the division of cells which requires equal distribution of the genetic material between the daughter cells. Errors in this process are often lethal or otherwise associated with disease (Hassold et al., 1984; Levine et al., 2018). Understanding the mechanisms by which cells ensure mitotic fidelity is therefore of great importance.

1.1 Histones

The human genome contains approximately 3 billion (3×10^9) basepairs of DNA with each cell containing two full copies. Chromatin is a complex and dynamic structure that packages the genomic DNA in the nucleus of eukaryotic cells. It is composed of DNA, histone proteins, and various associated non-histone proteins (Wolffe, 1998).

Together with DNA, histones form the most basic repeating unit of chromatin; the nucleosome (Olins et al., 1974). Approximately 147 bp are wrapped around a histone hetero-octamer core in 1.65 turns. 10 to 80 bp of linker DNA connect individual nucleosomes forming the so-called ”beads on a string” (Felsenfeld, 1978; Luger et al., 1997). The histone core consists of 2 copies of each of the histones H2A, H2B, H3 and H4 (Kornberg et al., 1974). The linker histone H1 binds the linker DNA, stabilising the nucleosome and allowing for further compaction of the nucleosome chain. The core histones all feature a histone fold domain (HFD), consisting of 3 α helices making up the globular part, as well as N-terminal and C-terminal unstructured tails (Arents et al., 1995). While histones in this form are exclusive for eukaryotes, similar proteins with HFDs can also be found in bacteria and archaea (Alva et al., 2019; Hocher et al., 2023) and even in some viruses (Erives, 2017; Yoshikawa et al., 2019; Bryson et al., 2022). The HFD α-helices mediate the interaction of the histone proteins with each other, allowing their assembly into an octamer. H2A and H2B, as well as H3 and H4, form dimers by interacting via their α2 helices. Two H3-H4 dimers then form a hetero-tetramer by interaction between the H3 proteins. The H3-H4 tetramer and 2 H2A-H2B dimers assemble the core particle in a DNA dependent manner (Eickbush et al., 1978). The histone core is largely positively charged by enrichment of lysine and arginine residues (DeLange et al., 1971) allowing the negatively charged DNA to bind with high affinity. The mostly unstructured

histone tails partially protrude from the nucleosome and are accessible to a range of proteins interacting with them and are subject to a variety of post-translational modifications (Zhang et al., 2021).

Although DNA and the histone octamer form stable interactions, nucleosomes are flexible structures. They can be removed and replaced, slide along the DNA strand or be modified. Because these nucleosomes tightly bind the DNA, they have to be removed for transcription or replication to allow polymerases to bind and process the DNA and replaced afterwards (Adams et al., 1993).

The transport of histone proteins, the assembly of nucleosomes as well as their deposition is facilitated by histone chaperones. Although histones can assemble in the absence of histone chaperones and can form nucleosomes *in vitro*, histone chaperones aid in nuclear uptake of histone proteins and prevent unstructured aggregation of histones with DNA (De Koning et al., 2007; Gurard-Levin et al., 2014).

1.1.1 Post-translational modifications of histones

Histones, like most other proteins, are extensively post-translationally modified as shown in Figure 1 (Allfrey et al., 1964; Peterson et al., 2004). Post-translational modifications (PTMs) are the addition of functional groups to the amino acid residues such as methylation and acetylation of lysine residues, phosphorylation of serine/threonine residues or ubiquitination (Uy et al., 1977). A plethora of other modifications, including crotonylation, succinylation, biotinylation as well as many more have also been identified on histones as well (Hymes et al., 1995; Tan et al., 2011; Xie et al., 2012). In the case of histones, a large number of these modifications, also known as histone marks, occur on the unstructured tails (Figure 1). In recent years, an increasing number of PTMs has also been identified in the globular domains of histones as well (Tropberger et al., 2013; Jack et al., 2014), where they are more likely to directly influence nucleosome structure.

Phosphorylation of histone residues is often the result of activation of signalling pathways (Lau et al., 2010). Histone phosphorylation is generally greatly increased during mitosis where several histone residues are phosphorylated, including H3 T3, H3 S10, H3 S28, H3 T80, CENP-A S7, H3.3 S31, H2A T120 and H2B S6, among others (Schmitz et al., 2020). Some of these modifications have been found to fulfil multiple roles in different contexts. For example, H3 S10ph and H3 S28ph are involved in early chromosome condensation in mitosis. They have also been detected in interphase where they are involved in transcriptional activation on certain genes upon external stimuli (Nowak et al., 2000; Lau et al., 2011). However, the regulatory networks controlling these PTMs are different in interphase and mitosis. Other reported phosphorylations include phosphorylation of the variant histone H2A.X S139, also called γH2AX. This modification is specifically installed around DNA double-strand breaks (DSBs), marking them for the DNA repair machinery (Rogakou et al., 1998). During apoptosis, phosphorylation of H2B S14 and S32 have been found to be involved in

DNA fragmentation (Cheung et al., 2003). Apart from these examples a number of other histone phosphorylations can be found on all core histones as reviewed by Banerjee et al. (2011).

Modifications are installed by specific 'writer' proteins and removed by 'eraser' proteins (Bannister et al., 2011). Phosphorylations are catalysed by protein kinases which are able to add phosphate groups specifically to serine/threonine or tyrosine residues. Removal of phosphate groups is catalysed by protein phosphatases. While the human genome expresses around 500 different kinase in multiple kinase families, it contains less than 200 phosphatases (Manning et al., 2002; Chen et al., 2017). This dysbalance between kinases and phosphatases is countered by the diverse composition of functioning protein-phosphatases. One of the most abundant protein phosphatases, the PP1 family, contains 3 catalytic subunits with low substrate specificity (Ceulemans et al., 2004). They form complexes with one or more regulatory subunits targeting them to their substrates and regulating their activity (Goldberg et al., 1995). Some of these regulatory subunits are involved in histone dephosphorylation, such as RepoMan, PNUTS, Ki-67, NIPP1, GADD34, PHAP1 and others (Brautigan et al., 2018). They play a role in removing mitotic phosphorylations, but also the regulation of phosphorylations found during DNA damage signalling (Grallert et al., 2015; Ramos et al., 2019).

Histone PTMs rarely occur as singular modifications but rather in a complex group of modifications influencing each other (Fischle et al., 2003; Lee et al., 2010). This grouping of histone modifications has been recognised as forming a rich code in addition to the genetic code itself (Strahl et al., 2000; Jenuwein et al., 2001). The combined presence of a particular set of histone PTMs, and the factors they recruit, gives identity to genetic elements such as promoters, enhancers, exons, introns and all other features. Similar to language, this histone code is written and erased, but also read in order to convey its meaning. 'Reader' proteins bind specifically to the modified amino acids and convey their function by directly modifying chromatin or by recruiting additional factors such as remodellers, transcription factors, etc.

Chromatin accessibility is a key mechanism by which genetic elements are either activated or repressed. Since most of the genome does not contain genes or their related regulatory elements, large parts of the genome are constitutively repressed by a high degree of compaction (Morrison et al., 2021). These regions form the constitutive heterochromatin and contain mostly repetitive sequences such as centromeres, pericentromeres, telomeres and transposable elements. Facultative heterochromatin mostly contains genes which are not required and therefore not expressed in a given cell type or under current environmental conditions. These regions are more dynamic as they can change to active regions depending on the cells needs. Euchromatin represents the loosely packed, actively transcribed regions and their regulatory elements (Morrison et al., 2021).

Some modifications, such as acetylations and phosphorylations change the overall positive charge of the histone octamer and thereby reduce the binding strength to DNA. As such, acetylations are typically associated with actively transcribed genes (Grunstein, 1997). Other histone modifications

recruit additional factors that modify the chromatin environment by adding or removing further modifications or by actively altering the local chromatin environment by instructing remodelling complexes (Swygert et al., 2014).

Installation and removal of these histone PTMs is a highly dynamic process. Not only does the presence of histone marks influence the activity of genetic elements, but the activity of these elements also influences histone PTMs. Active transcription, for example, is known to promote further activation of genomic loci by the installation of chromatin marks supporting gene expression (Martin et al., 2021). Furthermore, these modifications underlie highly dynamic changes in the course of cell differentiation and the changing expression programmes during this process, but also in response to other external stimuli like inflammation, hypoxia and many more (Haas et al., 2020). Histone PTMs are very diverse and ever new modifications and functions for these modifications are constantly being discovered. It is very likely that histone PTMs are involved in every chromatin associated process. For example, while splicing of mRNAs is dependent on signalling sequences, histone modifications have recently been implicated in the regulation of alternative splicing (Luco et al., 2010). On the other hand splicing has also been found to influence the deposition of chromatin marks (Kim et al., 2011), highlighting the complexity of regulatory networks of which histone PTMs are part of.

As the histone code carries important information needed for cell identity it must be passed on to progeny cells. Therefore, during replication the histone modifications from the parent strand have to be replicated faithfully along with the DNA. Although there are several models that explain the inheritance of chromatin state after replication, the exact mechanism is not entirely clear, and there is probably more than one mechanism (Budhavarapu et al., 2013). It is generally assumed that after replication, both nascent DNA strands contain half newly synthesised nucleosomes and half parental nucleosomes including their histone modifications. Histone modifications on the recycled nucleosomes then template and re-establish the pattern of histone modifications on the newly synthesised nucleosomes (Reverón-Gómez et al., 2018).

1.1.2 Histone variants

In addition to histone modifications, histone variants play an important role in chromatin regulation (Zink et al., 2016). Histone variants are specialised forms of the core histone proteins. They differ from their canonical counterparts by sometyimes only a few amino acids, (e.g. in the case for the H3 variant H3.3) or show larger differences with the addition of larger domains (e.g. in the case of macroH2A), as schematically displayed in Figure 2. These variants can replace canonical histones, leading to altered chromatin structure and function (Venkatesh et al., 2015). Histone variants are expressed in a developmental and tissue-specific manner and are associated with specific biological processes, such as mitosis, DNA repair, and transcriptional regulation (Buschbeck et al., 2017).

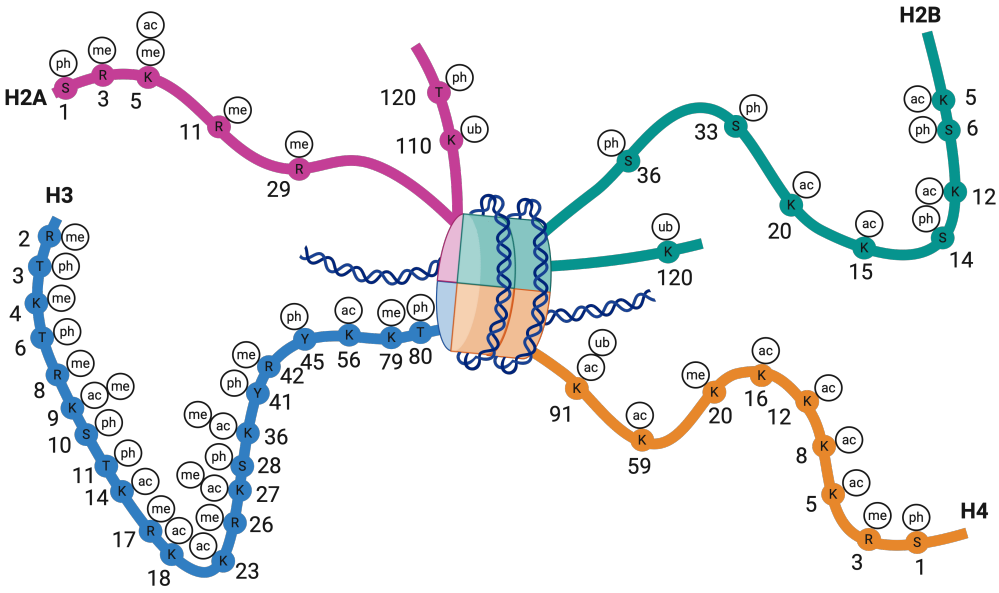

Figure 1: Post-translational modifications of histone tails.

The protruding unstructured histone tails are subject to extensive post-translational modifications. Many relevant modifications are found on the long N-terminal tail of histone H3. *Created with biorender.com*

As such, they are distinct from histone isoforms which are products of the multiple copies of histone genes in a genome (subsection 1.1.3). By incorporating variants into chromatin, cells can modulate gene expression and adapt to different cellular states. Dysregulation of their expression or deposition has been linked to diseases such as cancer (Buschbeck et al., 2017). There are several histone variants in humans and other mammals, the most common being variants of H2A with 8 variants, H3 with 6 variants and H2B with 2 variants (Buschbeck et al., 2017). Histone H4, the most highly conserved histone, has variants described in some eukaryotes, but a possible H4 variant in higher eukaryotes has only recently been discovered (Long et al., 2019). The variants H2A.X, H2A.Z, the centromeric H3 variant CENP-A and H3.3 appeared before the divergence of eukaryotes and are considered to be universal histone variants (Talbert et al., 2010). H2A.X is mainly studied in the context of the DNA damage response where it carries an important damage signal (subsection 1.1.1). H2A.Z is a highly studied variant which is involved in transcriptional activation and repression (Kreienbaum et al., 2022). H3.3 is a ubiquitous variant which is deposited in various genomic locations and associated with genetic elements such as promoters and enhancers (Goldberg et al., 2010).

The histone H3 variant CENP-A replaces H3 at centromeric regions and is installed specifically via its depositor HJURP after replication (Dunleavy et al., 2009). This loading of CENP-A gives centromeres their identity and allows for assembly of other centromeric proteins, namely the kinetochores. This is facilitated by the recruitment of members of the constitutive centromere

associated network (CCAN), the CENP proteins (subsection 1.3.2) (Hori et al., 2008). CENP-A is therefore an important histone variant for allowing chromosome segregation during cell division.

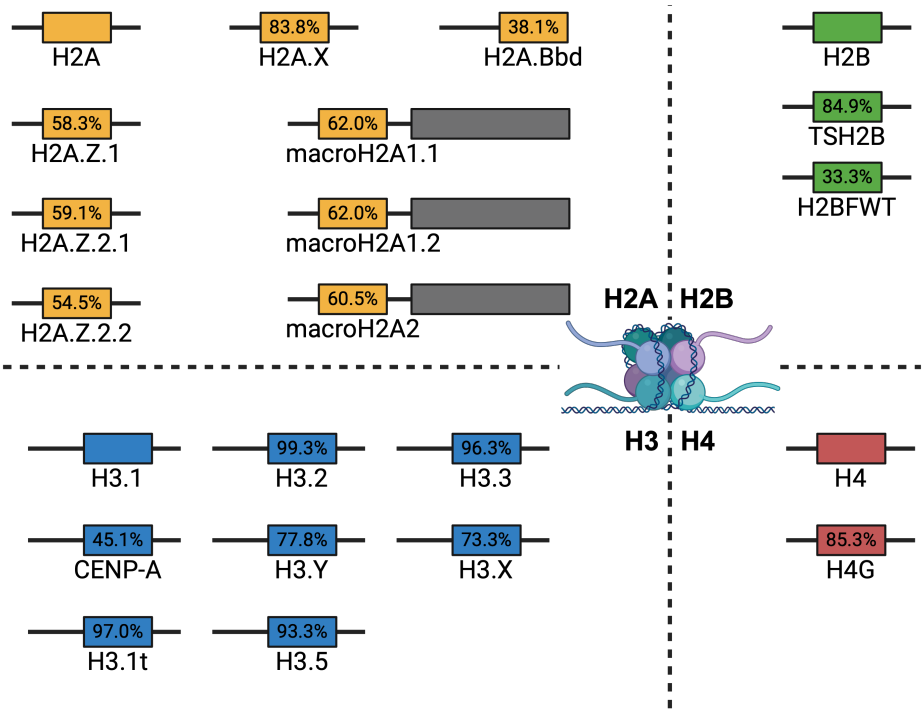

Figure 2: Histone variants.

Histone variants are similar to their canonical versions, but feature either sequence differences or additional domains. The rectangles indicate the globular domains while the lines indicate the unstructured histone tails. Percentages indicate amino acid sequence conservation compared to the canonical histone. Adapted from Buschbeck et al. (2017). *Created with biorender.com*

1.1.3 Histone gene expression

Histones are integral to every eukaryote. This is also reflected in the organisation of histone genes in the genome. The lower eukaryote *Saccharomyces cerevisiae* has two copies of each core histone which are expressed in tandem with their respective binding partners (Eriksson et al., 2012). In vertebrates on the other hand, histones are usually expressed from multiple copies. H2B has 22 copies in the human genome, and the other core histones have similar copy numbers (Marzluff et al., 2002; Amatori et al., 2021). All histone genes are contained in 2 or more histone gene clusters, as shown at the example of the human genome in Figure 3. These are highly accessible, highly transcribed regions in the genome which are proposed to form phase separated histone expression loci (histone locus bodies, HLB). They contain the factors required for the expression and processing of histone mRNA (Hur et al., 2020). While in some organisms histone gene copies are highly structured in repeating units, in mammals histones are apparently randomly clustered into a few large sections without repeating units (Amatori et al., 2021).

Canonical histones present a unique form of mRNA. Unlike other mRNAs, histones do not undergo splicing as they do not contain introns. They are also the only mRNAs not being terminated in a polyA-tail but rather in a highly conserved histone stem loop (HSL) (Pandey et al., 1987). The HSL is located approximately 20 to 50 bp downstream of the stop codon and is followed by a histone downstream element (HDE). These conserved structures are recognised by a processing machinery, mainly a snRNP, which cleaves the nascent mRNA after the HSL (Mowry et al., 1987). Stem loop binding protein (SLBP) then binds the mRNA and protects it from nucleolytic degradation, similar to the protective function exerted by a polyA-tail (Battle et al., 2001). As the canonical core histones are only required during replication to package the newly replicated DNA, their expression is tightly linked to the cell cycle, with an approximately 40-fold increase in mRNA levels in S-phase (Heintz et al., 1983; Marzluff et al., 1988; Harris et al., 1991). As such, they are also described as replication dependent histones. While the activity of the promoters driving expression of the histone genes does fluctuate with the cell cycle (approximately 5-fold), most of the cell cycle regulation is mediated by the HSL (Pandey et al., 1987; Son, 1999). In S-phase, binding of the HSL by SLBP protects the mRNA from degradation, just like a polyA-tail. SLBP is degraded at S-phase exit and therefore protection of histone mRNAs is lost, leading to their decay (Whitfield et al., 2000; Zheng et al., 2003). The HSL is also proposed to aid in achieving high expression levels for the histone genes by recruiting the histone mRNAs to the polyribosomes associated with the endoplasmic reticulum (Hanson et al., 1996; Whitfield, 2004; Gorgoni et al., 2005).

Histone variants (as described in subsection 1.1.2) are expressed more like typical genes. They often contain introns and undergo splicing or even alternative splicing. They are present in only 1 or 2 copies and are, as other mRNAs, terminated with a polyA-tail.

1.1.4 Functional analysis of histone modifications

As discussed above, histone modifications influence a wide range of chromatin related processes by mediator factors or direct effects (Bannister et al., 2011). While structural consequences of histone modifications or their mutations can be studied in cell free assay effectively, studying the function of histone modifications involved in signalling processes requires cellular systems. Traditionally, the function of individual modifications is investigated by correlating the occurrence of these modifications with gene expression profiles or chromatin accessibility profiles. The main method for this is chromatin immunoprecipitation followed by deep sequencing as well as RNA deep sequencing (ChIP-seq). By fragmenting chromatin and binding of specific PTMs with an antibody, chromatin fragments featuring this PTM can be precipitated. By sequencing the bound DNA, its genomic location can be determined. At the same time, sequencing of all expressed RNAs gives information about the transcriptional activity of all genes. The spatial information of

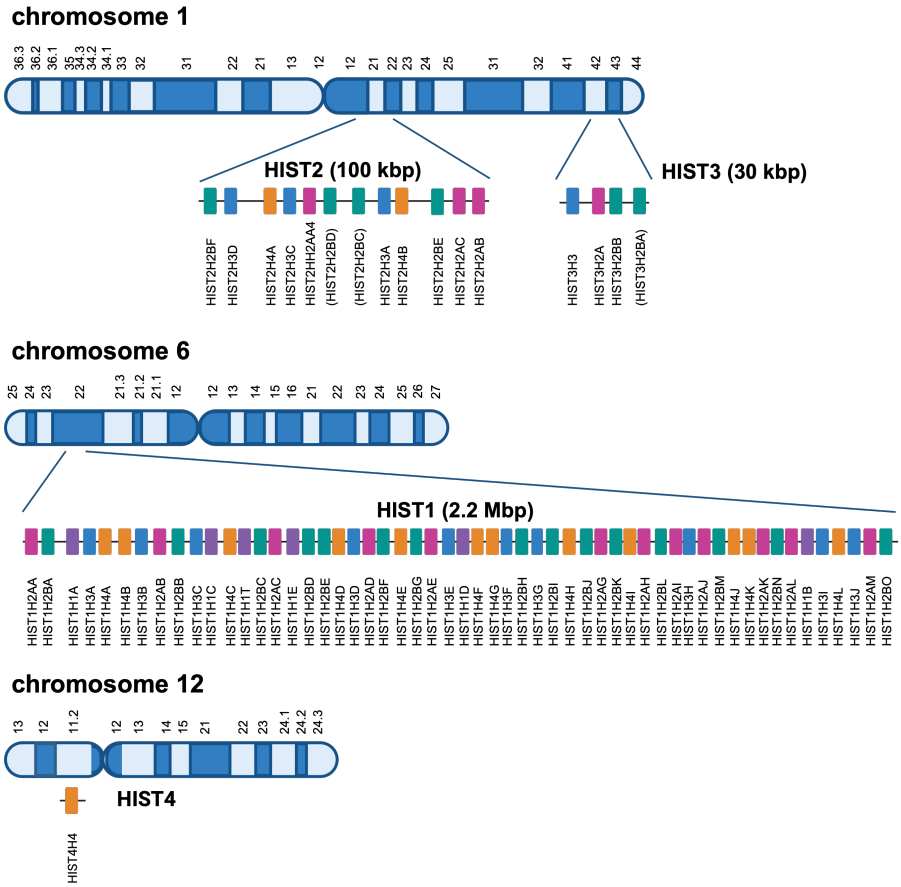

Figure 3: Organisation of histone genes in the human genome.

The 82 histone genes in the human genome are located in 3 distinct clusters on the chromosomes 1 and 6, with an additional single locus on chromosome 12. The largest cluster on chromosome 6 contains more that 66 % of the total histone genes. Adapted from Amatori et al. (2021). *Created with biorender.com*

PTMs can then be mapped to the transcriptional activity of genes. However, by definition, these experiments only show correlations, not necessarily functional relationships.

Specific functions can be investigated by modulation of the activity of writer or eraser proteins for specific histone PTMs, either by mutation or small molecules. As many of these proteins are part of larger protein complexes and regulate more than one PTM, these methods inevitably suffer from off-target effects. While a function can be attributed to a group of modifications regulated by a certain writer or eraser, it is very difficult to pinpoint the function of one PTM. Finally, mutation of the histones themselves allows for the direct linking of a histone residue to a function. The nature of histone gene organisation in many organisms (see subsection 1.1.3) limits the expression of histone mutants. While for many proteins, knock-down or gene mutation are viable options, histones as essential multi-copy genes are difficult to mutate efficiently. Systems for the complete replacement of wildtype histone have been available for a longer time in *Saccharomyces cerevisiae*

with only two copies per histone (Schuster, 1986), in higher eukaryotes these systems are a more recent development (Sankar et al., 2022). In human cells, to date no such systems exists.

1.1.5 Histones and their modifications in cancer

Cancerous transformation is driven by mutations of critical proliferation control genes. Cancer cells subsequently acquire a wide range of mutations, further driving cancer development (Vogelstein et al., 1993). These mutations affect chromatin regulators, the readers/writer/erasers of histone PTMs, but, not surprisingly, also the histones themselves. Histone genes mutations are commonly found in paediatric cancers, including glioblastoma (Mohammad et al., 2017; Nacev et al., 2019). Many of these mutations concern the variant histone H3.3. However, the canonical histones are also target of mutations including the highly conserved residues H3 K27 and H3 K36 (Morgan et al., 2013; Li et al., 2019). Due to the nature of histones as multi-copy genes, mutations in one or more genes result in only a part of total histone protein to be mutated. Nonetheless, some of the mutations, including H3 K27M and H3 G34V/R, exert a dominant negative effect. For example, H3 K27M was shown to dominantly inhibit PRC mediated H3 methylation, causing loss of gene silencing through a global reduction in H3 K27me3 (Lewis et al., 2013) leading to large scale derepression and general transcriptional activation. For many other residues the functional consequences of their mutation is not clear and generally understudied. This is in part due to the limited technical possibilities, as described above.

1.2 The cell cycle

Proliferating cells undergo an orchestrated series of events that enable growth, duplication of genetic material and ultimately division into two progeny cells. The cell cycle is divided into two sections; interphase and mitosis. Interphase is further subdivided into the first and second gap-phases (G1 & G2), which precede and follow synthesis phase (S). Progression through these phases is tightly controlled by cyclin-dependent kinases (CDKs) together with their respective cyclins, which together ensure correct order and of phases irreversibility of the cell cycle (Graña et al., 1995; Johnson et al., 1999). While CDKs are constitutively expressed throughout the cell cycle, cyclins fluctuate in their protein levels. CDKs are only active in the presence of their respective cyclins together with the removal of inhibitory phosphorylations (Obaya et al., 2002). The ordered expression and degradation of cyclins determines the order of the cell cycle phases, as schematically shown in Figure 4

In multicellular organisms, most cells do not proliferate but rest in a G1-like quiescent state called G0. From this stage, cells can enter the cell cycle upon mitogenic stimulation. This increases expression of cyclin D and activity of CDK4 and 6 (Matsushime et al., 1994). This activity in turn

increases expression of cyclin E, which triggers activity of CDK2, the driver for entry into S-phase. Once a threshold for CDK2/cyclin E activity is reached, cells irreversibly enter S-phase by initiating replication of the genome (Ohtsubo et al., 1995). In S-phase, the genomic material is copied so that a diploid set of chromosomes can be passed to each daughter cell in the next mitosis. This forms two-chromatid chromosomes, with the sister-chromatids connected at the centromere. In addition, the microtubule-organising organelle of the mitotic spindle, the centrosome, is duplicated. Cyclin E is degraded after S-phase onset and expression cyclin A is initiated. CDK2/cyclin A activity is needed to complete replication and facilitate entry into G2-phase (Cardoso et al., 1993). In G2-phase, CDK1 becomes activated by the rising cyclin A levels. Rising cyclin B levels activate the mitosis driver CDK1/cyclin B (Nurse, 1990) and cells enter mitosis.

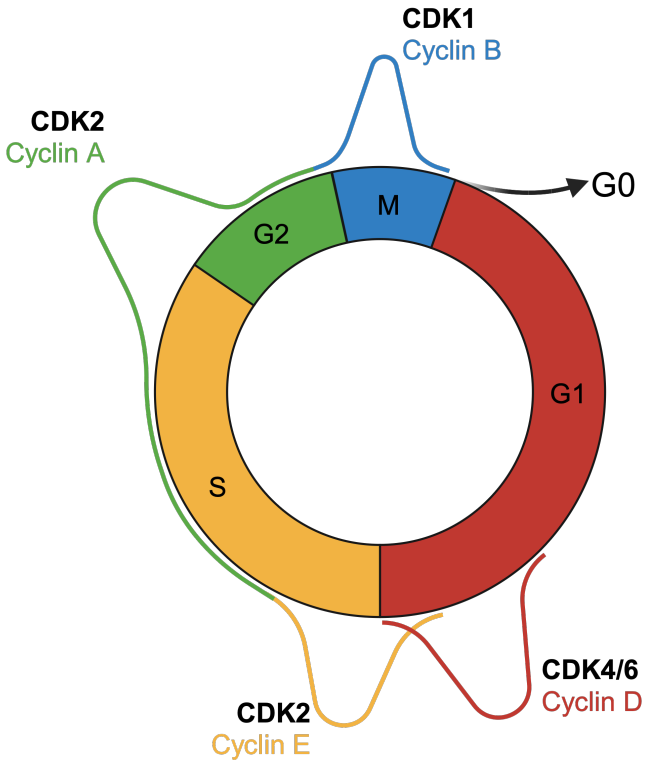

Figure 4: The cell cycle is driven by CDKs and Cyclins.
CDKs are constitutively expressed throughout the cell cycle, while the expression of the accompanying cyclins is subject to change with the cell cycle. Adapted from Belapurkar (2021). *Created with biorender.com*

1.3 Mitosis

Mitosis is the ultimate step of the cell cycle, after which the cell is divided into two daughter cells. The faithful division of the genomic information between the daughter cells is of highest importance to maintain genomic integrity over multiple generations. Mitosis is therefore a highly

regulated, complex multi-step process (McIntosh, 2016). It is divided into multiple phases where from prophase to metaphase chromatin is prepared for the subsequent segregation in anaphase, as schematically depicted in Figure 5.

In prophase, the largely uncondensed chromatin becomes compacted into the highly condensed iconic chromosomes (Belmont, 2006) (subsection 1.3.1). Cohesion, a physical connection between the sister chromatids, is resolved by removing cohesin from chromosome arms (subsection 1.3.1) (Miyazaki et al., 1994; Ishiguro et al., 2007) to allow for later separation of sister-chromatids. At the centromeres, cohesion is retained. This is critical to the correct function of (pro-)metaphase and the spindle assembly checkpoint (subsubsection 1.3.2.1). Finally, the nuclear envelope, which forms a strict barrier between the nuclear area and cytoplasm in interphase, is dissolved. This allows microtubules to invade the nuclear area in prometaphase. The mitotic spindle is formed by centrosomal microtubules attaching to the kinetochores on the condensed chromosomes. The chromosomes are then moved towards the cell equator to be aligned in the metaphase plate, which helps formation of bipolar spindle attachments. It is essential that both kinetochores of one chromosome are attached only to opposing spindle poles (subsubsection 1.3.2.2). Highly dynamic kinetochore-microtubule attachments ensure that erroneous attachments can be corrected. The spindle assembly checkpoint (SAC) monitors correct attachments and prevents progression of mitosis until all attachments have been made correctly (subsubsection 1.3.2.3). When the SAC is silenced, cohesion between the sister chromatids is fully resolved by Separase mediated proteolytic cleavage of centromeric cohesin. With the sister chromatids no longer attached to each other, microtubules from opposing centrosomes pull the sister chromatids apart in anaphase. When the chromosomes reach the poles in telophase, the nuclear membranes reforms and encloses the decondensing chromatin. A the cell equator a contractile ring divides the cells.

1.3.1 Chromatin structure in mitosis

The most dramatic changes in chromatin structure occur during mitosis. As cells enter mitosis, their chromosomes become highly condensed, reducing chromatin volume anywhere from 5- to 50-fold (Belmont, 2006). This is facilitated by establishing a higher order chromatin structure in a hierarchical order, similar to the structures formed by proteins. While the exact structural formation during condensation is debated (Antonin et al., 2016), as cells enter mitosis, the mostly homogeneously distributed chromatin of interphase nuclei becomes regionally more compacted, forming filamentous structures. This process depends on condensin protein complexes, which form ring like structures, enclosing two strands of DNA in a similar way to the structurally related cohesin complexes (Hudson et al., 2003, 2009). It is proposed that condensin creates loop like structures decreasing the linear length of the chromatids. Depletion of condensin still allows for chromosome condensation, with delayed kinetics in the initial phase, suggesting that condensin

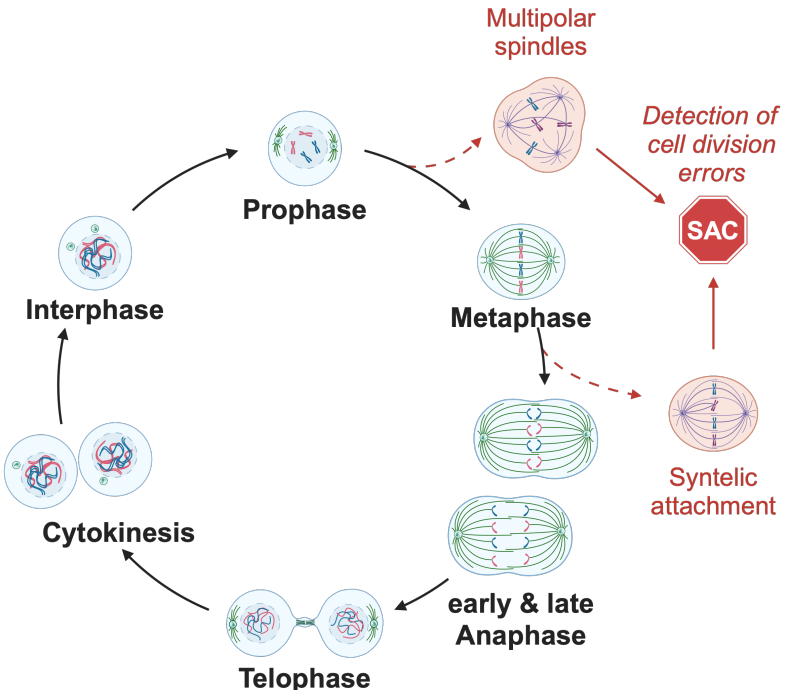

Figure 5: Phases of mitosis.

Mitosis is a multi-step process beginning in prophase with chromosome condensation and breakdown of the nuclear membrane. Chromosomes are then oriented by the mitotic spindle in metaphase, pulled apart in anaphase and decondensed in telophase. Cells are then divided and nuclei form around the decondensing chromosomes. Mitosis is safeguarded against erroneous spindle attachments and spindle formation errors by the spindle assembly checkpoint (SAC). *Created with biorender.com*

is not the only player involved in condensation (Wilkins et al., 2014). Condensin independent condensation is likely to be mediated by interaction of H4 tails with neighbouring nucleosomes. This interaction is dependent on deacetylation of H4 K16ac (Shogren-Knaak et al., 2006; Kruitwagen et al., 2015). H3 S10ph installed on chromatin by Aurora B recruits a histone deacetylase to promote the deactelyation of H4 K16ac (Wilkins et al., 2014). Chromatin decondensation at mitotic exit temporally correlates with the dephosphorylation of H3 S10ph by the phosphatase PP1. The timing suggests that dephosphorylation of H3 is necessary to allow for the re-acetylation of H4 K16 for decondensation (Antonin et al., 2016).

In addition to the structural changes in mitosis, transcription is largely inhibited as transcription factors and other transcription machinery are ejected from the condensing chromatin (Gottesfeld, 1997). Recent evidence shows that some transcription still occurs or is even necessary for mitosis in certain locations, such as centromeres, where transcription is required for the maintenance of sister chromatid cohesion (Liu et al., 2015; Palozola et al., 2017; Chen et al., 2021; Zhang et al., 2024).

1.3.2 The centromere and kinetochore

Key mitotic events, cohesion and kinetochore attachments, are orchestrated by a network of kinases located at and around the centromeres (Trivedi et al., 2016). The centromere is the region of the chromosome that links the two sister chromatids together (Choo, 1997). On DNA level, centromeres consist of repetitive sequences, α-satellite repeats (Kalitsis et al., 1997). These regions are decorated with the centromeric histone H3 variant CENP-A (Dunleavy et al., 2009). CENP-A containing nucleosomes provide a scaffold on which further proteins assemble to form the kinetochores, the binding sites for the mitotic spindle (Hori et al., 2008). The inner kinetochore is formed by recruitment of members of the CCAN to CENP-A. The CCAN links the microtubule-binding KMN network, which forms the outer kinetochores, to the centromere (Cheeseman et al., 2006; Hori et al., 2008).

Key players at the centromere include the chromosomal passenger complex (CPC) which contains the kinase Aurora B and its interactors INCENP, Borealin and Survivin (Carmena et al., 2012). It is located at the inner centromere during early stages of mitosis and later relocalises away from chromatin to the central spindle region where it plays a role in cytokinesis (Basant et al., 2015). In addition to the CPC, several kinases and phosphatases play important roles such as the monopolar spindle kinase (Mps1), Budding uninhibited by benzimidazoles 1 kinase (Bub1), Haspin, Shugoshin like 1 (Sgo1), Polo like kinase 1 (Plk1) as well as the phosphatases PP1 and PP2A (Trivedi et al., 2016).

Upon mitotic entry, the CPC is recruited to the inner centromere and fully established at the centromeres in prophase. Its Survivin subunit binds H3 T3ph, which is installed by Haspin kinase (Wang et al., 2011). The CPC in turn stimulates Haspin kinase, thereby enhancing its own centromeric location (Qian et al., 2013). Secondly, Bub1 phosphorylates H2A T120 (Kawashima et al., 2010). H2A T120ph recruits Sgo1 which binds Borealin and thereby the CPC (Bonner et al., 2020). Aurora B recruits the kinase Mps1 to the kinetochores which itself recruits Bub1 to phosphorylate H2A T120 (Yamagishi et al., 2012). This creates a second positive feedback loop by which the CPC enhances its own localisation by generating its own recruitment signals as shown in Figure 6.

1.3.2.1 Sister chromatid cohesion

One of the major functions of the CPC is the maintenance of sister chromatid cohesion at the centromeres (Trivedi et al., 2016). After replication, sister chromatids of one chromosome are physically linked by a multi-protein complex called cohesin. During prophase, cohesion between the chromosome arms is removed in a phosphorylation-dependent manner (prophase pathway) to allow for the later separation of the sister chromatids in anaphase (Waizenegger et al., 2000; Ishiguro et al., 2007). Centromeric cohesion on the other hand is critical to form correct microtubule

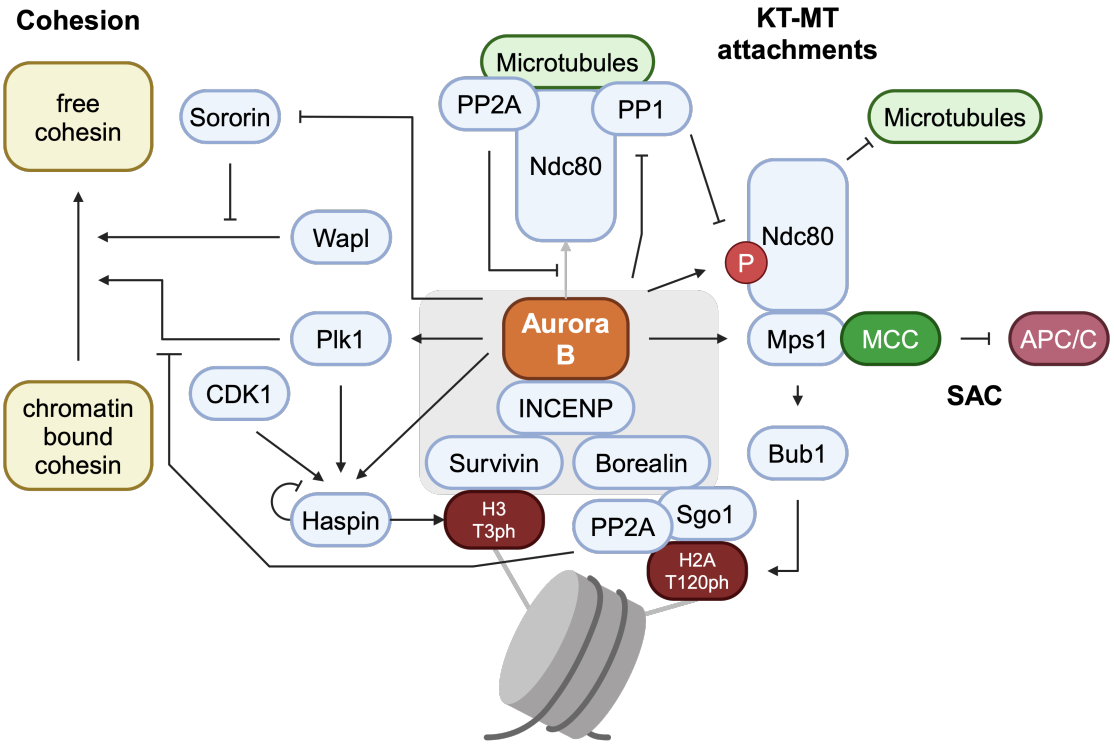

Figure 6: The CPC controls centromeric regulatory networks.
The chromosomal passenger complex and its catalytic subunit Aurora B control both centromeric cohesion and kinetochore function. Aurora B is also a key player in signalling for the spindle assembly checkpoint. In prophase, before being established at the centromeres, the CPC mediates removal of cohesin from chromosome arms via Plk1 and Wapl. At the centromeres, indirect recruitment of Sgo1 protects cohesion by opposing phosphorylation mediated removal via PP2A. At the kinetochores Aurora B destabilises microtubule attachments by phosphorylating Ndc80. Unattached Ndc80 causes assembly of the mitotic checkpoint complex (MCC) via Mps1. After attachment Aurora B mediated destabilisation is inhibited by recruitment of phosphatases. Mps1 is displaced and the SAC is silenced. Adapted from Trivedi et al. (2016). *Created with biorender.com*

spindle attachments as its loss would cause premature segregation. Therefore, centromeric cohesion is protected from prophase pathway removal (Liu et al., 2013). The CPC has an interesting dual role in cohesion regulation as it is both involved in its removal as well as maintenance. Aurora B (and CDK1) mediated phosphorylation of cohesion protection factors allow for Wapl mediated cohesin removal in addition to Plk1 mediated cohesin removal (Kueng et al., 2006; Nishiyama et al., 2013). At the same time the CPC recruits Bub1, which, through H2A T120 phosphorylation, allows for its own centromeric location, but critically also recruits Sgo1. Sgo1, located at the centromeres, recruits the protein phosphatase PP2A, which directly opposes the phosphorylation mediated cohesin removal process of the prophase pathway (Kitajima et al., 2006; Zhang et al., 2020). This CPC-dependent protection maintains centromeric cohesion until the SAC is satisfied and silenced after all kinetochores have made correct spindle attachments (subsubsection 1.3.2.3) (Hengeveld et al., 2017). Once the SAC is satisfied, the protease Separase is activated by proteasomal degradation of its inhibitor Securin. This allows for the cleavage of cohesin at the centromeres and for the

sister chromatids to be pulled apart (Zou et al., 1999; Nakajima et al., 2007). It is possible that SET/I2PP2A, a cellular PP2A inhibitor, is required to mediate the removal of Sgo1 by inhibiting PP2A or by binding Sgo1 and thereby displacing it from cohesin (Higgins et al., 2013; Qu et al., 2019). While a critical requirement for SET in anaphase II of meiosis has been demonstrated, the significance of this protein in mitosis is less clear. It is also unclear whether its function as a PP2A inhibitor is critical for the removal of cohesin. SET has also been demonstrated to have inhibitory potential for acetyltransferases as a member of INHAT (Seo et al., 2001). If this plays a role in centromeric cohesion is unclear.

1.3.2.2 Kinetochore-microtubule attachments

Kinetochores are complex protein structures that assemble on the CENP-A-containing regions of the outer centromere. They provide an interface for mitotic spindle microtubules to attach to chromatids and pull them to the poles during anaphase. It has to be ensured that one, and only one, chromatid of each chromosome is pulled to each cell pole. If one kinetochore were to bind microtubules from opposite poles of the spindle (merotelic attachment), the chromatid attached to that kinetochore could not be pulled to either pole and would be trapped in the cleavage furrow. If both kinetochores make attachments to one spindle pole (syntelic attachment), both chromatids could be pulled to one cell pole. In both cases, the resulting aneuploidy would lead to cell death or possibly transformation of the cell (Kops et al., 2005). Kinetochores, however, make multiple microtubule connections (Lampson et al., 2017). Correct orientation of the chromosomes with the kinetochores towards opposing cell poles helps in making bipolar attachments (Magidson et al., 2011). Additionally the CPC helps to make correct spindle attachments. Aurora B directly inhibits kinetochore-microtubule attachments (KT-MT) by phosphorylating the outer kinetochore KMN network member Ndc80. This destabilisation of KT-MT attachments allows for the dissociation of erroneous attachments (Cheeseman et al., 2006). Unbound Ndc80 recruits Mps1, which indirectly increases localisation of the CPC to the centromere via Bub1. Binding of microtubules to Ndc80 displaces Mps1 and therefore also reduces CPC activity (Hiruma et al., 2015). The reduction in CPC activity leads to a stabilisation of the attachment as Ndc80 phosphorylation is reduced. Additionally, KT-MT attachments recruit PP1 which opposes Aurora B mediated phosphorylation further stabilising the attachment. Importantly, only attachments from opposing poles (amphitelic attachments) create tension between the sister kinetochores. This tension physically increases the distance between the centromeric CPC and the outer kinetochore (Nezi et al., 2009). This ultimately reduces Aurora B activity on the outer kinetochore proteins, fully stabilising the attachments (Liu et al., 2009).

1.3.2.3 The spindle assembly checkpoint

Critically, correct attachment is also surveilled by the CPC, which establishes the SAC. The spindle assembly checkpoint is mediated by the MCC (Chao et al., 2012). One of its members is the kinase Mps1. As described above, Mps1 is directly recruited to the kinetochores by Aurora B (Saurin et al., 2011). Localisation of SAC proteins, like Mps1, at unattached kinetochores allows assembly of the MCC, a multi-protein complex which is a potent inhibitor of the anaphase promoting complex/cyclosome (APC/C) (Izawa et al., 2015; Faesen et al., 2017). The APC/C is a ubiquitin E3 ligase which targets the Separase inhibitor Securin as well as cyclin B for proteosomal degradation. Its activation allows resolution of centromeric sister chromatid cohesion via Separase and mitotic exit by suppressing CDK1 activity. The MCC is produced on unattached kinetochores. As a very potent inhibitor of APC/C, one unattached kinetochore can signal for the SAC to be upheld (Rieder et al., 1995). Critically, only correct attachments can be stabilised due to the requirement for tension across the kinetochores and centromere for stabilisation which can only be provided by opposing attachments. By this mechanism only when all kinetochore attachments are stable (i.e. correct) is MCC no longer produced and the APC/C inhibition lifted. As Aurora B is required for both the formation of stable KT-MT attachments and resolution of erroneous ones, as well as recruitment of essential SAC proteins to kinetochores, successful mitosis is critically dependent on Aurora B kinase activity.

1.3.3 Chromosomal instability

Failures in the intricate control mechanisms described above can cause a variety of mitotic defects resulting in the unequal distribution of chromosomes (Thompson et al., 2010) and ultimately an aberrant number of chromosomes in the daughter cells, called aneuploidy. While this should lead to immediate cell death, some aneuploidies are tolerated, especially in the absence of functioning control mechanisms. As such, cancer cells often show chromosomal instability (CIN), a high rate of division defects causing aberrant karyotypes (Negrini et al., 2010). Aberrant cohesion between the sister chromatids which opposes the pulling forces of the mitotic spindle can cause ”lagging” chromosomes, which might ultimately be trapped in the cleavage furrow between the forming daughter cells (Thompson et al., 2010). On the other hand, premature loss of cohesion at the centromeres also causes segregation defects as without this cohesion the control mechanism ensuring proper KT-MT attachments does not work and erroneous attachments are formed. These erroneous attachments can cause lagging chromosomes, where a kinetochore is attached to opposing spindles effectively stopping the chromatid to be pulled to either pole. Attachments of both kinetochores to one pole cause aneuploidy as both chromatids are pulled to one pole resulting in a daughter cell with a trisomy and another with a monosomy. In addition to mitotic defects, failure to resolve chromosome interactions as they are formed during HR DNA repair can cause bridges

between the anaphase plates to form (Chan et al., 2018). Under the pulling forces of the spindle these bridges can break and cause loss of genetic material (Hoffelder et al., 2004; Shimizu et al., 2005).

1.3.4 Meiosis

Meiosis is a specialform of nuclear division found only in the reproductive cells (Moens, 1987). In contrast to mitosis, meiosis divides the duplicated diploid genome into four haploid cells, forming the gametes. This involves two divisions following only one replication. While the processes are similar, a large difference is apparent in the first meiotic division (meiosis I). Instead of segregating the sister chromatids, the homologous chromosomes are segregated forming two haploid genomes but with two-chromatid chromosomes. Only during the second division (meiosis II), which follows immediately without an interphase, are the sister chromatids separated similarly to mitosis forming 4 haploid genomes with single-chromatid chromosomes. Chromosomal rearrangements are intentionally introduced by homologous recombination (HR) between homologous chromosomes in the prolonged prophase of meiosis I (Zickler et al., 2015). To allow for these recombination events, cohesion between sister chromatids is maintained until anaphase I and removed only once recombination is finished. However, as homologous chromosomes are segregated in meiosis I, sister chromatids remain attached to each other via centromeric cohesion. Only before anaphase II, when sister chromatids are segregated, is centromeric cohesion resolved similar to mitosis (Ohkura, 2015).

1.3.5 H2B Serine 6 phosphorylation

One of the many mitotic histone modifications is a centromere-specific phosphorylation of H2B S6. While histones are generally conserved proteins among eukaryotes, H2B S6 is conserved only among vertebrates. H2B S6ph is detected in many vertebrate organisms like humans, mice, pigs and chickens, indicating a possibly conserved function. Whether a similar mitotic phosphorylation site exists in invertebrates like *Drosophila melanogaster* or lower eukaryotes like *Saccharomyces cerevisiae* is not yet known. H2B is phosphorylated by CDK1 upon mitotic entry and persists at the inner centromeres from prophase to early anaphase (Seibert et al., 2019) (Figure 7). In addition to CDK1, H2B S6ph is strictly dependent on Aurora B kinase activity. Opposing CDK1, protein phosphatase PP1 is essential for the dephosphorylation of H2B S6ph in later stages of mitosis as well as restriction of this PTM to the centromere as inhibition of PP1 causes spreading of H2B S6ph along the chromosome arms. However, the exact regulatory network controlling this phosphorylation remains to be identified.

The spatiotemporal regulation of H2B S6ph correlates with cohesin occupancy at centromeres (Figure 7). A functional connection is not yet established. However, masking of H2B S6ph by

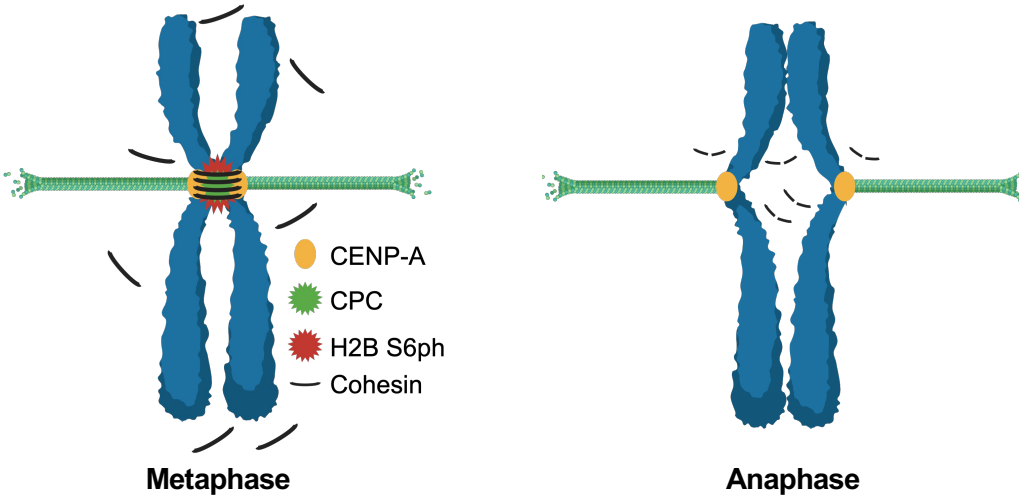

Figure 7: Localisation of H2B S6ph on mitotic chromosomes.

H2B S6ph is found specifically at the inner centromere on condensed mitotic chromosomes. It colocalises with the chromosomal passenger complex (CPC) and with centromeric cohesin. After anaphase onset, the CPC is displaced from the centromere together with cohesin and H2B S6ph is lost. Adapted from Seibert et al. (2019). *Created with biorender.com*

antibody injection into mitotic cells caused mitotic defects and failed chromosome segregation, indicating a possible functional relevance of this modification in mitosis (Seibert et al., 2019). Interestingly, phosphorylated H2B can be bound by 14-3-3 proteins, whereas SET/I2PP2A is repelled by the phosphorylation, implicating it with cohesion.

1.4 Aims of this study

Previous studies identified H2B S6 to be phosphorylated by CDK1 upon mitotic entry. The regulatory mechanism underlying the regulation of this modification, which is quickly lost after anaphase onset, however, is hitherto incompletely understood. While the writers, erasers and readers have been previously identified, it is unclear how they interact to provide the tight spatiotemporal control over H2B S6ph together with other mitotic histone PTMs. To gain insight into the possible function of this modification, its context should be understood. Therefore, this study aims to elucidate the network controlling H2B S6ph. Furthermore, H2B S6ph has been implicated with mitotic fidelity. Therefore, this study investigates a possible role in cancer cell chromosomal instability.

To help establish a function for H2B S6ph, this study aims to develop a new system that allows for the complete replacement of histones in vertebrate cells with mutant histone versions. This would open up new possibilities for linking the function of specific modified (and unmodified) amino acids of histones to a specific function, including H2B S6ph. So far, such systems only exist in non-vertebrate cells.

2 Material and Methods

2.1 Materials

2.1.1 Primary antibodies

Target	Clone	Host	Supplier	Cat. No.	Dilution
ACA		Human	Antibodies inc.	15-234	1:200
Aurora B		Mouse	abcam	ab3609	1:1000
CDK1	POH1	Mouse	Cell Signaling	9116	1:1000
GFP	7.1 and 13.1	Mouse	Merck	11814460001	1:1000
H2B		Rabbit	abcam	ab1790	1:20000
H2B S6ph	1D4-1-1	Rat	Custom made		1:400
H3 S10ph	6G3	Mouse	Cell Signaling	9706	1:1000
H3 S28ph		Rabbit	Cell Signaling	9713	1:1000
H3 T3ph	D5G1I	Rabbit	Cell Signaling	13576	1:5000
Ki-67		Mouse	Santa Cruz	sc-23900	1:1000
LNGFR	D4B3	Rabbit	Cell Signaling	8238	1:1000
Mklp2		Rabbit	Biomol	A300-879A	1:1000
PNUTS		Rabbit	Biomol	A300-439A	1:1000
PP1α	10C6-3	Mouse	Thermo Fisher	43-8100	1:1000
PP1γ		Rabbit	Biomol	A300-906A	1:1000
RepoMan	D7T4P	Rabbit	Cell Signaling	14976	1:1000
β-Tubulin	E7	Mouse	DHSB	E7	1:1000
Vinculin	hVIN-1	Mouse	Sigma	V9131	1:1000

2.1.2 Secondary antibodies

Target	Conjugate	Supplier	Cat. No.	Dilution
Goat-α-rabbit	Alexa Fluor 488	Dianova	111-545-003	1:500
Goat-α-rat	Alexa Fluor 488	Dianova	112-545-167	1:500
Goat-α-mouse	Alexa Fluor 488	Dianova	115-545-003	1:500
Donkey-α-rabbit Fab	Alexa Fluor 488	Dianova	711-547-003	1:500
Goat-α-rabbit	Alexa Fluor 594	Dianova	111-585-144	1:500
Goat-α-rat	Alexa Fluor 594	Dianova	112-585-167	1:500
Goat-α-mouse	Alexa Fluor 594	Dianova	115-585-062	1:500
Donkey-α-human	Alexa Fluor 594	Dianova	709-585-149	1:500
Goat-α-rabbit	Cy5	Dianova	111-175-144	1:500
Goat-α-rabbit	HRP	Dianova	111-035-144	1:5000
Goat-α-rat	HRP	Dianova	112-035-143	1:5000
Goat-α-mouse	HRP	Dianova	115-035-146	1:5000

2.1.3 Antibiotics

Name	Working conc.	Selection	Supplier
Ampicillin	100 µg/mL	bacteria	Carl Roth
Blasticidin	10 µg/mL	eukaryotes	InvivoGen
Chloramphenicol	25 µg/mL	bacteria	Fluka
G418	400 µg/mL	eukaryotes	Capricorn
Hygromycin B	50 µg/mL	eukaryotes	InvivoGen
Kanamycin	50 µg/mL	bacteria	Carl Roth
Penicillin/Streptomycin	100 U/mL / 100 µg/mL	bacteria	Thermo Fisher
Puromycin	0.33 µg/mL to 1 µg/mL	eukaryotes	InvivoGen

2.1.4 Bacterial strains

Name	Genotype	Supplier	Usage
DH5α (*Escherichia coli* K12)	F– Φ80lacZΔM15 Δ(lacZYA-argF) U169 recA1 endA1 hsdR17 (rK– mK+) phoA supE44 λ- thi–1 gyrA96 relA1	Invitrogen	general cloning
NEB 10β (*Escherichia coli* K12)	Δ(ara-leu) 7697 araD139 fhuA ΔlacX74 galK16 galE15 e14- Φ80dlacZΔM15 recA1 relA1 endA1 nupG rpsL (StrR) rph spoT1 Δ(mrr-hsdRMS-mcrBC)	NEB	large plasmids
Stbl3 (*Escherichia coli* K12)	F-mcrB mrrhsdS20(rB- mB-) recA13 supE44 ara-14 galK2 lacY1 proA2 rpsL20(StrR) xyl-5 Δ-leumtl-1	Invitrogen	plasmids with repetetive elements
SURE2 (*Escherichia coli* K12)	e14-(McrA-) Δ(mcrCB-hsdSMR-mrr)171 endA1 gyrA96 thi-1 supE44 relA1 lac recB recJ sbcC umuC::Tn5 (Kanr) uvrC [F' proAB lacIqZΔM15 Tn10 (Tetr) Amy Camr]	Stratagene	plasmids with repetetive elements
TOP10 (*Escherichia coli* K12)	F-mcrA Δ(mrr-hsdRMS-mcrBC) Φ80LacZΔM15 ΔLacX74 recA1 araD139 Δ(araleu) 7697 galU galK rpsL (StrR) endA1 nupG	Invitrogen	general cloning

2.1.5 Eukaryotic cell lines

Name	Cell type	Growth medium
Caco-2	human colorectal adenocarcinoma	DMEM
DF-1	chicken fibroblast	DMEM/F-12

Name	Cell type	Growth medium
HCT116	human colorectal carcinoma	DMEM
HeLa	human cervical adenocarcinoma	DMEM
HT-29	human colorectal adenocarcinoma	RPMI 1640
LN-229	human glioblastoma	DMEM
MCF-7	human mammary gland carcinoma	DMEM
RPE-1 hTERT	human pigmented retinal epithelial cell; immortalised	DMEM/F-12
SW620	human colorectal adenocarcinoma	RPMI 1640
T98G	human glioblastoma	DMEM
U2OS	human osteosarcoma	DMEM

2.1.6 Inhibitors

Name	Working conc.	Target	Supplier
AZD1152	1 µM	Aurora B	Sigma
Calyculin A	50 nM	PP1/PP2A	Sigma
Nocodazole	100 ng/mL	microtubules	Sigma
Thymidine	2 mM	nucleotide synthesis	Sigma

2.1.7 Chemicals

Name	Formula	Supplier
2-Propanol	C_3H_8O	Sigma
Acetic acid	$C_2H_4O_2$	Carl Roth
Acrylamide/Bis-acrylamide 37.5:1	C_3H_5NO and $C_7H_{10}N_2O_2$	Carl Roth
Adenosine triphosphate	$C_{10}H_{14}N_5O_{13}P_3Na_2$	Sigma
Ammonium persulfate (APS)	$(NH_4)_2S_2O_8$	Carl Roth

Name	Formula	Supplier
Aprotinin	$C_{284}H_{432}N_{84}O_{79}S_7$	Sigma
beta-mercaptoethanol	C_2H_6OS	Carl Roth
Bromphenol blue	$C_{19}H_{10}Br_4O_5S$	Merck
Calcium chloride	$CaCl_2$	Riedel de Haen
Citric acid	$C_6H_8O_7$	Carl Roth
Coomassie Brilliant Blue R-250	$C_{45}H_{44}N_3NaO_7S_2$	Fluka
Crystal violet	$C_{25}H_{30}ClN_3$	Sigma
Dimethyl Sulfoxide (DMSO)	C_2H_6OS	Sigma
Disodium hydrogen phosphate	Na_2HPO_4	Carl Roth
Dithiothreitol (DTT)	$C_4H_{10}O_2S_2$	Promega
EDTA	$C_{10}H_{16}N_2O_8$	Acros
EGTA	$C_{14}H_{24}N_2O_{10}$	Carl Roth
Ethanol	C_2H_6O	Sigma
Ethidium bromide (soln. 1 %)	$C_{21}H_{20}BrN_3$	Carl Roth
Formaldehyde	CH_2O	Carl Roth
Glycerol	$C_3H_8O_3$	Carl Roth
Glycine	$C_2H_5NO_2$	Carl Roth
Guanidinium chloride	CH_6ClN_3	Carl Roth
HEPES	$C_8H_{18}N_2O_4S$	Carl Roth
Hoechst 33342	$C_{27}H_{31}Cl_3N_6O$	Thermo Fisher
Hydrochloric acid	HCl	Carl Roth
Hydrogen peroxide	H_2O_2	Merck
IGEPAL C-630	$(C_2H_4O)nC_{14}H_{22}O$	Sigma
Isopropanol	C_3H_8O	Sigma
Leupeptin	$C_{20}H_{38}N_6O_4 \cdot \frac{1}{2}\,H_2SO_4$	Sigma
Magnesium chloride hexhydrate	$MgCl_2 \cdot 6\,H_2O$	Fluka
Manganese chloride dihydrate	$MnCl_2 \cdot 2\,H_2O$	Merck

Name	Formula	Supplier
Methanol	Ch_4O	Sigma
Mowiol 4-88	$(CH_2CHOH)n$	Sigma
PEG 4000	$(C_2H_4O)n$	Thermo Fisher
PEG 8000	$(C_2H_4O)n$	Carl Roth
PMSF	$C_7H_7FO_2S$	Sigma
Polyethyleenimine linear (PEI)	$(C_2H_5N \cdot HCl)n$	PolyScience
Ponceau S	$C_{22}H_{12}N_4Na_4O_{13}S_4$	Applichem
Potassium acetate	$C_2H_3KO_2$	Carl Roth
Potassium chloride	KCl	Sigma
Potassium dihydrogenphosphate	KH_2PO_4	Sigma
Potassium hydroxide	KOH	Merck
Propidium Iodide	$C_{27}H_{34}I_2N_4$	Sigma
Sodium acetate	$C_2H_3NaO_2$	Carl Roth
Sodium azide	NaN_3	Sigma
Sodium chloride	NaCl	Carl Roth
Sodium citrate	$C_6H_5Na_3O_7$	Fluka
Sodium deoxycholate	$C_{24}H_{39}NaO_4$	Sigma
Sodium dodecyl sulfate	$C_{12}H_{25}NaO_4S$	Bio-Rad
Sodium fluoride	NaF	Carl Roth
Sodium hydroxide	NaOH	Carl Roth
Sodium orthovanadate	Na_3VO_4	Sigma
Sulfuric acid	H_2SO_4	Merck
SYBR Green I	$C_{32}H_{37}N_4S$	Thermo Fisher
3, 3', 5, 5'-Tetramethylbenzidin (TMB)	$C_{16}H_{20}N_2$	Sigma
N, N, N', N'-tetramethylethylendiamine (TEMED)	$C_6H_{16}N_2$	Carl Roth
Tris	$C_4H_{11}NO_3$	Carl Roth

Name	Formula	Supplier
Triton X-100	$C_{14}H_{22}O(C_2H_4O)n$	Sigma
Trypan blue	$C_{34}H_{24}N_6Na_4O_{14}S_4$	Sigma
Tween 20	$C_{58}H_{114}O_{26}$	Gerbu

2.1.8 Kits

Name	Cat. No.	Supplier
NucleoBond PC500 Maxi	740574100	Macherey-Nagel
NucleoSpin Plasmid Mini	740588250	Macherey-Nagel
NucleoSpin RNA	740955250	Macherey-Nagel
NucleoSpin Tissue	740952	Macherey-Nagel
Pierce BCA protein assay	23225	Thermo Fisher
PrimeScript RT Master Mix cDNA synthesis	RR036B	Takara
QuikChange II XL Mutagenesis	200522	Takara
SmartPure Gel Purification	SK-GEPU-100	Eurogentec
SmartPure PCR Purification	SK-PCPU-100	Eurogentec

2.1.9 Enzymes and proteins

Enzyme	Cat. No.	Supplier
CDK1/Cyclin B	PV3292	Thermo Fisher
FastAP phosphatase	EF0651	Thermo Fisher
GST	SRP5348	Sigma
H2B, recombinant	SRP0407	Sigma
Micrococcal nuclease (MNase)	M0247S	NEB
NEB HiFi assembly Master Mix	E2621	NEB

Enzyme	Cat. No.	Supplier
Phusion HF DNA polymerase	F530	Thermo Fisher
PP1α	NBP1-72418	Novus Biologicals
PP1β	H00005500-Q01	Abnova
PP1γ	NBP2-59582	Novus Biologicals
Q5 DNA Polymerase	M0491	NEB
Restriction enzymes and buffers		Thermo Fisher & NEB
RNase A	R5503	Thermo Fisher
SuperScript II reverse transcriptase	18064014	Thermo Fisher
T4 DNA Ligase	EL0014	Thermo Fisher
T4 DNA Polymerase	EP0062	Thermo Fisher
T4 PNK	EK0031	Thermo Fisher
T5 Exonuclease	M0663S	NEB
Taq DNA Polymerase	EP0402	Thermo Fisher
TrypLE Express	12605010	Thermo Fisher

2.1.10 Peptides

Name	Sequence	Supplier
H2B(1-20)unmodified	PEPAKSAPAPKKGSKKAVTK[Biotin]	ProteoGenix
H2B(1-20)S6ph	PEPAK(pSer)APAPKKGSKKAVTK[Biotin]	ProteoGenix
H3(18-37)unmodified	KQLATKAARKSAPATGGVKK[Biotin]	ProteoGenix
H3(18-37)S28ph	KQLATKAARK(pSer)APATGGVKK[Biotin]	ProteoGenix

2.1.11 Oligonucleotides

2.1.11.1 Oligonucleotides for qPCR

Name	Sequence
GAPDH-fwd	GTCAGCCGCATCTTCTTTTGC
GAPDH-rev	AGTTAAAAGCAGCCCTGGTGA
PPP1CA-fwd	GAGACCATCTGCCTGCTGCT
PPP1CA-rev	CAGTTTGATGTTGTAGCGTCTCTTG
PPP1CB-fwd	CGAGTTTGATAATGCTGGTGGAATG
PPP1CB-rev	GCTGTTCGAGTTGGAGTGAC
PPP1CC-fwd	AAAGAGGCAGTTGGTCACTCTG
PPP1CC-rev	TTACAGGTCTCGTGGCATTTGG
PNUTS-fwd	AGGATGGGACACAGGTTTGAA
PNUTS-rev	GGGCAAGATAGGTGGGAAGG
MKI67-fwd	GCCTGCTCGACCCTACAGA
MKI67-rev	GCTTGTCAACTGCGGTTGC
CDCA2-fwd	GCTCTCCTGAAACAAACCATCT
CDCA2-rev	GCTGACTGGAAGGCTGATATT
KIF20A-fwd	CTTCGGCGACTAGGTGTGAG
KIF20A-rev	GACATCGTCATCGGACAGCA

2.1.11.2 Oligonucleotides for cloning

Refer to Appendix

2.1.12 siRNAs

Target	Vendor	Sequence	Reference
CDCA2	Origene	CAGAAGAAAUCAAUUGGUCAGUG	SR315905-A
CDCA2	Origene	AGAUCUUUCUGAGAUAUCAUCUA	SR315905-B

Target	Vendor	Sequence	Reference
PPP1CA	Sigma	CCGCATCTATGGTTTCTAC	Qian et al., 2011
PPP1CC	Sigma	GCATGATTTGGATCTTATA	Qian et al., 2011
KIF20A	Sigma	CCACCTATGTAATCTCATG	Qian et al., 2013
MKI67	Sigma	GGUCACACUGAGGAAUCAA	Vanneste et al., 2009
PNUTS	Sigma	GGAUGAAACUGAACGAGUA	Sigma SASI_Hs01_00133264

2.1.13 Plasmids

Plasmid	Vector	Reference
pUC19		Yanisch-Perron et al., 1985
pEGFP-N1		Clontech
pEGFP-C1		Clontech
pEGFP-H2B	pEGFP-N1	Kanda et al., 1998
pEGFP-H2B S6A	pEGFP-N1	Markus Seibert
pEGFP-H2B S6E	pEGFP-N1	Markus Seibert
pEGFP-H3.1	pEGFP-C1	Sandra Hake
pEGFP-H3.1 S28A	pEGFP-C1	This study
pEGFP-H3.1 S28E	pEGFP-C1	This study
pH2B-EGFP-MCS	pEGFP-C1	This study
pEGFP-H2B-Aurora B WT	H2B-GFP-MCS	This study
pEGFP-H2B-Aurora B KD	H2B-GFP-MCS	This study
pEGFP-H2B-INCENPΔcen	H2B-GFP-MCS	This study
pEGFP-RepoMan-WT	pEGFP-C1	This study
pEGFP-RepoMan-RATA	pEGFP-RepoMan-WT	This study
pEGFP-RepoMan-T394A	pEGFP-RepoMan-WT	This study
pEGFP-RepoMan-S893D	pEGFP-RepoMan-WT	This study

Plasmid	Vector	Reference
pEGFP-RepoMan-ΔC(1-890)	pEGFP-RepoMan-WT	This study
pSBtet-Hyg	pUC19	Kowarz et al., 2015
pSBtet-Neo	pUC19	Kowarz et al., 2015
pINDUCER10	pGIPZ	Meerbrey et al., 2011
pEGFP-ggH2B7	pEGFP-N1	This study
pEGFP-ggH2B8	pEGFP-N1	This study
pMIR30	pCDNA3	This study
pMIR30-shCtrl	pMIR30	This study
pMIR30-shH2B-1	pMIR30	This study
pMIR30-shH2B-2	pMIR30	This study
pMIR30-shH2B-3	pMIR30	This study
pMIR30-shH2B-4	pMIR30	This study
pMIR30-shH2B-5	pMIR30	This study
pMIR30-shH2B-6	pMIR30	This study
pMIR30-shH2B-7	pMIR30	This study
pMIR30-shH2B-3+7	pMIR30	This study
pMIR30-shH2B-3+7+5	pMIR30	This study
pMIR30-short-DsRed2	pCDNA3	This study
pMIR30-short-shH2B-3	pMIR30-short	This study
pMIR30-short-shH2B-3(5p)	pMIR30-short	This study
pSB-Puro-mir30short-Neo	pSBtet-Hyg	This study
pSB-Puro-mir30short-shH2B-3(5p)Neo	pSB-Puro-mir30short-Neo	This study
pCAG-SB100X-pA	pCAG	Mark Groudine
pSBtet-IRES-Bla-Hygro	pSBtet-Hyg	This study
pUC57-ggH2B-shResist	pUC57	This study

Plasmid	Vector	Reference
pSBtet-ggH2B-IRES-Bla-Hygro	pSBtet-IRES-Bla-Hygro	This study
pSB-Puro-mir30short-shH1-71-Neo	pSB-Puro-mir30short-Neo	This study
pSB-Puro-mir30short-shH1-368-Neo	pSB-Puro-mir30short-Neo	This study
pSB-Puro-mir30short-shH1-389-Neo	pSB-Puro-mir30short-Neo	This study
pSB-Puro-mir30short-shH1-393-Neo	pSB-Puro-mir30short-Neo	This study
pSB-Puro-mir30short-shH1-404-Neo	pSB-Puro-mir30short-Neo	This study
pSB-Puro-mir30short-shH1-482-Neo	pSB-Puro-mir30short-Neo	This study
pSB-Puro-mir30short-shH1-503-Neo	pSB-Puro-mir30short-Neo	This study
pSB-Puro-mir30short-shH1-521-Neo	pSB-Puro-mir30short-Neo	This study
pSB-Puro-mir30short-shH2A-87-Neo	pSB-Puro-mir30short-Neo	This study
pSB-Puro-mir30short-shH2A-92-Neo	pSB-Puro-mir30short-Neo	This study
pSB-Puro-mir30short-shH2A-104-Neo	pSB-Puro-mir30short-Neo	This study
pSB-Puro-mir30short-shH2A-107-Neo	pSB-Puro-mir30short-Neo	This study
pSB-Puro-mir30short-shH2A-152-Neo	pSB-Puro-mir30short-Neo	This study
pSB-Puro-mir30short-shH2A-155-Neo	pSB-Puro-mir30short-Neo	This study
pSB-Puro-mir30short-shH2A-206-Neo	pSB-Puro-mir30short-Neo	This study
pSB-Puro-mir30short-shH2A-215-Neo	pSB-Puro-mir30short-Neo	This study
pSB-Puro-mir30short-shH3-41-Neo	pSB-Puro-mir30short-Neo	This study
pSB-Puro-mir30short-shH3-44-Neo	pSB-Puro-mir30short-Neo	This study
pSB-Puro-mir30short-shH3-86-Neo	pSB-Puro-mir30short-Neo	This study
pSB-Puro-mir30short-shH3-155-Neo	pSB-Puro-mir30short-Neo	This study
pSB-Puro-mir30short-shH3-167-Neo	pSB-Puro-mir30short-Neo	This study
pSB-Puro-mir30short-shH3-173-Neo	pSB-Puro-mir30short-Neo	This study
pSB-Puro-mir30short-shH3-245-Neo	pSB-Puro-mir30short-Neo	This study
pSB-Puro-mir30short-shH3-287-Neo	pSB-Puro-mir30short-Neo	This study
pSB-Puro-mir30short-shH4-38-Neo	pSB-Puro-mir30short-Neo	This study
pSB-Puro-mir30short-shH4-47-Neo	pSB-Puro-mir30short-Neo	This study

Plasmid	Vector	Reference
pSB-Puro-mir30short-shH4-116-Neo	pSB-Puro-mir30short-Neo	This study
pSB-Puro-mir30short-shH4-119-Neo	pSB-Puro-mir30short-Neo	This study
pSB-Puro-mir30short-shH4-150-Neo	pSB-Puro-mir30short-Neo	This study
pSB-Puro-mir30short-shH4-158-Neo	pSB-Puro-mir30short-Neo	This study
pSB-Puro-mir30short-shH4-161-Neo	pSB-Puro-mir30short-Neo	This study
pSB-Puro-mir30short-shH4-236-Neo	pSB-Puro-mir30short-Neo	This study
pSBtet-Puro-shggH2B-3(5p)-Neo-rtTAV16	pSB-Puro-mir30short-Neo	This study
pHEX-SB-Bxb1-RMCE-LNGFR-BpI-free		This study
pSBtet-Hygro-ggH2B-GFP11	pSBtet-Hyg	This study
pHEX-RMCE-LNGFR-1xggH2B-GFP11	pHEX-SB-Bxb1-RMCE-LNGFR-BpI-free	This study
pHEX-RMCE-LNGFR-2xggH2B-GFP11	pHEX-SB-Bxb1-RMCE-LNGFR-BpI-free	This study
pHEX-RMCE-LNGFR-3xggH2B-GFP11	pHEX-SB-Bxb1-RMCE-LNGFR-BpI-free	This study
pHEX-RMCE-LNGFR-4xggH2B-GFP11	pHEX-SB-Bxb1-RMCE-LNGFR-BpI-free	This study

2.1.14 Other reagents and materials

Name	Supplier
8-well coverslip slides	ibidi
ABsolute qPCR SYBR Green ROX Mix	Thermo Fisher
Agar	Applichem
Agarose	PeqLab
Bovine serum albumine	Sigma

Name	Supplier
Cell culture plastics	Sarstedt & TPP & Greiner
Coulter Clenz	Beckman Coulter
Coverslips	Langenbrinck
Cytospin microscope slides	Tharmac
Deoxynucleoside triphosphates	Thermo Fisher
DMEM high Glucose with GlutaMAX	Thermo Fisher
DMEM/F-12 high Glucose with GlutaMAX	Thermo Fisher
DNA loading dyes	Thermo Fisher & NEB
E-Z 96 DNA Plate	Omega Bio-tek
FACSClean	BD Bioscience
FACSFlow	BD Bioscience
FACSRinse	BD Bioscience
Fetal calf serum	Thermo Fisher
GFP-Trap Agarose beads	chromotek
Immersion oil	Carl Roth
Immobilon ECL Ultra Western HRP Substrate	Merck
Lipofectamine 3000	Thermo Fisher
NeutrAvidin coated Plates	Thermo Fisher
Oligo-dT primer	Thermo Fisher
OptiMEM	Thermo Fisher
PageRuler prestained protein ladder plus	Thermo Fisher
Parafilm M	Bemis
Primers	Sigma & Eurofins
Random hexamer primer	Genaxxon
RPMI 1640 with GlutaMAX	Thermo Fisher
Sanger sequencing	Seqlab
Skimmed milk powder	Sucofin

Name	Supplier
Standard glass microscope slides	Langenbrinck
Tryptone	Carl Roth
Western Lightning ECL Solution	Perkin Elmer
Whole plasmid sequencing	Seqlab
Yeast extract	Carl Roth

2.1.15 Lab equipment and other devices

Name	Purpose	Supplier
BioPhotometer 6131	DNA quantification	Eppendorf
Cellspin III UNI	chromosome spreading	Tharmac
ChemiDoc MP	Western blot ECL imaging	Bio-Rad
Elix water purification	water purification	Millipore
FACSCalibur	flow cytometry	BD Bioscience
FACSMelody	flow cytometry (sorting)	BD Bioscience
GloMax Discover plate reader	absorbance and fluorescence measurement	Promega
LUNA II	cell counting	logos biosystems
Mini-Protean III gel tanks	SDS-PAGE	Bio-Rad
Sonifier 250 with micro tip	cell lysis	Branson
StepOne Plus	qPCR	Applied biosystems
T100 gradient thermal cycler	PCR	Bio-Rad
TE2000E inverted microscope; coolLED pE-300; ORCA Spark	brightfield and fluorescence microscopy	Nikon; coolLED; Hamamatsu
Tpersonal Cycler	PCR	Biometra

Name	Purpose	Supplier
Trans-Blot SD semi-dry transfer cells	Western blotting	Bio-Rad
Vilber UV illuminator	agarose gel imaging	Vilber
Wilovert PH 20	cell culture microscopy	Hund Wetzlar

2.1.16 Software

Name	Versions	Purpose	Supplier
BioRender	n/a	Figure generation	BioRender
CellQuest Pro	5.2.1	FACS data acquisition and analysis	BD Bioscience
DeepL Write	n/a	Spell & grammar checking	DeepL SE
Excel	2019	Data analysis	Microsoft
FACSChorus	1.0	FACS data acquisition	BD Bioscience
FIJI / ImageJ	2.3.0	Image analysis and editing	ImageJ project
FlowJo	10.8.1	FACS data analysis	BD Bioscience
Image Lab	6.0.1	Western blot ECL image analysis	Bio-Rad
NEBuilder	2.8.2	NEB HiFi assembly planning	NEB
NIS Elements AR	3.10	Image acquisition	Nikon
PowerPoint	2019	Figure generation	Microsoft
RNA fold	2.4.18	RNA folding simulation	University of Vienna
SnapGene	5.3.0 - 6.3.2	Cloning simulation	GSL Biotech
StepOne Software	2.3	qPCR setup and analysis	Applied Biosystems
TeX Live	2023	Writing	TeX Users Group
Texifier	1.9.21	Writing	Valletta Ventures

2.2 Methods in Molecular Biology

2.2.1 *In vitro* kinase and phosphatase assay

Kinase reaction mix: 6 mM HEPES (pH 7.5); 3 mM $MgCl_2$; 3 mM $MnCl_2$; 1.2 mM DTT; 5 % (v/v) glycerol; 20 µM ATP

In vitro kinase assays were performed with recombinant proteins. 0.5 µg of CDK1 and Cyclin B1 and 2 µg H2B were added to a kinase reaction mix and incubated at 37 °C for 30 min. Reactions were stopped by heat inactivation at 95 °C for 10 min. 0.5 µg recombinant GST or PP1 enzyme were added and mixtures were incubated for another 30 min at 37 °C. Reactions were stopped by the addition of SDS sample buffer (subsection 2.3.6) and samples were further analysed by Western blotting or Coomassie staining.

2.2.2 Transformation of bacteria

LB medium: 1 % (w/v) tryptone; 0.5 % (w/v) yeast extract; 1 % (w/v) NaCl
LB agar: LB medium with 1.5 % (w/v) agar and antibiotics

Chemically competent cells were prepared with the $CaCl_2$ method (Mandel et al., 1970) and stored at −80 °C until use. All chemically competent *Escherichia coli* strains were transformed with the heat shock method (Bergmans et al., 1981). Briefly, 100 µL of chemically competent bacteria were thawed on ice and less than 100 ng of plasmid or ligation reaction were added. Cells were incubated on ice for 30 min Bacteria were heat-shocked at 42 °C for 60 s and placed on ice for another 2 min. 900 µL of LB medium without antibiotics was added. Bacteria were allowed to recover at 37 °C for 15 to 60 min, for ampicillin or kanamycin resistance respectively, shaking at 1500 rpm. Cells were centrifuged at 13 000 rcf for 1 min and the supernatant was partly aspirated. The pellet was resuspended in the remaining volume and cells were plated on an LB-agar plate containing the appropriate selection antibiotic (2.1.3). Plates were incubated at 37 °C overnight or at room temperature over weekend.

2.2.3 Isolation of plasmids

LB medium: 1 % (w/v) tryptone; 0.5 % (w/v) yeast extract; 1 % (w/v) NaCl

Plasmids were isolated from overnight cultures of *Escherichia coli* (subsection 2.1.4) in LB medium (Bertani, 1951), that were grown at 37 °C shaking.

2.2.3.1 Minipreparation

For minipreparations, 5 to 6 mL of LB medium with appropriate selection antibiotic were inoculated and grown overnight. Bacteria were centrifuged at 13 000 rcf for 5 min and supernatant was aspirated. Cell pellet was then subjected to alkaline lysis and silica column purification as per the manufacturers protocol using the Thermo GenJET Mini purification kit. Eluted plasmid DNA was quantified and quality checked via UV photometry and also checked on an agarose gel.

96-well miniprep

Buffer P1:	50 mM Tris-HCl (pH 8.0); 10 mM EDTA; 50 µg/mL RNase A
Buffer P2:	200 mM NaOH; 1 % (w/v) SDS
Buffer N3:	4.2 M guanidinium chloride; 500 mM potassium-acetate
Buffer PE:	10 mM Tris-HCl (pH 7.5); 80 % (v/v) ethanol
Buffer EB:	10 mM Tris-HCl (pH 8.5)

For minipreparations in 96-well format, bacteria were grown in 96 deep-well blocks with 1.5 mL of LB medium overnight, shaking at 37 °C. Blocks were centrifuged at 3500 rcf for 10 min. Medium was removed and cells were resuspended in 200 µL resuspension buffer P1. 200 µL lysis buffer P2 was added and mixed by inversion. 280 µL neutralisation buffer N3 was added and mixed and precipitate was centrifuged off at 3500 rcf for 30 min. Cleared lysates were transferred to 96-well silica blocks and centrifuged at 2250 rcf for 5 min. 600 µL wash buffer PE was added and blocks were centrifuged at 2250 rcf for 5 min. Wells were washed once more and blocks were dried by centrifugation at 2250 rcf for 15 min. Plasmid DNA was eluted in 100 µL elution buffer EB by centrifugation at 2250 rcf for 15 min.

96-well DNA quantification

PBS:	137 mM NaCl; 2.7 mM KCl; 8 mM Na_2HPO_4; 1.47 mM KH_2PO_4
DNA staining solution:	1X SYBR Green I, PBS

DNA concentrations in 96-well format were measured with SYBR Green I DNA staining. 100 µL of staining solution were mixed in 96-wells with 2 µL sample or 2 µL of pUC19 DNA standard with concentrations of 1.95 to 125 ng/µL. Samples were incubated for 15 min at room temperature. Fluorescence with excitation at 475 nm and emission at 500 to 550 nm was measured. Concentrations were calculated by linear regression of the DNA standard.

2.2.3.2 Maxipreparations

For maxipreparations, 200 to 400 mL of LB medium with appropriate selection antibiotic were inoculated and grown overnight. Bacteria were centrifuged at 6000 rcf for 15 min at 4 °C and supernatant was discarded. Cell pellet was then subjected to alkaline lysis and silica column purification as per the manufacturers protocol using the MN NucleoBond Maxi kit. Eluted DNA was isopropanol and ethanol precipitated, dried and resuspended in water. Eluted plasmid DNA was quantified and quality checked via UV photometry.

2.2.4 Polymerase chain reaction (PCR)

PCR (Mullis, 1987) was performed to amplify DNA fragments for restriction digestion, mutagenesis, transformed colony identification or mRNA/gDNA quantification.

2.2.4.1 Colony PCR

For colony PCR, primers were chosen to either detect the presence or order of certain sequences to identify successful assembly of a desired construct. Primers were chosen or designed to yield amplicons between 300 and 2000 bp.

Single cell clones were picked from overnight agar-plates and added to a prepared PCR master mix using Taq DNA polymerase. Depending on the cloning, between 4 and 32 colonies were screened. PCRs were performed using a standard colony-PCR protocol with 40 cycles adjusting annealing temperatures and elongation times to the primers being used.

Reagent	Volume	Amount
10X Taq Polymerase Buffer ($(NH_4)_2SO_4$)	2.5 µL	1X
$MgCl_2$ (25 mM)	2.0 µL	2 mM
dNTPs (10 mM)	0.5 µL	0.2 mM
Primer 1 (10 µM)	0.25 µL	1 µM
Primer 2 (10 µM)	0.25 µL	1 µM
Taq DNA polymerase	0.5 µL	2.5 U
deion. H_2O	19 µL	

Step	Temperature	Time	Cycles
Initial denaturation	95 °C	180 s	1
Denaturation	95 °C	30 s	40
Annealing	50 to 70 °C	30 s	40
Extension	72 °C	60 s/kbp	40
Final extension	72 °C	600 s	1

2.2.4.2 Preparative PCR

For cloning, DNA was amplified using high-fidelity polymerases (Phusion or Q5) in a PCR program following the manufacturers recommendations.

Reagent	Volume	Amount
5X Q5 Buffer or 5X Phusion HF/GC Buffer	10 µL	1X
dNTPs (10 mM)	1 µL	0.2 mM
Primer 1 (10 µM)	2.5 µL	0.5 µM
Primer 2 (10 µM)	2.5 µL	0.5 µM
Template DNA	X	less than 200 ng
Q5/Phusion polymerase	0.5 µL	2.5 U
deion. H_2O	33.5 µL	

Step	Temperature	Time	Cycles
Initial denaturation	98 °C	30 s	1
Denaturation	98 °C	10 s	
Annealing	50 to 70 °C	30 s	
Extension	72 °C	30 s/kbp	40
Final extension	72 °C	600 s	1

For PCR reactions using primers for the addition of overhangs for NEB HiFi assembly or restriction cloning, a modified 2-stage PCR protocol was used.

Step	Temperature	Time	Cycles
Initial denaturation	98 °C	30 s	1
Denaturation	98 °C	10 s	
Annealing	50 to 70 °C	30 s	
Extension	72 °C	30 s/kbp	10
Denaturation	98 °C	10 s	
Annealing & extension	72 °C	30 s	30
Final extension	72 °C	600 s	1

2.2.4.3 Site directed mutagenesis

Mutagenesis PCRs were performed with QuikChange II XL kit as per manufacturers instructions or Phusion polymerase. Primers were designed with 15 bases perfectly matching the target sequence upstream and downstream of the mismatch. After PCR, template plasmid was digested by adding 10 U of DpnI restriction enzyme and incubation for 1 h at 37 °C. After heat inactivation, 10 µL of PCR were used for bacterial transformation.

Reagent	Volume	Amount
5X Phusion HF	10 µL	1X
dNTPs (10 mM)	1 µL	0.2 mM
Primer 1 (10 µM)	2.5 µL	0.5 µM
Primer 2 (10 µM)	2.5 µL	0.5 µM
Template plasmid	X	less than 50 ng
$MgCl_2$ (50 mM)	1 µL	
DMSO	2.5 µL	
Q5/Phusion polymerase	0.5 µL	2.5 U
deion. H_2O	ad 50 µL	

Step	Temperature	Time	Cycles
Initial denaturation	98 °C	30 s	1
Denaturation	98 °C	10 s	
Annealing	55 °C	60 s	
Extension	72 °C	60 s/kbp	18

2.2.4.4 qPCR

qPCRs were performed on a Applied Biosystems StepOne Plus 96-well qPCR cycler and ABsolute SYBR Green master mix as 10 µL reactions. SYBR Green fluorescence was quantified. ROX was used a passive reference.

Reagent	Volume	Amount
2X ABsolute SYBR Green Master Mix	5 µL	1X
DNA	1 to 4 µL	
Primer 1 (10 µM)	0.2 µL	200 nM
Primer 2 (10 µM)	0.2 µL	200 nM
deion. H_2O	ad 10 µL	

Step	Temperature	Time	Cycles
Initial denaturation	95 °C	10 min	1
Denaturation	95 °C	15 s	
Annealing & extension	60 °C	60 s	40
Melt Curve	60 to 95 °C		1

All measurements were performed in technical duplicates or triplicates and analysed with StepOne software. Fold changes were calculated with $\Delta\Delta C_T$-method (Livak et al., 2001).

2.2.5 Molecular cloning

Plasmids cloned in this study were cloned by different methods. All sequences were verified by Sanger sequencing or whole plasmid sequencing and control digest.

2.2.5.1 Restriction digests

Restriction digests of plasmid DNA or DNA fragments were performed according to manufacturer instructions. Depending on the application between 0.5 and 5 µg of DNA were digested with 10 to 30 U of restriction enzyme for 1 to 3 h at 37 °C (or different, depending on the enzyme). For single enzyme digests, the optimal buffer was used. For digestions with multiple enzymes the buffer with the overall highest activity was determined with the Thermo Fisher Double Digest tool. Restriction digests of backbones for cloning were supplemented with FastAP phosphatase to reduce re-ligation of the backbone. Restriction digests with unintended products smaller than 60 bp were purified with the SmartPure PCR cleanup kit. If multiple products larger than 60 bp were expected a gel purification was performed of the intended fragment.

2.2.5.2 Ligations

Ligations were performed with T4 DNA Ligase and 50 ng of backbone DNA and insert(s) in a 3:1 molar ratio. Ligations were incubated for 30 min in case of sticky-end ligations and 60 min for blunt-end ligations or multi-fragment ligations at room temperature as per manufacturers instructions.

2.2.5.3 Golden Gate Assembly

Golden Gate assembly was performed with either Esp3I or BpiI as described previously (Bhakta, 2017).

For assemblies of shRNA plasmids with Esp3I, annealed DNA oligos were used to produce compatible overhangs in the insert. Annealed oligos were added to the assembly reaction with the appropriate backbone. For assemblies of histone plasmids with BpI, PCR products and plasmid DNA were used in the assembly reaction.

Reagent	Volume	Amount
10X T4 DNA Ligase Buffer	1.5 µL	1X
DNA fragments	X	25 fmol each
Esp3I or BpiI	0.5 µL	5 U
T4 DNA Ligase	0.5 µL	2.5 U
deion. H_2O	ad 15 µL	

Golden Gate assembly with Esp3I

Step	Temperature	Time	Cycles
Initial digest	37 °C	10 min	
Digestion	37 °C	1.5 min	
Annealing & Ligation	16 °C	3 min	10
Digestion	37 °C	5 min	
Digestion & Ligase inactivation	50 °C	5 min	
Inactivation	80 °C	10 min	

Golden Gate assembly with BpiI

Step	Temperature	Time	Cycles
Initial digest	37 °C	10 min	
Digestion	37 °C	1.5 min	20
Annealing & Ligation	16 °C	3 min	20
Digestion	37 °C	10 min	
Digestion & Ligase inactivation	50 °C	10 min	
Inactivation	80 °C	10 min	

2.2.5.4 NEB HiFi Assembly

Primers to create fragments with overhangs for NEB HiFi assembly were designed with SnapGene or NEBuilder. Fragments were created by either restriction digest or preparative PCR (2.2.4.2). Purified fragments were added to NEB Hifi assembly reaction mixture and incubated at 37 °C for 15 to 60 min.

Reagent	Volume	Amount
NEB HiFi Assembly Master Mix	10 µL	1X
DNA fragments	X	200 fmol each
deion. H_2O	ad 15 µL	

2.2.5.5 TEDA Cloning

5X TEDA Master Mix: 500 mM Tris (pH 7.5); 50 mM $MgCl_2$; 50 mM DTT; 0.25 g PEG 8000; 10 U T5 exonuclease

TEDA cloning (Xia et al., 2019) was used for assembly of DNA fragments as an alternative to NEB HiFi assembly. Fragments were created the same way as for NEB HiFi assembly but assembled with self-made TEDA cloning Master Mix. Briefly, 4 µL of 5X TEDA Master Mix were used with a total of 16 µL of DNA fragments with a 3:1 ratio of inserts to backbone. Assemblies were carried out at 30 °C for 40 min and then used for transformation.

2.2.6 Agarose gel electrophoresis

TAE buffer: 4 mM Tris (pH 8.3); 50 mM acetic acid; 1 mM EDTA

For fragment size analysis agarose gels were prepared with 0.8 to 4 % (w/v) agarose in TAE-buffer with 0.2 µg/µL Ethidiumbromide. Samples were loaded and gels were run at a constant voltage of 70 to 180 V until separation was sufficient. Gels were imaged on an UV illuminator and camera.

For fragment purification, gels were prepared with 0.7 to 1.5 % (w/v) agarose in TAE-buffer with 0.2 µg/µL Ethidiumbromide. Samples were loaded and gels were run at a constant voltage of 70 to 100 V until separation was sufficient. Gels were illuminated on an UV transilluminator (set to 70 % intensity) and fragments of the desired size were cut from the gel. DNA was extracted and purified using Eurogentec SmartPure Gel extraction kit. DNA was quantified and quality checked via UV photometry and also checked on an agarose gel.

2.2.7 Isolation of RNA

Cells were trypsinised until fully detached and resuspended in PBS. Cells were centrifuged at 500 rcf for 5 min and cell pellet was washed once more in PBS. Cell pellet was then processed according to manufacturer protocol with MN NucleoBond RNA mini kit. Eluted RNA was quantified and purity checked by UV photometry. RNA was then stored at −80 °C.

2.2.8 cDNA synthesis

Pure total RNA was subjected to reverse transcription by either SuperScript III RT with oligo-dT primers or random-hexamers or by Takara PrimeScript Master Mix according to the manufacturer protocol. In both cases a maximum of 500 ng of RNA were reverse transcribed. After the reaction, cDNA was diluted 1:5 in preparation for qPCR and was used immediately or stored at −20 °C or −80 °C for long term storage.

2.3 Methods in Cellular Biology

2.3.1 Cell culture

Cells were cultured in appropriate cell culture media (section 2.1.5) supplemented with 10 % (v/v) FCS and Penicillin/Streptomycin in a humidified 5 % (v/v) CO_2 atmosphere. Stable cell lines were kept under selective pressure with the appropriate antibiotics (section 2.1.3) in the medium. Cells were regularly passaged to keep cells in log-phase and checked for mycoplasma contamination by DNA staining and fluorescence microscopy. For cell seeding, cells were counted with a Logos LUNA-II automated cell counter using trypan blue for dead cell exclusion.

2.3.2 Cryopreservation of eukaryotic cells

Freezing medium: 10 % (v/v) DMSO; FCS

Cells were trypsinised until fully detached and resuspended in warm PBS. Cells were then centrifuged at 300 rcf for 5 min and resuspended in freezing medium. Cells were aliquoted in cryo-tubes and initially frozen at −80 °C for 1-4 days. For long term storage stocks were kept at −150 °C.

For thawing, cryostocks were thawed in a 37 °C waterbath. Cells were resuspended in fresh medium and centrifuged at 300 rcf for 3 min. Cells were then resuspended in fresh medium again and plated for recovery and outgrowth.

2.3.3 Transfection of mammalian cells

Cells were seeded the day before transfection to yield 50 to 80 % confluency at transfection depending on the time course of the experiment. Culture medium was exchanged for medium supplemented with 10 % (v/v) FCS but without antibiotics. HCT116, HEK293T and HeLa cells were transfected with PEI (Boussif et al., 1995). DF1 cells were transfected with Lipofectamine 3000.

2.3.3.1 Lipofectamine 3000

DNA and P3000 were diluted in OptiMEM and Lipofectamine 3000 was diluted in OptiMEM separately. The amount of DNA was chosen according to manufacturers recommendations. The two dilutions were combined, mixed and incubated for 15 min at room temperature before being added to the cells dropwise.

2.3.3.2 PEI

PEI: 1 mg/mL PEI (pH 7.0)

DNA was diluted in blank DMEM and PEI was diluted in blank DMEM in a ratio of 3 µg/mL PEI per 1 µg/mL DNA. The DNA and PEI dilutions were combined, mixed and incubated for 30 min at room temperature and mixture was added to cells dropwise. After 4 h medium was exchanged to normal growth medium.

Culture dish	12-well	6-well	6 cm dish	10 cm dish
DNA	1 µg	2 µg	2.5 µg	5 µg
DNA mix	50 µL	75 µL	100 µL	200 µL
PEI mix	50 µL	75 µL	100 µL	200 µL
Total volume	100 µL	150 µL	200 µL	400 µL
Transfection medium	0.5 mL	1 mL	2 mL	5 mL

2.3.4 Generation of stable cell clones

For the generation of stable cell clones, cells were transfected as described above with the appropriate plasmids. 1 d after transfection, cells were selected with the appropriate selection antibiotic for 2 to 4 d to select for transfected cells. In some cases, cells were also sorted via FACS to enrich stably transfected cells. Selected cell pools were then seeded in a large dish in a high dilution for clonal expansion of single cells or seeded in 96-well plates in a limiting dilution. Clones were then grown until colonies were large enough for picking or further analysis.

For clone picking, cells were briefly trypsinised for 60 s and quickly diluted with cold PBS. Colonies were then aspirated with a micropipette and transferred into a 96-well plate.

2.3.5 siRNA mediated knock-down

Cells were transfected with siRNAs using Lipofectamine 3000 reagent. Transfections were carried out as for plasmid DNA, without the addition of P3000. Transfections were carried out with an siRNA total concentration of 37.5 nM. Knock-down efficiencies were tested on RNA level with qPCR, and protein level via Western blotting after 24 h or 48 h, respectively.

2.3.6 Whole cell lysis

RIPA Buffer: 50 mM Tris-HCl (pH 7.4); 150 mM NaCl; 1 % (v/v) IGEPAL CA-630; 0.1 % (w/v) SDS; 1 mM EDTA; 0.5 % (w/v) sodium-deoxycholate ***freshly added:*** 1 mM PMSF; 10 µg/mL Aprotinin; 10 µg/mL Leupeptin; (10 mM NaF; 0.5 mM Na_3VO_4)

5x SDS sample buffer: 250 mM Tris-HCl (pH 6.8); 10 % (w/w) SDS; 40 % (v/v) glycerol; 15 % (v/v) β-mercaptoethanol; 0.02 % (w/v) bromphenolblue

Medium was removed and cells were washed with cold PBS. Depending on the experimental setting, medium and PBS were discarded or collected. Cells were scraped off in a small volume of cold PBS and then collected. Culture dishes were rinsed with cold PBS again and cells were collected by centrifugation at 500 rcf for 5 min at 4 °C. The cell pellet was resuspended in 5-times its volume of cold RIPA buffer (Alcaraz et al., 1990) freshly supplemented with protease and phosphatase inhibitors. Cells were lysed on ice for 30 min. Lysates were then sonicated for 20 s twice on continuous setting with output power 1.5 to shear DNA and fully solubilise the cells. Protein concentration was measured by BCA assay (Smith et al., 1985) on a plate reader and samples were adjusted to equal concentrations with PBS. 5x SDS sample buffer was added and samples were boiled for 10 min at 95 °C.

2.3.7 Chromosome spreads

Hypotonic buffer: 30.9 mM (0.8 % (w/v)) tri-sodium citrate

KCM buffer: 120 mM KCl; 20 mM NaCl; 10 mM Tris-HCl (pH 7.5); 0.5 mM EDTA; 0.1 % (v/v) Triton X-100

Chromosome spreads were prepared with cytospin technqiue (Jeppesen, 2000; Shrestha et al., 2017). Cells were treated with 100 ng/mL nocodazole for 1 to 16 h to enrich mitotic cells. Cells were collected by shake-off and centrifuged at 300 rcf for 5 min at room temperature. Cells were resuspended in hypotonic buffer and swollen for 15 min at room temperature. Cell density was determined and adjusted to 1×10^5 cells/mL. Cells were placed on ice and 500 µL cell suspension was spun onto a glass slide at 1500 rpm for 10 min in a cytospin with medium acceleration. Slides were immediately placed in 3.7 % (w/v) formaldehyde/PBS for 10 min for fixation. Slides were then washed in KCM buffer for 30 min at room temperature similar to the procedure described by Oestergaard (2017).

Slides were then used for normal immunofluorescence staining. Slides were stained in a custom made humidified chamber. All solutions were placed on the slide under parafilm to keep it on the sample.

2.3.8 Immunofluorescence

Staining buffer: 3 % (w/v) BSA; 0.3 % (v/v) Triton X-100; PBS

Mounting medium: 100 mM Tris (pH 8.5); 10 % (w/v) Mowiol 4-88; 6 % (w/v) glycerol; 18 % (v/v) H_2O

Cells were seeded onto isopropanol disinfected glass coverslips or 8-well ibidi coverslip slides. For fixation, medium was removed, cells were washed with PBS and cells were incubated in 3.7 % (w/v) formaldehyde/PBS for 5 min at room temperature. Cells were washed with PBS again and permeabilised for 30 min at room temperature with staining buffer. Coverslips were moved to a custom made humidified chamber (Pfisterer et al., 2022). Primary antibodies were diluted in staining buffer and kept on coverslips overnight at 4 °C. Cells were then washed twice with staining buffer and stained with secondary antibodies diluted in staining buffer for 1 h at room temperature. Cells were washed twice with PBS, DNA was stained with 0.1 µg/mL Hoechst 33342 for 5 min at room temperature and washed again with PBS. Coverslips were then mounted on standard microscope glass slides with Mowiol mounting medium.

Samples were imaged on a Nikon TE2000E inverted fluorescence microscope equipped with a coolLED pE-300ultra light source, a Hamamatsu ORCA Spark scientific camera and a Nikon T-RCP controller and NIS Elements 3.10.

All images were processed with FIJI/ImageJ for brightness/contrast adjustment. All adjustments were performed without gamma correction and were applied to the complete image equally. Deconvolution was performed with Microvolution. For quantifications all images of one experiment were acquired with equal imaging parameters. Any measurements were performed in FIJI/ImageJ (Schindelin et al., 2012; Schneider et al., 2012) on raw images.

2.3.8.1 Counting and classification of cells

For counting of cells showing H2B S6ph positive cells, samples were analysed in a blinded manner. Cells were classified as positive or negative for H2B S6ph or other PTMs if they showed a clearly distinct staining above background signal. Mitotic phases were morphologically classified. Early and late anaphases were distinguished based on the distance between the anaphase plates. A clearly separate gap with no overlap between chromosome arms was classified as late anaphase (Vukušić et al., 2021). Telophases were distinguished from them by beginning decondensation, a rounding of the anaphase plates around the spindle pole or a clearly defined cleavage furrow.

2.3.9 Flow cytometry

PI staining solution:	0.1 % (v/v) Triton X-100, 200 µg/mL RNase A, 20 µg/mL propidium iodide, PBS
FACS sorting buffer:	1 mM EDTA, 1 % (w/v) BSA, PBS
Conditioned medium:	50 % (v/v) used culture medium; 40 % (v/v) fresh culture medium; 10 % (v/v) additional FCS

For non-sorting cytometry, cells were trypsinised until fully detached and resuspended in PBS. Cells were collected by centrifugation at 300 rcf for 5 min. Cells were washed once in PBS and centrifuged again. The cells were fixed by adding 70 % (v/v) ethanol dropwise while vortexing to avoid cell clumping. Cells were then incubated for at least 1 h at −20 °C.

For cell cycle analysis, cells were washed with PBS twice and resuspended in PI staining solution and incubated for 15 min at 37 °C, put on ice and immediately analysed for DNA content. Cells were analysed on a BD FACSCalibur (2-laser, 4-colour) and gated based on SSC and FSC, singlets were gated by FL2-A and FL-2W and ultimately DNA content was analysed from FL-2A signal.

For immediate GFP only analysis, fixation was skipped and cells were only collected, washed, and immediately analysed. For later analysis of GFP, cells were fixed but not PI stained.

2.3.9.1 Live cell sorting

For live cell sorting cells were trypsinised with TrypLE until they were fully detached, resuspended in cold PBS and collected by centrifugation at 300 rcf for 5 min at 4 °C. Cell pellets were then resuspended in cold FACS sorting buffer and kept cool during transport to sorter. Prior to sort, cells were resuspended, filtered through a nylon mesh and dead cells were stained with 0.1 µg/µL propidium-iodide. Cells were sorted with a 3-laser (BGR, 8-colour, 2-2-4) BD FACSMelody cell sorter and a 100 µm nozzle. Cells were chilled to 4 °C during sort. Single cells were gated with SSC and FSC, live cells were gated with PI staining and positive cells were gated in the GFP channel. Up to 1×10^6 cells were sorted into a FACS tube with cold FCS. After sorting cells were centrifuged and plated in sterile filtered conditioned medium to recover. On the following day medium was exchanged back to fresh culture medium or renewed to sterile filtered conditioned medium for further recovery depending on cell morphology. To verify sort, recovered cell pools were subjected to post-sort analysis via flow cytometry.

2.3.10 Crystal Violet cell survival staining

Staining solution: 0.5 % (w/v) crystal violet, 25 % (v/v) methanol, H_2O
Destaining solution: 2 % (w/v) SDS, H_2O

Culture medium was discarded, and cells were washed once in cold PBS. Cells were fixed with ice-cold methanol for 10 min at room temperature. Cells were then stained with staining solution for 10 min at room temperature (Saotome et al., 1989). After that, cells were rinsed with tap water until no more crystal violet came off. Cells were then dried at room-temperature or at 37 °C. Crystal violet was solubilised with destaining solution for 30 min at room temperature on an orbital shaker at 500 rpm. Absorbance at 600 nm was measured on a plate reader.

2.4 Methods in Biochemistry

2.4.1 GFP-Trap

NP-40 lysis buffer: 20 mM Tris-HCl (pH 7.5); 150 mM NaCl; 10 % (v/v) glycerol, 1 % (v/v) IGEPAL C-630
GFP-Trap Dilution/Wash buffer: 10 mM Tris-HCl (pH 7.5); 150 mM NaCl; 0.5 mM EDTA

Cells were harvested like for whole cell lysis (see 2.3.6) but resuspended in NP-40 lysis buffer. For GFP-Trap of nuclear proteins, lysis buffer was supplemented with 2 mM $MgCl_2$ and 5 U MNase. 200 µL of cell lysate was diluted with dilution buffer to 1 mL. 20 µL of washed GFP-Trap agarose beads were added and samples were rotated for 4 h at 4 °C. Beads were sedimented at 2700 rcf for 5 min at 4 °C and washed 3 times with 500 µL of wash buffer. Beads were resuspended in 50 µL of 1.25X SDS sample buffer (see 2.3.6).

2.4.2 SDS polyacrylamide gel electrophoresis

SDS running buffer: 25 mM Tris; 192 mM glycine; 0.1 % (w/v) SDS
4X Lower buffer: 1.5 M Tris-HCl (pH 8.8); 0.4 % (w/v) SDS
4X Upper buffer: 500 mM Tris-HCl (pH 6.8); 0.4 % (w/v) SDS
Separating gel: 7 to 20 % (w/v) acrylamide/bis-acrylamide; 25 % (v/v) lower buffer; 0.75 % (v/v) APS; 0.1 % (v/v) TEMED
Stacking gel: 4 % (w/v) acrylamide/bis-acrylamide; 25 % (v/v) upper buffer; 1 % (v/v) APS; 0.2 % (v/v) TEMED

SDS-PAGE was performed as described by Laemmli (1970). Denaturing acrylamide gels were freshly prepared with Bio-Rad casting stands, 1.5 mm glass plates and combs. Acrylamide contents between 7 % and 20 % were chosen depending on the size of the proteins of interest. Separating gels were prepared with acrylamide and lower buffer, stacking gels with upper buffer. Samples were prepared as described in 2.3.6 and between 10 and 30 µg protein were loaded into each well. Gels were run with SDS electrophoresis buffer at a constant voltage of 80 V for around 15 min until the ladder had started to separate in the lower gel. Gels were then run at 100 to 130 V until separation was sufficient.

2.4.3 Coomassie staining

Coomassie staining solution: 0.25 % (w/v) Coomassie Brilliant Blue R-250; 45 % (v/v) methanol; 10 % (v/v) acetic acid; H_2O
Strong destaining solution: 30 % (v/v) methanol; 20 % (v/v) acetic acid; H_2O
Weak destaining solution: 20 % (v/v) methanol; 10 % (v/v) acetic acid; H_2O

For protein staining in gels, the gels were covered in Coomassie staining solution and stained for around 15 min. Then gels were rinsed in weak destaining solution to remove excess staining solution. Gels were then destained for around 1 h twice and then overnight in weak destaining solution. Gels were then imaged on a light-box or a transillumination scanner.

2.4.4 Western blotting

Transferbuffer: 50 mM Tris; 40 mM glycine; 20 % (v/v) methanol; 0.04 % (w/v) SDS
TBS-T: 25 mM Tris (pH 7.4); 137 mM NaCl; 5 mM KCl; 0.7 mM $CaCl_2$; 0.1 mM $MgCl_2$; 0.1 % (v/v) Tween 20
Ponceau S solution: 0.1 % (w/v) Ponceau S; 0.5 % (v/v) acetic acid
Blocking solution: 5 % (w/v) skimmed-milk powder in TBS-T
1st antibody solution: 1 % (w/v) skimmed-milk powder in TBS-T; 0.1 % (w/v) NaN_3
2nd antibody solution: 1 % (w/v) skimmed-milk powder in TBS-T

For immuno-detection of proteins and their modifications, proteins separated via SDS-PAGE (2.4.2) were blotted onto PVDF membranes. Blots were prepared in a stack of 2 Whatman papers, a methanol activated membrane, the gel and another Whatman paper soaked thoroughly in transfer buffer according to Bjerrum et al. (1986). Blots were assembled in Bio-Rad semi-dry blotting chambers. Blots were run at a constant voltage of 25 V first and then at a constant current of 100 mA per membrane for 2.25 h. After transfer, membranes were rinsed once in TBS-T and then

blocked with blocking solution. If necessary, membranes were stained with Ponceau S staining solution to verify transfer before the incubation in primary antibody. Membranes were transferred to the appropriate primary antibodies and incubated overnight at 4 °C. Membranes were rinsed briefly in TBS-T and then washed in TBS-T for 10 min twice. Membranes were transferred to secondary antibodies and incubated for 1 h at room temperature. Membranes were again rinsed and washed 3 times in TBS-T. Membranes were analysed on a ChemiDoc Touch with Perkin Elmer ECL or stronger Immobilon Ultra ECL solution depending on signal intensity.
Images were analysed and edited in ImageLab and FIJI/ImageJ. Only uniform, linear brightness and contrast adjustments were used. For blot quantification only unaltered, correctly exposed raw images were used. Quantifications were performed with the ImageJ gel analysis tool.

2.4.5 Enzyme-linked immunosorbent assay (ELISA)

ELISA wash buffer:	0.1 % (w/v) BSA; TBS-T
Substrate solution:	110 mM sodium-acetate (pH 5.5); 0.1 % (v/v) H_2O_2; 0.06 µg/mL TMB
Stop solution:	10 % (v/v) sulfuric acid

NeutrAvidin coated 96-well plates were washed with 200 µL ELISA wash buffer 3 times. Wells were coated with 10 µg biotynilated peptide (subsection 2.1.10) per well for 2 h at room temperature. Wells were washed 3 times. 100 µL primary antibodies, diluted in wash buffer, were added and incubated for 20 min at room temperature. Wells were again washed 3 times, and 100 µL secondary antibody diluted in wash buffer was added for 20 min. Wells were washed 3 times and 100 µL substrate solution was added for 5 min. Reaction was stopped by addition of 100 µL stop buffer. Absorbance was measured at 450 nm on a plate reader.

2.5 Statistical analysis

Statistical analyses were performed using GraphPad Prism using appropriate statistical tests with recommended corrections for the dataset. Experiments were performed in 3 technical and/or biological replicates unless otherwise noted. P-values are abbreviated with asterisks in figures as following: * $p<0.05$, ** $p<0.01$, *** $p<0.001$.

3 Regulation and pathophysiology of H2B Serine 6 phosphorylation

---

Parts of the results presented in this chapter have been accepted for publication in:
Pfisterer M, Robert R, Saul VV, Pritz A, et al. (2024)
"The Aurora B-controlled PP1/RepoMan complex determines the spatial and temporal distribution of mitotic H2B S6 phosphorylation"
Open Biology, doi: 10.1098/rsob.230460

Previous studies from this laboratory have shown that histone H2B Serine 6 is phosphorylated at the inner centromere specifically during mitosis (Seibert et al., 2019). While the writer, eraser and reader of this modification were identified, the molecular mechanisms governing the spatial and temporal regulation of this modification have not yet been understood. To understand the functional significance and relevance of H2B S6ph, a thorough understanding of its regulation is essential.

3.1 Validation of a new monoclonal antibody against H2B S6ph

As most methods for the detection of amino acid modifications are based on antibodies, highly specific antibodies are required. In previous studies, a polyclonal rabbit antibody was used for the detection of H2B S6ph. For higher specificity, reproducibility and easier co-staining in immunofluorescence, a new rat monoclonal antibody was raised against a peptide corresponding to the amino acids 1-11 of histone H2B with a phosphorylated serine 6. Briefly, in collaboration with Dr. Regina Feederle (Helmholtz Center Munich), rats were immunised with the peptide and antibody producing hybridoma cell clones were established and screened via ELISA. Supernatants of positive clones were tested by Western blotting (Markus Seibert, unpublished). This resulted in the H2B S6ph monoclonal antibody 1D4. As cross-reactivity between different histone PTMs is a common problem, even with monoclonal antibodies (Bock et al., 2011; Egelhofer et al., 2011), further experiments for the validation of sensitivity and specificity of this new antibody were performed.

In order to evaluate the specificity, whole cell lysates of cells arrested in mitosis or treated with calyculin A were analysed by Western blotting using the new monoclonal antibody 1D4.

Figure 8A shows that the antibody recognised only one band of the correct size (approximately 15 kDa) in mitotic extracts, but not in unsynchronised extracts. Upon treatment of mitotic cells with the phosphatase inhibitor calyculin A, this signal was strongly increased. Importantly, there was no apparent increase in unspecific signal. Minor unspecific bands were detected at approximately 35 kDa and 70 kDa, but these were also present in unsynchronised cells (Figure 8A) and were therefore not specific for mitosis.

Serine 6 of H2B is surrounded by a 5 amino acid sequence (KSAPA) which is also present in the N-terminal tail of histone H3 surrounding serine 28 (Figure 8B). As such, validation of the specificity of the 1D4 monoclonal antibody towards H2B S6ph is of high importance for all subsequent experiments.

To test whether the 1D4 monoclonal antibody cross-reacts with H3 S28ph, the histone phosphomutants H2B S6A and S6E as well as H3 S28A and S28E were created. Phospho-specific antibodies should not detect the A mutant while they often react with the phosphomimetic E mutant. HEK293T cells were transfected with plasmids expressing these histone mutants and cell extracts were analysed via Western blotting and staining with 1D4 antibody. This revealed the specific detection of H2B S6E but not H3S 28E (Figure 8C).

To further validate this with a more quantitative approach, a peptide ELISA was performed to exclude H3 S28ph as a potential cross-reactive PTM for this antibody. Peptides corresponding to the amino acids 1-20 of histone H2B and amino acids 18-37 of histone H3 in either phosphorylated or unphosphorylated form were used. Probing these peptides with 1D4 antibody revealed that it recognised H2B S6ph with high affinity as seen by binding of highly diluted antibodies (Figure 8D). Crucially, while the sequence surrounding S6 on H2B and S28 on H3 is very similar, the antibody recognised H3 S28ph only to a minor extent even in low dilutions.

Together, these data indicate that the monoclonal 1D4 antibody shows high sensitivity and specificity towards H2B S6ph. While cross-reactivity towards other PTMs cannot be formally excluded, recognition of a different amino acid sequence by this monoclonal antibody is highly unlikely (Frank, 2002, Chapter 4).

3.2 PP1α and PP1γ dephosphorylate H2B Serine 6

Previous studies have shown that PP1 protein phosphatase contributes to the dephosphorylation of H2B S6ph after anaphase onset (Seibert et al., 2019). As PP1 in its active form is a protein complex of one of 3 different catalytic and at least one regulatory subunit (Peti et al., 2013), it was important to identify which PP1 subunit(s) contribute to H2B S6ph dephosphorylation.

For that purpose, an *in vitro* kinase and phosphatase assay was performed. Recombinant H2B was *in vitro* phosphorylated by recombinant CDK1/cyclin B and then subjected to dephosphorylation

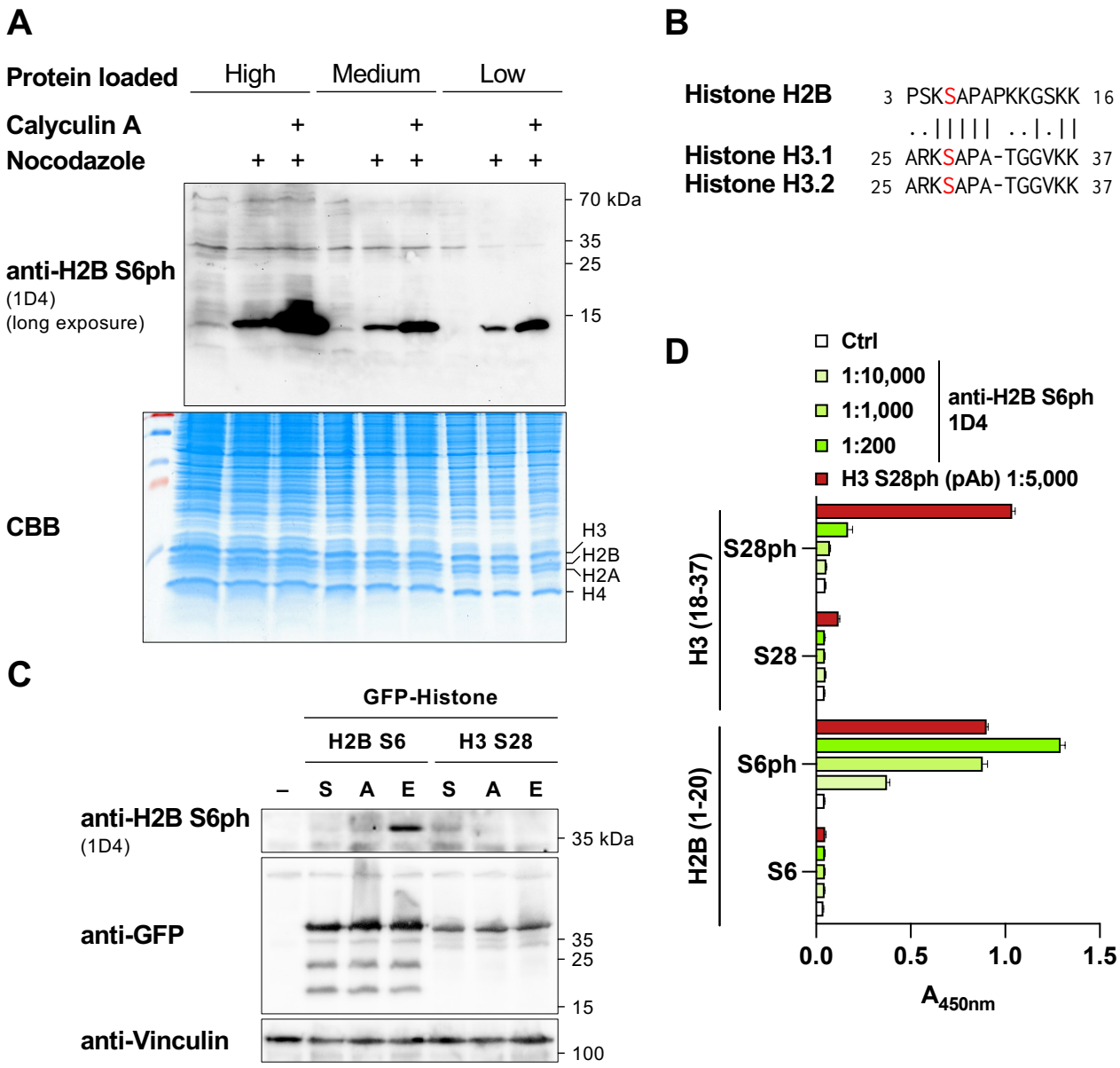

Figure 8: 1D4 monoclonal antibody specifically recognises H2B S6ph.

(A) HEK293T cells were treated with calyculin A (30 min, 50 nM) to enrich phosphorylations and/or nocodazole (16 h, 100 ng/mL) to arrest cells in mitosis. Whole cell extracts were analysed via high resolution SDS-PAGE and Western blotting and probed with 1D4 H2B S6ph antibody. The positions of molecular weight markers are indicated. The lower parts shows a Coomassie (CBB) stained gel. **(B)** Serine 6 of H2B and serine 28 of H3 share a similar motif. H2B, H3.1 and H3.2 were aligned with EMBOSS Water (Madeira et al., 2022). The phosphorylated residues are shown in red. **(C)** H2B serine 6 and H3 serine 28 mutants were expressed in HEK293T cells. Samples were analysed via Western blot and stained with the 1D4 H2B S6ph antibody after Western blotting. **(D)** Peptides corresponding to the amino acids 1-20 and 18-37 of H2B and H3, respectively, with unphosphorylated and phosphorylated serine 6 or 28 were coated onto Strepatvidin plates. An ELISA experiment was performed using the indicated dilutions of the 1D4 antibody. Data from 3 technical replicates are shown as means ± SD.

by either recombinant PP1α, PP1β or PP1γ. Detection of H2B S6ph by Western blotting showed that while PP1α and PP1γ exerted phosphatase activity on H2B S6ph, PP1β did not (Figure 9).

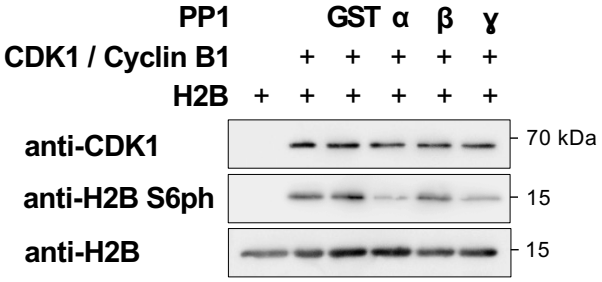

Figure 9: PP1α and PP1γ dephosphorylate H2B *in vitro*.
Recombinant H2B was *in vitro* phosphorylated with recombinant CDK1/cyclin B. Phosphorylated H2B was used as a substrate for dephosphorylation by recombinant PP1α, β or γ or GST as a control. Reactions were analysed via Western blotting for phosphorylation of H2B S6 as shown.

To substantiate the selective contribution of these two PP1 subunits for H2B S6ph dephosphorylation in cells, knock-down experiments targeting these subunits were performed. For these experiments, the colon cancer cell line HCT116 was chosen, as it is characterised by high genomic stability (Camps et al., 2005) and thus frequently used in mitosis research (Varmark et al., 2009; Rello-Varona et al., 2010).
HCT116 cells were transfected with siRNAs targeting PP1α or PP1γ or with an unspecific siRNA as a control. siRNA transfected cells were synchronised with a single thymidine block overnight and released for 10 h to enrich cells in mitosis for microscopic analysis (Figure 10A). Staining of H2B S6ph revealed that only approximately 20 % of untransfected (not shown) or control transfected HCT116 cells showed H2B S6ph in late anaphase (Figure 10B and C), in line with previous results (Seibert et al., 2019). After knock-down of PP1α or PP1γ, approximately 50 % of cells showed H2B S6ph in late anaphase (Figure 10B and C), indicating their involvement in H2B S6ph dephosphorylation. Combined knock-down of both PP1α and PP1γ together yielded a further increase in H2B S6ph positive late anaphase cells to approximately 70 % (Figure 10C). This additive effect suggests that both subunits are capable of dephosphorylating H2B S6ph independently.

Knock-down experiments against PP1β were performed without an apparent effect on H2B S6ph during anaphase, however these experiments remained inconclusive as knock-down efficiencies for PP1β were too low to be reliable (data not shown).

3.3 RepoMan targets PP1 to dephosphorylate H2B S6ph

It is well established that PP1 enzymes gain their substrate specificity by interaction with targeting factors that bind PP1 via its short linear interaction motif (SLiM) and target it to its substrate (Hubbard et al., 1993; Brautigan et al., 2018) or by direct interaction with a SLiM containing

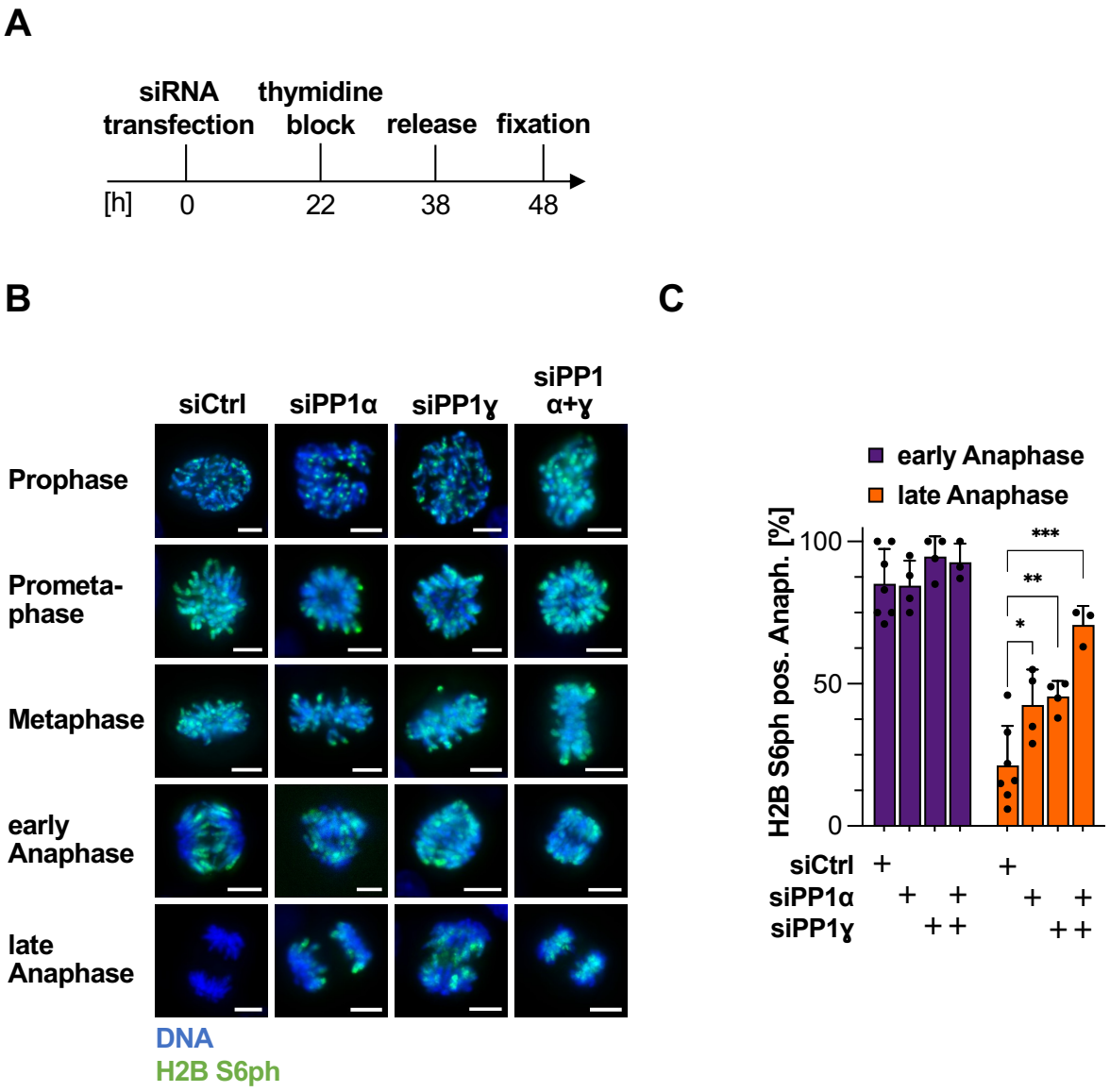

Figure 10: PP1α and PP1γ dephosphorylate H2B S6ph in cells.

(A) Schematic representation of experimental setup. HCT116 cells were transfected with siRNAs against the indicated mRNAs and further grown until cells were subjected to thymidine block for 16 h and released for 10 h to enrich mitotic cells. **(B)** HCT116 cells were transfected with the indicated siRNAs as shown in (A). After 48 h cells were fixed and stained for H2B S6ph using immunofluorescence. Representative images of mitotic cells are shown. Scale bar = 10 µm. **(C)** Mitotic figures as shown in (B) were scored as H2B S6ph positive or negative and classified for their mitotic phase. Data from 3 independent biological replicates are shown as means ± SD, individual data points are displayed as black dots. Data were statistically analysed with two-way ANOVA with Tukey's multiple comparisons correction. * $p<0.05$, ** $p<0.01$, *** $p<0.001$.

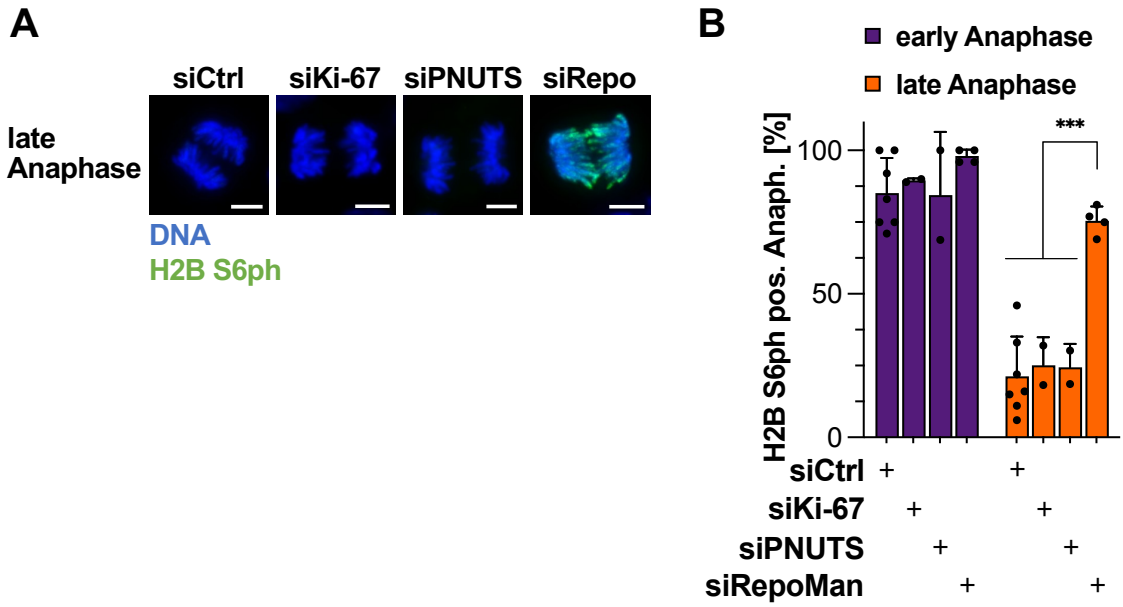

Figure 11: RepoMan is required for dephosphorylation of H2B S6ph.

(A) HCT116 cells were transfected with the indicated siRNAs and further grown until cells were subjected to thymidine block for 16 h and released for 10 h to enrich mitotic cells. Cells were fixed and stained for H2B S6ph using immunofluorescence. Representative images of anaphase cells are shown. Scale bar = 10 µm. **(B)** Cells from (A) were scored for their H2B S6ph staining in early or late anaphase. Means from 3 independent biological replicates are shown as means ± SD. Data were statistically analysed with two-way ANOVA with Tukey's multiple comparisons correction. * $p<0.05$, ** $p<0.01$, *** $p<0.001$.

substrate (Vietri et al., 2006). Different chromatin targeting factors serve to regulate PP1 activity during mitosis. These include PNUTS, RepoMan and the proliferation marker Ki-67 (Allen et al., 1998; Trinkle-Mulcahy et al., 2006; Bollen et al., 2010; Booth et al., 2014).

To test whether one of these targeting factors is responsible to target PP1 to dephosphorylate H2B S6ph after anaphase onset, knock-down experiments against these targeting factors were performed. HCT116 cells were transfected with siRNAs against the mentioned targeting factors and subjected to a single thymidine block and release. After 2 days, mitotic cells were analysed for the presence of H2B S6ph in late anaphase cells by immunofluorescence (Figure 10A). Microscopic analysis of late anaphase cells showed that only RepoMan knock-down increased the number of H2B S6ph positive late anaphase cells to approximately 70 % (Figure 11A and B). When combining the knock-down of PP1 catalytic subunits and RepoMan, the number of H2B S6ph positive late anaphases was not increased further (Figure 12A and B).

Under normal conditions, H2B S6ph shows a characteristic centromeric localisation throughout mitosis. When PP1 activity is inhibited, H2B S6ph spreads along the chromosome axis (Seibert et al., 2019). As the dephosphorylation of H2B S6ph was delayed when depleting either PP1α or

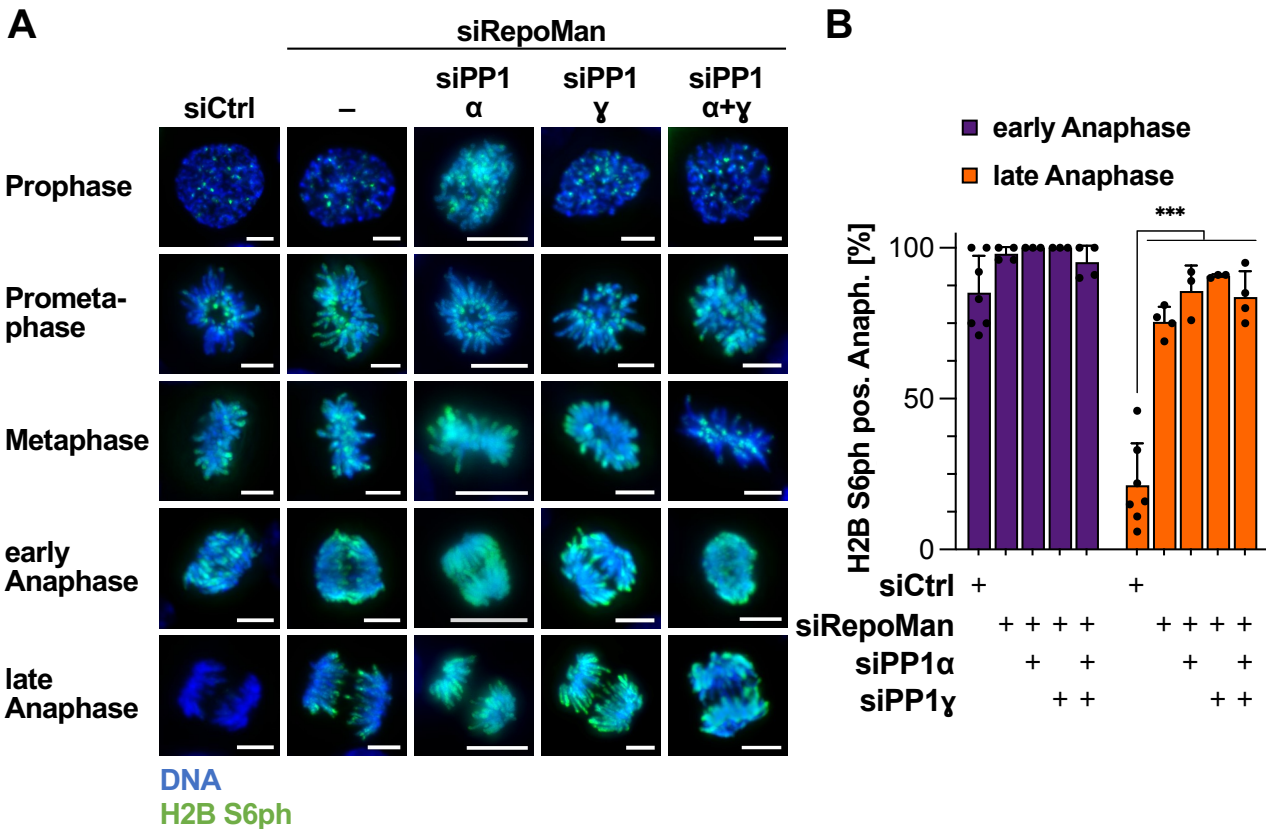

Figure 12: PP1/RepoMan dephosphorylates H2B S6ph.

(A) HCT116 cells were transfected with the indicated siRNAs and further grown until cells were subjected to thymidine block for 16 h and released for 10 h to enrich mitotic cells. Cells were fixed and stained for H2B S6ph using immunofluorescence. Representative images of mitotic cells are shown. Scale bar = 10 µm. **(B)** Cells from (A) were scored for their H2B S6ph staining and classified for their mitotic state. Means from 3 independent biological replicates are shown as means ± SD. Data were statistically analysed with two-way ANOVA with Tukey's multiple comparisons correction. * $p<0.05$, ** $p<0.01$, *** $p<0.001$.

PP1γ levels, it was interesting to see wether the knock-down of PP1 subunits also affects the spatial regulation of H2B S6ph.

To test this, chromosome spreads of cells transfected with siRNAs targeting PP1 and/or RepoMan were prepared. Figure 13A and B show that in control siRNA transfected cells, H2B S6ph was restricted to the inner centromere as previously described. After knock-down of only a single catalytic PP1 subunit, H2B S6ph did not spread along the chromosome axis (Figure 13A and B). In contrast, the knock-down of RepoMan led to spreading of the phosphorylation along to the entire chromosome (Figure 13A and B), together with an overall increase in H2B S6ph intensity (Figure 13C). Similar results were obtained after a combined knock-down of both PP1α and PP1γ together with RepoMan.

As RepoMan is most commonly described to be an interactor of PP1γ rather than PP1α (Trinkle-Mulcahy et al., 2006), it was relevant to examine whether RepoMan interacts with PP1α. Therefor,

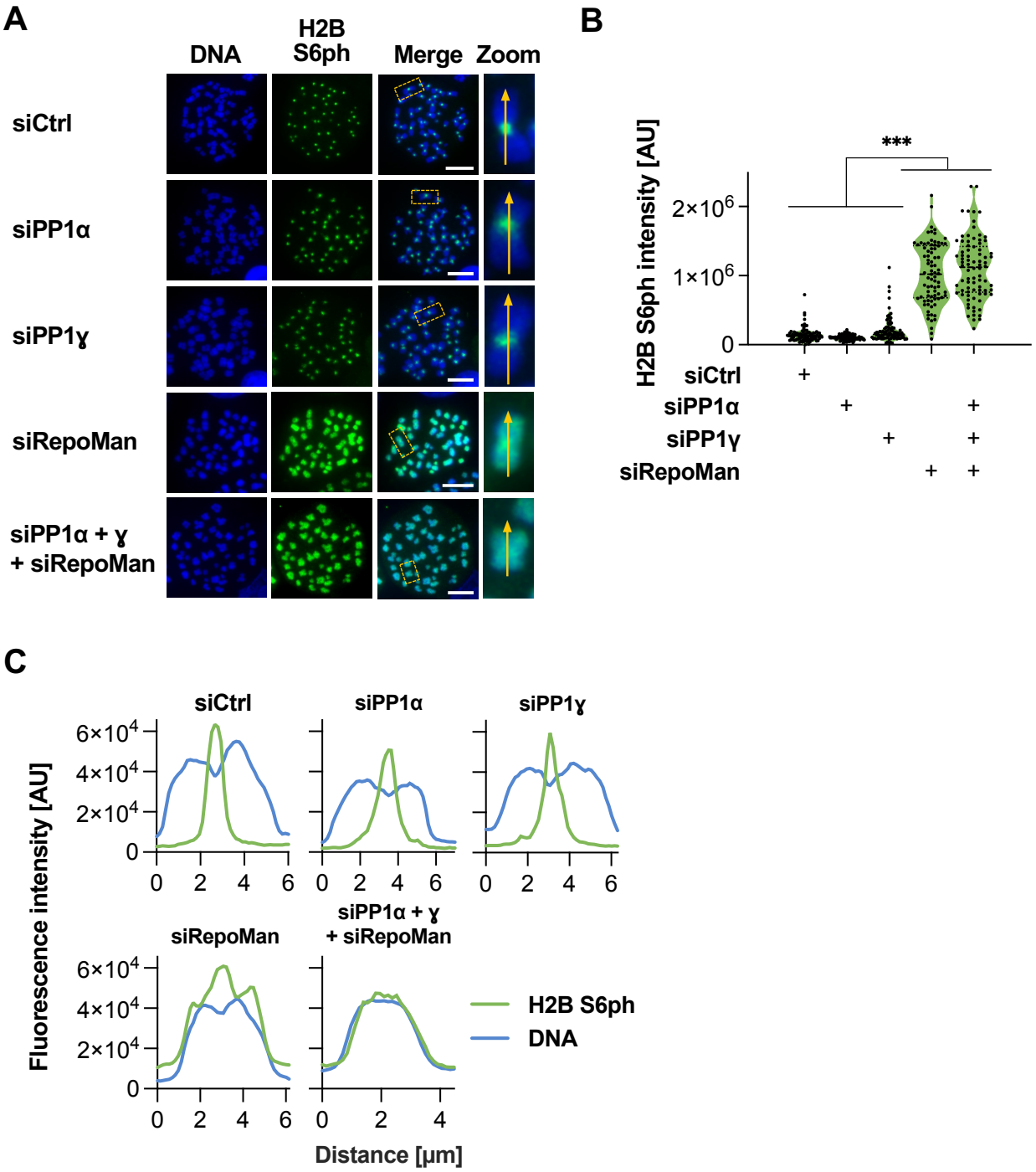

Figure 13: PP1/RepoMan is essential for spatial restriction of H2B S6ph.

(A) HCT116 cells were transfected with the indicated siRNAs and after 48 h cells were arrested in mitosis with nocodazole (100 ng/mL, 16 h). Chromosome spreads were prepared and stained for H2B S6ph. Representative images are shown. Scale bar = 10 µm. **(B)** Staining intensities of DNA and H2B S6ph along the chromosome axis from chromosomes shown in (A) were quantified. Data were statistically analysed with one-way ANOVA and Dunnett multiple comparisons correction. * $p<0.05$, ** $p<0.01$, *** $p<0.001$. **(C)** H2B S6ph intensities from chromosomes shown in (A) were measured with ImageJ.

a semi-endogenous co-immunoprecipitation of RepoMan was performed. HEK293T cells were transfected with plasmids expressing EGFP or EGFP-RepoMan. Whole cell lysates were prepared and used for GFP-Trap to pull down RepoMan. Subsequent Western blotting of the pulldowns revealed that both PP1α and PP1γ co-precipitated together with EGFP-RepoMan (Figure 14A). Quantification of the pulldown efficiency revealed that approximately 5 times more PP1γ was precipitated along with RepoMan than PP1α (Figure 14B). This value is largely in line with previous studies reporting a 3:1 ratio (Trinkle-Mulcahy et al., 2006).

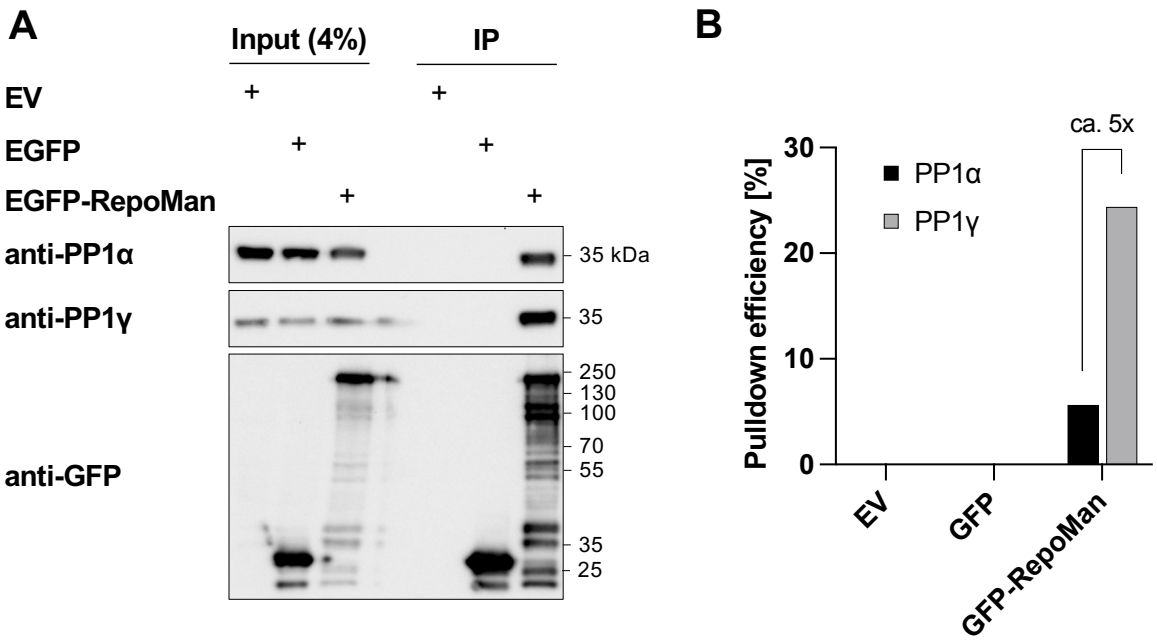

Figure 14: RepoMan interacts with both PP1α and PP1γ.

(A) HEK293T cells were transfected with the indicated plasmids. Cells were then lysed and GFP was immunoprecipitated with GFP-Trap beads. Input and pulldowns were analysed via Western blotting for association of PP1α and γ. **(B)** Pulldown efficiencies for PP1α and PP1γ were quantified from the blots shown in (A) by comparing the signal after IP with the input.

Together these data suggest that RepoMan in association with PP1α and PP1γ works to dephosphorylate H2B S6ph. While the involvement of other PP1 regulatory subunits cannot be excluded, RepoMan can be assumed to be a key regulatory factor in the regulation of H2B S6ph.

3.4 Aurora B maintains centromeric H2B S6ph until Anaphase

While CDK1 directly phosphorylates H2B S6ph, Aurora B kinase activity was previously shown to be essential for the maintenance of H2B S6ph (Seibert et al., 2019). Aurora B is a known regulator of both RepoMan and PP1 (Manzione et al., 2020; Xin et al., 2020). As such it is possible that Aurora B, which is normally located at the inner centromere until anaphase, locally inhibits RepoMan and PP1 to protect H2B S6ph from phosphatase activity.

To test this possibility, a tethering approach was chosen by which Aurora B was covalently linked to H2B, allowing the anchoring of Aurora B outside of the centromeres, as schematically shown in Figure 15A. For this, plasmids expressing fusion proteins of H2B-EGFP and Aurora B wt as well as kinase-deficient point mutant Aurora B (Aurora B KD) were cloned.

HCT116 cells were transiently transfected with these plasmids or an empty H2B-EGFP control plasmid. Chromosome spreads were prepared and stained for H2B S6ph. Chromosomes from cells expressing the control plasmid showed an EGFP signal on the chromosome arms, while H2B S6ph was still restricted to centromeres (Figure 15B). Chromosomes from cells expressing the H2B-EGFP-Aurora B wt fusion protein showed spreading of H2B S6ph to the chromosome arms (Figure 15B). This was dependent on Aurora B kinase activity, as expression of a kinase-deficient Aurora B fusion protein did not lead to spreading. Additionally, inhibition of Aurora B with the small molecule inhibitor AZD1152 lead to the complete loss of both distal and centromeric H2B S6ph.

In order to substantiate this finding in a setting where Aurora B is not covalently bound to chromatin, a a plasmid expressing a fusion protein of H2B-EGFP and Aurora B's binding partner INCENP lacking the centromere binding domain (Δcen) was cloned in order to non-covalently recruit Aurora B. Transfection of cells with this plasmid led to the anchoring of INCENPΔcen to chromatin and the subsequent recruitment of Aurora B (Figure 15C). This resulted in spreading of H2B S6ph to distal chromatin, which also was dependent on Aurora B kinase activity (Figure 15C).

Together, these results are in line with a model in which Aurora B kinase activity locally maintains H2B S6ph at the centromere due to its inhibitory effect on PP1/RepoMan.

3.5 PP1/RepoMan/Chromatin interaction is controlled by Aurora B

A mechanism by which Aurora B inhibits PP1/RepoMan function was described by previous studies (Qian et al., 2011, 2013). RepoMan is known to harbour multiple Aurora B target sites in the chromatin binding domain as well as PP1 binding domain of the protein. These phosphorylations control the binding of PP1 to RepoMan and RepoMan to the chromatin (Qian et al., 2013; Xin et al., 2020).

To investigate whether these Aurora B mediated modifications are also important for the regulation of H2B S6ph, mutants of the conserved PP1 SLiM RVxF, as well as mutants of the chromatin binding domain at the C-terminus of RepoMan were created. (Figure 16A). To allow for the expression of these mutants in the absence of endogenous wildtype RepoMan, HCT116 cells were co-transfected with siRNAs targeting endogenous RepoMan together with siRNA resistant RepoMan wt or mutants. HCT116 cells were transfected, stained for H2B S6ph and anaphases were microscopically analysed for the presence of H2B S6ph.

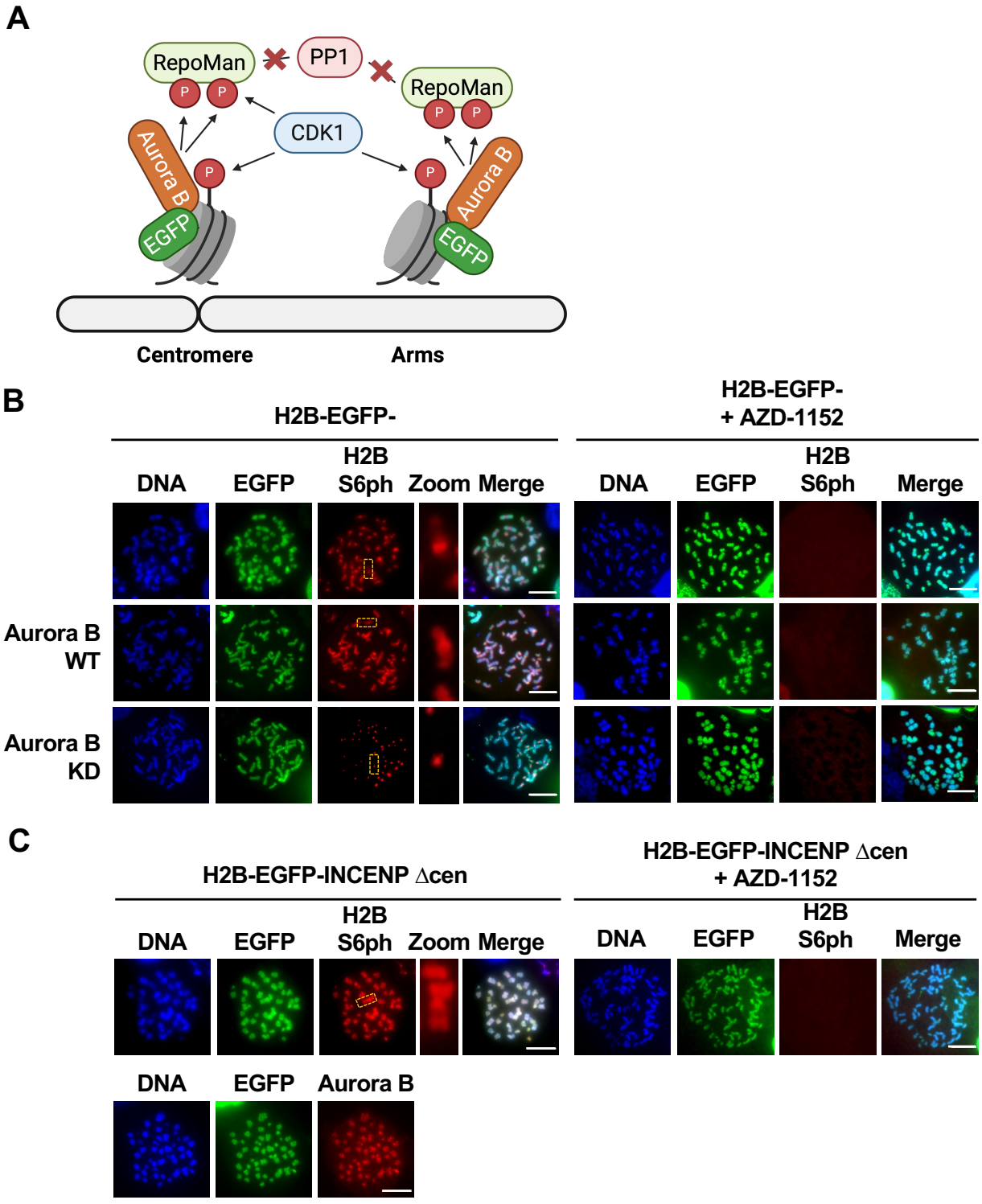

Figure 15: Aurora B maintains H2B S6ph on chromatin.

Caption is continued on page 66 .

Figure 15 (cont.): Aurora B maintains H2B S6ph on chromatin.

(A) Schematic representation of the experimental setup. Aurora B is tethered to chromatin via fusion to H2B and therefore inhibits PP1 activity along the entire chromosome. *Created with biorender.com* **(B)** HCT116 cells were transfected with H2B-EGFP, H2B-EGFP-Aurora B wt or H2B-EGFP-Aurora B KD plasmids. Mitotic chromosome spreads were prepared and stained for H2B S6ph. Cells were also transfected and treated with Aurora B inhibitor AZD1152 (1 µM, 30 min) before preparing spreads. Scale bar = 10 µm. **(C)** HCT116 cells were transfected with H2B-EGFP-INCENPΔcen. Mitotic chromosome spreads were prepared and stained for H2B S6ph or Aurora B. Cells were also transfected and treated with Aurora B inhibitor AZD1152 (1 µM, 30 min) before preparing the spreads. Scale bar = 10 µm.

Cells transfected with siRNAs against RepoMan but without re-expression of RepoMan showed the previously described (section 3.3) increase in late anaphase H2B S6ph positive cells (Figure 16A and B). This effect was fully rescued by the re-expression of an siRNA resistant wildtype EGFP-RepoMan. Expression of a PP1 binding deficient mutant (RATA) did not rescue the knock-down mediated increase in anaphase H2B S6ph positive cells, indicating that PP1/RepoMan binding is crucial for the dephosphorylation of H2B S6ph. Mutation of the PP1 binding site T394 to a phosphomimetic T394D showed a similar increase in late anaphase H2B S6ph, as the phosphorylation of the PP1 binding site reduces the binding of PP1 (Kumar et al., 2016) (Figure 16E). In contrast, phosphomutant RepoMan T394A was proficient in H2B S6ph dephosphorylation as it also rescued the effect of RepoMan knock-down (Figure 16A and B).

Mutation of S893 of the chromatin binding site to a phosphomimetic S893D, which should reduce binding of RepoMan to chromatin (Qian et al., 2013), increased the number of late anaphases with H2B S6ph. A truncation mutant of RepoMan lacking the chromatin binding domain (RepoManΔC) was also not able to facilitate dephosphorylation of H2B S6ph (Figure 16C and D).

3.6 H2B S6ph dephosphorylation is delayed in some cancer cell lines

H2B S6ph has been previously implicated with mitotic fidelity (Seibert et al., 2019). As the factors regulating spatial and temporal distribution of H2B S6ph, such as RepoMan and Aurora B, are known to be deregulated in some cancers (Manzione et al., 2020), it was interesting to evaluate whether cancer cell lines, especially those featuring chromosomal instability, showed any abnormal H2B S6ph staining in mitotic cells.

For this, a panel of 10 different cell lines, including the non-cancerous retinal epithelial cell line RPE-1, the colorectal carcinoma lines HCT116 and HT-29 and the osteosarcoma line U2OS, was screened for H2B S6ph in mitosis. This panel intentionally included near diploid cancerous cells like HCT116 as well as chromosomally unstable cell lines like the hyper-pentaploid T98G cells. Cells were analysed for the occurrence of H2B S6phph via immunofluorescence microscopy. Mitotic

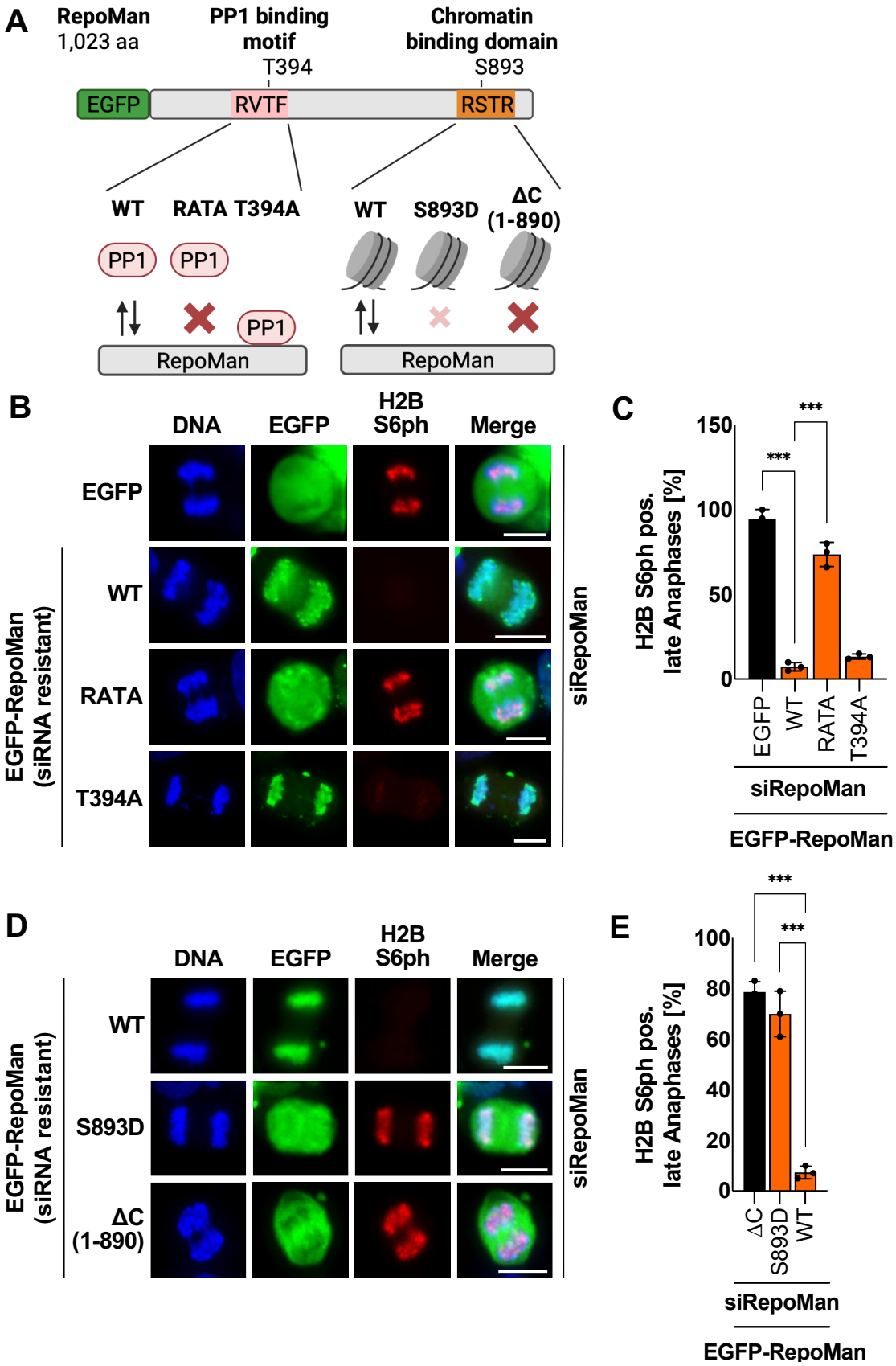

Figure 16: RepoMan mutants influence H2B S6ph dephosphorylation.

Caption is continued on page 68 .

Figure 16 (cont.): RepoMan mutants influence H2B S6ph dephosphorylation.

(A) Overview of the proposed effect of the RepoMan mutants used in the experiment. *Created with biorender.com* **(B)** HCT116 cells were transfected with an siRNA targeting the endogenous RepoMan and plasmids coding for the indicated siRNA resistant RepoMan PP1 binding mutants. Cells were stained for H2B S6ph using immunofluorescence. Representative images are shown. Scale bar = 10 µm. **(C)** The experiment shown in (B) was quantified for the occurrence of H2B S6ph in late anaphase cells. **(D)** HCT116 cells were transfected with an siRNA targeting the endogenous RepoMan and plasmids coding for the indicated siRNA resistant RepoMan chromatin binding mutants. Cells were stained for H2B S6ph using immunofluorescence. Mitotic cells were imaged, representative images are shown. Scale bar = 10 µm. **(E)** The experiment shown in (D) was quantified for the occurrence of H2B S6ph in late anaphase cells. **(C and E)** Data from 3 independent biological replicates are shown as means ± SD, individual data points are displayed as black dots. Data was statistically analysed with one-way ANOVA and Dunnett multiple comparisons correction. * $p<0.05$, ** $p<0.01$, *** $p<0.001$.

figures were classified into mitotic stages and scored for their H2B S6ph signal. This revealed that 60 % of HT-29 and U2OS cells showed H2B S6ph during late anaphase, while the majority of HCT116 cells showed no phosphorylation. Other tested cell lines did not differ significantly from HCT116 cells in this regard (Figure 17A and B). Interestingly, there was no apparent correlation between the number of H2B S6ph positive late anaphase cells and CIN (not shown). However, aberrant mitotic figures like anaphase bridges or lagging chromosomes were often still decorated with H2B S6ph, even though bulk chromatin was negative for H2B S6ph (Figure 17B and C).

With the regulatory network responsible for the timely dephosphorylation of H2B S6ph identified, it was interesting to investigate whether the cell lines displaying delayed dephosphorylation of H2B showed any differences in the regulation by RepoMan or Aurora B.

First, RepoMan binding to chromatin was analysed by staining of RepoMan and H2B S6ph in HCT116, U2OS, HT-29 and RPE-1 cells. This revealed that regardless of the H2B phosphorylation status, RepoMan was always located on chromatin in late anaphases (data not shown). This suggests that the previously observed effects are independent from correct chromatin localisation of RepoMan but rather caused by PP1 or any of its regulators.

As Aurora B is a known regulator of PP1 (Qian et al., 2013; Xin et al., 2020) stainings for H2B S6ph and Aurora B were performed and anaphases were analysed microscopically for the localisation of this kinase. This revealed that, in the majority of anaphases in HCT116 cells, Aurora B was localised at the central spindle. However, there was a clear correlation between Aurora B localisation at the chromatin and the occurrence of H2BS6ph in anaphase. This was also observed in RPE1, HT29 and U2OS cells (Figure 18A and B), showing that this correlation in not retsticted to a specific cell type.

Aurora B is normally relocalised from the centromeres to the central spindle after anaphase onset by the motor protein Mklp2 (Adams et al., 2001; Serena et al., 2020). To test whether

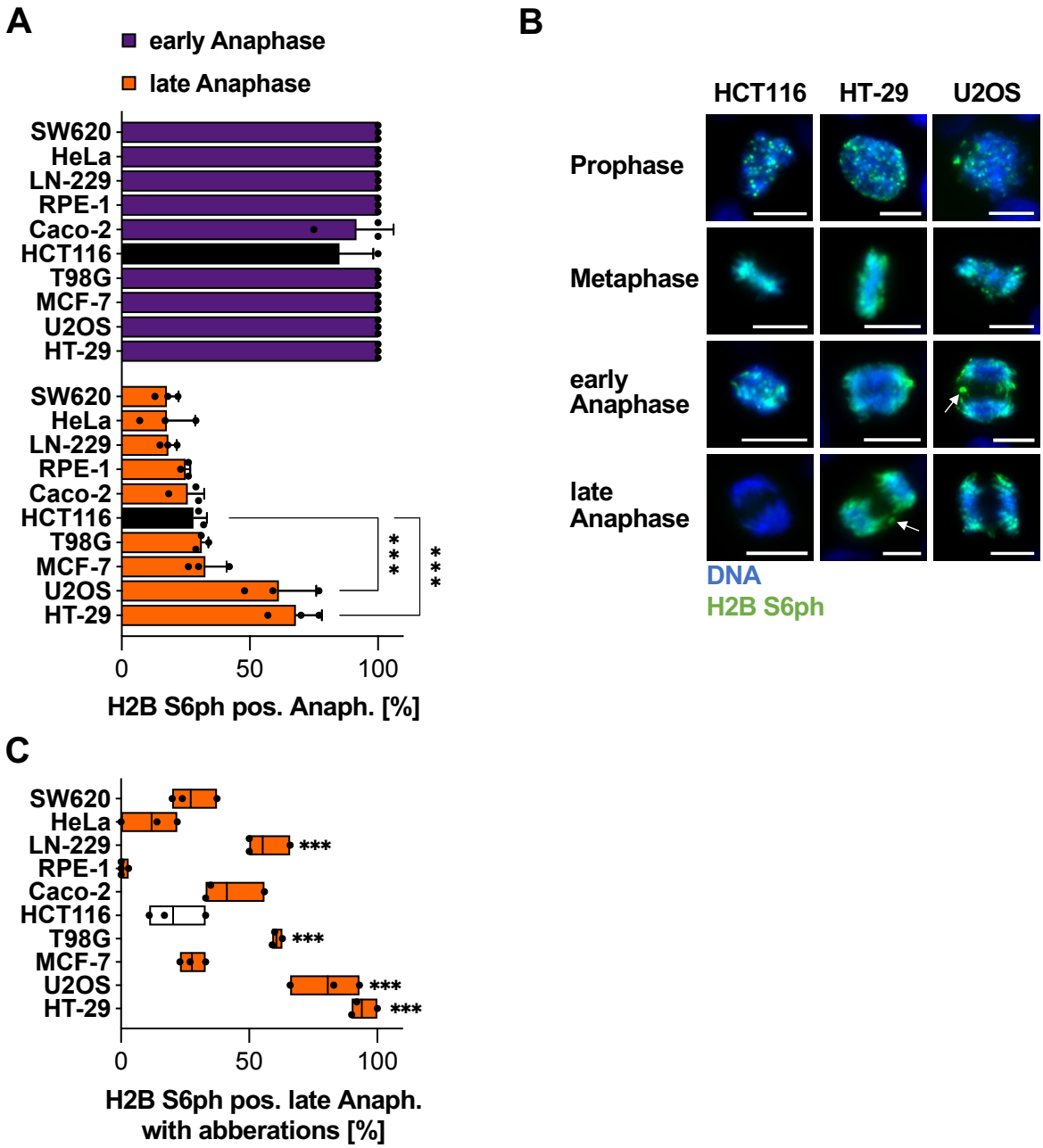

Figure 17: H2B S6ph dephosphorylation is delayed in some cancer cell lines.

(A) The indicated cell lines were prepared for immunofluorescence and stained for H2B S6ph. Mitotic figures were classified for their mitotic stage and scored for their H2B S6ph staining. Data from 3 independent biological replicates are shown as means ± SD, individual data points are displayed as black dots. Data from HCT116 cells are indicated by a black bar as these cells were used in previous experiments. **(B)** Representative images of mitotic figures for the indicated cell lines from (A). The occurrence of H2B S6ph on aberrant lagging chromosomes or bridging chromatin is indicated by arrows. Scale bar = 15 µm. **(C)** Anaphases were classified as normal or aberrant based on the presence of anaphase bridges or lagging chromosomes. Boxes indicate the minimum and maximum values, lines indicate the means, individual data points are displayed as black dots. **(A and C)** Data was statistically analysed with one-way ANOVA with Dunnett multiple comparisons correction.* $p<0.05$, ** $p<0.01$, *** $p<0.001$.

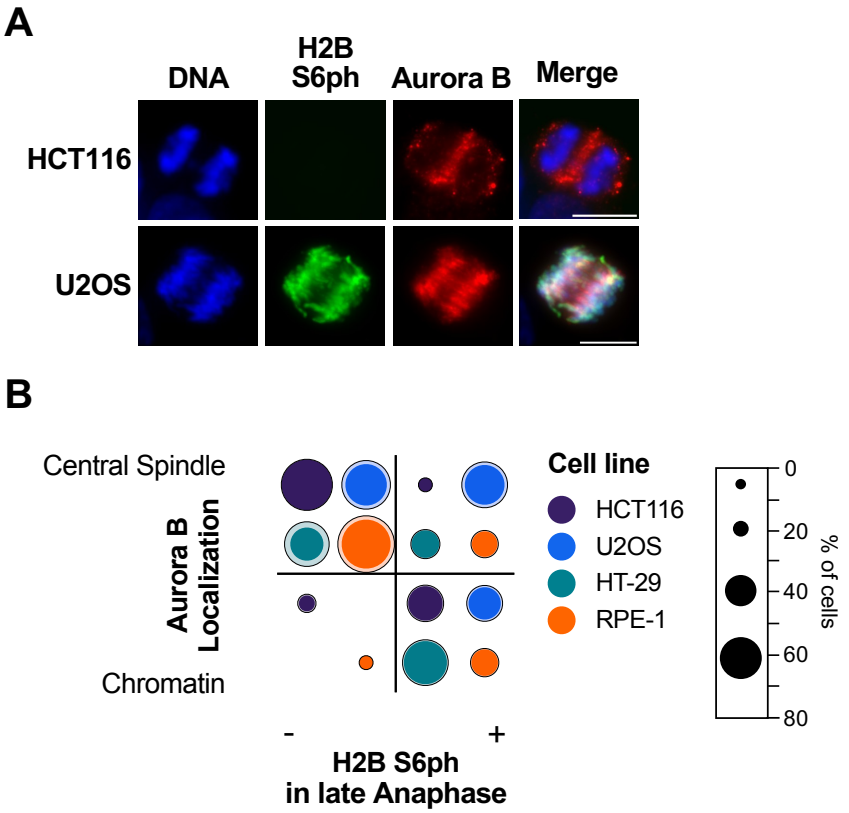

Figure 18: Aberrant Aurora B localisation occurs in some cancer cell lines.

(A) HCT116 and U2OS cells were prepared for immunofluorescence imaging and stained for H2B S6ph and Aurora B. Mitotic cells were imaged, representative results are shown. Scale bar = 15 µm. **(B)** Cells shown in (A) were counted and classified based on the presence of H2B S6ph staining and Aurora B location. Data from 3 independent biological replicates are shown. The inner circle indicates the percentage of cells showing this distribution, the outer circle indicates standard deviation.

Mklp2 itself is mislocalised in these cells, stainings for Aurora B and Mklp2 were performed. Indeed, in all cell lines analysed, Mklp2 localisation matched Aurora B localisation and correlated with H2B S6ph (Figure 19A). To verify that mislocalisation of Aurora B causes a delay in H2B dephosphorylation, HCT116 cells were transfected with an siRNA targeting Mklp2 (Gruneberg et al., 2004). After Mklp2 knock-down, Aurora B was predominantly located on chromatin and the number of anaphases showing H2B S6ph was increased from the previously observed 20 % to approximately 70 %. This matches the ratio H2B S6ph positive anaphases found in U2OS and HT29 cells (Figure 19B and C).

Aurora B and RepoMan are not only important regulators of H2B S6ph but also control localisation and timing of H3 T3ph and H3 S10ph (Qian et al., 2011; Vagnarelli et al., 2011). To test whether these PTMs are regulated with the same kinetics, co-stainings for these and H2B S6ph were prepared and microscopically analysed. This showed that these histone PTMs occur with overlapping but distinct kinetics. Around 50 % of anaphase cells were negative for H2B S6ph while being still

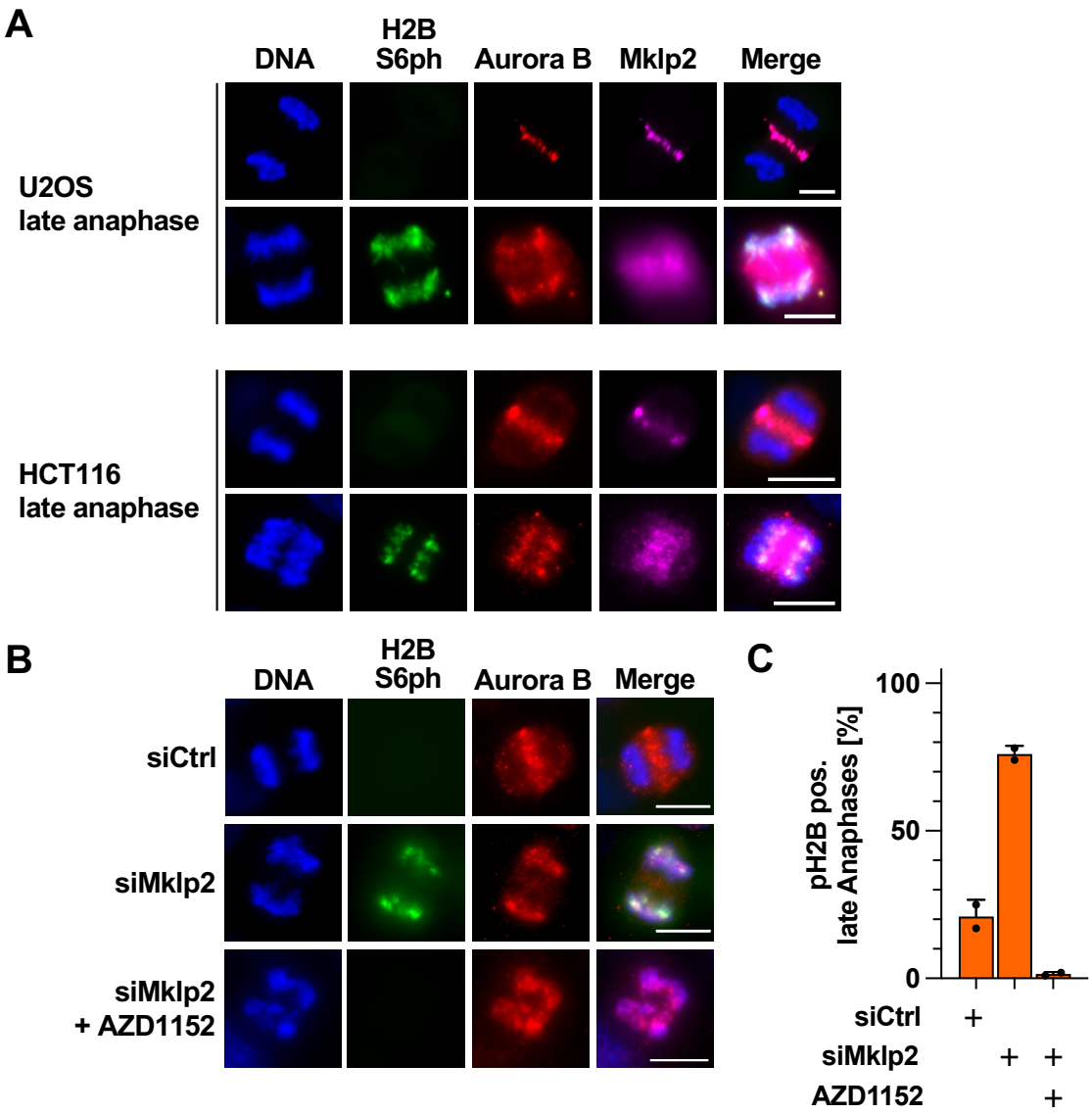

Figure 19: Aberrant localisation of Mklp2 and Aurora B coincide with aberrant H2B S6ph.

(A) HCT116 and U2OS cells were stained for H2B S6ph, Aurora B and Mklp2 using immunofluorescence. Representative images of mitotic cells are shown. Scale bar = 15 µm. **(B)** HCT116 cells were transfected with control siRNA or siRNA targeting Mklp2. After 48 h cells were treated with AZD1152 (1 µM, 30 min) as indicated and stained for H2B S6ph and Aurora B using immunofluorescence. Representative images of mitotic cells are shown. Scale bar = 15 µm. **(C)** Cells as shown in (B) were scored for their presence of H2B S6ph in late anaphase. Data from 2 independent biological replicates are shown as means ± SD, individual data points are displayed as black dots.

positive for H3 T3ph or H3 S10ph (Figure 20). This suggests that other factors, together with PP1/RepoMan and Aurora B, are involved in specification of timing of these different PTMs. Together, these data show that H2B S6ph is indeed deregulated in some cancer cell lines. The functional significance of this finding is so far elusive and needs to be investigated further.

3.7 Over-expression of H2B S6 mutants does not impact mitotic fidelity

Previous studies, using antibody injection experiments, have indicated an involvement of H2B S6ph in mitotic fidelity (Seibert et al., 2019). Furthermore, H2B S6ph has been implicated in sister-chromatid cohesion during mitosis as its presence precludes binding of the cohesin removal factor SET. To investigate the potential relevance of H2B S6ph by an independent experimental approach, H2B serine 6 mutants were created and expressed in HCT116 cells. Cells were stably transfected with plasmids allowing for the doxycycline inducible expression of H2B-wt-EGFP, H2B-S6A-EGFP or H2B-S6E-EGFP. Single cell clones were picked, expanded and selected based on their expression of EGFP-H2B as evaluated by fluorescence microscopy. Multiple clones were then pooled to avoid clonal effects.

Wildtype and mutant cell pools as well as normal HCT116 cells were treated with doxycycline for 14 d to allow for the expression of EGFP-H2B and analysed microscopically. Mitotic figures were scored for the presence of either anaphase bridges and lagging chromosomes. This revealed that in HCT116 cells, approximately 20 % of anaphases show bridges or lagging chromosomes. No further increase in mitotic defects was observed in cells expressing either H2B wt, H2B S6A or S6E (Figure 21A).

While no effect on mitotic fidelity could be observed in this setting, previous data suggest that H2B S6ph protects cohesin from premature removal at the centromeres (Seibert et al., 2019).

To test whether H2B S6 mutants have an effect on cohesion, cell pools expressing EGFP-H2B pools were treated with doxycycline as before. Chromosome spreads were prepared and centromeres were stained. The inter-centromeric distance was measured (Figure 21B). This revealed that the inter-centromeric distance was not significantly different between normal HCT116 cells, H2B-wt, S6A or S6E expressing cells (Figure 21C).

While these data do not reveal evidence for a functional relevance of H2B S6i n mitosis, the experimental setting is ultimately limited. As over-expressed mutant histone represents only 10 to 20 % of total histone, any mutant that does not cause a strong or dominant effect might not yield a phenotype in such a setting. Therefore, endogenous histone should be replaced by the mutant in question to exclude this possibility. Such systems, in vertebrates, however, do not yet exist.

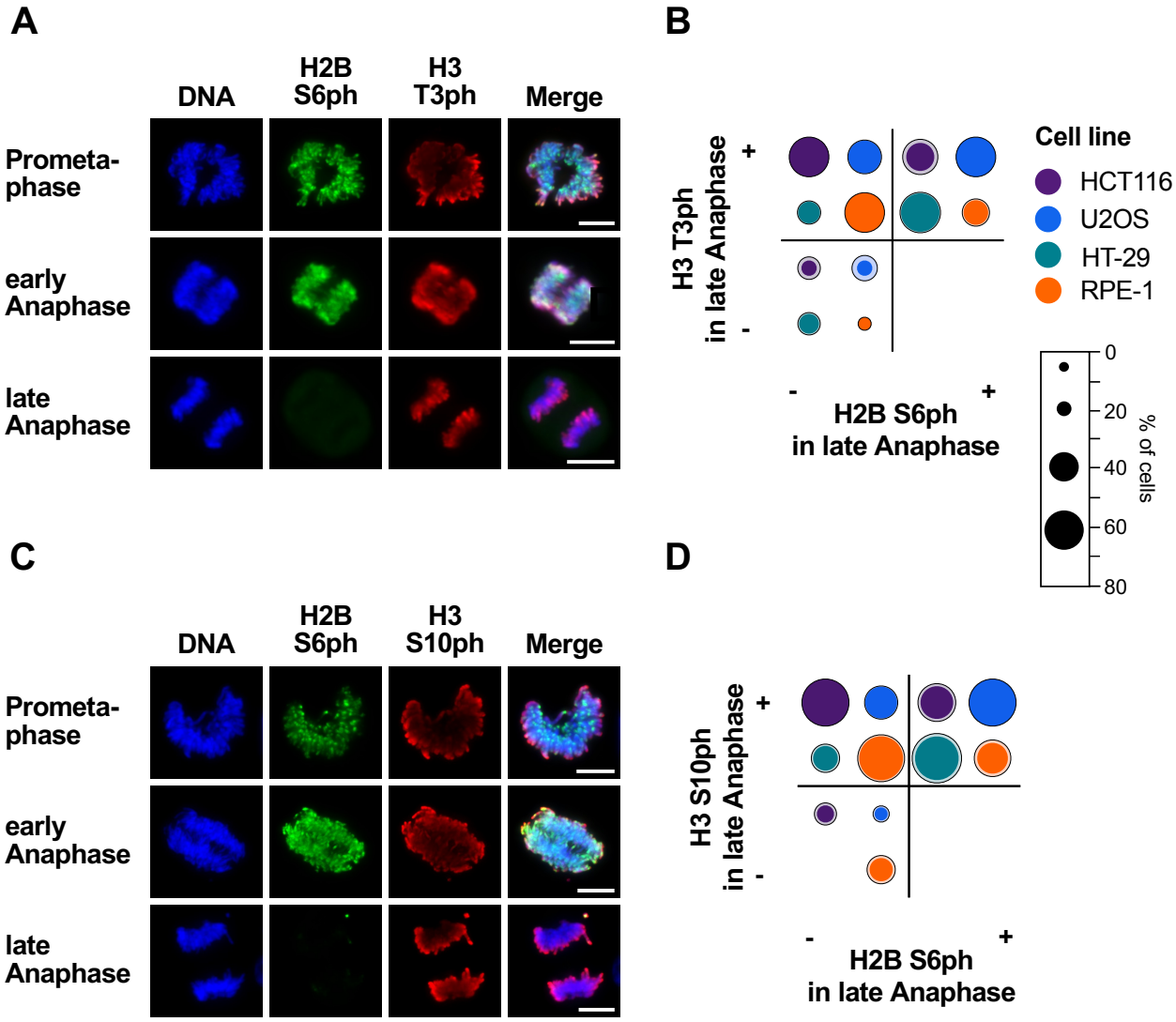

Figure 20: H2B S6ph is dephosphorylated independently from other mitotic histone PTMs.

(A) HCT116 cells were stained for H2B S6ph and H3 T3ph using immunofluorescence. Representative images of mitotic cells are shown. Scale bar = 15 µm. **(B)** The indicated cell lines were analysed for the occurrence of H2B S6ph and H3 T3ph in late anaphase. **(C)** HCT116 cells were stained for H2B S6ph and H3 S10ph using immunofluorescence. Representative images of mitotic cells are shown. Scale bar = 15 µm. **(D)** The indicated cell lines were analysed for the occurrence of H2B S6ph and H3 T3ph in late anaphase. **(B and D)** Data from 3 independent biological replicates are shown. The inner circle indicates the percentage of cells showing this distribution, the outer circle indicates standard deviation.

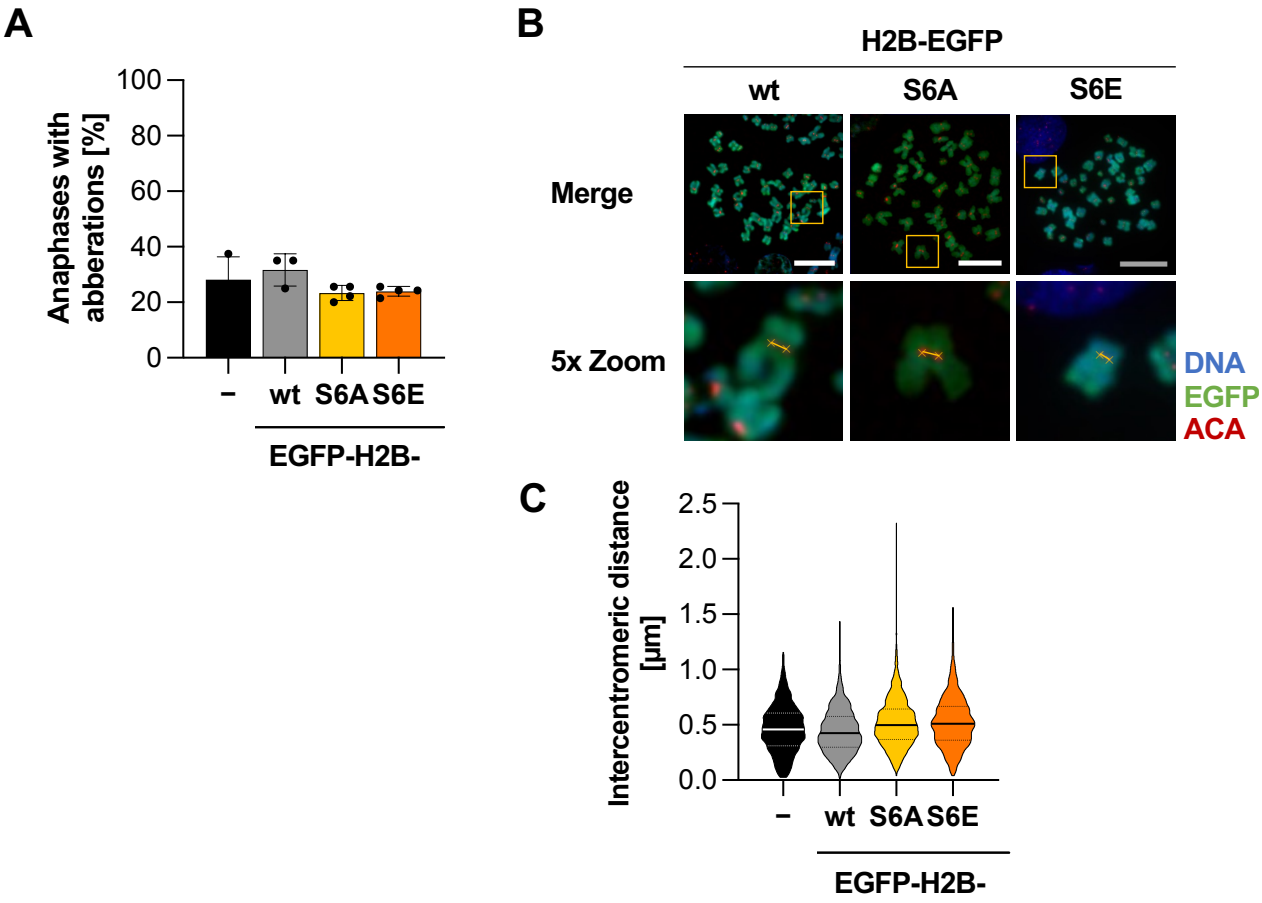

Figure 21: H2B Serine 6 phospho-mutants do not influence mitotic fidelity.

(A) Stable HCT116 cells inducibly expressing either EGFP-H2B wt, S6A or S6E were created. Cells were then induced (1 µg/mL doxycycline, 14 d) and analysed microscopically. Anaphases were classified as normal or aberrant based on the presence of anaphase bridges or lagging chromosomes. Data from 2 independent biological replicates are shown as means ± SD, individual data points are displayed as black dots. **(B)** H2B mutant cells were arrested with nocodazole and chromosome spreads were prepared. Cells were stained for H2B S6ph and with human-ACA using immunofluorescence. Representative images are shown. Scale bar = 15 µm. Crosses mark the centromeres, the line between them indicates the distance measured. **(C)** Distance between the centromeres of the sister chromatin was measured as shown in (B). Data from 3 independent biological replicates are shown, continuous black line indicates mean, dashed lines indicate quartiles. Data were statistically analysed with one-way ANOVA and Dunnett multiple comparisons correction. * $p<0.05$, ** $p<0.01$, *** $p<0.001$.

4 Development of a novel histone replacement system in higher eukaryotes

The functional consequences of histone modifications are typically investigated by correlating their occurrence with their genomic and transcriptional context (Millán-Zambrano et al., 2022). In order to study the function of histone modifications in a more targeted way, histone replacement systems aim to deplete or reduce the levels of wildtype histone protein and simultaneously express mutant versions.

Such systems are already established in organisms like *Drosophila melanogaster* and *Saccharomyces cerevisiae* as well as *Arabidopsis thaliana* (Matsubara et al., 2007; Zhang et al., 2019; Corcoran et al., 2022, 2023). However, as these organisms do not have H2B S6, which is only conserved among vertebrates, these cannot be used to study the function of H2B S6ph.
Therefore it is the goal of this study to test the feasibility of histone replacement in vertebrate cells.

A comprehensive histone replacement system should have the following characteristics:

- Applicable to all canonical histones
- Applicable to all residues
- Inducible switch from endogenous histone to replacement histone
- Allows for combination of multiple histone replacements
- Adjustable replacement efficiency
- Non-detrimental for normal chromatin function
- Fast cell creation to facilitate screening approaches

The lack of comprehensive histone replacement systems in vertebrates can likely be attributed to their complicated histone gene landscape (Figure 3), strength of histone expression and infeasibility of stable knock-out approaches due to the essential nature of histones (Günesdogan et al., 2014).

While genome editing approaches, directly mutating the genes *in situ*, have been successfully implemented before (Sankar et al., 2022), they suffer from labour intensive cell clone generation. For the generation of various mutant histone cell lines, only knock-down and re-expression strategies remain as viable options. Such approaches have been successfully implemented in the past for other highly expressed multi-copy genes like Ubiquitin (Xu et al., 2009).

4.1 Histone replacement strategy

A knock-down and re-expression system for histones would consist of two main parts (Figure 22A):

1. An shRNA targeting the endogenous histone to be replaced
2. A replacement histone (shRNA resistant)

These would be delivered as a single or two separate plasmids and would be stably integrated into the host cells genome to yield a stable histone replacement cell line (Figure 22B). To allow for the expression of potentially deleterious histone mutants, an inducible system is desirable as it allows for the creation of stable cell lines that can be maintained without the expression of the replacement histone.

After induction, expression of the histone targeting shRNA would lead to a gradual decrease in endogenous histone mRNA, as it is degraded via RNA interference (RNAi). At the same time, induction of an shRNA resistant histone would compensate for this loss of endogenous histone mRNA, thereby replacing the endogenous histone mRNA with a replacement version (Figure 22C). This replacement histone could be wildtype histone or a mutant of choice.

As a cell replicates its genome during S-phase, it doubles its genomic DNA and the total amount of histone (Spalding et al., 1966). If only replacement histone is being synthesised after induction, the existing endogenous histone protein, which is not degraded, becomes diluted by the newly made replacement histone. Therefore, in each replication a maximum of 50 % of histone can be replaced. Within a few cell cycles, almost all of the original wildtype histone would be replaced by the mutant version. If the replacement efficiency is lower, the ratio of replacement to wildtype histone is lowered accordingly (Figure 22D and E).

RNAi mediated knock-down of the endogenous histone partially relies on perfect base-pairing between the effector siRNA and the target mRNA (Bofill-De Ros et al., 2016). Therefore, a histone targeting shRNA has to be designed such that it targets the mRNA of all gene copies of that histone. The human genome contains 22 H2B genes, with a sequence similarity of only approximately 75 % between the different H2B copies (Amatori et al., 2021). While multiple shRNAs could certainly be used to target these, a simpler vertebrate cell line is used for this study. In the chicken genome, only 8 H2B genes with sequence similarities of approximately 90 % are present (Takami, 1996). As opposed to *Drosophila melanogaster* or *Saccharomyces cerevisiae*, chicken H2B does contain a phosphorylated serine 6 (Nakayama et al., 1993). As histones are generally highly conserved, especially in vertebrates, studies on the function of histone PTMs are likely to be of great significance in chicken cells as well.

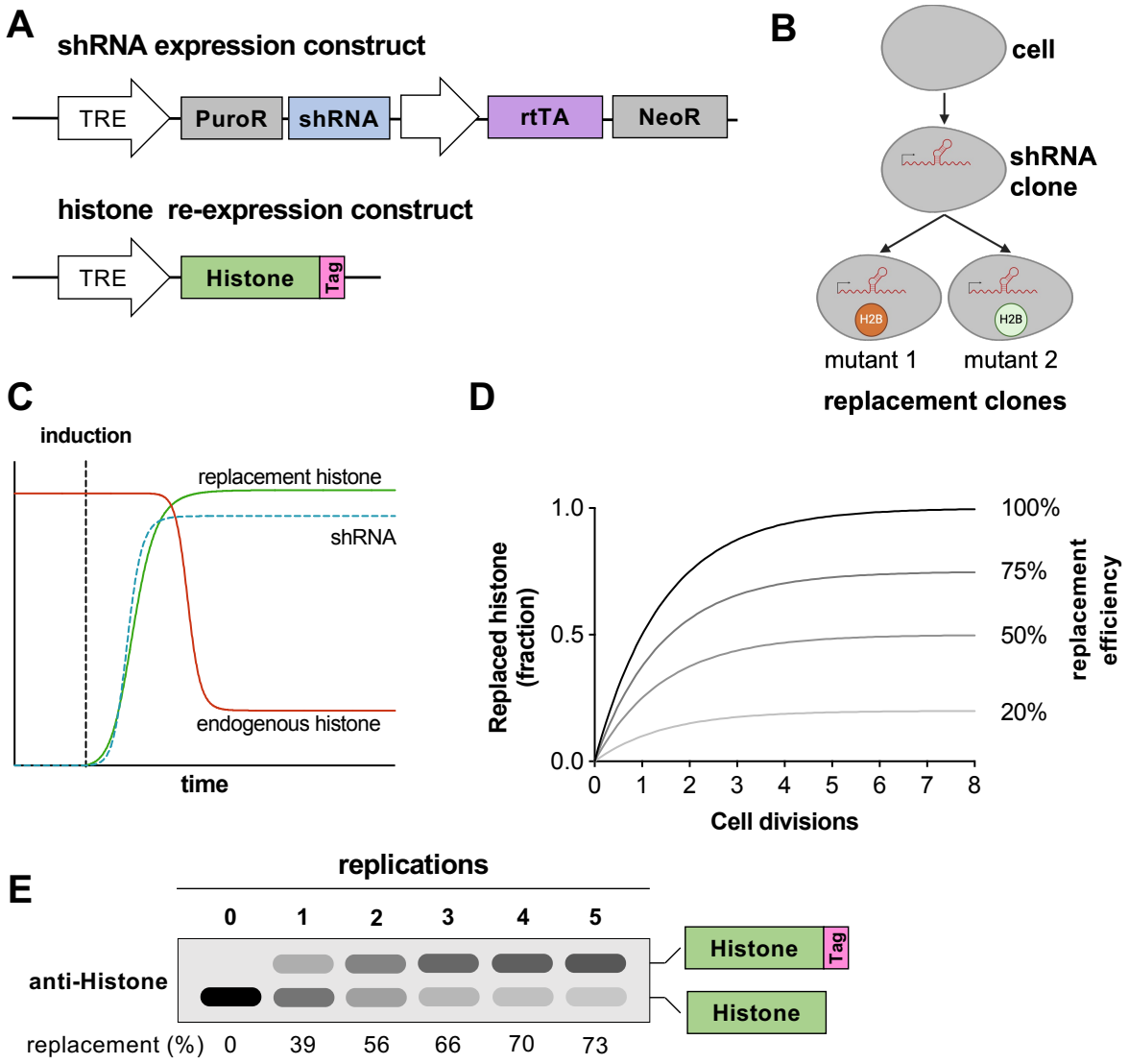

Figure 22: Histone replacement strategy.

(A) Schematic representation of an inducible histone replacement system consisting of a plasmid expressing a histone targeting shRNA expressing and a second plasmid expressing shRNA resistant replacement histone. **(B)** First an shRNA expressing parental cell line is generated from which histone mutant replacement cell clones can be generated by integration of the plasmids as shown in (A). *Created with biorender.com* **(C)** Induction of the replacement system results in the expression and processing of histone targeting shRNA. Subsequently endogenous histone mRNA decays overtime. shRNA resistant histone mRNA simultaneously increases, replacing the endogenous histone mRNA. **(D)** With each replication, the amount of histone in the cell is doubled. With a replacement efficiency of 100 % at most 50 % of total histone could be replaced with each replication. This leads to a dilution of endogenous histone over time. With a lower replacement efficiency, the maximum amount of histone that can be replaced is lowered accordingly as indicated on the right side. **(E)** Schematic Western blot showing replacement over time with an assumed replacement efficiency of 75 %. The upper band corresponds to the tagged replacement histone.

4.2 Designing chicken H2B targeting shRNAs

As a first step, shRNAs against chicken H2B were designed and tested in order to allow for the knock-down of endogenous H2B. shRNAs were designed against the consensus sequence of chicken H2B according to sequence requirements as identified by Matveeva et al. (2012) or by other shRNA design tools (*BLOCK-iT™ RNAi Designer* 2021; *InvivoGen siRNA Wizard* 2021). A total of 7 shRNAs were selected for testing (see Appendix). An shRNA vector allowing for easy cloning of the shRNAs as annealed oligos via Golden Gate assembly was designed and cloned (pMIR30) and selected shRNA sequences were inserted.

To test the efficacy of the designed shRNAs, human HEK293T cells were transfected with plasmids expressing EGFP fusion proteins of the two main chicken H2B isoforms; ggH2B7 and ggH2B8, along with plasmids containing the different shRNAs.

After 4 d, cell extracts were analysed by Western blotting for H2B. This showed that the ggH2B-EGFP fusion proteins were expressed at the expected size of approximately 40 kDa (Figure 23A). Lower mass bands corresponding to degradation products of the fusion protein were always observed. In cells co-transfected with plasmids coding for shRNA #3 or #7, protein levels of the fusion protein were strongly reduced for both ggH2B7 and ggH2B8 (Figure 23A). Interestingly, the knock-down was most apparent for the degradation products rather than the full-length protein. This is likely because once the H2B-EGFP is incorporated into chromatin its protein turnover is strongly reduced (Chalkley et al., 1965; Bondy, 1971).

To test whether the combination of multiple shRNAs would increase the overall knock-down efficiency, a plasmid was cloned allowing for the expression of the shRNAs #3, #7 and #5 from one mRNA. HEK293T cells were transfected with plasmids expressing H2B-EGFP fusion protein and the combined shRNAs and analysed as described before. This showed that the combination did not result in a higher knock-down efficiency (Figure 23B). Chicken H2B shRNA #3 was chosen as the most effective shRNA for knock-down of endogenous chicken H2B in all subsequent experiments.

4.3 Design and testing of 1st generation histone replacement system

For the first generation histone replacement system, a two plasmid strategy was chosen with the first plasmid expressing the shRNA and the second plasmid expressing the replacement histone (Figure 22A). The required integration copy number for shRNA and replacement histone plasmids are not known but possibly larger than 1. Using two plasmids allows for the separate creation and functional testing of stable cell clones containing these plasmids (Figure 22B). This was intended to provide the proof-of-concept for the technical feasibility of histone replacement in vertebrate

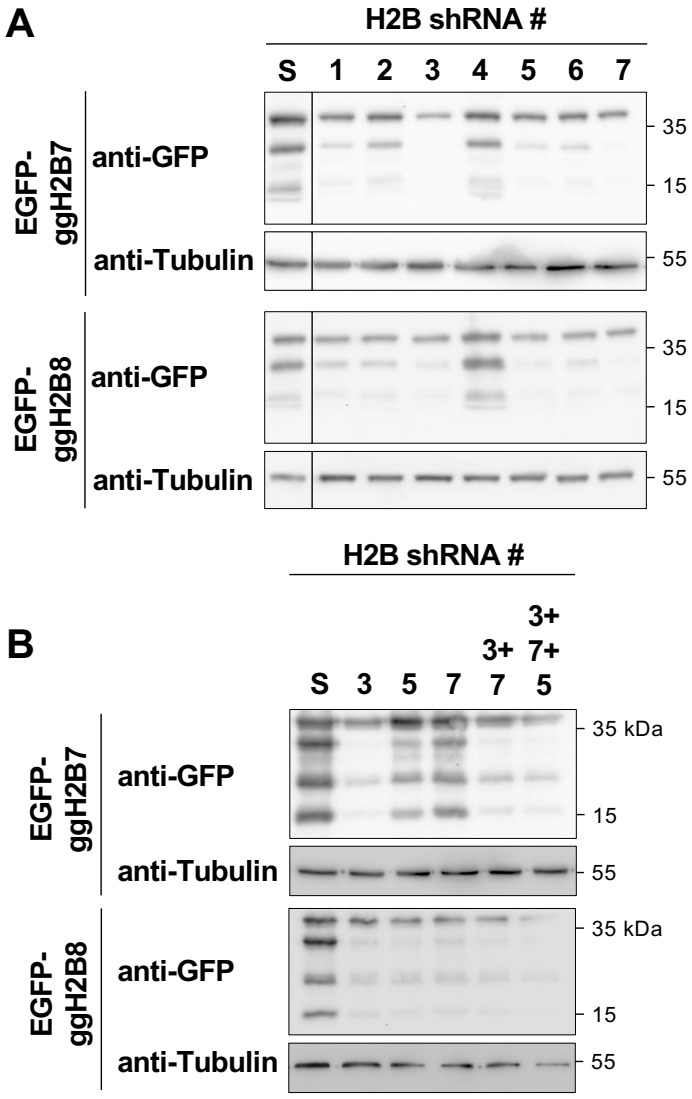

Figure 23: Testing knock-down efficiencies of chicken H2B shRNAs.

(A) HEK293T cells were transfected with plasmids expressing EGFP-ggH2B7 or EGFP-ggH2B8 and plasmids expressing the indicated shRNAs. S = scramble shRNA. Cells were grown for 2 d and cell extracts were analysed via Western blotting and staining for GFP. Representative results are shown. **(B)** Cells were transfected as shown in (A) but with the indicated shRNA combination plasmids. S = scramble shRNA.

cells as well as showing potential difficulties and technical hurdles that could be addressed in a second generation.

4.3.1 shRNA expression plasmid

4.3.1.1 shRNA expression optimisation

Knock-down of high abundance targets is often less efficient than for low abundance targets (Arvey et al., 2010). As histones are highly expressed during S-phase, optimisation potential for the expression of shRNAs was investigated.

To test the efficacy of different shRNA expression backbones, the commonly used human mir30a shRNA sequence (Zeng et al., 2002) (used in the initial shRNA screening) was compared to the chicken ortholog of mir30a as well as a synthetic shortened mir30 sequence (Sun et al., 2006). Plasmids carrying these backbones with the previously selected H2B shRNA #3 were cloned. Functional experiments showed that the knock-down efficiencies between the different backbones did not differ (data not shown). Therefore, the synthetic shortened mir30 backbone was chosen for further use due to its smaller size.

Additionally, the influence of the location of the guide (antisense) strand on the stem loop was tested. Traditionally, the guide strand is placed on the 3' half of the stem loop (Mcintyre et al., 2011; Fellmann et al., 2013; Bofill-De Ros et al., 2016; Sheng et al., 2020). However, some groups previously reported an increase in efficiency when placing the guide on the 5' half (Ge et al., 2010). Indeed the 5' version did show slightly higher knock-down efficiency (data not shown) and thus for the final shRNA plasmid, the guide strand was placed on the 5' side (Figure 24D).

4.3.1.2 Inducible shRNA plasmid design

For the stable integration of an inducible shRNA expression system, an integration plasmid was designed (pSB-Puro-mir30short-Neo) (Figure 24A). This plasmid is based on a Sleeping Beauty plasmid (pSBtet-Neo) designed by Kowarz et al. (2015), which allows for tetracycline inducible expression and Sleeping Beauty transposase mediated integration into a host cells genome (Ivics et al., 1997; Izsvák et al., 2004). Sleeping Beauty transposase is known to integrate more than once per genome, potentially allowing for stronger shRNA expression and better knock-down efficiency. The plasmid contains a tet-responsive promoter (TRE) driving an shRNA expression cassette based on the shortened mir30 backbone together with a puromycin resistance gene (Figure 24B). This allows for the selection of cells actively expressing the shRNA after induction, as it was anticipated that strong expression of the shRNA might present a selective disadvantage. A constitutive promoter drives expression of a 3rd generation tet-activator (rtTA3) needed for the induction of the TRE. Compatible self-destructing restrictions sites were added upstream and downstream of the miRNA

backbone that allow for the addition of further shRNAs or for multimerisation, if required (Fink et al., 2018) (Figure 24C).

4.3.2 Histone re-expression plasmid

The second plasmid, carrying the replacement H2B, was also designed based on a Sleeping Beauty backbone with a different antibiotic resistance (pSBtet-Hygro) to allow for double selection (pSBtet-ggH2B-IRES-Bla-Hygro) (Kowarz et al., 2015) (Figure 24D).

As the re-expressed histone H2B must not be targeted by the simultaneously expressed shRNA, chicken H2B7 was rendered shRNA resistant by changing the DNA sequence at the shRNA binding site without changing the amino acid sequence by using synonymous codons. In order to be able to distinguish replaced from endogenous histone in subsequent analyses, replacement H2B was tagged with a His-tag followed by a tandem OLLAS-tag (Park et al., 2008) (Figure 24C). This allows for the distinction by size after gel-electrophoresis as well as staining with tag-specific antibodies in immunofluorescence. Generally, tagging H2B is well tolerated even with larger tags such as a full GFP *in vivo* (Lois et al., 2002; Hadjantonakis et al., 2004). The OLLAS-tag was chosen because it contains less charged amino-acids compared to a FLAG- or V5-tag. Together with the replacement H2B, a blasticidin resistance is expressed from an IRES sequence to allow for the selection of expressing cells.

4.4 Preliminary test of histone replacement components

In order to test whether the components of the histone replacement system work, DF-1 chicken fibroblasts were transfected with plasmids expressing the H2B specific or control shRNA, as well as the re-expression plasmids and were induced with doxycycline for 4 d. Cell survival was measured using the crystal violet assay. As expected, expression of the H2B specific shRNA lead to a strong and significant decrease in cell survival of about 70 % compared to control shRNA (Figure 25). Strikingly, co-transfection with the re-expression plasmid rescued the lower cell survival to some extent, significantly increasing cell survival from 25 % to 60 %. This suggests that re-expression of shRNA resistant histone can rescue histone depletion mediated cell death.

4.5 Generation of 1st generation stable histone replacement cells

4.5.1 Generation of stable histone knock-down cell clones

To generate functional histone replacement cells for H2B, in a next step, a stable cell line with the inducible H2B shRNA expressing plasmid was created. For that, DF-1 chicken fibroblasts

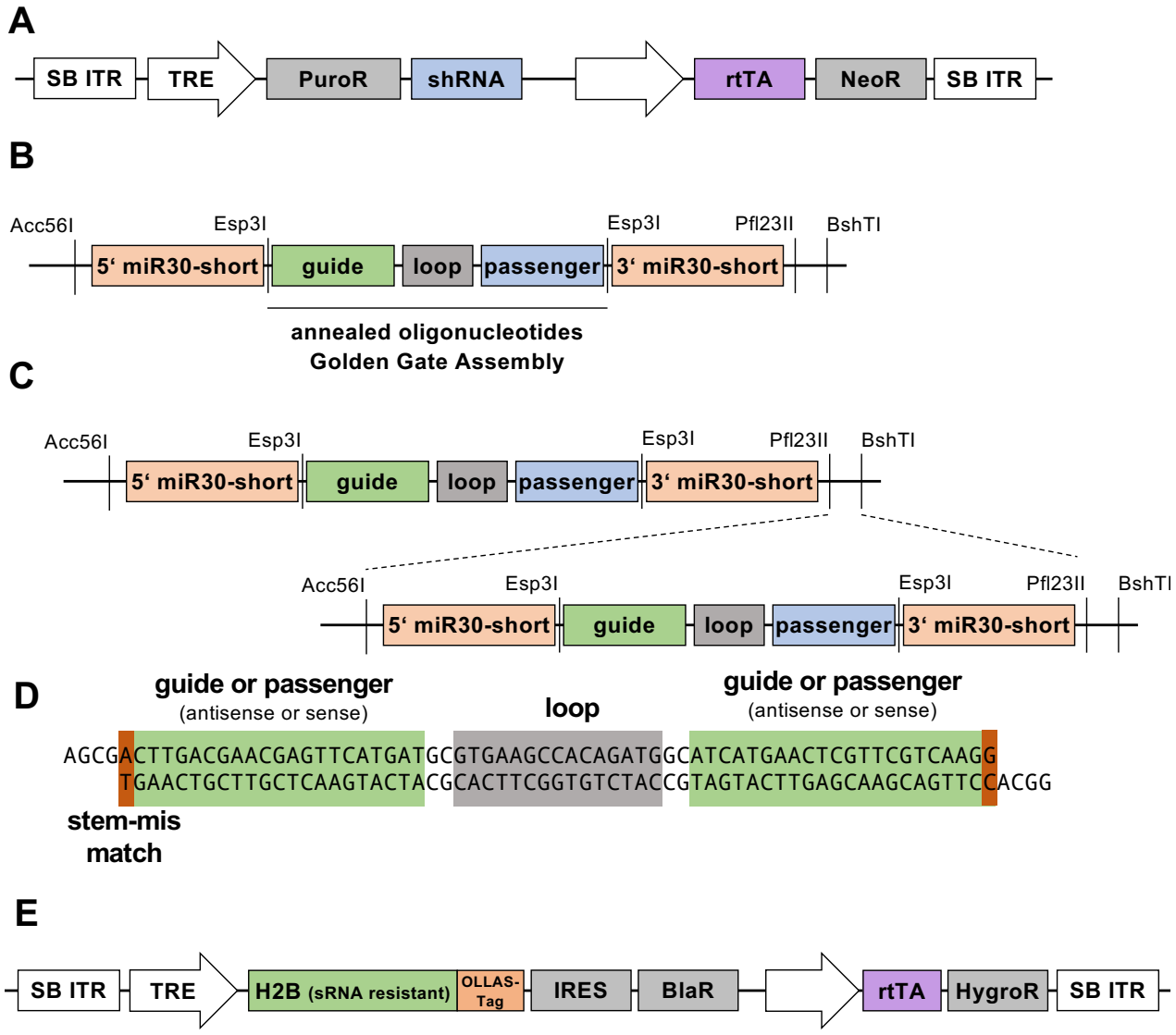

Figure 24: Design of histone replacement system expression plasmids.

(A) Schematic representation of the shRNA expressing plasmid. The plasmid contains a tet-responsive promoter (TRE) driving expression of a puromycin resistance gene and the shRNA. It also contains a constitutively expressed tet-activator (rtTA-VP16) to allow for expression from the TRE. The plasmid is flanked by Sleeping Beauty sequences (SB ITR) to allow for transposase mediated genomic integration. PuroR = puromycin resistance, NeoR = Neomycin resistance. **(B)** Schematic representation of the shRNA expression backbone using a shortened mir30a backbone as described in Sun et al., 2006. Esp3I sites allow for the insertion of shRNAs via Golden Gate assembly. **(C)** Schematic representation of the shRNA multimerisation cloning strategy using compatible self-destructing restriction sites. **(D)** Schematic representation of the stem-loop oligos used for Golden Gate assembly via the Esp3I restriction sites shown in (B). **(E)** Schematic representation of the histone re-expression construct. A TRE drives expression of an shRNA resistant histone tagged with a double OLLAS tag for easy discrimination between endogenous and replaced histone. An additional expression cassette for the rtTA allows for induction of the TRE. The construct is flanked by SB ITR sequences to allow for transposase mediated genomic integration. BlaR = blasticidin resistance, HygroR = hygromycin resistance.

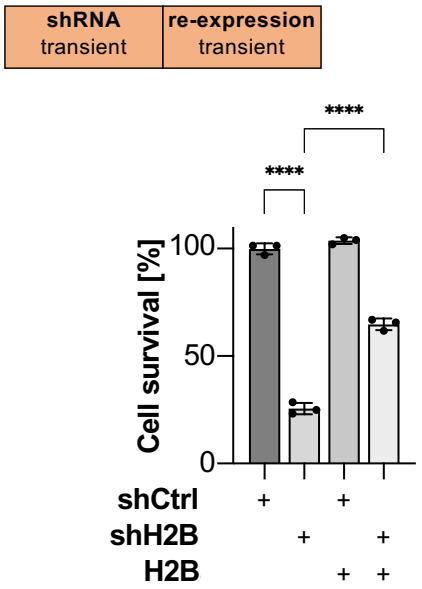

Figure 25: Re-expression of H2B rescues knock-down mediated cell death.

DF-1 chicken fibroblasts were transiently transfected with control shRNA or H2B targeting shRNA together with shRNA resistant chicken H2B7. Expression of shRNAs and shRNA resistant histone was induced with doxycycline for 4 days. Cell survival was measured with crystal violet. Data from 3 independent biological replicates are shown. Data was statistically analysed with one-way ANOVA and Dunnett multiple comparisons correction. * $p<0.05$, ** $p<0.01$, *** $p<0.001$.

were transfected with the shRNA plasmid (pSB-Puro-mir30short-shH2B-3[5p]-Neo) and a plasmid expressing the Sleeping Beauty transposase for stable integration. The day after transfection, cells were put under selective pressure with G418 to select for cells which have stably integrated the plasmid into the genome. After 14 d of selection, 96 single cell clones were picked and further analysed.

First, a functional screen of the picked clones was performed by testing cell survival of uninduced and induced cells. Single cell clones were left untreated, induced by the addition of doxycycline for 4 d or induced and selected with puromycin (Figure 26A). Live cells were stained with crystal violet and staining was quantified. Clones were selected based on uninduced growth and growth after induction and selection. A cut-off of 10 % was used, as cells were expected to not survive efficient histone knock-down as seen before (Figure 25). This resulted in 2 shRNA cell clones (G10 and G12) which were inducibly killed by expression of an H2B shRNA (Figure 26B)

4.5.2 Generation of stable histone replacement cell clones

In order to create H2B replacement cell clones, the two shRNA expression clones G10 and G12 were transfected with the plasmid for the inducible expression of shRNA resistant H2B together

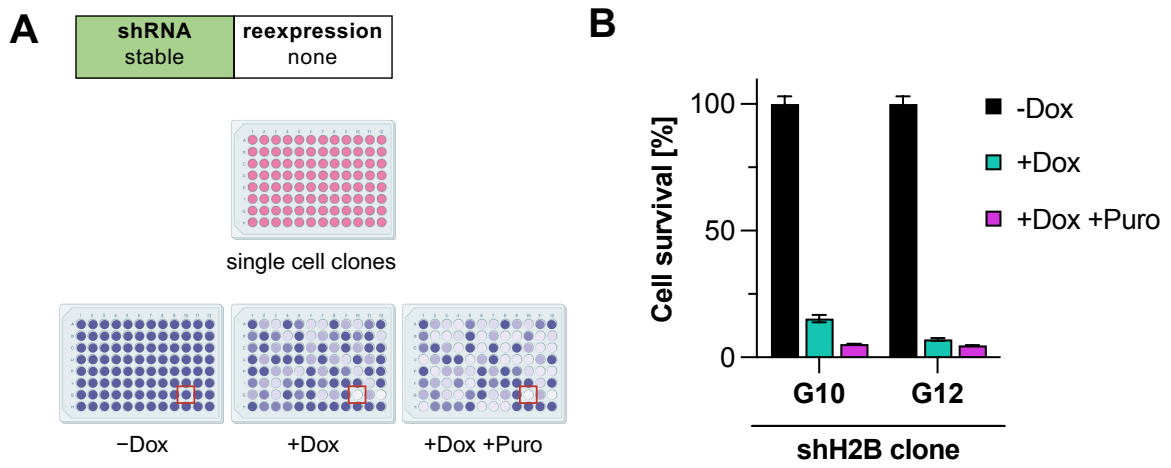

Figure 26: Generation and testing of stable inducible chicken H2B knock-down cell clones.
(A) Schematic representation of experimental setup. Cells were transfected with chicken H2B targeting shRNA plasmid together with a Sleeping Beauty expressing plasmid and single cell clones were seeded into 96-well plates. Clones were split into 3 different plates that remained untreated (-Dox), were induced (+Dox, 1 µg/mL, 4 d) or were induced and selected with puromycin (+Dox +Puro). Cell survival was determined by crystal violet staining, a schematic result is shown. The red box marks a clone growing in the absence of Dox but not after induction of histone knock-down, therefore qualifying as a good candidate for efficient knock-down. *Created with biorender.com*
(B) After initial functional screening as shown in (A), two selected shRNA expressing clones (G10 and G12) were induced with doxycycline (1 µg/mL, 4 d), induced and additionally selected with puromycin or left untreated. Cell survival was measured with crystal violet assay and normalised to uninduced controls. Data from 3 independent biological replicates shown as means ± SD.

with a plasmid expressing the Sleeping Beauty transposase to mediate stable integration. Cells were selected for 14 d with hygromycin to yield a stable cell pool.

To test whether the histone replacement system works after stable integration, the generated pools were used for a preliminary test. Cell pools were treated with doxycycline and with doxycycline plus puromycin for 4 d and cell survival was measured with the crystal violet assay. Indeed, the stable replacement pools showed increased survival after induction of approximately 25 % and 18 % respectively, compared to under 10 % of just the shRNA clones (Figure 27A). To analyse replacement of H2B, the replacement pools were induced with doxycycline and selected for 8 d to 12 d, followed by analysis of H2B expression by Western blotting. This showed that, in addition to the endogenous H2B at around 15 kDa, a second band of approximately 18 kDa, corresponding to the tagged replacement H2B, was present (Figure 27B). Quantification of the ratio of the upper band to total H2B showed that a replacement efficiency of 65 % and 25 % for the G10 and G12 based pools respectively was reached after 12 d (Figure 27C). Total H2B levels were reduced to approximately 20 % and 45 % for G10 and G12 based pools respectively after 12 d (Figure 27D).

Next, 96 single cell clones per stable pool were picked and expanded for further testing. Clones were screened for survival after induction of the shRNA and replacement histone. Cells were grown

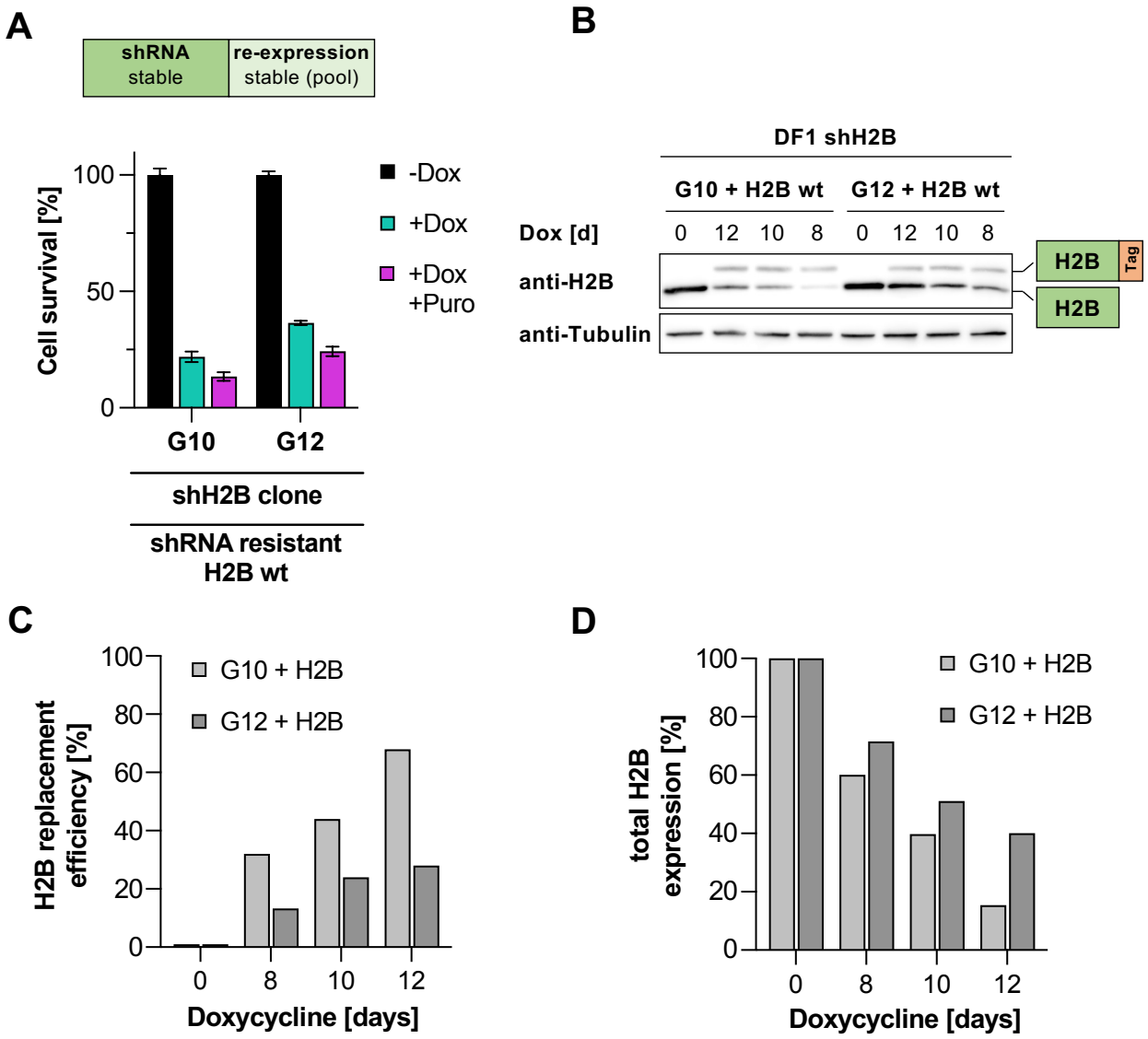

Figure 27: Generation and testing of stable chicken H2B re-expression cells.

(A) 2 cell clones with stable integration of inducible H2B targeting shRNA (G10 and G12) were transfected with plasmids for the expression of shRNA resistant wildtype replacement H2B and selected for the integration of that plasmid with hygromycin for 14 d. The resulting stable cell pools were induced with doxycycline (+Dox, 1 µg/mL, 4 d), induced with additional puromycin selection (+Dox +Puro) or remained uninduced. Cell survival was measured by crystal violet staining. Data from 3 independent biological replicates shown as means ± SD. **(B)** Replacement cell pools shown in (A) were induced with doxycycline (1 µg/mL, 8 to 12 d) or left untreated. Cell extracts were analysed via Western blotting for H2B, a representative blot is shown. The lower and upper band in the H2B blot correspond to endogenous or tagged replacement H2B, as schematically indicated on the right. **(C)** Replacement efficiency from the blot shown in (B) was quantified as the ratio of the upper (replacement) histone H2B to the total H2B level (replacement + endogenous H2B) and plotted. **(D)** Total H2B expression level from blot shown in (B) was quantified and normalised to the uninduced control.

in the absence or presence of doxycycline and selected with puromycin for 4 d and cell survival was measured using crystal violet. Most of the clones showed poor survival after induction of under 50 % or did not survive additional selection for shRNA expression via puromycin (Figure 28A). Ultimately, 4 re-expression clones based on the G10 shRNA clones were expanded for testing of histone replacement. These still showed low cell survival of only 15 % to 60 % (Figure 28B) under selective pressure for shRNA expression.

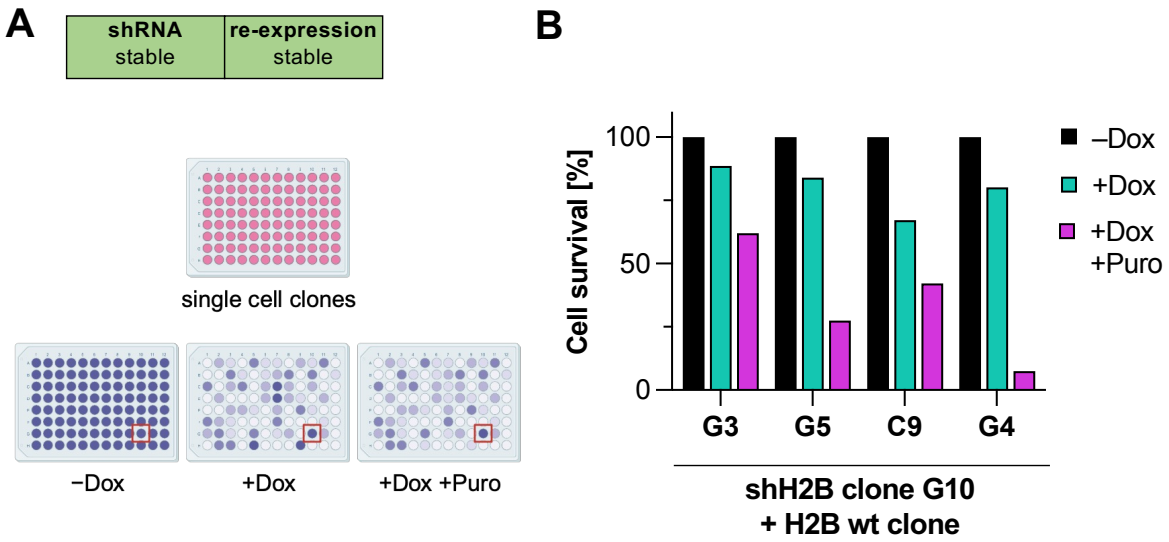

Figure 28: Generation and testing of stable chicken H2B re-expression cell clones.

(A) Schematic representation of experimental setup. Single cell clones were generated from stable cell pools containing both the inducible H2B targeting shRNA and inducible wildtype replacement H2B plasmids. Clones were split into 3 different plates that remained untreated (-Dox), were induced (+Dox, 1 µg/mL, 4 d) or were induced and selected with puromycin (+Dox +Puro). Cell survival was determined by crystal violet staining. A schematic result is shown. The red box marks a clone growing in the absence of Dox and also after induction with Dox and also surviving additional selection for shRNA expression with puromycin. *Created with biorender.com* **(B)** After initial functional screening as shown in (A), 4 selected H2B replacement clones based on the shRNA expression clone G10 were treated with doxycycline (1 µg/mL, 4 d), doxycycline and additionally selected with puromycin or left untreated. Cell survival was measured with crystal violet assay and normalised to uninduced controls.

To test histone replacement efficiency, cells were again induced for 4 d and H2B was analysed via Western blotting. Strikingly, endogenous H2B was almost completely lost after induction of the replacement system (Figure 29A) in all clones with a second band corresponding to tagged replacement H2B present. Quantification of the ratio of replacement H2B to total H2B showed replacement efficiencies were above 75 % for all clones, with clone G10D5 almost reaching the theoretical maximum of 95 % (Figure 29B and Figure 22D). Quantification of total H2B revealed that for 2 of the 4 clones, H2B levels were not reduced below the uninduced state, and for 2 levels were strongly reduced below 75 % Figure 29C.

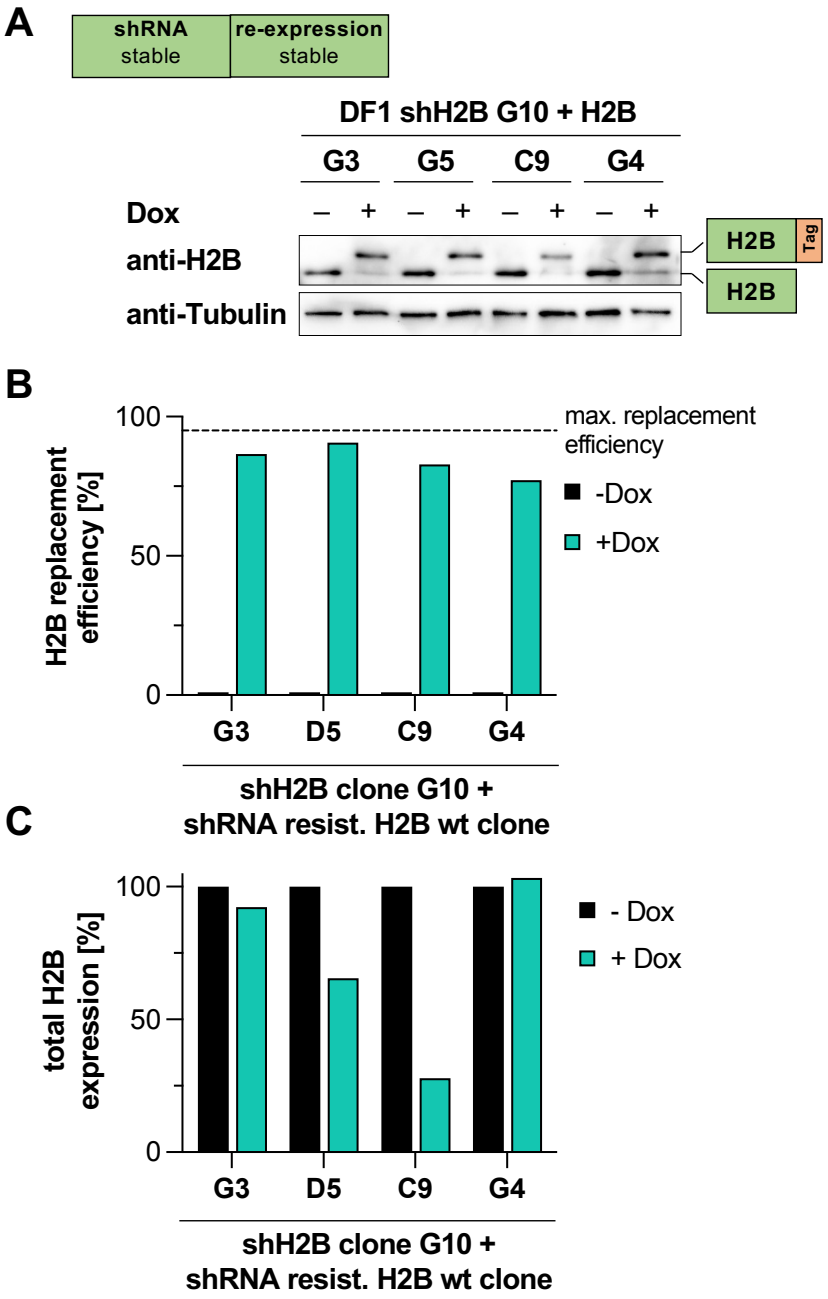

Figure 29: Histone H2B can be efficiently replaced in chicken cells.

(A) The indicated 4 selected stable replacement cell clones based on shRNA expressing clone G10 were induced with doxycycline (1 µg/mL, 4 d) or left untreated. Cell extracts were analysed by Western blotting for H2B. A representative blot is shown. The lower and upper band in the H2B blot correspond to endogenous or tagged replacement H2B as schematically indicated on the right. **(B)** Replacement efficiency from blot shown in (A) was quantified as the ratio of the upper (replacement) histone H2B to the total H2B level (replacement + endogenous H2B) and plotted. **(C)** Total H2B expression level from blot shown in (A) was quantified and normalised to uninduced control.

These data show that efficient histone replacement is technically possible in chicken cells with a knock-down and re-expression approach as used here. However, poor cell growth and reduced histone levels after induction of the system call for further optimisation to make a reliable tool useful for research questions.

Generation of replacement clones expressing H2B S6A and S6E mutants was successfully tested, although with even lower cell survival of the best clones and poor histone expression level (data not shown).

4.6 Design and testing of shRNAs for all canonical histones

To enable replacement of all canonical histones and after proving the technical feasibility of histone replacement with shRNA mediated knock-down, shRNAs against all canonical chicken histones (H1, H2A, H3 and H4) were designed and tested. To facilitate the design of shRNAs according to the criteria described in Matveeva et al. (2012), which proved to be reliable before, a Python script was developed that scored all possible shRNAs for a given mRNA sequence according to those criteria.

In short, input mRNAs were divided into 22-nucleotide sequences with a rolling window. Candidate shRNA sequences were first filtered to only include sequences present in all histone genes of a given type. shRNAs were then filtered to remove sequences with deleterious motifs (Matveeva et al., 2012). Correlation coefficients for each position and the nucleotide at that position were summed up to form an efficiency prediction score. The top 8 shRNAs (see Appendix) were then cloned as shRNA expression plasmids (pSB-Puro-mir30short-Neo) and tested against chicken histone GFP fusions as described before (section 4.2).

Human HEK293T cells were transfected with plasmids expressing EGFP-tagged chicken histones (EGFP-ggH1, EGFP-ggH2A, H3-ggEGFP or EGFP-ggH4) together with plasmids containing a control shRNA or histone specific shRNAs. Samples were analysed by Western blotting for EGFP to assess the knock-down efficiency on protein level (data not shown), as described before (section 4.2). Additionally, knock-down efficiency was assessed by RT-qPCR. Cells were transfected as before and total RNA was extracted. EGFP expression was quantified, revealing that all tested shRNAs showed high knock-down efficiencies (Figure 30). The best shRNA were selected for creating knock-down clones (shH1-503, shH2A-155, shH3-86, shH4-47).

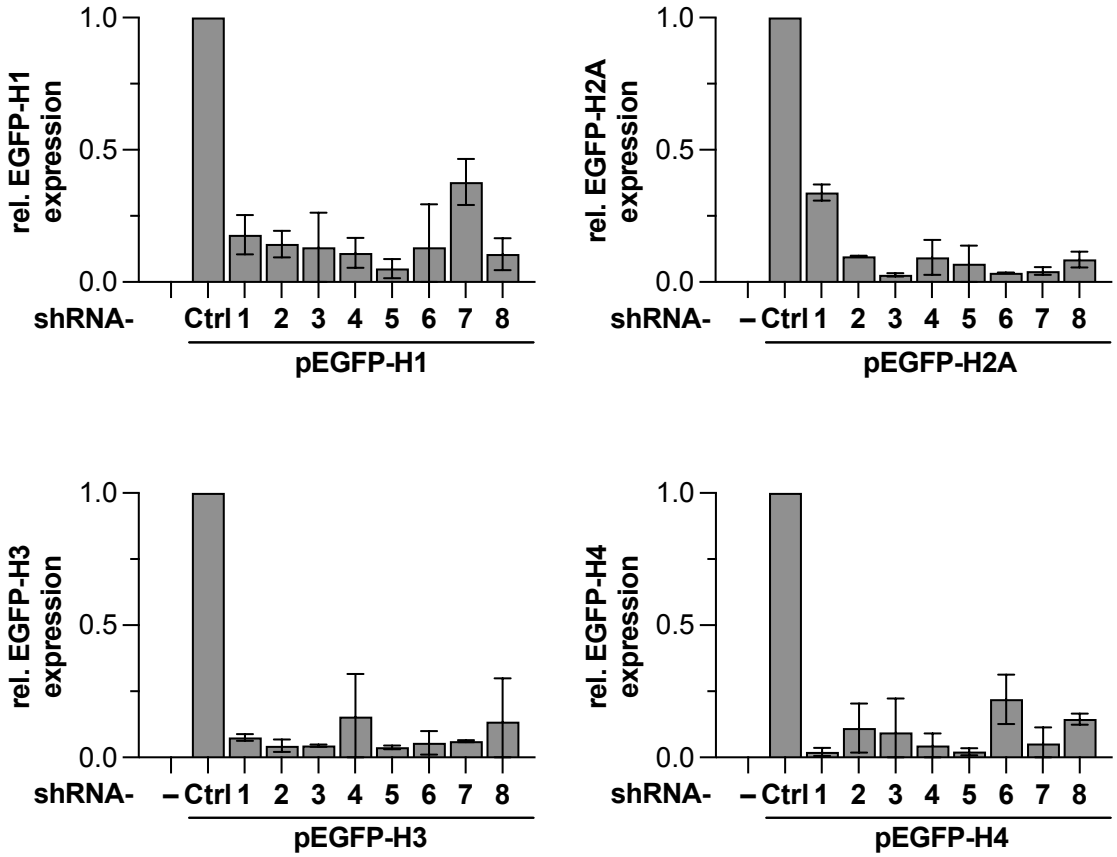

Figure 30: Testing of shRNAs against all canonical chicken histones.

Human HEK293T cells were transfected with plasmids expressing shRNAs against chicken H1, H2A, H3 or H4 or control shRNA together with the respective chicken histone as an EGFP fusion protein as indicated. After 2 d, total RNA was extracted and mRNA levels were measured by qPCR against GFP and normalised to control. Data from 3 independent biological replicates are shown as means ± SD with all samples normalised to their respective shRNA control.

4.7 Design and testing of an improved 2nd generation histone replacement system

While the proof-of-concept for histone chicken replacement has provided important experience, for research use it needs to be further optimised. For this, a few parts of the histone replacement system were taken under consideration in order to improve 3 main points:

1. Expression strength of replaced histone
2. Cell survival after induction of replacement
3. Comparability between histone mutant clones

4.7.1 Re-expression histone copy number and expression strength

In the first version of histone replacement system, H2B levels after induction of the system did not match endogenous expression levels and cell survival was low in many of the clones. To address that, the integration copy number of replacement histone could be increased, resembling the endogenous organisation of histone genes which are also present in multiple copies (Grandy et al., 1987). While integration via the Sleeping Beauty transposase already mediates multi-copy integration (Wächter et al., 2014), each integrated plasmid could contain more than one copy of replacement histone to further simplify the generation of clones with sufficient H2B copy numbers.

Additionally, in order to increase the expression strength from the tet-responsive promoters, an improved tet-activator (rtTA-V16) (Zhou et al., 2006) with higher sensitivity and stronger expression could be used instead of the traditional tet-activator (rtTA3) (Gossen et al., 1992; Gossen et al., 1995).

4.7.2 Semi-targeted integration of replacement histone

For integration of both the shRNA and replacement histone expressing plasmid, random integration via the Sleeping Beauty transposase was used. Random integration of plasmids into the host genome poses the risk of damaging important genomic regions such as actively transcribed genes (Liang et al., 2009; Huang et al., 2010). Moreover, when creating cell clones from pools with random integration, these clones will inherently be different in both the location of integration and copy number, ultimately reducing comparability between mutants (Figure 31A).

As the needed copy number for efficient knock-down and re-expression is unknown but likely larger than 1, rational selection of integration locations is difficult. Not all genomic locations are equally suitable for plasmid integration due to locus specific accessibility, expression strength and long-term stability (Sadelain et al., 2012). As such, random integration with a subsequent functional screening has several benefits for this purpose. To combine random-integration with a more targeted approach, recombination sites, so called ”landing-pads”, can be used (Sauer et al., 1988; Schlake et al., 1994). Once integrated, landing pads can be targeted specifically to integrate a donor DNA at their specific location (Figure 31B).

4.7.2.1 Recombinase mediated cassette exchange

To integrate the histone mutants into the landing pads, recombinases such as Cre or FRT can be used (Turan et al., 2013). As more than one landing pad will be integrated into the genome, integrases such as Bxb1 are the preferred choice as they do not recombine between multiple landing pads causing chromosomal translocations or inversions (Xu et al., 2013; Gaidukov et al., 2018). Flanking

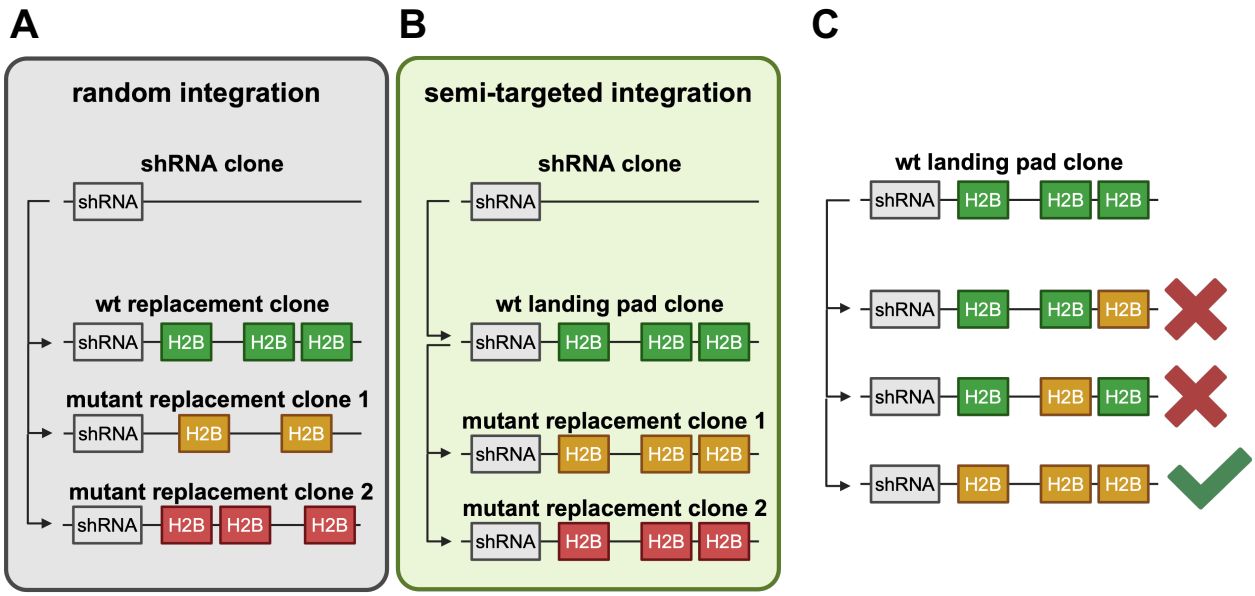

Figure 31: Strategy for semi-targeted integration of replacement histone.

Schematic representation of the creation of histone replacement cell clones by different methods. **(A)** Random integration. A parental shRNA knock-down cell clones is used to randomly integrate wt or mutant replacement histone. The integration copy number and locations between cell clones will inherently be different, reducing comparability between clones. **(B)** Semi-targeted integration. A parental shRNA knock-down cell clones is used to randomly integrate wt replacement histone landing pads. These landing pads are subsequently targeted to exchange the contained wt histone with mutants. This results in cell clones that have identical integration copy numbers and locations, improving comparability between clones. **(C)** Negative selection for semi-targeted integration. After targeting landing pads, cells in which not all landing pads have been successfully targeted need to be eliminated. *Created with biorender.com*

landing pads with two Bxb1 recombination sites, a longer sequence of DNA can be replaced by recombination with another template (Inniss et al., 2017).

This recombinase mediated cassette exchange (RMCE) would be ideal for a histone replacement system. A wildtype replacement histone could first be randomly integrated into the genome and cells screened for their survival, resulting in cell clones with replacement histone integrated in sufficient amounts in favourable loci. The wildtype replacement histone expression cassette can then be exchanged for one containing a desired histone mutant. Cells would then be selected for the successful exchange of all wildtype expressing loci. This way, the resulting cells should be isogenic, apart from the histone mutation.

4.7.2.2 Negative selection

When performing RMCE on multiple landing pads, a selection system is needed to ensure targeting of all landing pads (Figure 31C). This is only possible with a negative selection marker, as opposed to positive selection markers like antibiotic resistance. There are multiple negative selection markers

available, for example so called ”suicide genes” which can produce toxic metabolites or trigger cell death (Tiberghien, 1994). If a landing pad remains untargeted, expression of the suicide gene from this locus will trigger cell death. Inducible Caspase9 (iCasp9, Straathof et al., 2005), herpes simplex virus thymidine kinase (HSVtk) and bacterial cytosine deaminase (bCD) were tested as suicide genes in chicken cells but were found to not be sensitive enough or to produce toxic compounds which also kill cells not expressing the gene (data not shown).

Therefore sortable markers were selected for selection of fully targeted cells. The truncated cell surface protein LNGFR was used for magnetic cell sorting (Siebenkotten et al., 1997) and EGFP for fluorescence based cell sorting (Hulett et al., 1969).

4.7.3 Design of 2nd generation plasmids

The 2nd generarion histone replacement plasmids were created to incorporate the improved design features. The shRNA expressing plasmid was changed to include the optimised rtTA-V16 tet-activator to drive stronger expression from tet-responsive promoters (Zhou et al., 2006) (Figure 32A). The new landing pad plasmid was created with a constitutive promoter driving expression of the selectable surface marker LNGFR, the sortable marker EGFP and a hygromycin resistance gene. Downstream BpiI restriction sites allow for the integration of inducible histone expression cassettes in multiple copies by using Golden Gate assembly. Between the constitutive promoter and LNGFR as well as downstream of the histone expression cassettes, an attP-wt and modified attP-GA sequence (Jusiak et al., 2019; Low et al., 2022) are inserted to be used for Bxb1 mediated RMCE (Figure 32B). The replacement histone was tagged with a splitGFP tag instead of the previously used OLLAS tag, as the splitGFP can be used for visualisation of chromatin for live cell microscopy by complementation with the larger GFP fragment (Kamiyama et al., 2016; Romei et al., 2019) (Figure 32C).

4.8 Generation of 2nd generation stable histone replacement cells

4.8.1 Generation of stable histone knock-down cell clones

To allow for the later creation of cell clones for the replacement of any canonical histone, shRNA cell clones were created for all histones using the new, improved plasmids and the shRNAs selected before (section 4.6). DF-1 chicken fibroblasts were transfected with the appropriate plasmids (pSBtet-Puro-shggH2B-3(5p)-Neo-rtTAV16-Cloning et seq.) together with a plasmid expressing the Sleeping Beauty transposase to integrate the shRNA into the genome. Cells were selected with G418 for two weeks and single cell clones were prepared by limited dilution.

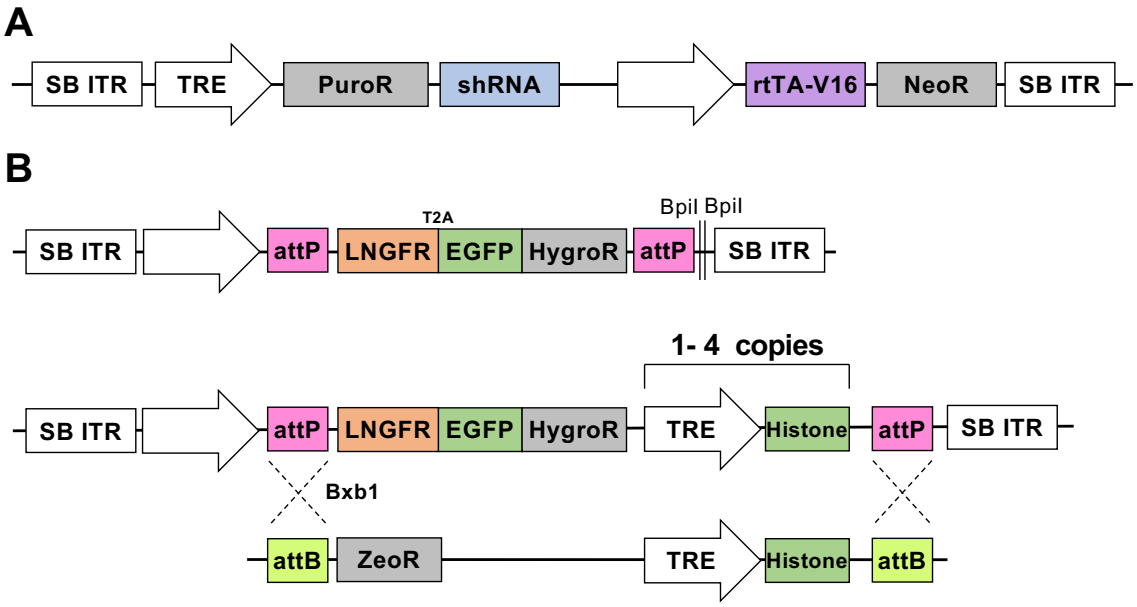

Figure 32: Design of 2nd generation histone replacement plasmids.

(A) Schematic representation of the revised shRNA expressing plasmid. A tet-responsive promoter drives expression of a puromycin resistance and a histone targeting shRNA. A constitutive promoter drives expression of an improved tet-activator and a neomycin resistance gene to select for genomic integration of the construct. Sleeping beauty sequences flank the cassette to allow for transposase mediated genomic integration. PuroR = puromycin resistance, NeoR = neomycin resistance. **(B)** A constitutive promoter drives expression of a truncated NGFR surface protein that allows for the sorting and enrichment of cells expressing this construct. A T2A site allows separate expression of an EGFP-hygromycin resistance fusion protein. A cloning site allows for the integration of multiple copies of shRNA resistance replacement histone under control of a tet-responsive promoter. attP-wt and attP-GA sites between the promoter and LNGFR and after the histone expression cassette allow for the recombinase mediated cassette exchange (RMCE) via the Bxb1 integrase. The RMCE plasmid exchanges the LNGFR-EGFP-HygroR construct for a zeocin resistance gene to allow for the enrichment of cells with successful recombination. At the same time the replacement histone can be exchanged for a mutant. Loss of LNGFR and EGFP expression can be used for sorting recombined cells. HygroR = hygromycin resistance, ZeoR = zeocin resistance.

Cell clones were expanded and functionally tested based on cell survival after induction of the shRNA as described before (subsection 4.5.1). Clones were selected based on overall growth in the uninduced condition, survival after induction and survival after induction with selection for shRNA expression with puromycin. This yielded 2 cell clones for each of the canonical histones, which died within 4 days after induction of the histone targeting shRNA (Figure 33).

4.8.2 Generation of stable histone replacement cell clones

As H2B is the main research interest in this study, H2B replacement cells were created by stably transfecting the H2B shRNA clones A2 and D3 with wildtype chicken H2B expressing landing pad plasmids containing 1 to 4 H2B expression cassettes per landing pad (pHEX-RMCE-LNGFR-

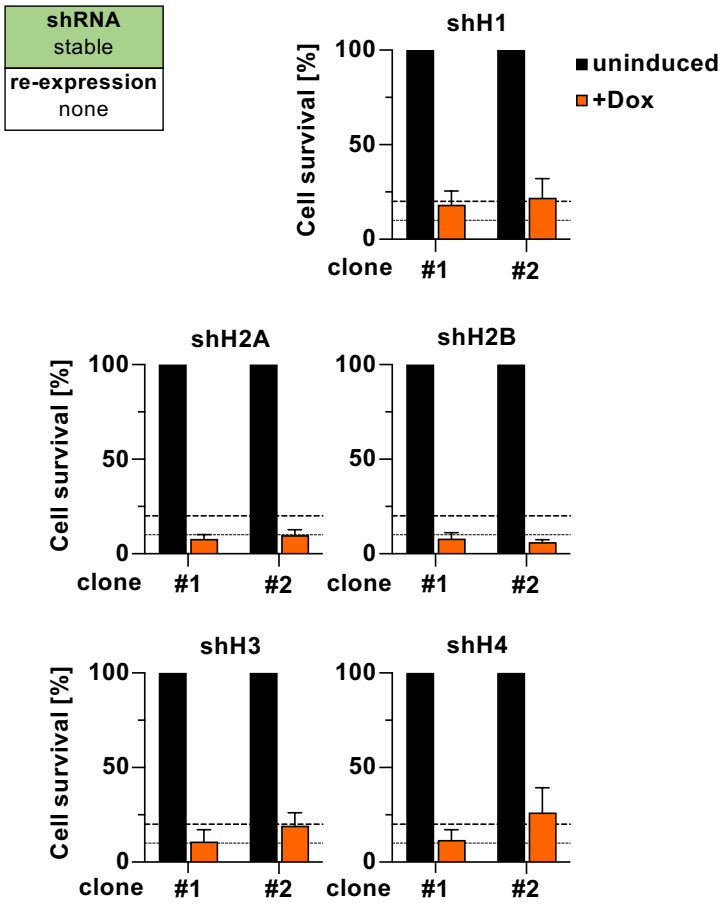

Figure 33: Generation of stable histone knock-down cell clones.

DF-1 chicken fibroblasts were transfected with inducible chicken histone targeting shRNA plasmids as indicated and single cell clones were seeded into 96-well plates. The resulting clones were initially functionally screened by measuring cell survival after induction of the shRNA with doxycycline (1 µg/mL, 4 d) compared to uninduced cells. Clones with highest reduction in cell survival after induction were selected and cell survival data from 3 independent biological experiments is shown as means ± SD for 2 shRNA expressing clones per shRNA. 10 % and 20 % are indicated by dashed lines.

1xggH2B-GFP11 et seq.). Cells were selected with hygromycin for two weeks and FACS sorted based on EGFP expression to yield stable cell pools.

First, the obtained cell pools were functionally tested based on cell survival after induction of the replacement system as described before. Figure 34A shows that after induction cell survival in the shRNA cell clones is only approximately 10 % as observed before (Figure 26 and Figure 33). However, stable pools containing one H2B copy per landing pad plasmids based on the shRNA clone A2 show an increased survival of approximately 40 %. This survival increased with each additional H2B copy per plasmid to almost 60 % for the 3 copy plasmid. Interestingly, survival of the pools with the 4 copy plasmid was lower and on a similar level as with the 1 copy plasmid. Survival for the pools based on the D3 shRNA clone was overall lower with only a moderate increase in cell survival with increasing copy number (Figure 34A). H2B replacement efficiency

was assessed by inducing the cell pools with doxycycline for 4 d and subjecting whole cell lysates to SDS-PAGE and immunoblotting with staining against H2B. This showed a replacement efficiency of approximately 20 % in the A2 based pools with 1 H2B copy. This increased to an efficiency of approxiamately 60 % with the 3 copy plasmids. No further increase with 4 H2B was observed (Figure 34B). This indicates that the knock-down of endogenous H2B is rescued to some extent by the replacement H2B. Moreover, survival of the cell pool at this stage was much higher than with the first generation histone replacement (Figure 27).

As the 3x H2B pool based on the A2 shRNA cell clone showed the highest overall survival after induction, single cell clones were prepared from this cell pool by limited dilution. Also, these single cell clones were tested functionally based on cell survival after induction of the replacement system as described before (subsection 4.5.2 and Figure 34C). Picked clones did reflect the survival of the pools they originated from (Figure 34D). As histone replacement clones before showed problems with matching the endogenous expression level, a larger number 24 of clones was selected for a preliminary expression screen and further narrowed down to 8 clones.

To test replacement efficiency and histone expression level, clones were grown for 4 d without or in the presence of doxycycline and total protein was extracted. Samples were analysed by Western blotting with staining against H2B. This revealed that for all clones expressed the replacement H2B but the average expression levels remained significantly lower than the levels of the endogenous H2B (Figure 35A and B). Replacement efficiency, as quantified from the ratio of replacement H2B to total H2B was between 40 % to 50 % for all clones (Figure 35C).

In summary, these experiments show that an inducible reduction of endogenous histones is possible, although they belong to the group of the most abundant proteins. The work also demonstrates that the inducible re-expression of histones is possible. However, in the 2nd generation system, the endogenous histone protein levels were not reached. Possible reasons and strategies for improvement will be discussed in the next section.

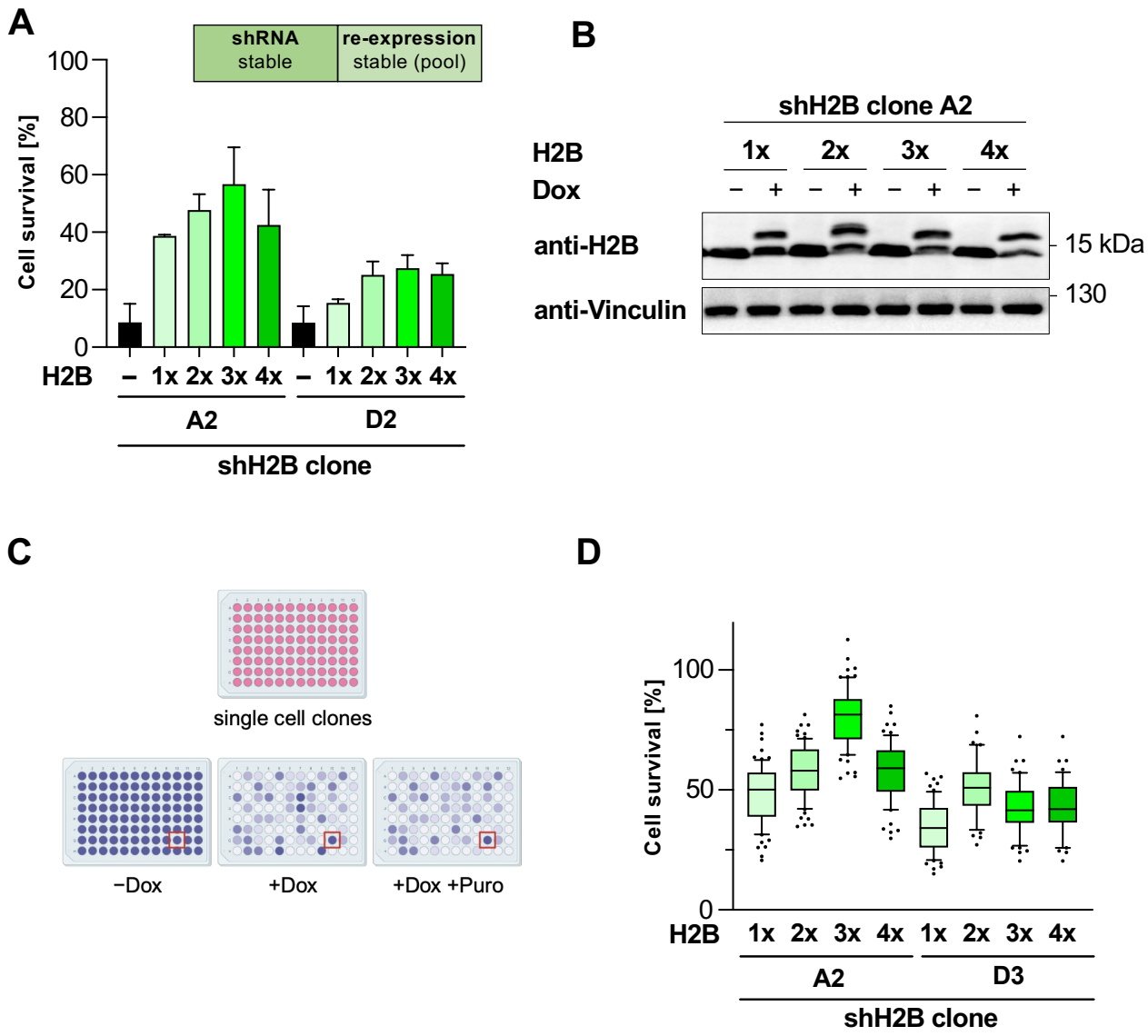

Figure 34: Generation and testing of 2nd generation chicken H2B replacement cell clones.

(A) 2 cell clones with stable integration of inducible H2B targeting shRNA (A2 and D2) were transfected with landing pad plasmids containing 1 to 4 copies of shRNA resistant wildtype replacement H2B and selected for the integration of that plasmid with hygromycin for 14 d. The resulting stable cell pools were induced with doxycycline (+Dox, 1 µg/mL, 4 d) or remained uninduced. Cell survival was measured by crystal violet staining and normalised to uninduced controls. Data from 3 independent biological replicates as means ± SD. **(B)** Replacement cell pools based on shRNA clone A2 as shown in (A) were induced with doxycycline (1 µg/mL, 4 d) or left untreated. Cell extracts were analysed via Western blotting for H2B. A representative blot is shown. The lower and upper band in the H2B blot correspond to endogenous or tagged replacement H2B. **(C)** Single cell clones were prepared from stable replacement pools based on H2B shRNA expressing clone A2 as shown in (A) by limited dilution seeding into 96-well plates. Clones were split into 3 different plates that remained untreated (-Dox), were induced (+Dox, 1 µg/mL, 4 d) or were induced and selected with puromycin (+Dox +Puro). Cell survival was determined by crystal violet staining. *Caption is continued on page 97.*

Figure 34 (cont.): Generation and testing of 2nd generation chicken H2B replacement cell clones.

A schematic result is shown. The red box marks a clone growing in the absence of Dox and also after induction with Dox and also surviving additional selection for shRNA expression with puromycin. *Created with biorender.com* **(D)** Cell clones obtained in (C) were functionally tested as in (A). Cell survival was measured by crystal violet staining and normalised to uninduced controls. Data from 3 independent biological replicates are shown. Boxes indicate interquartile range (IQR), whiskers indicate 1.5 IQR and means are indicated by horizontal lines.

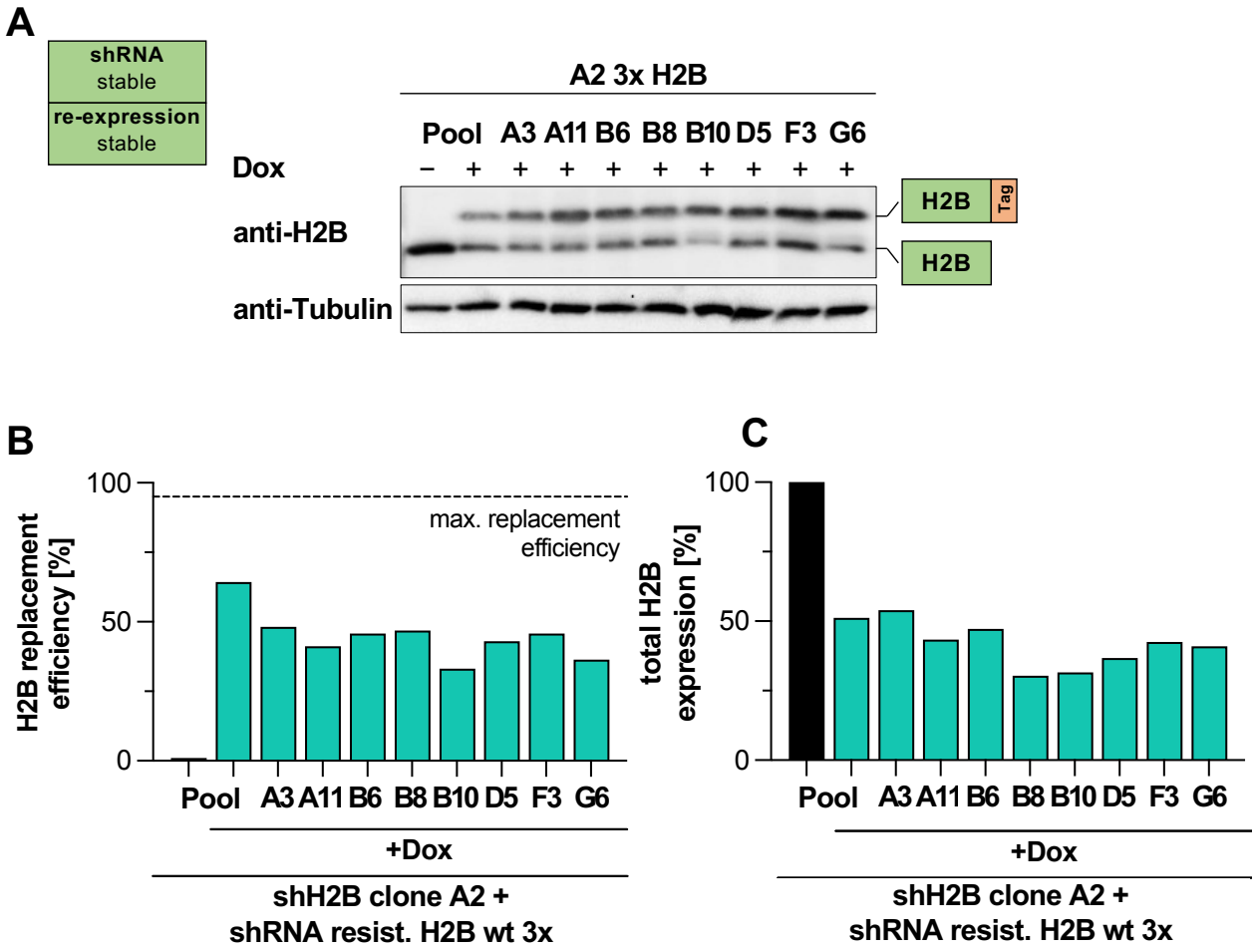

Figure 35: Generation and testing of 2nd generation chicken H2B replacement cell clones.

(A) 8 selected stable H2B replacement clones and the parent pool were induced with doxycycline (1 µg/mL, 4 d) or left uninduced. Cell extracts were analysed via Western blotting for H2B. A representative blot is shown. The lower and upper band in the H2B blot correspond to endogenous or tagged replacement H2B as schematically indicated on the right. **(B)** Replacement efficiency from blot shown in (A) was quantified as the ratio of the upper (replacement) histone H2B to the total H2B level (replacement + endogenous H2B). **(C)** Total H2B expression level from blot shown in (A) was quantified and normalised to uninduced control.

5 Discussion

Post-translational modifications of histones are fundamental to many cellular functions. This work addresses the molecular mechanisms leading to the spatio-temporal control of H2B S6ph in mitosis as well as the development of a novel histone replacement system to better study the function of such PTMs.

5.1 Mechanisms governing regulation of H2B S6ph

Mitosis is a tightly regulated and intricate process that relies on the orchestration of multiple signalling mechanisms to ensure faithful chromosome segregation (Nigg, 2001; Gelens et al., 2018). Any error in this process can potentially lead to the loss of genetic material and promote genetic instability, a hallmark of cancer (Pihan et al., 1999; Negrini et al., 2010). Therefore, understanding the mechanisms underlying this critical cell cycle phase is fundamental. Mitosis is driven by a sequence of events that rely heavily on signalling cascades involving kinases, phosphatases, and their substrates (Poon, 2007; Dephoure et al., 2008). One of many such substrates is histone H2B which is specifically phosphorylated during mitosis (Seibert et al., 2019) among other histones (Schmitz et al., 2020). While previous studies have shown that H2B S6ph is maintained only in the early stages of mitosis at centromeres (Seibert et al., 2019), this study investigates the regulation of this modification in more detail.

Data presented here suggest a model in which global CDK1 activity in mitosis phosphorylates H2B S6ph. This kinase activity is opposed by the phosphatase complex PP1/RepoMan. The phosphatase is locally inhibited by Aurora B kinase located at the inner centromere as part of the chromosomal passenger complex, effectively protecting H2B S6ph from dephosphorylation until Aurora B activity declines in anaphase, as schematically shown in Figure 36.

5.1.1 PP1 dephosphorylates H2B S6ph

PP1 phosphatases all contain one of three catalytic subunits and form a complex with one or more regulatory subunits to achieve substrate specificity (Peti et al., 2013). While the importance of PP1 for the dephosphorylation of H2B S6ph has been previously identified, it was not clear which PP1 enzyme complex catalyses this reaction. Data shown here demonstrate that although PP1 catalytic subunits on their own show no pronounced substrate specificity, only two of the three PP1 subunits can dephosphorylate in a cell-free setting. PP1α, PP1β and PP1γ share a high

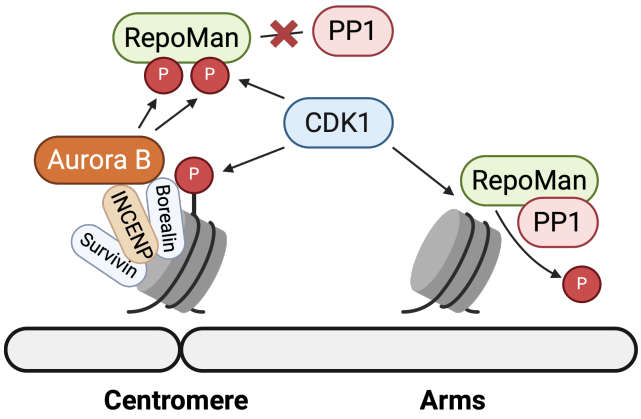

Figure 36: Model of regulatory network controlling H2B S6ph.
In mitosis, global CDK1 activity phosphorylates bulk H2B. PP1/RepoMan counteracts this kinase activity locally. At the inner centromere, Aurora B (as part of the CPC) prevents PP1/RepoMan activity by phosphorylation of RepoMan to inhibit PP1 binding to RepoMan and RepoMan to chromatin, thereby protecting H2B S6ph. Additional regulation of this is provided by CDK1. *Created with biorender.com*

sequence similarity in their catalytic domains and differ mainly in their extreme termini (Shima et al., 1993). The mechanism by which only PP1α and PP1γ are able to dephosphorylate H2B is not clear. In cells, depletion of either PP1α or PP1γ independently both delayed dephosphorylation of H2B S6ph from early to late anaphase. Combined depletion of both subunits abolished H2B S6ph dephosphorylation almost completely, suggesting that it is exclusively dephosphorylated by PP1α and PP1γ, independently. While a contribution of PP1β to the dephosphorylation of H2B S6ph seems unlikely, depletion experiments performed here remained inconclusive due to insufficient knock-down efficiencies. Future experiments could follow up by creating stable PP1β knock-out cells using CRISPR/Cas9. Interestingly, until metaphase in cells, PP1β is mainly associated with chromosomes while PP1γ and PP1α localise to the centrosomes and spindle, respectively (Andreassen et al., 1998). In interphase, all three catalytic subunit isoforms are located in cytoplasm and nucleus (Andreassen et al., 1998). There, PP1β was shown to be involved in histone dephosphorylation in different processes (Zhang et al., 2013). Yet, for H2B S6ph and many other histone PTMs, PP1γ and possibly PP1α are most likely the major phosphatase subunits (Shimada et al., 2010; Qian et al., 2011, 2013).

5.1.2 PP1/RepoMan controls H2B S6ph in space and time

While direct binding of PP1 catalytic subunits has been shown for other substrates, H2B does not contain a canonical binding site for PP1 (RVxF). Thus, a targeting factor that recruits PP1 to H2B, or chromatin in general, is likely to be involved in the dephosphorylation of H2B S6ph in cells. Of the various regulatory subunits which are known to target PP1 to chromatin in mitosis,

this work identified RepoMan to be essential for the timely dephosphorylation of H2B S6ph by depletion experiments. PP1/RepoMan is a well-studied PP1 complex that not only dephosphorylates H2B S6ph, but also other mitotic phosphorylations such as H3 T3ph (Qian et al., 2011), while for the dephosphorylation of H3 S10ph and H3 S28ph there is conflicting evidence regarding the involvement of RepoMan as a targeting factor (Qian et al., 2011; Vagnarelli et al., 2011). RepoMan directly binds PP1 subunits with differing affinities (Kumar et al., 2016) and also directly binds the tails of H2B and H3, thereby targeting PP1 catalytic subunits to chromatin (Vagnarelli et al., 2011; De Castro et al., 2017).

The almost exclusive reliance of H2B S6ph dephosphorylation on RepoMan in anaphase suggests that RepoMan is the main PP1 targeting subunit in this context. However, under combined knock-down conditions for RepoMan, PP1α and PP1γ, an extension of H2B S6 phosphorylation beyond anaphase into telophase was observed. While this could be explained by additive effects of knock-down efficiencies, it is also possible that other PP1 targeting factors, besides RepoMan, can compensate for its loss to a limited extent. Knock-down experiments presented in this study failed to support a role for the PP1 chromatin targeting subunits PNUTS and Ki-67, but the involvement of one of the $>$200 regulatory PP1 subunits in H2B S6ph dephosphorylation can not be excluded. Such targeting factors include NIPP1 (Aleyde et al., 1995; Trinkle-Mulcahy et al., 1999, 2001), Neurabin I (Hsieh-Wilson et al., 1999) and several others (Sukackaite et al., 2017). It will be interesting to investigate if any of these targeting factors fulfil a function in H2B S6ph in the absence of RepoMan.

RepoMan is often described as interacting mainly with PP1γ and only to a very limited extent with PP1α (Trinkle-Mulcahy et al., 2006; Peng et al., 2010; Kumar et al., 2016). Additionally, PP1α is not described to be recruited to chromatin after anaphase onset (Trinkle-Mulcahy et al., 2006). Nonetheless, in this study, both PP1α and PP1γ were found to be necessary for the dephosphorylation of H2B S6ph after metaphase. As discussed above both subunits likely work in an independent manner but in conjunction with RepoMan. Together with the direct interaction between RepoMan and PP1α, this suggests a functional relationship between both proteins. Whether PP1α is targeted to chromatin by RepoMan directly or if PP1α fulfils important regulatory functions, such as opposing regulatory phosphorylations of RepoMan, is unclear. Further studies will investigate this in more detail.

5.1.2.1 Temporal control

The involvement of PP1/RepoMan in the dephosphorylation of H2B S6ph is not surprising given that PP1/RepoMan is also responsible for the dephosphorylation of the mitotic histone PTM H3 T3ph, and possibly H3 S28ph and H3 S10ph (Qian et al., 2011; Vagnarelli et al., 2011). However, the dephosphorylation of these modifications occurs with different kinetics where H2B S6ph is removed first as shown in this study. This could be explained by the involvement of additional regulatory

factors restricting PP1/RepoMan phosphatase activity to H2B, before allowing dephosphorylation of H3. It is also possible, and more likely, that these differences are a result of the different kinases responsible for these modifications. While H2B S6 is phosphorylated by CDK1, H3 S10 is phosphorylated by Aurora B and H3 T3 is phosphorylated by Haspin (Wei et al., 1998; Hsu et al., 2000; Dai et al., 2005; Wang et al., 2010). CDK1 drives mitotic entry and remains active during the early stages of mitosis through its association with cyclin B1 (Solomon et al., 1990; Gavet et al., 2010). This activity is rapidly lost after satisfaction of the SAC which triggers ubiquitination of cyclin B1 by APC/C and its subsequent proteasomal degradation (Murray et al., 1989; Clute et al., 1999; Chang et al., 2003). Aurora B on the other hand, while most active during active SAC signalling, retains its activity even after anaphase onset when it is removed from the centromeres and relocalises to the central spindle and ultimately the forming midbody (Emanuele et al., 2008). This creates a gradient of Aurora B activity which might maintain phosphorylation of H3 S10 (Carmena et al., 2012; Afonso et al., 2014; Papini et al., 2021). Haspin is similarly retained on chromosomes for a while after anaphase onset (Dai et al., 2005), again possibly allowing for H3 T3ph to remain phosphorylated while H2B S6ph is already dephosphorylated by PP1/RepoMan.

5.1.2.2 Spatial control

H2B S6ph, H3 T3ph and H3 S10ph differ not only in their temporal regulation but also in their spatial distribution. Both H2B S6ph and H3 T3ph are localised at the centromeres (Dai et al., 2005; Seibert et al., 2019) and are restricted to the inner centromere by local inhibition of PP1/RepoMan through Aurora B mediated phosphorylation of PP1 and RepoMan. The association of RepoMan with PP1 and chromatin is regulated via phosphorylation by both CDK1 and Aurora B and additionally by dephosphorylation via PP1 and PP2A (Qian et al., 2015). On the other hand, Aurora B localisation itself is partially dependent on RepoMan activity, as RepoMan restricts H3 T3ph to the centromeres, which controls localisation of the CPC and hence Aurora B. Aurora B phosphorylates the PP1 binding site of RepoMan at multiple locations including the SLiM at T394 (Vagnarelli et al., 2011; Qian et al., 2013; Kumar et al., 2016; Manzione et al., 2020). Additionally, phosphorylations in the chromatin binding domain around S893 dissociate RepoMan from chromatin (Xin et al., 2020). This essentially protects centromeric phosphorylation of histone residues from PP1/RepoMan. At the chromosome arms, in the absence of Aurora B, PP1/RepoMan constantly opposes phosphorylation. Although bulk PP1/RepoMan is recruited to chromatin after anaphase onset, this suggest that a limited pool of PP1/RepoMan is already associated in earlier mitotic stages as has been observed before (Trinkle-Mulcahy et al., 2003).

H3 S10ph and H3 S28ph are spread along the chromosome arms (Hendzel et al., 1997; Goto et al., 2002). Both are phosphorylated by Aurora B. Interestingly, Aurora B activity is mostly restricted to the centromeres where it is located as part of the CPC and should not phosphorylate chromosome arms due to being physically located away from them. Additionally, constant phosphatase activity

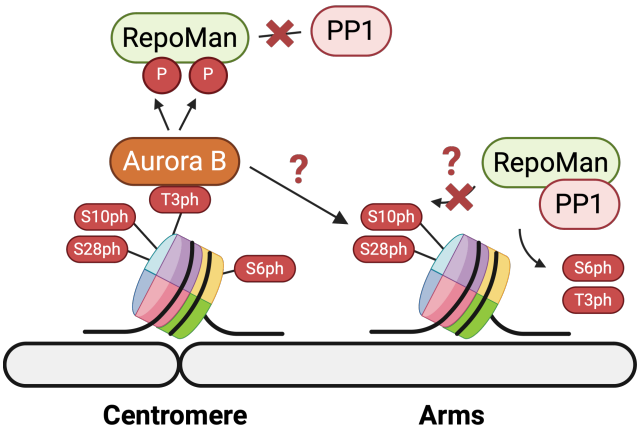

Figure 37: PP1/RepoMan act differently on histone PTMs.
While Aurora B protects H2B S6ph and H3 T3ph from dephosphorylation at centromeres but not chromosome arms, it apparently phosphorylates and protects H3 S10 and H3 S28 on chromosome arms. *Created with biorender.com*

is exhibited on chromatin as shown by the restriction of H2B S6ph to the centromeres and its spreading after removal of RepoMan. This raises the question of how PP1/RepoMan distinguishes between H3 S10 and H2B S6, since only the latter appears to be dephosphorylated prior to anaphase (Figure 37). How is peripheric H3 S10ph protected from dephosphorylation by PP1/RepoMan when its kinase, which is also protecting centromeric H2B S6ph, is restricted to centromeres? This may point to the involvement of additional, as yet unidentified factors.

5.2 Functional relevance of H2B Serine 6 phosphorylation

Despite the focus of this work being on the regulation of H2B S6ph in mitosis, the functional relevance of these modifications remains an open and interesting question. Studying the function of H2B S6ph is complicated by the fact that its regulators are essential mitotic players. Disruption of writers or erasers of H2B S6ph, such as CDK1 or Aurora B leads to mitotic catastrophe, as cells fail to enter mitosis or exit mitosis prematurely under inhibitory conditions (Hauf et al., 2003; Potapova et al., 2006). Mutant over-expression experiments have the potential to indicate whether a residue has strong dominant effects when applied ectopically (by mutation) but are not reliable. While reader proteins for H2B S6ph, like 14-3-3 proteins and SET have been identified before, they are not exclusive to H2B S6ph (Macdonald et al., 2005). Therefore, any effects observed when perturbing these proteins cannot be attributed to H2B S6ph alone. For most proteins, studies about the function of a specific residue or PTM rely on the over-expression or even complete replacement of the protein of interest with a mutant version (as exemplified in Dittmer et al. (1993)).

5.2.1 H2B S6ph in sister chromatid cohesion

Previous studies have suggested that H2B S6ph is potentially important for faithful chromosome segregation in mitosis and have shown that H2B S6ph prevents the binding of I2PP2A/SET to chromatin (Seibert et al., 2019). SET is a known cellular inhibitor of PP2A phosphatase and has been shown to regulate sister chromatid cohesion during meiosis and possibly mitosis as well (Chambon et al., 2013; Krishnan et al., 2017).

Cohesion between sister chromatids is established during replication by a protein complex called cohesin (Uhlmann et al., 1998). Cohesin forms a ring like structure which physically links both sister chromatids. Cohesion is important for normal chromatin function (e.g. in HR DNA repair), but must be removed in mitosis as the sister chromatids need to be separated (Hirano, 2000; Watrin et al., 2006; Piazza et al., 2021). In higher eukaryotes this is a two-step process in which bulk cohesin is removed from the chromosome arms by phosphorylation of one of the complex members (prophase pathway) (Waizenegger et al., 2000). At the centromere, cohesion is maintained as it is necessary to allow for tension by the pulling forces of the opposing spindles to build across the kinetochores and centromere (Zhou et al., 2002; Pinsky et al., 2005). Shugoshin protects cohesin from this removal by recruitment of PP2A phosphatase (Kitajima et al., 2004; McGuinness et al., 2005). Only when the SAC is satisfied, centromeric cohesin is removed via proteolytic cleavage by Separase (Separase pathway) (Hauf et al., 2001; Nakajima et al., 2007). SET binding, possibly through its PP2A inhibitor function, inactivates Shugoshin-PP2A and allows the subsequent removal of centromeric cohesion via proteolytioc cleavage by Separase (Higgins et al., 2013).

This model suggests that the presence of H2B S6ph or a phosphomimetic H2B S6E mutant protects cohesin from removal. Over-expression of such a mutant did not increase sister chromatid or centromere cohesion and also did not result in mitotic aberrations. While this could indicate that H2B S6ph does not function in the protection of cohesion and ensuring mitotic fidelity, it is also possible that H2B S6ph only functions in a group with other modifications. Indeed, SET has been shown to bind not only the unmodified tail of H2B but also of the tail H3. H3 T3ph and H3 S28ph have previously been shown to also prevent binding of SET as generally phosphorylations of the H3 histone tail do (Schneider et al., 2004; Kim et al., 2012). If both histone PTMs have overlapping functions in protecting centromere cohesion in mitosis, this could be tested by simultaneous expression of H2B S6 and H3 T3 mutants.

Although over-expression of histone mutants has been done for other histone residues (Ahmad et al., 2021; Sinha et al., 2023), these experiments do not necessarily result in a strong observable phenotype as the fraction of over-expressed mutant histone in the chromatin is generally low. Since a histone modification might only fulfil its function when present in higher densities, over expression experiments are not reliable for excluding a function. To further study the role of H2B S6ph in chromosome segregation, a more targeted approach for expression of mutant histone

could be used. Over-expression of a histone mutant generally leads to incorporation of that mutant into all genomic loci. If its incorporation could be targeted to specific locations, the local density of that mutant could be increased (Barnhart et al., 2011). Targeted incorporation of H2B mutants into centromeric nucleosomes could be achieved by targeting of the protein to CENP-A or centromeric alpha-satellite repeats as fusion protein with appropriate binding domains (Shuaib et al., 2010; Suntronpong et al., 2016). Even outside the centromere, this could be experimentally investigated by the expression of a LacI-EGFP-H2B mutant fusion protein to target mutant H2B specifically to genome-integrated LacO repeats (Janicki et al., 2004; Jegou et al., 2009). Alternatively, local H2B S6 phosphorylation by locus specific targeting of CDK1 could be used, as described before (Seibert et al., 2019). Cohesion or SET binding at this phosphorylated or mutant-containing locus could be monitored in mitosis. ChIP(-seq) experiments for these factors, especially the cohesin subunit Rad21, could be performed and cohesin presence in loci with H2B S6A/E mutant occupancy could be investigated.

Shindo et al. (2012) have developed a fluorescence based biosensor for the separase mediated cleavage of cohesin. This, or similar systems (Yaakov et al., 2012), could be used together with H2B S6A/E mutants to investigate whether these mutants induce changes in the timing of cohesin removal even though overall cohesion apparently remains unchanged.

5.2.1.1 H2B S6ph in meiosis

In mitosis, cohesion between sister chromatids along the chromosome arms is lost, beginning in prophase (Ishiguro, 2019). Only after triggering anaphase, cohesin is removed from centromeres. In meiosis I, cohesin is retained on chromosome arms until all recombination events between homologous sister chromatids have taken place. Before anaphase I, arm cohesion is then removed (Ishiguro, 2019). In contrast to mitosis, centromeric cohesion is maintained throughout anaphase I and only removed before anaphase II (Ishiguro, 2019). As H2B S6ph has been proposed as a protector of centromeric cohesion, it would be interesting to investigate its regulation in meiosis. Does H2B S6ph, which resembles regulation of cohesion in mitosis both in time and space, also resemble cohesion in meiosis? This would be a strong indicator of a relevant functional connection between H2B S6ph and cohesion. This is particularly relevant as the proposed H2B S6ph reader protein SET is a known cohesion regulator in meiosis (Chambon et al., 2013; Sanyal et al., 2013). Preliminary work by a collaborator has previously confirmed phosphorylation of H2B also during meiotic division in mice (Willy Baarends, Rotterdam, unpublished). It would therefore be interesting to investigate whether H2B S6ph is maintained along chromosome arms during prophase I similar to arm cohesion and at centromeres during anaphase I in order to understand more about its function.

5.2.2 H2B S6ph in cancer cells

Cancer cells differ from non-transformed cells in several ways (Hanahan et al., 2011), including disruption of regulatory networks. This is the case for the regulatory network identified in this work, comprising Aurora B, RepoMan and Mklp2 (Krasnoselsky et al., 2005; Qi et al., 2007; González-Loyola et al., 2015). This study demonstrates that the regulation of H2B S6ph is different in a subset of cancer cells compared to non-cancerous cells. While Aurora B and RepoMan are commonly over-expressed in some cancers (Manzione et al., 2020), it appears that in the cells identified here the localisation of Aurora B is dysregulated. Aurora B is normally relocalised from the centromeres to the central spindle and midbody shortly after anaphase onset (Earnshaw et al., 1991; Adams et al., 2001). This relocalisation, however, was shown to not always occur in a timely manner. Rather, it appears that Aurora B can be retained on chromatin and keep its protective function on H2B S6ph even after anaphase onset. While this occurs in all cells observed in this study, it is much more pronounced in some of the cancer cells such as HT-29.

The implications of this are not clear, however. Besides its function in the regulation of histone PTMs, Aurora B has an important function in the SAC and in later phases in cell division (Giet et al., 2001; Basant et al., 2015). At the central spindle and later midbody, Aurora B activity is needed for the correct formation of the contractile ring allowing for cytokinesis. A delayed localisation of Aurora B and delayed initiation of contraction might cause division defects.

In this context it is interesting to note that H2B S6ph was often observed on mitotic aberrations like lagging chromosomes and anaphase bridges. While both phenomena occur by different mechanisms, the former being caused by fragmented chromosomes that are not attached to the spindle or by chromosomes with erroneous attachments, the latter are caused by aberrant cohesion or ongoing DSB repair via HR (Elbakry et al., 2021). Whether H2B S6ph is important in either of these mechanisms is not clear at this point. It also not clear if this unexpected presence of this modification is a cause or a consequence of one of these mitotic errors. However, it is possible that erroneous Aurora B localisation itself leads to the observed defects and that H2B S6ph is a byproduct of this localisation.

While other histone residues are more frequently mutated in cancer cells, H2B S6A are described, mainly for thyroid cancers (Nacev et al., 2019). Interestingly, H2B S6ph was observed in a non-malignant prostatic cell line, while this modification did not occur in a prostate cancer cell line (Cang et al., 2016). It will thus be relevant to study whether dysregulation of H2B S6ph has a functional relevance in the growth of malignant cells.

5.2.3 H2B S6ph in interphase

Although H2B S6ph is not detected in non-synchronised cells by either immunoblotting or immunofluorescence, this does not exclude a potential occurrence and function of H2B S6ph in interphase. The common mitotic marker phosphorylation of H3 S10 has been shown to occur at specific genomic locations in interphase cells with a possible role in transcriptional activation (Nowak et al., 2000), as well as in apoptosis (Park et al., 2012) apart from its mitotic role in chromosome condensation. Phosphorylation of H3 S28 has also been previously observed in interphase cells in correlation with transcriptional activity and chromatin relaxation (Lau et al., 2011). In both cases, the kinases responsible for the phosphorylation of these residues are different from the kinases involved in mitosis. It would therefore be interesting to investigate a possible presence and function for H2B S6ph in interphase cells and to see whether it can be induced by external stimuli.

The activity of the mitotic driver kinase CDK1 is suppressed in interphase by the absence of cyclin B and by inhibitory phosphorylation of the kinase (Serpico et al., 2023). However, while CDK1 is the main kinase for H2B S6ph, this phosphorylation was first identified as a target of IKKε (Seibert, 2016). IKKε is a kinase involved in immune response (Fitzgerald et al., 2003; Mattioli et al., 2006). No enrichment for H2B S6ph after a variety of stimuli, including LPS, has been observed before (Seibert et al., 2019). However, other stimuli such as TNF-α might invoke such an enrichment. In a previously performed kinase targeting siRNA screen, several potential H2B S6ph regulating kinases were identified including, but not limited to, mitotic kinases such as Aurora B and CDK1 (Seibert et al., 2019). It is quite possible that other kinases can and do phosphorylate H2B S6ph in interphase cells. In order to test whether this is the case, histone extraction could be used to enrich histones in protein extracts to allow for the detection of smaller amounts of H2B S6ph as a first indicator of the presence of this PTM. This could be combined with different stimuli, such as TNF-α, which is known to induce H3 S10 phosphorylation at some promoters (Saccani et al., 2002; Anest et al., 2003; Yamamoto et al., 2003). Additionally, higher throughput *in vitro* kinase assays could be used to directly determine all kinases which can phosphorylate H2B (Butkevich et al., 2016; Walter et al., 2021). This could be combined with kinase inhibitor profile screens to identify additional H2B S6ph kinases apart from CDK1 in mitosis (Watson et al., 2020). This could be followed up by ChIP-seq or Cut&Run/Tag experiments to identify genomic locations in which H2B S6ph can be found. For H3 S10ph and H3 S28ph, differing localisations have been found depending on the acetylation state of H3 K27 (Khan et al., 2017). It would be interesting to see whether potential interphase H2B S6ph colocalises with any of these other mainly mitotic marks.

5.3 Histone replacement systems

5.3.1 Potential of histone replacement systems in chromatin research

Histone replacement systems have the potential to allow for fundamentally new approaches for studying the function of histone PTMs. Chromatin research to date has been largely correlative, analysing the co-occurrence of histone PTMs with specific genomic features, expression patterns or structural properties (Berger, 2002; Karlić et al., 2010). With the advent of next-generation sequencing it became possible to correlate the location of histone modifications with their genomic context on a genome-wide scale, allowing for the identification of groups of modifications found in different genomic features such as promoters, enhancers and others (Morozova et al., 2008; Hurd et al., 2009). Now, the AI revolution, using the large amounts of data, allows predictions of histone PTMs based on DNA sequence and accessibility (Zhou et al., 2015; Singh et al., 2016; Yin et al., 2019; Wen et al., 2024). More direct studies of the function of histone modifications by perturbing their regulatory networks, the writers/erasers or readers, always carry the risk of off-target effects and therefore do not always allow conclusions to be drawn about a single PTM. The ability to directly probe the function of individual amino acid residues by replacement of endogenous histone with mutant versions is very promising.

Histone replacement systems can and have been used (in organisms where they exist) to answer questions that other methods could not easily answer (Ravi et al., 2010; Graves et al., 2016; Truong et al., 2017). For many histone residues a high degree of conservation has been suggesting some functional relevance (Sullivan et al., 2003). Still, their specific function is often elusive. Histone replacement systems could be used in large screening approaches to find functional consequences of mutations of each residue (Matsubara et al., 2007). Additionally, mutations of histones are increasingly recognised as important features of some cancers. The direct functional consequences of these mutations are not always clear. Some studies link the mutation of certain residues directly to cancerous transformation (Sad et al., 2023). Histone replacement systems could aid in identifying such potentially oncogenic histone modifications as well as elucidating their impact on ongoing cancer cell development, chromosomal instability. Understanding these mechanisms might subsequently reveal possible targeting strategies, allowing for better treatment options. Moreover, histone variants have important functions in defining genomic features. While some are drastically different from their canonical versions, others are more similar (e.g. H2A.X or H3.3), differing by only a few amino acids. The ability to fully replace histones with chimeras, in which histone tails are swapped between different histones, between different species, or between variants and canonical histones, opens up new possibilities for identifying key features of variant histones or isoforms (Fachinetti et al., 2013).

5.3.2 A novel inducible histone replacement system in vertebrate cells

Established histone replacement systems in other organisms, such as *Saccharomyces cerevisiae* or *Drosophila melanogaster*, achieve complete histone replacement by mutation of the endogenous genes or by removal and replacement of the entire histone expression clusters (Matsubara et al., 2007; Günesdogan et al., 2010). This is possible because their histone gene landscape is simpler than that of vertebrates and therefore such systems do not yet exist in vertebrates.

In this study, a system which overcomes this limitation in vertebrates, by using a knock-down and re-expression approach, was designed. Such a system is advantageous for several reasons as outlined before; expression of an shRNA and replacement histone can be controlled using inducible expression systems, allowing for the potential replacement of histone mutants which are only tolerated for a short time. Additionally, inducible histone replacement keeps cells in a naive state before induction and does not allow for cells to develop escape mechanisms as opposed to constitutive mutant expression. Secondly, shRNA mediated knock-down is independent from the gene copy number of the target and therefore makes it easier to deplete multi-copy genes like histones as opposed to direct editing techniques. On the other hand, such a systems comes with a major disadvantage; Ectopic expression of histones potentially disturbs the endogenous tight regulation of their expression. While this issue could potentially be mitigated, ectopic expression is unlikely to be able to completely replicate endogenous control mechanisms.

5.3.2.1 Alternative strategies

Ultimately, any histone replacement system will have advantages and disadvantages that have to be taken under consideration depending on research interest. The advantages of some available systems and the system developed here are compared in Table 1. For future optimisation of the system developed here, certain elements from these systems could be used as outlined below.

Histone cluster replacement

In *Drosophila melanogaster*, a comprehensive histone replacement system was developed by complete replacement of the endogenous histone expression locus (Günesdogan et al., 2010). This was possible due to the repetitive nature of their histone genes. Approximately 100 repeats of all five canonical histones form their histone expression locus. By creating a histone null mutant and integrating multiple copies of modified histone repeat units, full replacement was achieved. In vertebrates, organisation of the histone loci is much more complex. Firstly, histones are distributed across multiple loci on different chromosomes. Secondly, these loci are much larger than the small repeating units in *Drosophila melanogaster* and therefore unlikely to be easily replaceable. Even if the large scale deletion of multiple histone clusters might be technically possible, the reintegration of simple repeat units would most likely be difficult. In contrast to *Drosophila melanogaster*,

the histone loci of vertebrates feature large intergenic regions, the function of which are not or poorly understood (Marzluff et al., 2002). However, certain elements of the endogenous loci, such as promoters and 3' UTRs could be used in attempt to replicate endogenous regulation and still reducing the size of a replacement cluster.

In situ histone gene mutation

With the availability of newer CRISPR/Cas9 based methods, such as Base or Prime editing, mutations can be induced directly in the genome (Komor et al., 2016; Anzalone et al., 2022). This could be used to target histone genes directly to introduce the desired mutations. Such an approach has the major advantage of not altering regulation of the expression, as the endogenous locus is mutated without any major genomic changes and could therefore be considered the "gold-standard. On the other hand, prime editing of multi-copy genes such as histones is extremely labour intensive. Yet, Sankar et al. (2022) have used such an approach to mutate all H3 K27 residues in mouse embryonic stem cells, clearly demonstrating its technical feasibility. Although available, the broad adoption of this technique, particularly for mutant screenings, is unlikely. Additionally, this technique in its current form is limited to mostly amino acid exchanges or small patch changes as with Prime editing the maximum editing length is around 40 bp (Komor et al., 2016). Furthermore, inducible expression of mutants is not possible with this approach. This is problematic for the expression of deleterious mutants which might not be tolerated for along time. It also allows cells to adapt to the expression of a mutant by the development of escape mechanisms.

Histone gene copy number reduction

A histone replacement system developed by Corcoran et al. (2022) in *Arabidopsis thaliana* for histone H4 takes an approach based on copy number reduction histone H4. The number of histone H4 copies is reduced from 8 to just 1 by CRISPR/Cas9 mediated knock-out of the remaining copies. Surprisingly, this is tolerated by the cells, albeit at the expense of impaired growth (Corcoran et al., 2022). The last copy is then also knocked out after integration of a replacement histone. Theoretically, such an approach could be used in vertebrate cells as well. Günesdogan et al. (2010) show that reduction in histone mRNA can be tolerated for a number of cell divisions in *Drosophila melanogaster* embryonic stem cells. It could be assumed that reducing the number of histone gene copies in human, mouse or chicken cells could be tolerated as well. In the form used by Corcoran et al. (2022), this system is not inducible. However, such a strategy could be combined with shRNA mediated knock-down an re-expression, as demonstrated here, where all but 1 histone copy is knocked-out and the last remaining copy is targeted by an shRNA, to allow for inducible replacement. Such a system still does not allow for the endogenous regulation of replacement histone expression and still lacks the expression of all endogenous histone isoforms. This copy number reduction approach could also be combined with *in situ* gene mutation as described before.

Table 1: Comparison between different histone-replacement strategies.

System	Advantage	Disadvantage
shRNA knock-down & re-expression	• Inducible • Applicable to all residues • Large changes possible	• Disrupted regulation of histone expression • Loss of histone isoform diversity • Variable histone replacement efficiency
In situ mutation	• Maintains native expression regulation • Keeps histone isoform diversity • Reliable 100 % replacement efficiency	• Not inducible • Labour intensive • Only small changes possible
Cluster replacement	• Reliable 100 % replacement efficiency • Can partially maintain native expression regulation	• Not inducible • Disrupted regulation of histone expression • Loss of histone isoform diversity
Copy number reduction & knock-out	• Applicable to all residues • Large changes possible	• Disrupted regulation of histone expression • Loss of histone isoform diversity • Variable histone replacement efficiency • Disruption of cell without replacement

The major disadvantage of this is the labour intensive targeting of many histone gene copies. By reducing the number of histone genes copies first, this would become easier.

5.4 Optimisation potential for tet-induced histone replacement

In this study, two versions of the histone replacement system were developed (Table 2.) In both versions, an endogenous histone was successfully replaced by an exogenous version.

The first version was based on random integration of the histone-targeting shRNA and replacement histone plasmids into the cell genome. It showed that an shRNA targeting a canonical histone can be designed and used to efficiently create histone knock-downs. In this first version the shRNA

Table 2: Comparison between 1st and 2nd generation histone replacement systems and a future, further optimised 3rd generation.

Feature	1st generation	2nd generation	*3rd generation*
Usability for screening	No	Yes	*Yes*
Inducibility	Yes	Yes	*Yes*
Regulated histone expression	No	No	*Yes*
Clonal variability	Yes	Not between mutants	*Not between mutants*
Replacement efficiency	High	Medium	*High*
Histone expression level	Normal	Low	*Normal*
Cell survival	Low	High	*High*
Cell morphology	Changed	Changed	*Normal*

design strategy and the shRNA expression system were optimised to allow for an efficient inducible knock-down of H2B from only a few integrated copies of the targeting shRNA. This first version also provided a proof-of-concept that a canonical histone could be rapidly and efficiently replaced in chicken cells. However, cell survival was strongly reduced after induction of the replacement system. Parts of this system were optimised for stronger expression of the replacement histone in order to increase cell survival because it seemed likely that the histone replacement system could not match the endogenous expression. Additionally, the second version used semi-targeted integration using landing pads for the integration of replacement histone to make mutant clones more comparable. While cell survival was drastically increased in the second version of the replacement system, replacement histone expression levels, as judged by Western blotting, appeared to lower than the endogenous histone. H2B levels in single cells clones remained below 20 % of the endogenous amount, an amount that was apparently high enough to rescue the knock-down mediated cell death. By expression of the shRNA alone, without replacement histone, cells die within a few days after induction of the shRNA, likely by apoptosis. This indicates that cells not only stop dividing under a lack of histone but actively sense a histone shortage and trigger cell death. It is therefore surprising that cells survive long term induction of the histone replacement system if it leads to a strong reduction in histone levels as seen in the second version replacement system. Further experiments have to identify the cause of under-performance and further optimisation is needed to rectify these issues and to design a third version of histone replacement system (Table 2). Multiple potential problems and other optimisations are outlined below.

5.4.1 Design and use of shRNAs

A histone replacement system based on shRNA mediated knock-down of the endogenous histone must overcome the hurdle of distinguishing between canonical histone mRNA and variant histone mRNA as only the canonical histone should be targeted. As is the case for H2A and H2A.X, the sequences for canonical and variant histone can be highly similar (subsection 1.1.2). As shRNA mediated knock-downs are based on base-pairing of the effector siRNA to the target mRNA, this presents the risk of targeting both the canonical histone as well as variant histone. Indeed, the shRNA designed against H2A in this study does also target H2A.X. While shRNA sequence can be chosen to avoid this, in some cases this is not possible. One potential solution is to mutate the variant histone *in situ* by Prime editing to render it shRNA resistant.

Moreover, even between canonical histones there are isoforms which differ in one or more amino acid residues (Singh et al., 2018). These may not be classified as histone variants but still have important functions which are not necessarily known (Singh et al., 2013, 2015). While shRNAs can be designed to not target histone variants if the sequence is different enough, it is more difficult to re-express all isoforms of a canonical histone with the endogenous stoichiometry (Singh et al., 2018). This problem is unlikely to be solved with a shRNA based knock-down approach.

5.4.2 Regulation of histone expression

Replication-dependent histone mRNAs are the only eukaryotic mRNAs not being terminated with a polyA-tail (Marzluff, 2005). Instead, a stem loop structure bound by SLBP protects the mRNA from degradation in S-phase and crucially also has important regulatory functions (Pandey et al., 1987; Marzluff et al., 1988; Harris et al., 1991; Marzluff et al., 2017). As canonical histones are only expressed in S-phase, their mRNA is quickly degraded upon entry into G2-phase (DeLisle et al., 1983; Graves et al., 1984). While histone variants like H3.3 are expressed throughout the cell cycle and are poly-adenylated, over expression of canonical histones in this way could disrupt the cell's regulatory machinery. While histones can be expressed with a polyA-tail instead of an HSL, and often are in over-expression experiments (Kanda et al., 1998; Ma et al., 2020), this approach loses the endogenous regulation of those histones. Cells normally maintain homeostasis of critical components by otherwise removing excess protein, for example by protein degradation (Gunjan et al., 2006; Singh et al., 2009; Chen et al., 2012). Uncontrolled over-expression of histones can overwhelm the cellular mechanisms and cause cytotoxicity, genetic instability and sensitivity to DNA damge (Gunjan et al., 1999; Singh et al., 2010). Preliminary experiments suggest that, indeed, in the second version histone replacement, mRNA levels for replacement histone are strongly increased above physiological levels, although this is apparently not reflected on the protein level. Here it is interesting to note that the TRE, used as promoters in both versions of the histone replacement system, is much stronger than the endogenous promoters for histones.

Nevertheless, many copies of replacement histone driven by those strong promoters are needed to express enough histone. While it would be possible that cells are overwhelmed by over-expression of replacement histone after induction, preliminary data show no evidence of protein degradation or mislocalisation of excess histone. It will be interesting to see how the overall increase in cell survival under histone replacement induction in the second version can be reconciled with the apparent shortcomings in histone expression levels.

Ideally, a histone replacement system would keep S-phase specific regulation of the replication dependent histones, although it is unclear whether controlled expression of histones is strictly necessary in continuously dividing cells. This could be achieved by the addition of an HSL to the re-expression histone instead of a polyA-sequence. In the system presented here, a polyA-tail was used as its performance in over-expression systems is well known. It is unclear, however, if replacing a polyA-tail with an HSL necessarily leads to regulated expression in the same way as the endogenous histones are regulated. Although cell cycle-specific regulation is mostly dependent on the HSL rather than the histone gene promoters, processing of the HSL terminated mRNAs requires a processing machinery (Mowry et al., 1987). At the 3' UTR, U7 snRNP base-pairs with the histone downstream element, a purine-rich region downstream of the HSL. CPSF73 then cleaves a few bases downstream of the HSL (Marzluff et al., 2008). The factors needed for to process the special histone mRNAs are located in HLBs (Liu et al., 2006; Marzluff et al., 2017). While previous experiments have demonstrated that recombinant genes terminated with an HSL and HDE instead of a polyA-tail are expressed and are partially cell cycle regulated (Pandey et al., 1987), it is unclear whether they are processed as efficiently as histone genes are. This could possibly be addressed by integrating the replacement histone cassette with HSL and HDE inside one of the histone gene clusters which form the HLB.

5.4.3 Factors potentially affecting expression and stability of histone proteins

Proteins fulfil their function based on the structure they assume after folding of the peptide chain into secondary, tertiary and ternary structures. Folding is a complex process driven by thermodynamic tendencies to assume low energy states. As a nascent peptide exits the ribosome, it begins folding immediately. Folding is therefore partially dependent on the speed of translation as slower or faster synthesis can lead to stable intermediary structures based on thermodynamic local minima (Shakhnovich, 2006). Translation speed is partially governed by tRNA availability, with rare codons slowing translation (Buhr et al., 2016; Engel et al., 2021). In the case of re-expressed histone, the H2B sequence was modified at the shRNA binding site to render the mRNA shRNA resistant. This sequence change may already alter translation speed and therefore protein structure of re-expressed histone as described above. This can be partially mitigated by choosing codons that occur with the same frequency as the codon to be replaced, although this is not always possible.

Additionally, protein tags can influence protein function (Araújo et al., 2000; Dave et al., 2016; Booth et al., 2018) because of misfolding of the protein, changed solubility of the protein, or masking of a surface feature that is necessary for normal protein function. Tagging of histone proteins is generally tolerated as mentioned before (Kimple et al., 2013; Bräuer et al., 2019). The histone tails protruding from the nucleosome can act as natural linkers separating the tag from the globular part of the histone. Nevertheless, careful consideration must be given to the terminus at which a histone is tagged. C-terminal tagging of H2B, as used in this study, has been used before, even *in vivo* (Hadjantonakis et al., 2004). While, therefore, misfolding is not a major concern in this case, the presence of the tag could interfere with proteins that bind the histone tail. This is particularly true for those binding at the very end of the tails which could be disturbed by the presence of additional amino acids. To reduce this risk, the OLLAS tag was chosen in the first version of the histone replacement system as it contains only few acidic amino acids. In the second version this was changed to a splitGFP tag for practical reasons as it can be used to stain chromatin for live cell microscopy by complementation with the larger GFP fragment. SplitGFP is a well-established protein tag which is well tolerated for a number of proteins, but its effect on histone proteins, however, is not known (Feng et al., 2017; Romei et al., 2019). In preliminary experiments, no detrimental effect on histone stability or expression was observed, however. Additional uncertainty for the effect of protein tags on histone function comes from the expected replacement fraction of tagged histone in different scenarios. Tagged histones are most often expressed simultaneously with endogenous untagged histone in simple over-expression setups. While this is often tolerated, it is unclear whether complete replacement with a tagged histone, as it is the case in this histone replacement system, is also tolerated. This could be addressed by replacement with an untagged histone. While the tag provides an easy way to distinguish replaced from endogenous histone to monitor replacement efficiency, as long as replacement is reliable and reproducible, an untagged histone could also be used.

All non-mitochondrial cellular proteins are synthesised by ribosomes in the cytoplasm (Robbins et al., 1967). Proteins needed in organelles such as the nucleus are actively transported there by carrier proteins that recognise targeting sequences and mediate the uptake into those organelles. The nucleus is a tightly guarded organelle; nuclear pores control entry and exit of all larger molecules(Davis, 1995). Even though histone proteins themselves are below the diffusion limit of the nuclear pore complex (NPC), they are actively imported as complexes with their histone chaperones. H2A-H2B and H3-H4 dimers are bound by the chaperones Nap1 (H2A-H2B) and Asf1 (H3-H4). These proteins were observed to shuttle between cyto- and nucleoplasm and are likely partially responsible for histone transport across the NPC (Keck et al., 2012). If the association of histone protein with their respective chaperones, or their histone binding partner, would be disrupted (e.g by addition of protein tags), transport to to the nucleus could be reduced, resulting in a shortage of nuclear in the presence of sufficient amounts of protein. Although no excess H2B

has been observed in cytoplasmic fractions of replacement cells, it is possible that free, unbound histone is quickly degraded and not available for nuclear uptake.

5.5 Conclusion and outlook

Although the regulatory network controlling H2B S6ph has been identified here, it will be interesting to investigate how one network can regulate distinct PTMs with different kinetics. This likely involves further enzymes and regulatory feedback loops which need to be identified in the future.

The biggest open question about H2B S6ph is undoubtedly about its function and relevance. While previous studies suggest a role for H2B S6ph as a protector of chromatid cohesion, it will be important to investigate whether this plays a relevant role in cells and if this is possibly related to disease. This study identified H2B S6ph regulation to be changed in somer cancer cell lines. However it will be important to study whether aberrant histone phosphorylations on lagging chromosomes of tumour cells are a cause or consequence of their genetic instability. The technical means for this are still limited.

To overcome these limitations, an inducible histone replacement system was developed in chicken cells. While this study provides a proof-of-principle showing that depletion of endogenous histone with an shRNA is possible, further optimisation of the re-expression of replacement histone will be needed to make it suitable for research use. When such a system is established, histone mutant expression will give more insight into the function of H2B S6ph and potentially other histone PTMs.

Summary

Histone modifications play a vital role in controlling the function of the genome. Some histone phosphorylations function as important signals during mitosis. Previous work showed transient phosphorylation of H2B S6 at the inner centromeres during mitosis between metaphase and early anaphase. To understand the molecular mechanisms restricting the occurrence of this histone modification in space and time, the responsible phosphatase complex and its regulation were identified by *in vitro* and *in vivo* experiments. CDK1 phosphorylates H2B upon mitotic entry, but this phosphorylation is counteracted by the phosphatase activity of PP1 on the chromosome arms. Two catalytic phosphatase subunits, PP1α and PP1γ, associate with the phosphatase regulator RepoMan. The local inhibition of the PP1/RepoMan complex by Aurora B through phosphorylation of PP1/RepoMan preserves H2B S6ph at the centromeres. The motor protein Mklp2 contributes to the re-localisation of Aurora B from chromatin to the central spindle during anaphase, which relieves Aurora B-dependent inhibition of the PP1/RepoMan complex to enable dephosphorylation of this histone modification. This relocalisation is observed to be dysregulated in some tumour cells. The resulting deregulation of the Aurora B/PP1/RepoMan axis can lead to delayed H2B S6 dephosphorylation, which might contribute to chromosomal instability.

To understand the physiological function of H2B S6ph (and other histone PTMs), this study initiated the development of a novel inducible histone replacement system in vertebrate cells. Towards this goal, the theoretical framework for a tetracycline-inducible histone replacement system based on shRNA-mediated knock-down and re-expression was developed. Chicken cells were identified as a suitable tetrapod model system due to their limited number of histone genes. The first version of this system (V1) optimised the shRNA design strategy to ensure efficient knock-down of endogenous H2B and further histones. Stable cell clones were generated that allowed efficient knocked-down of H2B expression, resulting in drastically reduced histone expression and cell death. Simultaneous re-expression of H2B rescued the knock-down cells and allowed robust re-expression of H2B in cell pools. As random chromatin integration of this system compromises the comparability of different cell clones, a second version of this system (V2) was developed. This employs the integration of genomic landing pads to allow Bxb1 recombinase-mediated cassette exchange of integrated histone cassettes with mutant histones. Maximal protein expression using this system was limited, requiring further analysis and optimisation. Together, this study provides a proof-of-concept for such a histone replacement system in tetrapods. Such a system will in the future allow for the investigation of the function of various histone PTMs.

Zusammenfassung

Histonmodifikationen spielen eine wichtige Rolle bei der Regulation aller Funktionen des Genoms. Einige Histonphosphorylierungen dienen als wichtige Signale während der Mitose. Frühere Studien zeigten eine transiente Phosphorylierung von H2B S6 an den inneren Centromeren während der Mitose zwischen der Metaphase und der frühen Anaphase. Um die molekularen Mechanismen zu verstehen, die diese Phosphorylierung räumlich und zeitlich begrenzen, wurde der Phosphatasekomplex, der diese Modifikation kontrolliert, durch *in vitro* and *in vivo* Experimente identifiziert. CDK1 phosphoryliert H2B S6 nach dem Eintritt in die Mitose. An den Chromosomenarmen wird diese Kinaseaktivität durch PP1α und PP1γ im Komplex mit ihrem Regulator RepoMan aufgehoben. An den Centromeren wird PP1/RepoMan lokal durch die Kinase Aurora B inhibiert. Dadurch wird H2B S6ph an den Centromeren vor Dephosphorylierung geschützt. Das Motorprotein Mklp2 trägt zur Relokalisierung von Aurora B vom Chromatin zur zentralen Spindel bei. Diese Relokalisierung hebt die lokale Inhibierung von PP1/RepoMan auf und ermöglicht so die Dephosphorylierung von H2B S6ph an den Centromeren. Diese Relokalisierung ist jedoch in einigen Krebszellen gestört Die resultierende Deregulation der Aurora B/PP1/RepoMan-Achse kann zu verspäteter Dephosphorylierung von H2B S6ph führen und damit möglicherweise zu chromosomaler Instabilität beitragen.

Um die physiologische Funktion von H2B S6ph (und anderen Histonmodifikationen) zu verstehen, beginnt diese Studie mit der Entwicklung eines umfassenden induzierbaren Histon-Austauschsystems. Zu diesem Zweck wurde die theoretische Grundlage für ein solches System auf der Basis von Tetracyclin-induziertem shRNA *knock-down* und Reexpression entwickelt. Hühnerzellen wurden als geeignetes Modell ausgewählt, da sie im Vergleich zum Menschen eine geringere Kopienzahl an Histonen aufweisen. In der ersten Version (V1) des Systems wurde die shRNA-Design-Strategie für den *knock-down* von H2B und anderen Histonen optimiert. Es wurden stabile Zellklone hergestellt, die einen effizienten *knock-down* ermöglichen, der zu einer Histonreduktion und damit zum Zelltod führt. Durch die gleichzeitige Reexpression eines Ersatz-Histons konnte das Überleben der Zellen wiederhergestellt und der Austausch von Histon H2B ermöglicht werden. Da die zufällige Integration der benötigten Komponenten in das Genom die Vergleichbarkeit der erzeugten Zellklone vermindert, wurde eine zweite Version (V2) entwickelt. Diese verwendet ein Kassettenaustauschverfahren, um bereits ins Genom integrierte Austauschhistone durch Mutanten ersetzen zu können. Die mit diesem neuen System erreichte Proteinexpression war deutlich reduziert, so dass weitere Untersuchungen und Optimierungen notwendig sind. Dennoch zeigt diese Studie einen *Proof-of-Concept* für ein solches Histon-Austauschsystem in Tetrapoden. Ein solches System wird es in Zukunft ermöglichen, die Funktion verschiedener Histonmodifikationen zu untersuchen.

Acronyms and Abbreviations

Acronym	Meaning
A	absorption
ac	acetylation
ACA	anti-centromere autoantibody
AI	artificial intelligence
Anaph.	anaphase
ANOVA	analysis of variance
APC/C	anaphase promoting complex / cyclosome
APS	ammonium persulfate
ATP	adenosine triphosphate
attB	attachment site of phage
attP	attachment site of bacteria
AU	arbitrary units
BCA	bicinchoninic acid
Bla(R)	blasticidin (resistance)
BSA	bovine serum albumin
C-terminal	carboxy-terminal
Cas9	CRISPR associated 9
Cat. No.	catalogue number
CBB	Coomassie Brilliant Blue
CCAN	constitutive centromere associated network
CDK	cyclin dependent kinase
cDNA	complementary DNA
ChIP-seq	chromatin immunoprecipitation followed by deep sequencing
CIN	chromosomal instability

Acronym	Meaning
CMV	cytomegalovius
cont.	continued
CPC	chromosomal passenger complex
CRISPR	Clustered Regularly Interspaced Short Palindromic Repeats
Ct	cycle threshold
Ctrl	Control
DMEM	Dulbecco's modified eagle medium
DMSO	dimethyl sulfoxide
DNA	desoxyribonucleic acid
dNTP	nucleoside triphosphate
Dox	doxycycline
DSB	DNA double-strand break
dsDNA	double-stranded DNA
DTT	Dithiothreitol
e.g.	exempli gratia / for example
ECL	enhanced chemiluminescence
EDTA	ethylenediaminetetraacetic acid
EGTA	triethylene glycol diamine tetraacetic acid
ELISA	enzyme-linked immunosorbent assay
et al.	*et alia* / and others
et seq.	*et sequens* / and following
etc.	*et cetera*
FACS	fluorescence activate cell sorting
FCS	fetal calf serum
FSC	forward-scatter
G1- & G2-phase	Gap 1 or Gap 2 phase
gDNA	genomic DNA
gg	*Gallus gallus*

Acronym	Meaning
GST	glutathion-S-transferase
HDE	histone downstream element
HEPES	hydroxyethylpiperazine ethane sulfonic acid
HFD	histone fold domain
His	histidin tag
HLB	histone locus body
HR	homologous recombination
HRP	horseradish peroxidase
HSL	histone stem loop
hTERT	human telomerase reverse transcriptase
Hygro(R)	hygromycin (resistance)
i.e.	*id est* / that is
IRES	internal ribosomal entry site
ITR	inverted terminal repeat sequences
IUPAC	International Union of Pure and Applied Chemistry
KCM	KCl buffer for cytospun metaphase spreads
KD	kinase dead
KT-MT	kinetochore-microtubule
LB	lysogeny broth
LPS	lipopolysaccharide
M-phase	mitotic phase
MCC	mitotic checkpoint complex
MEM	Eagle's Minimum Essential Medium
miRNA	micro RNA
MNase	micrococcal nuclease
mRNA	messenger RNA
N-terminal	amino-terminal
Neo(R)	neomycin (resistance)

Acronym	Meaning
NPC	nuclear pore complex
OLLAS	*Escherichia coli* OmpF Linker and mouse Langerin fusion Sequence
PBS	phosphate buffered saline
PCR	polymerase chain reaction
PEI	polyethylenimine
pH	potential of hydrogen
ph	phosphorylation
PMSF	phenylmethylsulfonylfluorid
PNK	polynucleotide kinase
polyA-tail	poly-adenine-tail on mRNA
pos.	positive
PRC	polycomb repressive complex
PTM	post-translational modification
Puro(R)	puromycin (resistance)
PVDF	polyvinylidene fluoride
qPCR	quantitative (real time) PCR
rcf	relative centrifugal force
resist.	resistant
RIPA	radio immunoprecipitation assay
RMCE	recombinase mediated cassette exchange
RNA	ribonucleic acid
RNAi	RNA interference
RPMI	Roswell Park Memorial Institute
RT	reverse-trancriptase
rtTA	reverse tet transactivator
S-phase	synthesis phase
SAC	spindle assembly checkpoint
SB	Sleeping Beauty transposase

Acronym	Meaning
Scr	Scramble
SD	standard deviation
SDS	sodium dodecyl sulfate
SDS-PAGE	SDS polyacrylamide gel electrophoresis
shRNA	small hairpin RNA
SI	Système international d'unités
siRNA	small interfering RNA
SLiM	short linear interaction motif
snRNP	small nuclear ribonucleoprotein
SSC	side-scatter
T2A	*Thosea asigna* virus 2A
TBS	Tris buffered saline
TEDA	T5 exonuclease DNA assembly
TEMED	tetramethylethylenediamine
Tet	tetracycline
TMB	3, 3', 5, 5'-tetramethylbenzidin
TNF-α	tumor-necrosis-factor-alpha
TRE	tet-responsive element
tRNA	transfer RNA
TSS	transcription start site
ub	ubiquitination
UTR	untranslated region
UV	ultraviolet
v/v	volume per volume
w/v	weight per volume
wt	wildtype

For abbreviating nucleotides and amino acids, standard IUPAC codes are used throughout this work.

Gene names

Name	Full name
(E)GFP	(enhanced) green fluorescent protein
Aurora B	Aurora kinase B
bCD	bacterial cytosine deaminase
Bub1	Budding uninhibited by benzimidazoles 1 mitotic checkpoint serine/threonine kinase
Bxb1	*Mycobacterium phage Bxb1* gp35 Serine integrase
Cas9	CRISPR-associated protein 9
CDK1/2/4/6	Cyclin-dependent kinase 1/2/4/6
CENP-A	centromeric protein A, centromeric variant H3
Cre	cyclization recombinase (*Escherichia phage P1*)
GADD34	protein phosphatase 1 regulatory subunit 15A
H1 / H2A / H2B / H3 / H4	histone H1 / H2A / H2B / H3 / H4
H2A.X / Z	H2A variant X / Z
HJURP	Holliday junction recognition protein
HSVtk	herpes simplex virus thymidine kinase
IKKε	I-kappaB kinase epsilon
INCENP	Inner centromere protein
Ki-67	marker of proliferation Ki-67
LNGFR	low-affinity nerve growth factor receptor
Mklp2	Mitotic kinesin-like protein 2
Mps1	serine/threonine/tyrosine protein kinase Monopolar spindle 1
Ndc80	NDC80 kinetochore complex component
NIPP1	Nuclear inhibitor of Protein phosphatase 1, protein phosphatase 1 regulatory subunit 8
PHAP1	acidic nuclear phosphoprotein 32 family member A
Plk1	polo like kinase 1
PNUTS	Phosphatase 1 nuclear targeting subunit

Name	Full name
PP1alpha/ beta/ gamma	Serine/threonine-protein phosphatase PP1-alpha/ beta/ gamma catalytic subunit
PP2A	Serine/threonine-protein phosphatase PP2
RepoMan	Cell division cycle-associated protein 2, recruits PP1 onto mitotic chromatin at anaphase
SET	SET nuclear proto-oncogene
Sgo1	shugoshin 1
SLBP	stem loop binding protein
Vinculin	
Wapl	wings apart-like cohesin release factor

Units

Throughout this work SI units, SI prefixes and their abbreviations are used for the units of measurement. In addition, common units in the field of biology, which are used in this work, are listed here.

Unit	Meaning	Definition
aa	number of amino acids	
bp	number of DNA/RNA bases	
M	molar concentration	mol/L
rcf	times earth gravity	9.81 m/s^2
U	enzymatic activity unit	enzyme specific

Collaborators

The experiments shown in this thesis were conceived by me or Prof. Lienhard Schmitz unless otherwise noted. All experiments were performed and evaluated by me unless otherwise noted. As part of this thesis' work I supervised medical PhD students, bachelor students and summer students. Some of the experiments shown here were performed and/or evaluated in close collaboration with these students as shown below.

Figure 14	Collaboration with Vera Saul
Figure 17	Collaboration with Roman Robert
Figure 18	Collaboration with Roman Robert
Figure 19A	Collaboration with Roman Robert
Figure 20	Collaboration with Roman Robert
Figure 21A and C	Collaboration with Johanna Segbers
Figure 30	Collaboration with Anna Parry
Figure 34A and D	Collaboration with Amelie Pritz
Figure 34B	Collaboration with Paulin Nikuradse
Figure 35A	Collaboration with Paulin Nikuradse
Figure 35B and C	Collaboration with Amelie Pritz

Appendix

Plasmid maps

pMIR30 (based on pCDNA3)

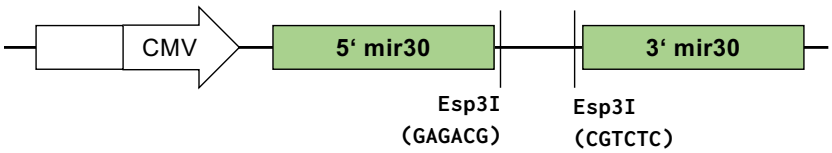

pMIR30-short (based on pCDNA3)

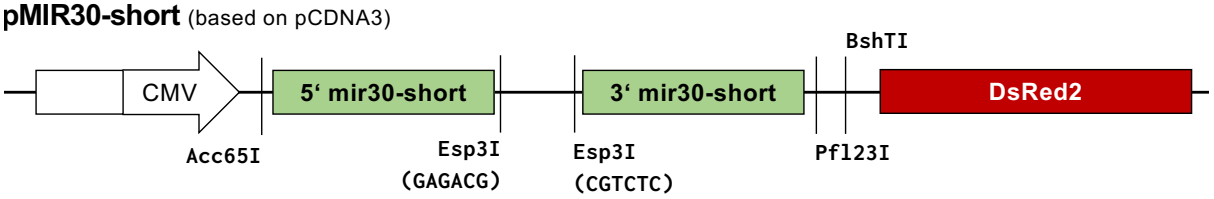

pSB-Puro-mir30short-Neo (based on pSBtet-Neo)

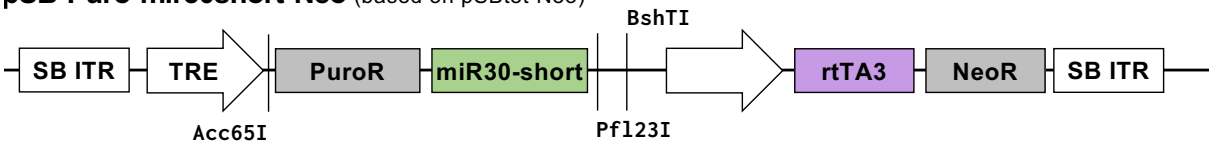

pSB-Puro-mir30short-Neo (based on pSBtet-Neo)

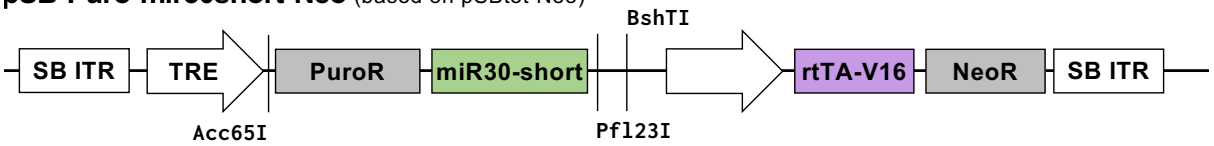

pHEX-SB-Bxb1-RMCE-LNGFR-BpI-free

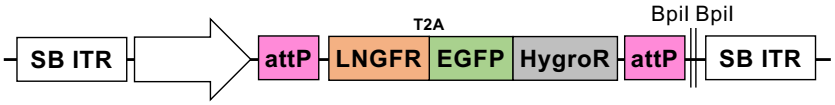

pHEX-RMCE-LNGFR-1xggH2B-GFP11

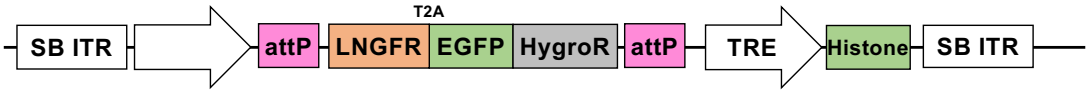

shRNA sequences

shRNAs against chicken histone H2B

Name	Sense
ggH2B-1	GCTACTCGATCTACGTGTACAA
ggH2B-2	CGACCATCACGTCGCGGGAGAT
ggH2B-3	GCATCATGAACTCGTTCGTCAA
ggH2B-4	CGTCGCGCCTGGCGCACTACAA
ggH2B-5	CCAAGGCCATGGGCATCATGAA
ggH2B-6	ACTACAACAAGCGCTCGACCAT
ggH2B-7	TCTACGTGTACAAGGTGCTGAA

shRNAs against chicken histone H1

Name	Antisense	Score
ggH1-sh404	TTGAGCCCCAGCTTGATGCGGC	0.612
ggH1-sh368	TTGGTCTGCACCAGGGTGCCCT	0.465
ggH1-sh71	TTGGGCTTCACCGCCTTTGCCT	0.363
ggH1-sh521	TTGGTGATCAGCTCGGTGACGC	0.361
ggH1-sh503	TTGGAGGCGGACACGGCCTTGG	0.263
ggH1-sh389	TTGCTGACGAGGCTCTTGAGCC	0.194
ggH1-sh482	AGGGAGAGCCCCTTGCGCTCCT	0.16
ggH1-sh393	TGACGAGGCTCTTGAGCCCCAG	0.16

shRNAs against chicken histone H2A

Name	Antisense	Score
ggH2A-sh107	TTGAGCTCCTCGTCGTTGCGGA	0.529
ggH2A-sh92	TTGCCCAGCAGCTTGTTGAGCT	0.526
ggH2A-sh152	ATGATGCGCGTCTTCTTGTTGT	0.332
ggH2A-sh104	TTGTTGAGCTCCTCGTCGTTGC	0.315
ggH2A-sh155	ATGCGCGTCTTCTTGTTGTCGC	0.284
ggH2A-sh215	AGGTACTCCAGCACGGCCGCCA	0.241
ggH2A-sh206	TCGGCCGTCAGGTACTCCAGCA	0.238
ggH2A-sh87	TCACCTTGCCCAGCAGCTTGTT	0.235

shRNAs against chicken histone H3

Name	Antisense	Score
ggH3-sh173	TTGAAGTCCTGCGCGATCTCGC	0.492
ggH3-sh155	TGGAAGCGCAGGTCGGTCTTGA	0.469
ggH3-sh44	TTGGGCATGATGGTGACGCGCT	0.414
ggH3-sh287	TAGCGGTGCGGCTTCTTCACGC	0.389
ggH3-sh86	TTGGTGTCCTCGAAGAGCCCCA	0.365

Name	Antisense	Score
ggH3-sh167	TCGGTCTTGAAGTCCTGCGCGA	0.317
ggH3-sh245	TGGTAGCGCCGGATCTCGCGCA	0.316
ggH3-sh41	TCCTTGGGCATGATGGTGACGC	0.307

shRNAs against chicken histone H4

Name	Antisense	Score
ggH4-sh47	TAGACCACGTCCATGGCCGTGA	0.53
ggH4-sh38	TTGAGCGCGTAGACCACGTCCA	0.449
ggH4-sh119	TTCTCCAGGAAGACCTTGAGCA	0.439
ggH4-sh236	TTGTCGCGCAGCACCTTGCGGT	0.402
ggH4-sh150	TCTCCTCGTAGATGAGCCCCGA	0.372
ggH4-sh161	ATGAGCCCCGAGATGCGCTTGA	0.348
ggH4-sh158	TAGATGAGCCCCGAGATGCGCT	0.329
ggH4-sh116	ACGTTCTCCAGGAAGACCTTGA	0.296

Oligonucleotides for cloning

Name	Sequence	Purpose
H3.1-S28A-fwd	AAGGCTGCTCGCAAGGCCGCGCCGGCTACCGGC	mutagenesis
H3.1-S28A-rev	GCCGGTAGCCGGCGCGGCCTTGCGAGCAGCCTT	mutagenesis
H3.1-S28E-fwd	AAGGCTGCTCGCAAGGAAGCGCCGGCTACCGGC	mutagenesis
H3.1-S28E-rev	GCCGGTAGCCGGCGCTTCCTTGCGAGCAGCCTT	mutagenesis
H2B-cloning-NheI-fwd	ATTGAGCTAGCATGCCAGAGCCAGCGAAG	cloning of pH2B-EGFP-MCS
EGFP-N	CGTCGCCGTCCAGCTCGACCAG	cloning of pH2B-EGFP-MCS
AurkB-Kpn2I-fwd	ATTAAAGATCCGGAACCCCATCTGCACTTGTCCTC	cloning of H2B-EGFP Aurora B

Name	Sequence	Purpose
AurkB-ApaI-rev	ATGATATGGGCCCGTTTAAACCTCGAGTGCGGCC	cloning of H2B-EGFP Aurora B
INCENPdCen-XhoI-fwd	TTAGCTACTCGAGTCAGCAAAGAGCCAGAGCTG	cloning of H2B-EGFP-INCENP
INCENPdCen-HindIII-rev	TTAGTACAAGCTTTTACTTCTTCAGGCTGTAGGCCAGG	cloning of H2B-EGFP-INCENP
RepoMan-RATA-fwd	ATGAGGAAGAGGAAGAGAGCTACTGCTGGAGAGGACTTAAGCCCG	mutagenesis
RepoMan-RATA-rev	CGGGCTTAAGTCCTCTCCAGCAGTAGCTCTCTTCCTCTTCCTCAT	mutagenesis
RepoMan-T394A-fwd	GAGGAAGAGGAAGAGAGTTGCTTTTGGAGAGGACTTAAG	mutagenesis
RepoMan-T394A-rev	CTTAAGTCCTCTCCAAAAGCAACTCTCTTCCTCTTCCTC	mutagenesis
RepoMan-S893D-fwd	GAAACCAAAGTGCGACGTGACACGAGGCTACAGAAGGA	mutagenesis
RepoMan-S893D-rev	TCCTTCTGTAGCCTCGTGTCACGTCGCACTTTGGTTTC	mutagenesis
RepoMan-1-890-fwd	CGCTTAGCCCGGGATCCACC	truncation
RepoMan-1-890-rev	GGTAGCCCCGGGCATCACTTTGGTTTCACTATTTCTCCTCTGAAAG	truncation
HIST1H2B7-NheIApaI-fwd	TTAGCTAGCGGGCCCGATGCCTGAGCCGGCCAAGT	cloning of pEGFP-H2B7
HIST1H2B8-BamHI-rev	GCGACCGGTGGATCCTTGGAGCTGGTGTACTTGGT	cloning of pEGFP-H2B7 and H2B8
HISTH2B8-NheIApaI-fwd	TTAGCTAGCGGGCCCGGATGCCAGAACCAGCGAAGT	cloning of pEGFP-H2B8
mir30a-BsiWI-BpiI-rev	ATGATAAGCTATAGTCTTCCGTACGTCCAATTGAAAAAAGTGATTTAATTTATACCATT	cloning of pMIR30
mir30a-Acc65I-fwd	GTATTATGGTACCGGCCGCAAGCCTTGTTAA	cloning of pMIR30

Name	Sequence	Purpose
mir30-Esp3I-insert-Oliogo-fwd	TCGAGAAGGTATATTGCTGTTGACAGTGAGCGAGAGACGTAACGTCTCGTGCCTACTGCCTCGGACTTCAAGGGGCTAG	cloning of pMIR30
mir30-Esp3I-insert-Oliogo-rev	AATTCTAGCCCCTTGAAGTCCGAGGCAGTAGGCACGAGACGTTACGTCTCTCGCTCACTGTCAACAGCAATATACCTTC	cloning of pMIR30
chicken H2B shRNA1 fwd	AGCGCCTACTCGATCTACGTGTACAATAGTGAAGCCACAGATGTATTGTACACGTAGATCGAGTAGC	cloning of H2B shRNA
chicken H2B shRNA1 rev	GGCAGCTACTCGATCTACGTGTACAATACATCTGTGGCTTCACTATTGTACACGTAGATCGAGTAGG	cloning of H2B shRNA
chicken H2B shRNA2 fwd	AGCGGGACCATCACGTCGCGGGAGATTAGTGAAGCCACAGATGTAATCTCCCGCGACGTGATGGTCG	cloning of H2B shRNA
chicken H2B shRNA2 rev	GGCACGACCATCACGTCGCGGGAGATTACATCTGTGGCTTCACTAATCTCCCGCGACGTGATGGTCC	cloning of H2B shRNA
chicken H2B shRNA3 fwd	AGCGCCATCATGAACTCGTTCGTCAATAGTGAAGCCACAGATGTATTGACGAACGAGTTCATGATGC	cloning of H2B shRNA
chicken H2B shRNA3 rev	GGCAGCATCATGAACTCGTTCGTCAATACATCTGTGGCTTCACTATTGACGAACGAGTTCATGATGG	cloning of H2B shRNA
chicken H2B shRNA4 fwd	AGCGGGTCGCGCCTGGCGCACTACAATAGTGAAGCCACAGATGTATTGTAGTGCGCCAGGCGCGACG	cloning of H2B shRNA
chicken H2B shRNA4 rev	GGCACGTCGCGCCTGGCGCACTACAATACATCTGTGGCTTCACTATTGTAGTGCGCCAGGCGCGACC	cloning of H2B shRNA
chicken H2B shRNA5 fwd	AGCGGCAAGGCCATGGGCATCATGAATAGTGAAGCCACAGATGTATTCATGATGCCCATGGCCTTGG	cloning of H2B shRNA
chicken H2B shRNA5 rev	GGCACCAAGGCCATGGGCATCATGAATACATCTGTGGCTTCACTATTCATGATGCCCATGGCCTTGC	cloning of H2B shRNA
chicken H2B shRNA6 fwd	AGCGTCTACAACAAGCGCTCGACCATTAGTGAAGCCACAGATGTAATGGTCGAGCGCTTGTTGTAGT	cloning of H2B shRNA
chicken H2B shRNA6 rev	GGCAACTACAACAAGCGCTCGACCATTACATCTGTGGCTTCACTAATGGTCGAGCGCTTGTTGTAGA	cloning of H2B shRNA
chicken H2B shRNA7 fwd	AGCGCCTACGTGTACAAGGTGCTGAATAGTGAAGCCACAGATGTATTCAGCACCTTGTACACGTAGA	cloning of H2B shRNA

Name	Sequence	Purpose
chicken H2B shRNA7 rev	GGCATCTACGTGTACAAGGTGCTGAATACATCTGTGGCTTCACTATTCAGCACCTTGTACACGTAGG	cloning of H2B shRNA
chicken H2B shRNA3(5p) fwd	AGCGACTTGACGAACGAGTTCATGATGCGTGAAGCCACAGATGGCATCATGAACTCGTTCGTCAAGG	cloning of H2B shRNA
chicken H2B shRNA3(5p) rev	GGCACCTTGACGAACGAGTTCATGATGCCATCTGTGGCTTCACGCATCATGAACTCGTTCGTCAAGT	cloning of H2B shRNA
mir-Short-BamHI	TAATACGGATCCCGTACGATCGTAGCCCTTGAAGTCC	cloning of pMIR30-short-DsRed2
mir-Short-SalI	GTATTAGTCGACGGTACCGATCCAAGAAGGTATATTGCTGTTG	cloning of pMIR30-short-DsRed2
miR-short-Oligo	GGTACCGATCCAAGAAGGTATATTGCTGTTGACAGTGAGCGAGAGACGGATGGATGGATCAATGATCCGTCTCATGCCTACTGCCTCGGACTTCAAGGGCTACGATCGTACG	cloning of pMIR30-short-DsRed2
PuroR-HiFi-new-fwd	ACTTCCTACCCTCGAAAGGCCTCTGATGACCGAGTACAAGCCCACGGTG	cloning of pSB-Puro-mir30short-Neo
PuroR-HiFi-new-rev	CGGTAGCGCTAGCTCGAGGCTGATCAGCGAGCTCTAGAG	cloning of pSB-Puro-mir30short-Neo
shShort-HiFi-new-fwd	GATCAGCCTCGAGCTAGCGCTACCGGACTCAGATCTCG	cloning of pSB-Puro-mir30short-Neo
shShort-HiFi-new-rev	TCTATCGATGGAAGCTTGGCCTGACTGGATCCCGTACGATCGTAGCCCTTG	cloning of pSB-Puro-mir30short-Neo
Puro-Esp3I-remove-fwd	GTCGGCGTTTCGCCCGACCACCAGGGCAAG	cloning of pSB-Puro-mir30short-Neo
Puro-Esp3I-remove-rev	GGGCGAAACGCCGACGGTGGCCAGGAAC	cloning of pSB-Puro-mir30short-Neo
Hifi-SB-IRES-fwd	TCCTACCCTCGAAAGGCCTCTGAGGCCCGCCGTGTAAGGCCTGTCAGGCCGCTGTTGGGGTGAGTACTCC	cloning pSBtet-IRES-Bla-Hygro
Hifi-SB-IRES-rev	GGCCATGGGGGTCATGGAAGGTCGTCTCCT	cloning pSBtet-IRES-Bla-Hygro
Hifi-SB-Blasti-fwd	TCCATGACCCCCATGGCCATGCCTTTG	cloning pSBtet-IRES-Bla-Hygro

Name	Sequence	Purpose
Hifi-SB-Blasti-rev	TCATGTCTATCGATGGAAGCTTACGACAGGCCTTCGAATTAGCCC	cloning pSBtet-IRES-Bla-Hygro
ggH1-sh404-fwd	AGCGTCCGCATCAAGCTGGGGCTCAATAGTGAAGCCACAGATGTATTGAGCCCCAGCTTGATGCGGC	cloning of shRNA plasmids
ggH1-sh404-rev	GGCAGCCGCATCAAGCTGGGGCTCAATACATCTGTGGCTTCACTATTGAGCCCCAGCTTGATGCGGA	cloning of shRNA plasmids
ggH1-sh368-fwd	AGCGCGGGCACCCTGGTGCAGACCAATAGTGAAGCCACAGATGTATTGGTCTGCACCAGGGTGCCCT	cloning of shRNA plasmids
ggH1-sh368-rev	GGCAAGGGCACCCTGGTGCAGACCAATACATCTGTGGCTTCACTATTGGTCTGCACCAGGGTGCCCG	cloning of shRNA plasmids
ggH1-sh71-fwd	AGCGCGGCAAAGGCGGTGAAGCCCAATAGTGAAGCCACAGATGTATTGGGCTTCACCGCCTTTGCCT	cloning of shRNA plasmids
ggH1-sh71-rev	GGCAAGGCAAAGGCGGTGAAGCCCAATACATCTGTGGCTTCACTATTGGGCTTCACCGCCTTTGCCG	cloning of shRNA plasmids
ggH1-sh521-fwd	AGCGTCGTCACCGAGCTGATCACCAATAGTGAAGCCACAGATGTATTGGTGATCAGCTCGGTGACGC	cloning of shRNA plasmids
ggH1-sh521-rev	GGCAGCGTCACCGAGCTGATCACCAATACATCTGTGGCTTCACTATTGGTGATCAGCTCGGTGACGA	cloning of shRNA plasmids
ggH1-sh503-fwd	AGCGGCAAGGCCGTGTCCGCCTCCAATAGTGAAGCCACAGATGTATTGGAGGCGGACACGGCCTTGG	cloning of shRNA plasmids
ggH1-sh503-rev	GGCACCAAGGCCGTGTCCGCCTCCAATACATCTGTGGCTTCACTATTGGAGGCGGACACGGCCTTGC	cloning of shRNA plasmids
ggH1-sh389-fwd	AGCGAGCTCAAGAGCCTCGTCAGCAATAGTGAAGCCACAGATGTATTGCTGACGAGGCTCTTGAGCC	cloning of shRNA plasmids
ggH1-sh389-rev	GGCAGGCTCAAGAGCCTCGTCAGCAATACATCTGTGGCTTCACTATTGCTGACGAGGCTCTTGAGCT	cloning of shRNA plasmids
ggH1-sh482-fwd	AGCGTGGAGCGCAAGGGGCTCTCCCTTAGTGAAGCCACAGATGTAAGGGAGAGCCCCTTGCGCTCCT	cloning of shRNA plasmids
ggH1-sh482-rev	GGCAAGGAGCGCAAGGGGCTCTCCCTTACATCTGTGGCTTCACTAAGGGAGAGCCCCTTGCGCTCCA	cloning of shRNA plasmids
ggH1-sh393-fwd	AGCGCTGGGGCTCAAGAGCCTCGTCATAGTGAAGCCACAGATGTATGACGAGGCTCTTGAGCCCCAG	cloning of shRNA plasmids

Name	Sequence	Purpose
ggH1-sh393-rev	GGCACTGGGGCTCAAGAGCCTCGTCATACATCTGTGG CTTCACTATGACGAGGCTCTTGAGCCCCAG	cloning of shRNA plasmids
ggH2A-sh107-fwd	AGCGGCCGCAACGACGAGGAGCTCAATAGTGAAGCCA CAGATGTATTGAGCTCCTCGTCGTTGCGGA	cloning of shRNA plasmids
ggH2A-sh107-rev	GGCATCCGCAACGACGAGGAGCTCAATACATCTGTGG CTTCACTATTGAGCTCCTCGTCGTTGCGGC	cloning of shRNA plasmids
ggH2A-sh92-fwd	AGCGCGCTCAACAAGCTGCTGGGCAATAGTGAAGCCA CAGATGTATTGCCCAGCAGCTTGTTGAGCT	cloning of shRNA plasmids
ggH2A-sh92-rev	GGCAAGCTCAACAAGCTGCTGGGCAATACATCTGTGG CTTCACTATTGCCCAGCAGCTTGTTGAGCG	cloning of shRNA plasmids
ggH2A-sh152-fwd	AGCGTCAACAAGAAGACGCGCATCATTAGTGAAGCCA CAGATGTAATGATGCGCGTCTTCTTGTTGT	cloning of shRNA plasmids
ggH2A-sh152-rev	GGCAACAACAAGAAGACGCGCATCATTACATCTGTGG CTTCACTAATGATGCGCGTCTTCTTGTTGA	cloning of shRNA plasmids
ggH2A-sh104-fwd	AGCGACAACGACGAGGAGCTCAACAATAGTGAAGCCA CAGATGTATTGTTGAGCTCCTCGTCGTTGC	cloning of shRNA plasmids
ggH2A-sh104-rev	GGCAGCAACGACGAGGAGCTCAACAATACATCTGTGG CTTCACTATTGTTGAGCTCCTCGTCGTTGT	cloning of shRNA plasmids
ggH2A-sh155-fwd	AGCGACGACAACAAGAAGACGCGCATTAGTGAAGCCA CAGATGTAATGCGCGTCTTCTTGTTGTCGC	cloning of shRNA plasmids
ggH2A-sh155-rev	GGCAGCGACAACAAGAAGACGCGCATTACATCTGTGG CTTCACTAATGCGCGTCTTCTTGTTGTCGT	cloning of shRNA plasmids
ggH2A-sh215-fwd	AGCGCGGCGGCCGTGCTGGAGTACCTTAGTGAAGCCA CAGATGTAAGGTACTCCAGCACGGCCGCCA	cloning of shRNA plasmids
ggH2A-sh215-rev	GGCATGGCGGCCGTGCTGGAGTACCTTACATCTGTGG CTTCACTAAGGTACTCCAGCACGGCCGCCG	cloning of shRNA plasmids
ggH2A-sh206-fwd	AGCGCGCTGGAGTACCTGACGGCCGATAGTGAAGCCA CAGATGTATCGGCCGTCAGGTACTCCAGCA	cloning of shRNA plasmids
ggH2A-sh206-rev	GGCATGCTGGAGTACCTGACGGCCGATACATCTGTGG CTTCACTATCGGCCGTCAGGTACTCCAGCG	cloning of shRNA plasmids
ggH2A-sh87-fwd	AGCGTACAAGCTGCTGGGCAAGGTGATAGTGAAGCCA CAGATGTATCACCTTGCCCAGCAGCTTGTT	cloning of shRNA plasmids

Name	Sequence	Purpose
ggH2A-sh87-rev	GGCAAACAAGCTGCTGGGCAAGGTGATACATCTGTGG CTTCACTATCACCTTGCCCAGCAGCTTGTA	cloning of shRNA plasmids
ggH3-sh173-fwd	AGCGCCGAGATCGCGCAGGACTTCAATAGTGAAGCCA CAGATGTATTGAAGTCCTGCGCGATCTCGC	cloning of shRNA plasmids
ggH3-sh173-rev	GGCAGCGAGATCGCGCAGGACTTCAATACATCTGTGG CTTCACTATTGAAGTCCTGCGCGATCTCGG	cloning of shRNA plasmids
ggH3-sh155-fwd	AGCGCCAAGACCGACCTGCGCTTCCATAGTGAAGCCA CAGATGTATGGAAGCGCAGGTCGGTCTTGA	cloning of shRNA plasmids
ggH3-sh155-rev	GGCATCAAGACCGACCTGCGCTTCCATACATCTGTGG CTTCACTATGGAAGCGCAGGTCGGTCTTGG	cloning of shRNA plasmids
ggH3-sh44-fwd	AGCGCGCGCGTCACCATCATGCCCAATAGTGAAGCCA CAGATGTATTGGGCATGATGGTGACGCGCT	cloning of shRNA plasmids
ggH3-sh44-rev	GGCAAGCGCGTCACCATCATGCCCAATACATCTGTGG CTTCACTATTGGGCATGATGGTGACGCGCG	cloning of shRNA plasmids
ggH3-sh287-fwd	AGCGCCGTGAAGAAGCCGCACCGCTATAGTGAAGCCA CAGATGTATAGCGGTGCGGCTTCTTCACGC	cloning of shRNA plasmids
ggH3-sh287-rev	GGCAGCGTGAAGAAGCCGCACCGCTATACATCTGTGG CTTCACTATAGCGGTGCGGCTTCTTCACGG	cloning of shRNA plasmids
ggH3-sh86-fwd	AGCGAGGGGCTCTTCGAGGACACCAATAGTGAAGCCA CAGATGTATTGGTGTCCTCGAAGAGCCCCA	cloning of shRNA plasmids
ggH3-sh86-rev	GGCATGGGGCTCTTCGAGGACACCAATACATCTGTGG CTTCACTATTGGTGTCCTCGAAGAGCCCCT	cloning of shRNA plasmids
ggH3-sh167-fwd	AGCGCCGCGCAGGACTTCAAGACCGATAGTGAAGCCA CAGATGTATCGGTCTTGAAGTCCTGCGCGA	cloning of shRNA plasmids
ggH3-sh167-rev	GGCATCGCGCAGGACTTCAAGACCGATACATCTGTGG CTTCACTATCGGTCTTGAAGTCCTGCGCGG	cloning of shRNA plasmids
ggH3-sh245-fwd	AGCGGGCGCGAGATCCGGCGCTACCATAGTGAAGCCA CAGATGTATGGTAGCGCCGGATCTCGCGCA	cloning of shRNA plasmids
ggH3-sh245-rev	GGCATGCGCGAGATCCGGCGCTACCATACATCTGTGG CTTCACTATGGTAGCGCCGGATCTCGCGCC	cloning of shRNA plasmids
ggH3-sh41-fwd	AGCGCCGTCACCATCATGCCCAAGGATAGTGAAGCCA CAGATGTATCCTTGGGCATGATGGTGACGC	cloning of shRNA plasmids

Name	Sequence	Purpose
ggH3-sh41-rev	GGCAGCGTCACCATCATGCCCAAGGATACATCTGTGG CTTCACTATCCTTGGGCATGATGGTGACGG	cloning of shRNA plasmids
ggH4-sh47-fwd	AGCGCCACGGCCATGGACGTGGTCTATAGTGAAGCCA CAGATGTATAGACCACGTCCATGGCCGTGA	cloning of shRNA plasmids
ggH4-sh47-rev	GGCATCACGGCCATGGACGTGGTCTATACATCTGTGG CTTCACTATAGACCACGTCCATGGCCGTGG	cloning of shRNA plasmids
ggH4-sh38-fwd	AGCGGGGACGTGGTCTACGCGCTCAATAGTGAAGCCA CAGATGTATTGAGCGCGTAGACCACGTCCA	cloning of shRNA plasmids
ggH4-sh38-rev	GGCATGGACGTGGTCTACGCGCTCAATACATCTGTGG CTTCACTATTGAGCGCGTAGACCACGTCCC	cloning of shRNA plasmids
ggH4-sh119-fwd	AGCGAGCTCAAGGTCTTCCTGGAGAATAGTGAAGCCA CAGATGTATTCTCCAGGAAGACCTTGAGCA	cloning of shRNA plasmids
ggH4-sh119-rev	GGCATGCTCAAGGTCTTCCTGGAGAATACATCTGTGG CTTCACTATTCTCCAGGAAGACCTTGAGCT	cloning of shRNA plasmids
ggH4-sh236-fwd	AGCGTCCGCAAGGTGCTGCGCGACAATAGTGAAGCCA CAGATGTATTGTCGCGCAGCACCTTGCGGT	cloning of shRNA plasmids
ggH4-sh236-rev	GGCAACCGCAAGGTGCTGCGCGACAATACATCTGTGG CTTCACTATTGTCGCGCAGCACCTTGCGGA	cloning of shRNA plasmids
ggH4-sh150-fwd	AGCGACGGGGCTCATCTACGAGGAGATAGTGAAGCCA CAGATGTATCTCCTCGTAGATGAGCCCCGA	cloning of shRNA plasmids
ggH4-sh150-rev	GGCATCGGGGCTCATCTACGAGGAGATACATCTGTGG CTTCACTATCTCCTCGTAGATGAGCCCCGT	cloning of shRNA plasmids
ggH4-sh161-fwd	AGCGCCAAGCGCATCTCGGGGCTCATTAGTGAAGCCA CAGATGTAATGAGCCCCGAGATGCGCTTGA	cloning of shRNA plasmids
ggH4-sh161-rev	GGCATCAAGCGCATCTCGGGGCTCATTACATCTGTGG CTTCACTAATGAGCCCCGAGATGCGCTTGG	cloning of shRNA plasmids
ggH4-sh158-fwd	AGCGCGCGCATCTCGGGGCTCATCTATAGTGAAGCCA CAGATGTATAGATGAGCCCCGAGATGCGCT	cloning of shRNA plasmids
ggH4-sh158-rev	GGCAAGCGCATCTCGGGGCTCATCTATACATCTGTGG CTTCACTATAGATGAGCCCCGAGATGCGCG	cloning of shRNA plasmids
ggH4-sh116-fwd	AGCGGCAAGGTCTTCCTGGAGAACGTTAGTGAAGCCA CAGATGTAACGTTCTCCAGGAAGACCTTGA	cloning of shRNA plasmids

Name	Sequence	Purpose
ggH4-sh116-rev	GGCATCAAGGTCTTCCTGGAGAACGTTACATCTGTGG CTTCACTAACGTTCTCCAGGAAGACCTTGC	cloning of shRNA plasmids
Hifi-pSBtet-replace-rttA-fwd	TCCGGCGCTACTAACTTCAGC	cloning of rtTA-V16 shRNA plasmid
Hifi-pSBtet-replace-rttA-rev	GTGGCCTCAGGTGCAGAGGT	cloning of rtTA-V16 shRNA plasmid
Hifi-rtTAV16-fwd	TAGAAACCTCTGCACCTGAGGCCACATGTCCAGACTG GACAAGAGCAAAATC	cloning of rtTA-V16 shRNA plasmid
Hifi-rtTAV16-rev	GCAGGCTGAAGTTAGTAGCGCCGGACCCGGGGAGCAT GTCAAGGT	cloning of rtTA-V16 shRNA plasmid
HSVtk-EGFP-NheI-fwd	TTAGAGCTAGCGGTTTGTCTGGTCAACCACCGCGGTC TCAGTGGTGTACGGTACAAACCTATACCATGGCTTCG TACCCCGGC	cloning of HSVtk RMCE cassette
HSVtk-EGFP-BshTI-rev	TACGACCGGTTTTGTACAGCTCGTCCATGCCAAGAGT GA	cloning of HSVtk RMCE cassette
Hygro-pA-BshTI-fwd	TAGCGAACCGGTGATCAGCACGTGATGAAAAAGCCTG AACTCACC	cloning of HSVtk RMCE cassette
Hygro-pA-PscI-rev	TTAGCACATGTGGTTTGTACCGTACACCACTGAGTCC GCGGTGGTTGACCAGACAAACCTCTACGTTTGTCTTC TGCTAGAAGACTTTGACGCCGCCAAGCTCTAGCTAGA GGTCGACGG	cloning of HSVtk RMCE cassette
pCDNA-Seq-rev	CTTTTTACGGTTCCTGGCCTTTTGC	cloning of pSBtet HSVtk RMCE plasmid
Hifi-CMV-fwd	AATCAGGGGATAACGCAGGAAAGAAACCGGTGACATT GATTATTGACTAGTTATTAATAGTAATCAATTACGGG G	cloning of pSBtet HSVtk RMCE plasmid
Hifi-SB-left-rev	GTAAGTTATGTAACGGTCTAGATAGCGGACCCCTTAC CGAAAC	cloning of pSBtet HSVtk RMCE plasmid
Hifi-SB-right-fwd	TTTTTGTGTCTCTCACTTCTGAGGCGGAAAGAACCAG CTG	cloning of pSBtet HSVtk RMCE plasmid

Name	Sequence	Purpose
NheI-attPwt-LNGFR-fwd	AAGCTGGCTAGCGGTTTGTCTGGTCAACCACCGCGGTCTCAGTGGTGTACGGTACAAACCGGCGCCGCCATGGGGGCAGGTGCCACCG	cloning of pSBtet LNGFR RMCE plasmid
LNGFR-T2A-Cfr9I-rev	TTATCTACCCGGGAGGGGCCGGGATTTTCCTCCACGTCCCCGCATGTTAGAAGACTTCCCCTGCCCTCCCTCTTGAAGGCTATGTAGGCCACAAGACCC	cloning of pSBtet LNGFR RMCE plasmid
T2A-BpiI-remove-fwd	GAGGGCAGGGGAAGTCTCCTAACATGCGGGGACGTGGAGG	cloning of pSBtet LNGFR RMCE plasmid
T2A-BpiI-remove-rev		cloning of pSBtet LNGFR RMCE plasmid
SfiI-ggH2B-fwd	TCGAAAGGCCTCTGAGGCCACCATGCCAGAGCCCGCAAAGTC	cloning of H2B-GFP11
HisGFP11-SfiI-ggHISTONE-rev	TCAGTATGGCCTGACAGGCCCTATGTAATCCCAGCAGCATTTACATACTCATGAAGGACCATGTGGTCACGATGGTGATGGTGATGGTGAAGCTT	cloning of H2B-GFP11
SB-GG-first-BbsI-fwd	CGTAAGAAGACTTGTCAGTTTCGGTAAGGGGTCCGCTATCTAGACG	cloning of H2B-GFP11 copy number plasmids
SB-GG-last-BbsI-rev	TTACCGAAGACTTACGTAAACCTCCCACATCTCCCCCTGAAC	cloning of H2B-GFP11 copy number plasmids
SB-GG-2x-BbsI-fwd	CGTAAGAAGACTTATTCGTTTCGGTAAGGGGTCCGCTATCTAGACG	cloning of H2B-GFP11 copy number plasmids
SB-GG-2x-BbsI-rev	TTACCGAAGACTTGAATAAACCTCCCACATCTCCCCCTGAAC	cloning of H2B-GFP11 copy number plasmids
SB-GG-3x-BbsI-fwd	CGTAAGAAGACTTCCTAGTTTCGGTAAGGGGTCCGCTATCTAGACG	cloning of H2B-GFP11 copy number plasmids

Name	Sequence	Purpose
SB-GG-3x-BbsI-rev	TTACCGAAGACTTTAGGAAACCTCCCACATCTCCCCC TGAAC	cloning of H2B-GFP11 copy number plasmids
SB-GG-4x-BbsI-fwd	CGTAAGAAGACTTATTGGTTTCGGTAAGGGGTCCGCT ATCTAGACG	cloning of H2B-GFP11 copy number plasmids
SB-GG-4x-BbsI-rev	TTACCGAAGACTTCAATAAACCTCCCACATCTCCCCC TGAAC	cloning of H2B-GFP11 copy number plasmids

References

Adams, Christopher C. and Jerry L. Workman (1993). "Nucleosome Displacement in Transcription". In: *Cell* 72.3, pp. 305–308. DOI: 10.1016/0092-8674(93)90109-4.

Adams, Richard R., Mar Carmena, and William C. Earnshaw (2001). "Chromosomal Passengers and the (Aurora) ABCs of Mitosis". In: *Trends in Cell Biology* 11.2, pp. 49–54. DOI: 10.1016/S0962-8924(00)01880-8.

Afonso, Olga et al. (2014). "Feedback Control of Chromosome Separation by a Midzone Aurora B Gradient". In: *Science* 345.6194, pp. 332–336. DOI: 10.1126/science.1251121.

Ahmad, Kami and Steven Henikoff (2021). "The H3.3K27M Oncohistone Antagonizes Reprogramming in Drosophila". In: *PLOS Genetics* 17.7. Ed. by Giovanni Bosco, e1009225. DOI: 10.1371/journal.pgen.1009225.

Alcaraz, Carlos et al. (1990). "Comparison of a Radioimmunoprecipitation Assay to Immunoblotting and ELISA for Detection of Antibody to African Swine Fever Virus". In: *Journal of Veterinary Diagnostic Investigation* 2.3, pp. 191–196. DOI: 10.1177/104063879000200307.

Aleyde, Van Eynde et al. (1995). "Molecular Cloning of NIPP-1, a Nuclear Inhibitor of Protein Phosphatase-1, Reveals Homology with Polypeptides Involved in RNA Processing". In: *Journal of Biological Chemistry* 270.47, pp. 28068–28074. DOI: 10.1074/jbc.270.47.28068.

Allen, Patrick B. et al. (1998). "Isolation and Characterization of PNUTS, a Putative Protein Phosphatase 1 Nuclear Targeting Subunit". In: *Journal of Biological Chemistry* 273.7, pp. 4089–4095. DOI: 10.1074/jbc.273.7.4089.

Allfrey, V. G., R. Faulkner, and A. E. Mirsky (1964). "Acetylation and Methylation of Histones and Their Possible Role in the Regulation of RNA Synthesis". In: *Proceedings of the National Academy of Sciences* 51.5, pp. 786–794. DOI: 10.1073/pnas.51.5.786.

Alva, Vikram and Andrei N Lupas (2019). "Histones Predate the Split between Bacteria and Archaea". In: *Bioinformatics* 35.14. Ed. by John Hancock, pp. 2349–2353. DOI: 10.1093/bioinformatics/bty1000.

Amatori, Stefano et al. (2021). "The Dark Side of Histones: Genomic Organization and Role of Oncohistones in Cancer". In: *Clinical Epigenetics* 13.1, p. 71. DOI: 10.1186/s13148-021-01057-x.

Andreassen, Paul R. et al. (1998). "Differential Subcellular Localization of Protein Phosphatase-1 α, Γ1, and δ Isoforms during Both Interphase and Mitosis in Mammalian Cells". In: *The Journal of Cell Biology* 141.5, pp. 1207–1215. DOI: 10.1083/jcb.141.5.1207.

Anest, Vasiliki et al. (2003). "A Nucleosomal Function for IκB Kinase-α in NF-κB-dependent Gene Expression". In: *Nature* 423.6940, pp. 659–663. DOI: 10.1038/nature01648.

Antonin, Wolfram and Heinz Neumann (2016). "Chromosome Condensation and Decondensation during Mitosis". In: *Current Opinion in Cell Biology* 40, pp. 15–22. DOI: 10.1016/j.ceb.2016.01.013.

Anzalone, Andrew V. et al. (2022). "Programmable Deletion, Replacement, Integration and Inversion of Large DNA Sequences with Twin Prime Editing". In: *Nature Biotechnology* 40.5, pp. 731–740. DOI: 10.1038/s41587-021-01133-w.

Araújo, A.P.U. et al. (2000). "Influence of the Histidine Tail on the Structure and Activity of Recombinant Chlorocatechol 1,2-Dioxygenase". In: *Biochemical and Biophysical Research Communications* 272.2, pp. 480–484. DOI: 10.1006/bbrc.2000.2802.

Arents, G and E N Moudrianakis (1995). "The Histone Fold: A Ubiquitous Architectural Motif Utilized in DNA Compaction and Protein Dimerization." In: *Proceedings of the National Academy of Sciences* 92.24, pp. 11170–11174. DOI: 10.1073/pnas.92.24.11170.

Arvey, Aaron et al. (2010). "Target mRNA Abundance Dilutes microRNA and siRNA Activity". In: *Molecular Systems Biology* 6.1, p. 363. DOI: 10.1038/msb.2010.24.

Banerjee, Taraswi and Debabrata Chakravarti (2011). "A Peek into the Complex Realm of Histone Phosphorylation". In: *Molecular and Cellular Biology* 31.24, pp. 4858–4873. DOI: 10.1128/MCB.05631-11.

Bannister, Andrew J and Tony Kouzarides (2011). "Regulation of Chromatin by Histone Modifications". In: *Cell Research* 21.3, pp. 381–395. DOI: 10.1038/cr.2011.22.

Barnhart, Meghan C. et al. (2011). "HJURP Is a CENP-A Chromatin Assembly Factor Sufficient to Form a Functional de Novo Kinetochore". In: *Journal of Cell Biology* 194.2, pp. 229–243. DOI: 10.1083/jcb.201012017.

Basant, Angika et al. (2015). "Aurora B Kinase Promotes Cytokinesis by Inducing Centralspindlin Oligomers That Associate with the Plasma Membrane". In: *Developmental Cell* 33.2, pp. 204–215. DOI: 10.1016/j.devcel.2015.03.015.

Battle, Daniel J. and Jennifer A. Doudna (2001). "The Stem-Loop Binding Protein Forms a Highly Stable and Specific Complex with the 3' Stem-Loop of Histone mRNAs". In: *RNA* 7.1, pp. 123–132. DOI: 10.1017/S1355838201001820.

Belapurkar, Ratnal (2021). "Molecular Mechanisms and Functional Consequences of HIF-1α Upregulation during the G1 Phase of the Cell Cycle in Normoxia". PhD thesis. Justus-Liebig-Universität Gießen. 127 pp.

Belmont, Andrew S (2006). "Mitotic Chromosome Structure and Condensation". In: *Current Opinion in Cell Biology* 18.6, pp. 632–638. DOI: 10.1016/j.ceb.2006.09.007.

Berger, Shelley L (2002). "Histone Modifications in Transcriptional Regulation". In: *Current Opinion in Genetics & Development* 12.2, pp. 142–148. DOI: 10.1016/S0959-437X(02)00279-4.

Bergmans, H E, I M Van Die, and W P Hoekstra (1981). "Transformation in Escherichia Coli: Stages in the Process". In: *Journal of Bacteriology* 146.2, pp. 564–570. DOI: 10.1128/jb.146.2.564-570.1981.

Bertani, G. (1951). "STUDIES ON LYSOGENESIS I: The Mode of Phage Liberation by Lysogenic Escherichia Coli". In: *Journal of Bacteriology* 62.3, pp. 293–300. DOI: 10.1128/jb.62.3.293-300.1951.

Bhakta, Shyam (2017). *Golden Gate Assembly Protocol*. Golden Gate Assembly. URL: https://wiki.rice.edu/confluence/display/BIODESIGN/Golden+Gate+Assembly (visited on 12/06/2023).

Bjerrum, OJ and C Schafer-Nielsen (1986). "Buffer Systems and Transfer Parameters for Semi Dry Electroblotting with a Horizontal Apparatus". In: *Electrophoresis '86: Proceedings of the Fifth Meeting of the International Electrophoresis Society*. Michael J. Dunn, (WCH), pp. 315–327.

BLOCK-iT™ RNAi Designer (2021). Thermo Fisher.

Bock, Ina et al. (2011). "Detailed Specificity Analysis of Antibodies Binding to Modified Histone Tails with Peptide Arrays". In: *Epigenetics* 6.2, pp. 256–263. DOI: 10.4161/epi.6.2.13837.

Bofill-De Ros, Xavier and Shuo Gu (2016). "Guidelines for the Optimal Design of miRNA-based shRNAs". In: *Methods* 103, pp. 157–166. DOI: 10.1016/j.ymeth.2016.04.003.

Bollen, Mathieu et al. (2010). "The Extended PP1 Toolkit: Designed to Create Specificity". In: *Trends in Biochemical Sciences* 35.8, pp. 450–458. DOI: 10.1016/j.tibs.2010.03.002.

Bondy, Stephen C. (1971). "The Synthesis and Decay of Histone Fractions and of Deoxyribonucleic Acid in the Developing Avian Brain". In: *Biochemical Journal* 123.3, pp. 465–469. DOI: 10.1042/bj1230465.

Bonner, Mary Kate et al. (2020). "The Borealin Dimerization Domain Interacts with Sgo1 to Drive Aurora B-mediated Spindle Assembly". In: *Molecular Biology of the Cell*, mbc.E20-05–0341. DOI: 10.1091/mbc.E20-05-0341.

Booth, Daniel G et al. (2014). "Ki-67 Is a PP1-interacting Protein That Organises the Mitotic Chromosome Periphery". In: *eLife* 3, e01641. DOI: 10.7554/eLife.01641.

Booth, William T. et al. (2018). "Impact of an N-terminal Polyhistidine Tag on Protein Thermal Stability". In: *ACS Omega* 3.1, pp. 760–768. DOI: 10.1021/acsomega.7b01598.

Boussif, O et al. (1995). "A Versatile Vector for Gene and Oligonucleotide Transfer into Cells in Culture and in Vivo: Polyethylenimine." In: *Proceedings of the National Academy of Sciences* 92.16, pp. 7297–7301. DOI: 10.1073/pnas.92.16.7297.

Bräuer, Maria et al. (2019). "The Influence of Commonly Used Tags on Structural Propensities and Internal Dynamics of Peptides". In: *Monatshefte für Chemie - Chemical Monthly* 150.5, pp. 913–925. DOI: 10.1007/s00706-019-02401-x.

Brautigan, David L. and Shirish Shenolikar (2018). "Protein Serine/Threonine Phosphatases: Keys to Unlocking Regulators and Substrates". In: *Annual Review of Biochemistry* 87.1, pp. 921–964. DOI: 10.1146/annurev-biochem-062917-012332.

Bryson, Terri D. et al. (2022). "A Giant Virus Genome Is Densely Packaged by Stable Nucleosomes within Virions". In: *Molecular Cell* 82.23, 4458–4470.e5. DOI: 10.1016/j.molcel.2022.10.020.

Budhavarapu, Varija N, Myrriah Chavez, and Jessica K Tyler (2013). "How Is Epigenetic Information Maintained through DNA Replication?" In: *Epigenetics & Chromatin* 6.1, p. 32. DOI: 10.1186/1756-8935-6-32.

Buhr, Florian et al. (2016). "Synonymous Codons Direct Cotranslational Folding toward Different Protein Conformations". In: *Molecular Cell* 61.3, pp. 341–351. DOI: 10.1016/j.molcel.2016.01.008.

Buschbeck, Marcus and Sandra B. Hake (2017). "Variants of Core Histones and Their Roles in Cell Fate Decisions, Development and Cancer". In: *Nature Reviews Molecular Cell Biology* 18.5, pp. 299–314. DOI: 10.1038/nrm.2016.166.

Butkevich, Eugenia et al. (2016). "Phosphorylation of FEZ1 by Microtubule Affinity Regulating Kinases Regulates Its Function in Presynaptic Protein Trafficking". In: *Scientific Reports* 6.1, p. 26965. DOI: 10.1038/srep26965.

Camps, Jordi et al. (2005). "Comprehensive Measurement of Chromosomal Instability in Cancer Cells: Combination of Fluorescence in Situ Hybridization and Cytokinesis-block Micronucleus Assay". In: *The FASEB Journal* 19.7, pp. 1–19. DOI: 10.1096/fj.04-2276fje.

Cang, Shundong et al. (2016). "Hypoacetylation, Hypomethylation, and Dephosphorylation of H2B Histones and Excessive Histone Deacetylase Activity in DU-145 Prostate Cancer Cells". In: *Journal of Hematology & Oncology* 9.1, p. 3. DOI: 10.1186/s13045-016-0233-x.

Cardoso, M.Cristina, Heinrich Leonhardt, and Bernardo Nadal-Ginard (1993). "Reversal of Terminal Differentiation and Control of DNA Replication: Cyclin A and Cdk2 Specifically Localize at Subnuclear Sites of DNA Replication". In: *Cell* 74.6, pp. 979–992. DOI: 10.1016/0092-8674(93)90721-2.

Carmena, Mar et al. (2012). "The Chromosomal Passenger Complex (CPC): From Easy Rider to the Godfather of Mitosis". In: *Nature Reviews Molecular Cell Biology*. DOI: 10.1038/nrm3474.

Ceulemans, Hugo and Mathieu Bollen (2004). "Functional Diversity of Protein Phosphatase-1, a Cellular Economizer and Reset Button". In: *Physiological Reviews* 84.1, pp. 1–39. DOI: 10.1152/physrev.00013.2003.

Chalkley, G R and H R Maurer (1965). "Turnover of Template-Bound Histone." In: *Proceedings of the National Academy of Sciences* 54.2, pp. 498–505. DOI: 10.1073/pnas.54.2.498.

Chambon, Jean-Philippe et al. (2013). "The PP2A Inhibitor I2PP2A Is Essential for Sister Chromatid Segregation in Oocyte Meiosis II". In: *Current Biology* 23.6, pp. 485–490. DOI: 10.1016/j.cub.2013.02.004.

Chan, Ying Wai, Kasper Fugger, and Stephen C. West (2018). "Unresolved Recombination Intermediates Lead to Ultra-Fine Anaphase Bridges, Chromosome Breaks and Aberrations". In: *Nature Cell Biology* 20.1, pp. 92–103. DOI: 10.1038/s41556-017-0011-1.

Chang, Donald C., Naihan Xu, and Kathy Q. Luo (2003). "Degradation of Cyclin B Is Required for the Onset of Anaphase in Mammalian Cells". In: *Journal of Biological Chemistry* 278.39, pp. 37865–37873. DOI: 10.1074/jbc.M306376200.

Chao, William C. H. et al. (2012). "Structure of the Mitotic Checkpoint Complex". In: *Nature* 484.7393, pp. 208–213. DOI: 10.1038/nature10896.

Cheeseman, Iain M. et al. (2006). "The Conserved KMN Network Constitutes the Core Microtubule-Binding Site of the Kinetochore". In: *Cell* 127.5, pp. 983–997. DOI: 10.1016/j.cell.2006.09.039.

Chen, Mark J., Jack E. Dixon, and Gerard Manning (2017). "Genomics and Evolution of Protein Phosphatases". In: *Science Signaling* 10.474, eaag1796. DOI: 10.1126/scisignal.aag1796.

Chen, Yu-Shan and Xiao-Bo Qiu (2012). "Transcription-Coupled Replacement of Histones: Degradation or Recycling?" In: *Journal of Genetics and Genomics* 39.11, pp. 575–580. DOI: 10.1016/j.jgg.2012.09.001.

Chen, Yujue et al. (2021). "Centromeric Transcription Maintains Centromeric Cohesion in Human Cells". In: *Journal of Cell Biology* 220.7, e202008146. DOI: 10.1083/jcb.202008146.

Cheung, Wang L. et al. (2003). "Apoptotic Phosphorylation of Histone H2B Is Mediated by Mammalian Sterile Twenty Kinase". In: *Cell* 113.4, pp. 507–517. DOI: 10.1016/S0092-8674(03)00355-6.

Choo, K H Andy (1997). "Centromere Proteins of Higher Eukaryotes". In: *The Centromere*. Oxford University PressOxford, pp. 143–253. DOI: 10.1093/oso/9780198577812.003.0006.

Clute, Paul and Jonathon Pines (1999). "Temporal and Spatial Control of Cyclin B1 Destruction in Metaphase". In: *Nature Cell Biology* 1.2, pp. 82–87. DOI: 10.1038/10049.

Corcoran, Emma Tung and Yannick Jacob (2023). "Direct Assessment of Histone Function Using Histone Replacement". In: *Trends in Biochemical Sciences* 48.1, pp. 53–70. DOI: 10.1016/j.tibs.2022.06.010.

Corcoran, Emma Tung et al. (2022). "Systematic Histone H4 Replacement in *Arabidopsis Thaliana* Reveals a Role for H4R17 in Regulating Flowering Time". In: *The Plant Cell* 34.10, pp. 3611–3631. DOI: 10.1093/plcell/koac211.

Dai, Jun et al. (2005). "The Kinase Haspin Is Required for Mitotic Histone H3 Thr 3 Phosphorylation and Normal Metaphase Chromosome Alignment". In: *Genes & Development* 19.4, pp. 472–488. DOI: 10.1101/gad.1267105.

Dave, Kapil et al. (2016). "The Effect of Fluorescent Protein Tags on Phosphoglycerate Kinase Stability Is Nonadditive". In: *The Journal of Physical Chemistry B* 120.11, pp. 2878–2885. DOI: 10.1021/acs.jpcb.5b11915.

Davis, Laura I. (1995). "The Nuclear Pore Complex". In: *Annual Review of Biochemistry* 64.1, pp. 865–896. DOI: 10.1146/annurev.bi.64.070195.004245.

De Castro, Inês J. et al. (2017). "Repo-Man/PP1 Regulates Heterochromatin Formation in Interphase". In: *Nature Communications* 8.1, p. 14048. DOI: 10.1038/ncomms14048.

De Koning, Leanne et al. (2007). "Histone Chaperones: An Escort Network Regulating Histone Traffic". In: *Nature Structural & Molecular Biology* 14.11, pp. 997–1007. DOI: 10.1038/nsmb1318.

DeLange, R J and E L Smith (1971). "Histones: Structure and Function". In: *Annual Review of Biochemistry* 40.1, pp. 279–314. DOI: 10.1146/annurev.bi.40.070171.001431.

DeLisle, Alice J. et al. (1983). “Regulation of Histone mRNA Production and Stability in Serum-Stimulated Mouse 3T6 Fibroblasts”. In: *Molecular and Cellular Biology* 3.11, pp. 1920–1929. DOI: 10.1128/mcb.3.11.1920-1929.1983.

Dephoure, Noah et al. (2008). “A Quantitative Atlas of Mitotic Phosphorylation”. In: *Proceedings of the National Academy of Sciences* 105.31, pp. 10762–10767. DOI: 10.1073/pnas.0805139105.

Dittmer, Dirk et al. (1993). “Gain of Function Mutations in P53”. In: *Nature Genetics* 4.1, pp. 42–46. DOI: 10.1038/ng0593-42.

Dunleavy, Elaine M. et al. (2009). “HJURP Is a Cell-Cycle-Dependent Maintenance and Deposition Factor of CENP-A at Centromeres”. In: *Cell* 137.3, pp. 485–497. DOI: 10.1016/j.cell.2009.02.040.

Earnshaw, William C. and Rebecca L. Bernat (1991). “Chromosomal Passengers: Toward an Integrated View of Mitosis”. In: *Chromosoma* 100.3, pp. 139–146. DOI: 10.1007/BF00337241.

Egelhofer, Thea A et al. (2011). “An Assessment of Histone-Modification Antibody Quality”. In: *Nature Structural & Molecular Biology* 18.1, pp. 91–93. DOI: 10.1038/nsmb.1972.

Eickbush, Thomas H. and Evangelos N. Moudrianakis (1978). “The Histone Core Complex: An Octamer Assembled by Two Sets of Protein-Protein Interactions”. In: *Biochemistry* 17.23, pp. 4955–4964. DOI: 10.1021/bi00616a016.

Elbakry, Amira and Markus Löbrich (2021). “Homologous Recombination Subpathways: A Tangle to Resolve”. In: *Frontiers in Genetics* 12, p. 723847. DOI: 10.3389/fgene.2021.723847.

Emanuele, Michael J. et al. (2008). “Aurora B Kinase and Protein Phosphatase 1 Have Opposing Roles in Modulating Kinetochore Assembly”. In: *The Journal of Cell Biology* 181.2, pp. 241–254. DOI: 10.1083/jcb.200710019.

Engel, Anja J. et al. (2021). “Codon Bias Can Determine Sorting of a Potassium Channel Protein”. In: *Cells* 10.5, p. 1128. DOI: 10.3390/cells10051128.

Eriksson, Peter R et al. (2012). “Regulation of Histone Gene Expression in Budding Yeast”. In: *Genetics* 191.1, pp. 7–20. DOI: 10.1534/genetics.112.140145.

Erives, Albert J. (2017). “Phylogenetic Analysis of the Core Histone Doublet and DNA Topo II Genes of Marseilleviridae: Evidence of Proto-Eukaryotic Provenance”. In: *Epigenetics & Chromatin* 10.1, p. 55. DOI: 10.1186/s13072-017-0162-0.

Fachinetti, Daniele et al. (2013). “A Two-Step Mechanism for Epigenetic Specification of Centromere Identity and Function”. In: *Nature Cell Biology* 15.9, pp. 1056–1066. DOI: 10.1038/ncb2805.

Faesen, Alex C. et al. (2017). “Basis of Catalytic Assembly of the Mitotic Checkpoint Complex”. In: *Nature* 542.7642, pp. 498–502. DOI: 10.1038/nature21384.

Fellmann, Christof et al. (2013). “An Optimized microRNA Backbone for Effective Single-Copy RNAi”. In: *Cell Reports* 5.6, pp. 1704–1713. DOI: 10.1016/j.celrep.2013.11.020.

Felsenfeld, Gary (1978). “Chromatin”. In: *Nature* 271.5641, pp. 115–122. DOI: 10.1038/271115a0.

Feng, Siyu et al. (2017). “Improved Split Fluorescent Proteins for Endogenous Protein Labeling”. In: *Nature Communications* 8.1, p. 370. DOI: 10.1038/s41467-017-00494-8.

Fink, Severin et al. (2018). “A Simple Approach for Multi-Targeted shRNA-mediated Inducible Knockdowns Using Sleeping Beauty Vectors”. In: *PLOS ONE* 13.10. Ed. by Wilfried A. Kues, e0205585. DOI: 10.1371/journal.pone.0205585.

Fischle, Wolfgang, Yanming Wang, and C David Allis (2003). “Histone and Chromatin Cross-Talk”. In: *Current Opinion in Cell Biology* 15.2, pp. 172–183. DOI: 10.1016/S0955-0674(03)00013-9.

Fitzgerald, Katherine A. et al. (2003). “IKKepsilon and TBK1 Are Essential Components of the IRF3 Signaling Pathway”. In: *Nature Immunology* 4.5, pp. 491–496. DOI: 10.1038/ni921.

Frank, Steven A. (2002). *Immunology and Evolution of Infectious Disease*. Princeton: Princeton University Press. 348 pp.

Gaidukov, Leonid et al. (2018). "A Multi-Landing Pad DNA Integration Platform for Mammalian Cell Engineering". In: *Nucleic Acids Research* 46.8, pp. 4072–4086. DOI: 10.1093/nar/gky216.

Gavet, Olivier and Jonathon Pines (2010). "Progressive Activation of CyclinB1-Cdk1 Coordinates Entry to Mitosis". In: *Developmental Cell* 18.4, pp. 533–543. DOI: 10.1016/j.devcel.2010.02.013.

Ge, Qing et al. (2010). "Minimal-Length Short Hairpin RNAs: The Relationship of Structure and RNAi Activity". In: *RNA* 16.1, pp. 106–117. DOI: 10.1261/rna.1894510.

Gelens, Lendert et al. (2018). "The Importance of Kinase–Phosphatase Integration: Lessons from Mitosis". In: *Trends in Cell Biology* 28.1, pp. 6–21. DOI: 10.1016/j.tcb.2017.09.005.

Giet, Régis and David M. Glover (2001). "*Drosophila* Aurora B Kinase Is Required for Histone H3 Phosphorylation and Condensin Recruitment during Chromosome Condensation and to Organize the Central Spindle during Cytokinesis". In: *The Journal of Cell Biology* 152.4, pp. 669–682. DOI: 10.1083/jcb.152.4.669.

Goldberg, Aaron D. et al. (2010). "Distinct Factors Control Histone Variant H3.3 Localization at Specific Genomic Regions". In: *Cell* 140.5, pp. 678–691. DOI: 10.1016/j.cell.2010.01.003.

Goldberg, Jonathan et al. (1995). "Three-Dimensional Structure of the Catalytic Subunit of Protein Serine/Threonine Phosphatase-1". In: *Nature* 376.6543, pp. 745–753. DOI: 10.1038/376745a0.

González-Loyola, Alejandra et al. (2015). "Aurora B Overexpression Causes Aneuploidy and P21 ^{Cip1} Repression during Tumor Development". In: *Molecular and Cellular Biology* 35.20, pp. 3566–3578. DOI: 10.1128/MCB.01286-14.

Gorgoni, Barbara et al. (2005). "The Stem–Loop Binding Protein Stimulates Histone Translation at an Early Step in the Initiation Pathway". In: *RNA* 11.7, pp. 1030–1042. DOI: 10.1261/rna.7281305.

Gossen, M and H Bujard (1992). "Tight Control of Gene Expression in Mammalian Cells by Tetracycline-Responsive Promoters." In: *Proceedings of the National Academy of Sciences* 89.12, pp. 5547–5551. DOI: 10.1073/pnas.89.12.5547.

Gossen, Manfred et al. (1995). "Transcriptional Activation by Tetracyclines in Mammalian Cells". In: *Science* 268.5218, pp. 1766–1769. DOI: 10.1126/science.7792603.

Goto, Hidemasa et al. (2002). "Aurora-B Phosphorylates Histone H3 at Serine28 with Regard to the Mitotic Chromosome Condensation". In: *Genes to Cells* 7.1, pp. 11–17. DOI: 10.1046/j.1356-9597.2001.00498.x.

Gottesfeld, J (1997). "Mitotic Repression of the Transcriptional Machinery". In: *Trends in Biochemical Sciences* 22.6, pp. 197–202. DOI: 10.1016/S0968-0004(97)01045-1.

Grallert, Agnes et al. (2015). "A PP1-PP2A Phosphatase Relay Controls Mitotic Progression". In: *Nature* 517.7532, pp. 94–98. DOI: 10.1038/nature14019.

Graña, X. and E. P. Reddy (1995). "Cell Cycle Control in Mammalian Cells: Role of Cyclins, Cyclin Dependent Kinases (CDKs), Growth Suppressor Genes and Cyclin-Dependent Kinase Inhibitors (CKIs)". In: *Oncogene* 11.2, pp. 211–219.

Grandy, David K. and Jerry B. Dodgson (1987). "Structure and Organization of the Chicken H2B Histone Gene Family". In: *Nucleic Acids Research* 15.3, pp. 1063–1080. DOI: 10.1093/nar/15.3.1063.

Graves, Hillary K. et al. (2016). "Mutations That Prevent or Mimic Persistent Post-Translational Modifications of the Histone H3 Globular Domain Cause Lethality and Growth Defects in Drosophila". In: *Epigenetics & Chromatin* 9.1, p. 9. DOI: 10.1186/s13072-016-0059-3.

Graves, Reed A. and William F. Marzluff (1984). "Rapid Reversible Changes in the Rate of Histone Gene Transcription and Histone mRNA Levels in Mouse Myeloma Cells". In: *Molecular and Cellular Biology* 4.2, pp. 351–357. DOI: 10.1128/mcb.4.2.351-357.1984.

Gruneberg, Ulrike et al. (2004). “Relocation of Aurora B from Centromeres to the Central Spindle at the Metaphase to Anaphase Transition Requires MKlp2”. In: *The Journal of Cell Biology* 166.2, pp. 167–172. DOI: 10.1083/jcb.200403084.

Grunstein, Michael (1997). “Histone Acetylation in Chromatin Structure and Transcription”. In: *Nature* 389.6649, pp. 349–352. DOI: 10.1038/38664.

Günesdogan, Ufuk, Herbert Jäckle, and Alf Herzig (2010). “A Genetic System to Assess in Vivo the Functions of Histones and Histone Modifications in Higher Eukaryotes”. In: *EMBO reports* 11.10, pp. 772–776. DOI: 10.1038/embor.2010.124.

– (2014). “Histone Supply Regulates S Phase Timing and Cell Cycle Progression”. In: *eLife* 3, e02443. DOI: 10.7554/eLife.02443.

Gunjan, Akash, Johanna Paik, and Alain Verreault (2006). “The Emergence of Regulated Histone Proteolysis”. In: *Current Opinion in Genetics & Development* 16.2, pp. 112–118. DOI: 10.1016/j.gde.2006.02.010.

Gunjan, Akash et al. (1999). “Effects of H1 Histone Variant Overexpression on Chromatin Structure”. In: *Journal of Biological Chemistry* 274.53, pp. 37950–37956. DOI: 10.1074/jbc.274.53.37950.

Gurard-Levin, Zachary A., Jean-Pierre Quivy, and Geneviève Almouzni (2014). “Histone Chaperones: Assisting Histone Traffic and Nucleosome Dynamics”. In: *Annual Review of Biochemistry* 83.1, pp. 487–517. DOI: 10.1146/annurev-biochem-060713-035536.

Haas, Jana et al. (2020). “Chromatin Targeting of HIPK2 Leads to Acetylation-Dependent Chromatin Decondensation”. In: *Frontiers in Cell and Developmental Biology* 8, p. 852. DOI: 10.3389/fcell.2020.00852.

Hadjantonakis, Anna-Katerina and Virginia E Papaioannou (2004). “Dynamic in Vivo Imaging and Cell Tracking Using a Histone Fluorescent Protein Fusion in Mice”. In: *BMC Biotechnology* 4.1, p. 33. DOI: 10.1186/1472-6750-4-33.

Hanahan, Douglas and Robert A. Weinberg (2011). “Hallmarks of Cancer: The Next Generation”. In: *Cell* 144.5, pp. 646–674. DOI: 10.1016/j.cell.2011.02.013.

Hanson, Roberta J. et al. (1996). “Efficient Extraction and Partial Purification of the Polyribosome-Associated Stem-Loop Binding Protein Bound to the 3‘ End of Histone mRNA”. In: *Biochemistry* 35.7, pp. 2146–2156. DOI: 10.1021/bi9521856.

Harris, M E et al. (1991). “Regulation of Histone mRNA in the Unperturbed Cell Cycle: Evidence Suggesting Control at Two Posttranscriptional Steps.” In: *Molecular and Cellular Biology* 11.5, pp. 2416–2424. DOI: 10.1128/MCB.11.5.2416.

Hassold, Terry J. and Patricia A . Jacobs (1984). “Trisomy in Man”. In: *Annual Review of Genetics* 18.1, pp. 69–97. DOI: 10.1146/annurev.ge.18.120184.000441.

Hatton, Ian A. et al. (2023). “The Human Cell Count and Size Distribution”. In: *Proceedings of the National Academy of Sciences* 120.39, e2303077120. DOI: 10.1073/pnas.2303077120.

Hauf, Silke, Irene C. Waizenegger, and Jan-Michael Peters (2001). “Cohesin Cleavage by Separase Required for Anaphase and Cytokinesis in Human Cells”. In: *Science* 293.5533, pp. 1320–1323. DOI: 10.1126/science.1061376.

Hauf, Silke et al. (2003). “The Small Molecule Hesperadin Reveals a Role for Aurora B in Correcting Kinetochore–Microtubule Attachment and in Maintaining the Spindle Assembly Checkpoint”. In: *Journal of Cell Biology* 161.2, pp. 281–294. DOI: 10.1083/jcb.200208092.

Heintz, Nathaniel, Hazel L. Sive, and Robert G. Roeder (1983). “Regulation of Human Histone Gene Expression: Kinetics of Accumulation and Changes in the Rate of Synthesis and in the Half-Lives of Individual Histone mRNAs During the HeLa Cell Cycle”. In: *Molecular and Cellular Biology* 3.4, pp. 539–550. DOI: 10.1128/mcb.3.4.539-550.1983.

Hendzel, Michael J. et al. (1997). “Mitosis-Specific Phosphorylation of Histone H3 Initiates Primarily within Pericentromeric Heterochromatin during G2 and Spreads in an Ordered Fashion Coincident with Mitotic Chromosome Condensation”. In: *Chromosoma* 106.6, pp. 348–360. DOI: 10.1007/s004120050256.

Hengeveld, Rutger C. C. et al. (2017). “Inner Centromere Localization of the CPC Maintains Centromere Cohesion and Allows Mitotic Checkpoint Silencing”. In: *Nature Communications* 8.1, p. 15542. DOI: 10.1038/ncomms15542.

Higgins, Jonathan M. G. and Mary Herbert (2013). “Nucleosome Assembly Proteins Get SET to Defeat the Guardian of Chromosome Cohesion”. In: *PLOS Genetics* 9.9, e1003829. DOI: 10.1371/journal.pgen.1003829.

Hirano, Tatsuya (2000). “Chromosome Cohesion, Condensation, and Separation”. In: *Annual Review of Biochemistry* 69.1, pp. 115–144. DOI: 10.1146/annurev.biochem.69.1.115.

Hiruma, Yoshitaka et al. (2015). “Competition between MPS1 and Microtubules at Kinetochores Regulates Spindle Checkpoint Signaling”. In: *Science* 348.6240, pp. 1264–1267. DOI: 10.1126/science.aaa4055.

Hocher, Antoine et al. (2023). “Histones with an Unconventional DNA-binding Mode in Vitro Are Major Chromatin Constituents in the Bacterium Bdellovibrio Bacteriovorus”. In: *Nature Microbiology* 8.11, pp. 2006–2019. DOI: 10.1038/s41564-023-01492-x.

Hoffelder, DianeR. et al. (2004). “Resolution of Anaphase Bridges in Cancer Cells”. In: *Chromosoma* 112.8. DOI: 10.1007/s00412-004-0284-6.

Hori, Tetsuya et al. (2008). “CCAN Makes Multiple Contacts with Centromeric DNA to Provide Distinct Pathways to the Outer Kinetochore”. In: *Cell* 135.6, pp. 1039–1052. DOI: 10.1016/j.cell.2008.10.019.

Hsieh-Wilson, Linda C. et al. (1999). “Characterization of the Neuronal Targeting Protein Spinophilin and Its Interactions with Protein Phosphatase-1”. In: *Biochemistry* 38.14, pp. 4365–4373. DOI: 10.1021/bi982900m.

Hsu, Jer-Yuan et al. (2000). “Mitotic Phosphorylation of Histone H3 Is Governed by Ipl1/Aurora Kinase and Glc7/PP1 Phosphatase in Budding Yeast and Nematodes”. In: *Cell* 102.3, pp. 279–291. DOI: 10.1016/S0092-8674(00)00034-9.

Huang, Xin et al. (2010). “Gene Transfer Efficiency and Genome-Wide Integration Profiling of Sleeping Beauty, Tol2, and PiggyBac Transposons in Human Primary T Cells”. In: *Molecular Therapy* 18.10, pp. 1803–1813. DOI: 10.1038/mt.2010.141.

Hubbard, Michael J. and Philip Cohen (1993). “On Target with a New Mechanism for the Regulation of Protein Phosphorylation”. In: *Trends in Biochemical Sciences* 18.5, pp. 172–177. DOI: 10.1016/0968-0004(93)90109-Z.

Hudson, Damien F., Kathryn M. Marshall, and William C. Earnshaw (2009). “Condensin: Architect of Mitotic Chromosomes”. In: *Chromosome Research* 17.2, pp. 131–144. DOI: 10.1007/s10577-008-9009-7.

Hudson, Damien F. et al. (2003). “Condensin Is Required for Nonhistone Protein Assembly and Structural Integrity of Vertebrate Mitotic Chromosomes”. In: *Developmental Cell* 5.2, pp. 323–336. DOI: 10.1016/S1534-5807(03)00199-0.

Hulett, H. R. et al. (1969). “Cell Sorting: Automated Separation of Mammalian Cells as a Function of Intracellular Fluorescence”. In: *Science* 166.3906, pp. 747–749. DOI: 10.1126/science.166.3906.747.

Hur, Woonyung et al. (2020). “CDK-Regulated Phase Separation Seeded by Histone Genes Ensures Precise Growth and Function of Histone Locus Bodies”. In: *Developmental Cell* 54.3, 379–394.e6. DOI: 10.1016/j.devcel.2020.06.003.

Hurd, P. J. and C. J. Nelson (2009). “Advantages of Next-Generation Sequencing versus the Microarray in Epigenetic Research”. In: *Briefings in Functional Genomics and Proteomics* 8.3, pp. 174–183. DOI: 10.1093/bfgp/elp013.

Hymes, J., K. Fleischhauer, and B. Wolf (1995). "Biotinylation of Histones by Human Serum Biotinidase: Assessment of Biotinyl-Transferase Activity in Sera from Normal Individuals and Children with Biotinidase Deficiency". In: *Biochemical and Molecular Medicine* 56.1, pp. 76–83. DOI: 10.1006/bmme.1995.1059.

Inniss, Mara C. et al. (2017). "A Novel Bxb1 Integrase RMCE System for High Fidelity Site-Specific Integration of mAb Expression Cassette in CHO Cells: Bxb1 RMCE for Site-Specific Integration". In: *Biotechnology and Bioengineering* 114.8, pp. 1837–1846. DOI: 10.1002/bit.26268.

InvivoGen siRNA Wizard (2021).

Ishiguro, Kei-ichiro and Yoshinori Watanabe (2007). "Chromosome Cohesion in Mitosis and Meiosis". In: *Journal of Cell Science* 120.3, pp. 367–369. DOI: 10.1242/jcs.03324.

Ishiguro, Kei-ichiro (2019). "The Cohesin Complex in Mammalian Meiosis". In: *Genes to Cells* 24.1, pp. 6–30. DOI: 10.1111/gtc.12652.

Ivics, Zoltán et al. (1997). "Molecular Reconstruction of Sleeping Beauty, a Tc1-like Transposon from Fish, and Its Transposition in Human Cells". In: *Cell* 91.4, pp. 501–510. DOI: 10.1016/S0092-8674(00)80436-5.

Izawa, Daisuke and Jonathon Pines (2015). "The Mitotic Checkpoint Complex Binds a Second CDC20 to Inhibit Active APC/C". In: *Nature* 517.7536, pp. 631–634. DOI: 10.1038/nature13911.

Izsvák, Zsuzsanna and Zoltán Ivics (2004). "Sleeping Beauty Transposition: Biology and Applications for Molecular Therapy". In: *Molecular Therapy* 9.2, pp. 147–156. DOI: 10.1016/j.ymthe.2003.11.009.

Jack, Antonia P. M. and Sandra B. Hake (2014). "Getting down to the Core of Histone Modifications". In: *Chromosoma* 123.4, pp. 355–371. DOI: 10.1007/s00412-014-0465-x.

Janicki, S. M. et al. (2004). "From Silencing to Gene Expression: Real-Time Analysis in Single Cells". In: *Cell* 116.5, pp. 683–98. DOI: 10.1016/s0092-8674(04)00171-0.

Jegou, Thibaud et al. (2009). "Dynamics of Telomeres and Promyelocytic Leukemia Nuclear Bodies in a Telomerase-Negative Human Cell Line". In: *Molecular Biology of the Cell* 20.7, pp. 2070–2082. DOI: 10.1091/mbc.e08-02-0108.

Jenuwein, Thomas and C. David Allis (2001). "Translating the Histone Code". In: *Science* 293.5532, pp. 1074–1080. DOI: 10.1126/science.1063127.

Jeppesen, Peter (2000). "Immunofluorescence in Cytogenetic Analysis: Method and Applications". In: *Genetics and Molecular Biology* 23.4, pp. 1107–1114. DOI: 10.1590/S1415-47572000000400059.

Johnson, D. G. and C. L. Walker (1999). "Cyclins and Cell Cycle Checkpoints". In: *Annual Review of Pharmacology and Toxicology* 39.1, pp. 295–312. DOI: 10.1146/annurev.pharmtox.39.1.295.

Jusiak, Barbara et al. (2019). "Comparison of Integrases Identifies Bxb1-GA Mutant as the Most Efficient Site-Specific Integrase System in Mammalian Cells". In: *ACS Synthetic Biology* 8.1, pp. 16–24. DOI: 10.1021/acssynbio.8b00089.

Kalitsis, Paul and K H Andy Choo (1997). "Centromere DNA of Higher Eukaryotes". In: Choo, K H Andy. *The Centromere*. Oxford University PressOxford, pp. 97–142. DOI: 10.1093/oso/9780198577812.003.0005.

Kamiyama, Daichi et al. (2016). "Versatile Protein Tagging in Cells with Split Fluorescent Protein". In: *Nature Communications* 7.1, p. 11046. DOI: 10.1038/ncomms11046.

Kanda, Teru, Kevin F. Sullivan, and Geoffrey M. Wahl (1998). "Histone–GFP Fusion Protein Enables Sensitive Analysis of Chromosome Dynamics in Living Mammalian Cells". In: *Current Biology* 8.7, pp. 377–385. DOI: 10.1016/S0960-9822(98)70156-3.

Karlić, Rosa et al. (2010). "Histone Modification Levels Are Predictive for Gene Expression". In: *Proceedings of the National Academy of Sciences* 107.7, pp. 2926–2931. DOI: 10.1073/pnas.0909344107.

Kawashima, Shigehiro A. et al. (2010). "Phosphorylation of H2A by Bub1 Prevents Chromosomal Instability Through Localizing Shugoshin". In: *Science* 327.5962, pp. 172–177. DOI: 10.1126/science.1180189.

Keck, Kristin M. and Lucy F. Pemberton (2012). "Histone Chaperones Link Histone Nuclear Import and Chromatin Assembly". In: *Biochimica et Biophysica Acta (BBA) - Gene Regulatory Mechanisms* 1819.3-4, pp. 277–289. DOI: 10.1016/j.bbagrm.2011.09.007.

Khan, Dilshad H. et al. (2017). "Mitogen-Induced Distinct Epialleles Are Phosphorylated at Either H3S10 or H3S28, Depending on H3K27 Acetylation". In: *Molecular Biology of the Cell* 28.6. Ed. by A. Gregory Matera, pp. 817–824. DOI: 10.1091/mbc.e16-08-0618.

Kim, Soojin et al. (2011). "Pre-mRNA Splicing Is a Determinant of Histone H3K36 Methylation". In: *Proceedings of the National Academy of Sciences* 108.33, pp. 13564–13569. DOI: 10.1073/pnas.1109475108.

Kim, Ji-Young et al. (2012). "H3K27 Methylation and H3S28 Phosphorylation-dependent Transcriptional Regulation by INHAT Subunit SET/TAF-Iβ". In: *FEBS Letters* 586.19, pp. 3159–3165. DOI: 10.1016/j.febslet.2012.06.026.

Kimple, Michelle E., Allison L. Brill, and Renee L. Pasker (2013). "Overview of Affinity Tags for Protein Purification". In: *Current Protocols in Protein Science* 73.1. DOI: 10.1002/0471140864.ps0909s73.

Kitajima, Tomoya S., Shigehiro A. Kawashima, and Yoshinori Watanabe (2004). "The Conserved Kinetochore Protein Shugoshin Protects Centromeric Cohesion during Meiosis". In: *Nature* 427.6974 (6974), pp. 510–517. DOI: 10.1038/nature02312.

Kitajima, Tomoya S. et al. (2006). "Shugoshin Collaborates with Protein Phosphatase 2A to Protect Cohesin". In: *Nature* 441.7089 (7089), pp. 46–52. DOI: 10.1038/nature04663.

Komor, Alexis C. et al. (2016). "Programmable Editing of a Target Base in Genomic DNA without Double-Stranded DNA Cleavage". In: *Nature* 533.7603, pp. 420–424. DOI: 10.1038/nature17946.

Kops, Geert J. P. L., Beth A. A. Weaver, and Don W. Cleveland (2005). "On the Road to Cancer: Aneuploidy and the Mitotic Checkpoint". In: *Nature Reviews Cancer* 5.10, pp. 773–785. DOI: 10.1038/nrc1714.

Kornberg, Roger D. and Jean O. Thomas (1974). "Chromatin Structure: Oligomers of the Histones: The Histones Comprise an (F2A1)\textsubscript{2} (F3)\textsubscript{2} Tetramer, a Different Oligomer of F2A2 and F2B, and Monomer of F1." In: *Science* 184.4139, pp. 865–868. DOI: 10.1126/science.184.4139.865.

Kowarz, Eric, Denise Löscher, and Rolf Marschalek (2015). "Optimized Sleeping Beauty Transposons Rapidly Generate Stable Transgenic Cell Lines". In: *Biotechnology Journal* 10.4, pp. 647–653. DOI: 10.1002/biot.201400821.

Krasnoselsky, Alexei L et al. (2005). "Altered Expression of Cell Cycle Genes Distinguishes Aggressive Neuroblastoma". In: *Oncogene* 24.9, pp. 1533–1541. DOI: 10.1038/sj.onc.1208341.

Kreienbaum, Carlotta, Lena W. Paasche, and Sandra B. Hake (2022). "H2A.Z's 'Social' Network: Functional Partners of an Enigmatic Histone Variant". In: *Trends in Biochemical Sciences* 47.11, pp. 909–920. DOI: 10.1016/j.tibs.2022.04.014.

Krishnan, Swathi et al. (2017). "Phospho-H1 Decorates the Inter-chromatid Axis and Is Evicted along with Shugoshin by SET during Mitosis". In: *Molecular Cell* 67.4, 579–593.e6. DOI: 10.1016/j.molcel.2017.07.008.

Kruitwagen, Tom et al. (2015). "Axial Contraction and Short-Range Compaction of Chromatin Synergistically Promote Mitotic Chromosome Condensation". In: *eLife* 4, e10396. DOI: 10.7554/eLife.10396.

Kueng, Stephanie et al. (2006). "Wapl Controls the Dynamic Association of Cohesin with Chromatin". In: *Cell* 127.5, pp. 955–967. DOI: 10.1016/j.cell.2006.09.040.

Kumar, Ganesan Senthil et al. (2016). "The Ki-67 and RepoMan Mitotic Phosphatases Assemble via an Identical, yet Novel Mechanism". In: *eLife* 5, e16539. DOI: 10.7554/eLife.16539.

Laemmli, U. K. (1970). "Cleavage of Structural Proteins during the Assembly of the Head of Bacteriophage T4". In: *Nature* 227.5259, pp. 680–685. DOI: 10.1038/227680a0.

Lampson, Michael and Ekaterina Grishchuk (2017). "Mechanisms to Avoid and Correct Erroneous Kinetochore-Microtubule Attachments". In: *Biology* 6.4, p. 1. DOI: 10.3390/biology6010001.

Lau, Priscilla Nga Ieng and Peter Cheung (2010). "Histone Phosphorylation". In: *Handbook of Cell Signaling*. Elsevier, pp. 2399–2408. DOI: 10.1016/B978-0-12-374145-5.00288-6.

– (2011). "Histone Code Pathway Involving H3 S28 Phosphorylation and K27 Acetylation Activates Transcription and Antagonizes Polycomb Silencing". In: *Proceedings of the National Academy of Sciences* 108.7, pp. 2801–2806. DOI: 10.1073/pnas.1012798108.

Lee, Jung-Shin, Edwin Smith, and Ali Shilatifard (2010). "The Language of Histone Crosstalk". In: *Cell* 142.5, pp. 682–685. DOI: 10.1016/j.cell.2010.08.011.

Levine, Michelle S. and Andrew J. Holland (2018). "The Impact of Mitotic Errors on Cell Proliferation and Tumorigenesis". In: *Genes & Development* 32.9-10, pp. 620–638. DOI: 10.1101/gad.314351.118.

Lewis, Peter W. et al. (2013). "Inhibition of PRC2 Activity by a Gain-of-Function H3 Mutation Found in Pediatric Glioblastoma". In: *Science* 340.6134, pp. 857–861. DOI: 10.1126/science.1232245.

Li, Jie, Jeong Hyun Ahn, and Gang Greg Wang (2019). "Understanding Histone H3 Lysine 36 Methylation and Its Deregulation in Disease". In: *Cellular and Molecular Life Sciences* 76.15, pp. 2899–2916. DOI: 10.1007/s00018-019-03144-y.

Liang, Qi et al. (2009). "Chromosomal Mobilization and Reintegration of *Sleeping Beauty* and *PiggyBac* Transposons". In: *genesis* 47.6, pp. 404–408. DOI: 10.1002/dvg.20508.

Liu, Dan et al. (2009). "Sensing Chromosome Bi-Orientation by Spatial Separation of Aurora B Kinase from Kinetochore Substrates". In: *Science* 323.5919, pp. 1350–1353. DOI: 10.1126/science.1167000.

Liu, Hong, Susannah Rankin, and Hongtao Yu (2013). "Phosphorylation-Enabled Binding of SGO1–PP2A to Cohesin Protects Sororin and Centromeric Cohesion during Mitosis". In: *Nature Cell Biology* 15.1 (1), pp. 40–49. DOI: 10.1038/ncb2637.

Liu, Hong et al. (2015). "Mitotic Transcription Installs Sgo1 at Centromeres to Coordinate Chromosome Segregation". In: *Molecular Cell* 59.3, pp. 426–436. DOI: 10.1016/j.molcel.2015.06.018.

Liu, Ji-Long et al. (2006). "The *Drosophila Melanogaster* Cajal Body". In: *The Journal of Cell Biology* 172.6, pp. 875–884. DOI: 10.1083/jcb.200511038.

Livak, Kenneth J. and Thomas D. Schmittgen (2001). "Analysis of Relative Gene Expression Data Using Real-Time Quantitative PCR and the 2-ΔΔCT Method". In: *Methods* 25.4, pp. 402–408. DOI: 10.1006/meth.2001.1262.

Lois, Carlos et al. (2002). "Germline Transmission and Tissue-Specific Expression of Transgenes Delivered by Lentiviral Vectors". In: *Science* 295.5556, pp. 868–872. DOI: 10.1126/science.1067081.

Long, Mengping et al. (2019). "A Novel Histone H4 Variant H4G Regulates rDNA Transcription in Breast Cancer". In: *Nucleic Acids Research* 47.16, pp. 8399–8409. DOI: 10.1093/nar/gkz547.

Low, Benjamin E. et al. (2022). "Efficient Targeted Transgenesis of Large Donor DNA into Multiple Mouse Genetic Backgrounds Using Bacteriophage Bxb1 Integrase". In: *Scientific Reports* 12.1, p. 5424. DOI: 10.1038/s41598-022-09445-w.

Luco, Reini F. et al. (2010). "Regulation of Alternative Splicing by Histone Modifications". In: *Science* 327.5968, pp. 996–1000. DOI: 10.1126/science.1184208.

Luger, Karolin et al. (1997). "Crystal Structure of the Nucleosome Core Particle at 2.8 Å Resolution". In: *Nature* 389.6648, pp. 251–260. DOI: 10.1038/38444.

Ma, Hoi Tang and Randy Y.C. Poon (2020). "Aurora Kinases and DNA Damage Response". In: *Mutation Research/Fundamental and Molecular Mechanisms of Mutagenesis* 821, p. 111716. DOI: 10.1016/j.mrfmmm.2020.111716.

Macdonald, Neil et al. (2005). “Molecular Basis for the Recognition of Phosphorylated and Phosphoacetylated Histone H3 by 14-3-3”. In: *Molecular Cell* 20.2, pp. 199–211. DOI: 10.1016/j.molcel.2005.08.032.

Madeira, Fábio et al. (2022). “Search and Sequence Analysis Tools Services from EMBL-EBI in 2022”. In: *Nucleic Acids Research* 50.W1, W276–W279. DOI: 10.1093/nar/gkac240.

Magidson, Valentin et al. (2011). “The Spatial Arrangement of Chromosomes during Prometaphase Facilitates Spindle Assembly”. In: *Cell* 146.4, pp. 555–567. DOI: 10.1016/j.cell.2011.07.012.

Mandel, M. and A. Higa (1970). “Calcium-Dependent Bacteriophage DNA Infection”. In: *Journal of Molecular Biology* 53.1, pp. 159–162. DOI: 10.1016/0022-2836(70)90051-3.

Manning, G. et al. (2002). “The Protein Kinase Complement of the Human Genome”. In: *Science* 298.5600, pp. 1912–1934. DOI: 10.1126/science.1075762.

Manzione, Maria Giulia et al. (2020). “Co-Regulation of the Antagonistic RepoMan:Aurora-B Pair in Proliferating Cells”. In: *Molecular Biology of the Cell* 31.6, pp. 419–438. DOI: 10.1091/mbc.E19-12-0698.

Martin, Benjamin J. E. et al. (2021). “Transcription Shapes Genome-Wide Histone Acetylation Patterns”. In: *Nature Communications* 12.1, p. 210. DOI: 10.1038/s41467-020-20543-z.

Marzluff, William F. (2005). “Metazoan Replication-Dependent Histone mRNAs: A Distinct Set of RNA Polymerase II Transcripts”. In: *Current Opinion in Cell Biology* 17.3, pp. 274–280. DOI: 10.1016/j.ceb.2005.04.010.

Marzluff, William F. and Kaitlin P. Koreski (2017). “Birth and Death of Histone mRNAs”. In: *Trends in Genetics* 33.10, pp. 745–759. DOI: 10.1016/j.tig.2017.07.014.

Marzluff, William F. and Niranjan B. Pandey (1988). “Multiple Regulatory Steps Control Histone mRNA Concentrations”. In: *Trends in Biochemical Sciences* 13.2, pp. 49–52. DOI: 10.1016/0968-0004(88)90027-8.

Marzluff, William F., Eric J. Wagner, and Robert J. Duronio (2008). “Metabolism and Regulation of Canonical Histone mRNAs: Life without a Poly(A) Tail”. In: *Nature Reviews Genetics* 9.11, pp. 843–854. DOI: 10.1038/nrg2438.

Marzluff, William F. et al. (2002). “The Human and Mouse Replication-Dependent Histone Genes”. In: *Genomics* 80.5, pp. 487–498. DOI: 10.1006/geno.2002.6850.

Matsubara, Kazuko et al. (2007). “Global Analysis of Functional Surfaces of Core Histones with Comprehensive Point Mutants”. In: *Genes to Cells* 12.1, pp. 13–33. DOI: 10.1111/j.1365-2443.2007.01031.x.

Matsushime, Hitoshi et al. (1994). “D-Type Cyclin-Dependent Kinase Activity in Mammalian Cells”. In: *Molecular and Cellular Biology* 14.3, pp. 2066–2076. DOI: 10.1128/mcb.14.3.2066-2076.1994.

Mattioli, Ivan et al. (2006). “Inducible Phosphorylation of NF-kappaB P65 at Serine 468 by T Cell Costimulation Is Mediated by IKKepsilin”. In: *Journal of Biological Chemistry* 281.10, pp. 6175–6183. DOI: 10.1074/jbc.M508045200.

Matveeva, Olga et al. (2012). “Optimized Models for Design of Efficient miR30-based shRNAs”. In: *Frontiers in Genetics* 3.

McGuinness, Barry E et al. (2005). “Shugoshin Prevents Dissociation of Cohesin from Centromeres During Mitosis in Vertebrate Cells”. In: *PLoS Biology* 3.3. Ed. by R. Scott Hawley, e86. DOI: 10.1371/journal.pbio.0030086.

McIntosh, J. Richard (2016). “Mitosis”. In: *Cold Spring Harbor Perspectives in Biology* 8.9, a023218. DOI: 10.1101/cshperspect.a023218.

Mcintyre, Glen J et al. (2011). “The Effects of Stem Length and Core Placement on shRNA Activity”. In: *BMC Molecular Biology* 12.1, p. 34. DOI: 10.1186/1471-2199-12-34.

Meerbrey, Kristen L. et al. (2011). "The pINDUCER Lentiviral Toolkit for Inducible RNA Interference in Vitro and in Vivo". In: *Proceedings of the National Academy of Sciences of the United States of America* 108.9, pp. 3665–3670. DOI: 10.1073/pnas.1019736108.

Millán-Zambrano, Gonzalo et al. (2022). "Histone Post-Translational Modifications — Cause and Consequence of Genome Function". In: *Nature Reviews Genetics* 23.9, pp. 563–580. DOI: 10.1038/s41576-022-00468-7.

Miyazaki, Wesley Y. and Terry L. Orr-Weaver (1994). "Sister-Chromatid Cohesion in Mitosis and Meiosis". In: *Annual Review of Genetics* 28.1, pp. 167–187. DOI: 10.1146/annurev.ge.28.120194.001123.

Moens, Peter B. (1987). "Introduction to Meiosis". In: *Meiosis*. Elsevier, pp. 1–17. DOI: 10.1016/B978-0-12-503365-7.50005-5.

Mohammad, Faizaan and Kristian Helin (2017). "Oncohistones: Drivers of Pediatric Cancers". In: *Genes & Development* 31.23-24, pp. 2313–2324. DOI: 10.1101/gad.309013.117.

Morgan, Marc Alard and Ali Shilatifard (2013). "(Poly)Combing the Pediatric Cancer Genome for Answers". In: *Science* 340.6134, pp. 823–824. DOI: 10.1126/science.1239223.

Morozova, Olena and Marco A. Marra (2008). "Applications of Next-Generation Sequencing Technologies in Functional Genomics". In: *Genomics* 92.5, pp. 255–264. DOI: 10.1016/j.ygeno.2008.07.001.

Morrison, Olivia and Jitendra Thakur (2021). "Molecular Complexes at Euchromatin, Heterochromatin and Centromeric Chromatin". In: *International Journal of Molecular Sciences* 22.13, p. 6922. DOI: 10.3390/ijms22136922.

Mowry, KL and JA Steitz (1987). "Identification of the Human U7 snRNP as One of Several Factors Involved in the 3' End Maturation of Histone Premessenger RNA's". In: *Science* 238.4834, p. 1682. DOI: 10.1126/science.2825355.

Mullis, Kary B. (1987). "Process for Amplifying Nucleic Acid Sequences". U.S. pat. 4683202A. Cetus Corp.

Murray, Andrew W and Marc W Kirschner (1989). "The Role of Cyclin Synthesis and Degradation in the Control of Maturation Promoting Factor Activity". In: 339.

Nacev, Benjamin A. et al. (2019). "The Expanding Landscape of 'Oncohistone' Mutations in Human Cancers". In: *Nature* 567.7749, pp. 473–478. DOI: 10.1038/s41586-019-1038-1.

Nakajima, Masato et al. (2007). "The Complete Removal of Cohesin from Chromosome Arms Depends on Separase". In: *Journal of Cell Science* 120.23, pp. 4188–4196. DOI: 10.1242/jcs.011528.

Nakayama, Tatsuo, Shinji Takechi, and Yasunari Takami (1993). "The Chicken Histone Gene Family". In: *Comparative Biochemistry and Physiology Part B: Comparative Biochemistry* 104.4, pp. 635–639. DOI: 10.1016/0305-0491(93)90189-C.

Negrini, Simona, Vassilis G. Gorgoulis, and Thanos D. Halazonetis (2010). "Genomic Instability — an Evolving Hallmark of Cancer". In: *Nature Reviews Molecular Cell Biology* 11.3, pp. 220–228. DOI: 10.1038/nrm2858.

Nezi, Luigi and Andrea Musacchio (2009). "Sister Chromatid Tension and the Spindle Assembly Checkpoint". In: *Current Opinion in Cell Biology* 21.6, pp. 785–795. DOI: 10.1016/j.ceb.2009.09.007.

Nigg, Erich A. (2001). "Mitotic Kinases as Regulators of Cell Division and Its Checkpoints". In: *Nature Reviews Molecular Cell Biology* 2.1, pp. 21–32. DOI: 10.1038/35048096.

Nishiyama, Tomoko et al. (2013). "Aurora B and Cdk1 Mediate Wapl Activation and Release of Acetylated Cohesin from Chromosomes by Phosphorylating Sororin". In: *Proceedings of the National Academy of Sciences* 110.33, pp. 13404–13409. DOI: 10.1073/pnas.1305020110.

Nowak, Scott J. and Victor G. Corces (2000). "Phosphorylation of Histone H3 Correlates with Transcriptionally Active Loci". In: *Genes & Development* 14.23, pp. 3003–3013. DOI: 10.1101/gad.848800.

Nurse, Paul (1990). "Universal Control Mechanism Regulating Onset of M-phase". In: *Nature* 344.6266, pp. 503–508. DOI: 10.1038/344503a0.

Obaya, A.J. and J.M. Sedivy (2002). "Regulation of Cyclin-Cdk Activity in Mammalian Cells". In: *Cellular and Molecular Life Sciences (CMLS)* 59.1, pp. 126–142. DOI: 10.1007/s00018-002-8410-1.

Oestergaard, Vibe (2017). "Immunostaining of Formaldehyde-fixed Metaphase Chromosome from Untreated and Aphidicolin-treated DT40 Cells". In: *BIO-PROTOCOL* 7.9. DOI: 10.21769/BioProtoc.2259.

Ohkura, Hiroyuki (2015). "Meiosis: An Overview of Key Differences from Mitosis". In: *Cold Spring Harbor Perspectives in Biology* 7.5, a015859. DOI: 10.1101/cshperspect.a015859.

Ohtsubo, Motoaki et al. (1995). "Human Cyclin E, a Nuclear Protein Essential for the G_1 -to-S Phase Transition". In: *Molecular and Cellular Biology* 15.5, pp. 2612–2624. DOI: 10.1128/MCB.15.5.2612.

Olins, Ada L. and Donald E. Olins (1974). "Spheroid Chromatin Units (ν Bodies)". In: *Science* 183.4122, pp. 330–332. DOI: 10.1126/science.183.4122.330.

Palozola, Katherine C. et al. (2017). "Mitotic Transcription and Waves of Gene Reactivation during Mitotic Exit". In: *Science* 358.6359, pp. 119–122. DOI: 10.1126/science.aal4671.

Pandey, NB and WF Marzluff (1987). "The Stem-Loop Structure at the 3' End of Histone mRNA Is Necessary and Sufficient for Regulation of Histone mRNA Stability." In: *Molecular and Cellular Biology* 7.12, pp. 4557–4559. DOI: 10.1128/MCB.7.12.4557.

Papini, Diana, Mark D. Levasseur, and Jonathan M.G. Higgins (2021). "The Aurora B Gradient Sustains Kinetochore Stability in Anaphase". In: *Cell Reports* 37.6, p. 109818. DOI: 10.1016/j.celrep.2021.109818.

Park, Choon-Ho and Kyong-Tai Kim (2012). "Apoptotic Phosphorylation of Histone H3 on Ser-10 by Protein Kinase Cδ". In: *PLoS ONE* 7.9. Ed. by Thomas G. Hofmann, e44307. DOI: 10.1371/journal.pone.0044307.

Park, Sung Ho et al. (2008). "Generation and Application of New Rat Monoclonal Antibodies against Synthetic FLAG and OLLAS Tags for Improved Immunodetection". In: *Journal of Immunological Methods* 331.1-2, pp. 27–38. DOI: 10.1016/j.jim.2007.10.012.

Peng, Aimin et al. (2010). "Repo-Man Controls a Protein Phosphatase 1-Dependent Threshold for DNA Damage Checkpoint Activation". In: *Current Biology* 20.5, pp. 387–396. DOI: 10.1016/j.cub.2010.01.020.

Peterson, Craig L and Marc-André Laniel (2004). "Histones and Histone Modifications". In: *Current Biology* 14.14, R546–R551. DOI: 10.1016/j.cub.2004.07.007.

Peti, Wolfgang, Angus C. Nairn, and Rebecca Page (2013). "Structural Basis for Protein Phosphatase 1 Regulation and Specificity". In: *FEBS Journal* 280.2, pp. 596–611. DOI: 10.1111/j.1742-4658.2012.08509.x.

Pfisterer, Maximilian and M. Lienhard Schmitz (2022). "Testing the Effect of Histone Acetyltransferases on Local Chromatin Compaction". In: *HDAC/HAT Function Assessment and Inhibitor Development*. 1st ed. Vol. 2. 2 vols. Methods in Molecular Biology. Springer Nature.

Pfisterer, Maximilian et al. (2024). "The Aurora B-controlled PP1/RepoMan Complex Determines the Spatial and Temporal Distribution of Mitotic H2B S6 Phosphorylation". In: *Open Biology*. DOI: 10.1098/rsob.230460.

Piazza, Aurèle et al. (2021). "Cohesin Regulates Homology Search during Recombinational DNA Repair". In: *Nature Cell Biology* 23.11, pp. 1176–1186. DOI: 10.1038/s41556-021-00783-x.

Pihan, German A. and Stephen J. Doxsey (1999). "The Mitotic Machinery as a Source of Genetic Instability in Cancer". In: *Seminars in Cancer Biology* 9.4, pp. 289–302. DOI: 10.1006/scbi.1999.0131.

Pinsky, Benjamin A. and Sue Biggins (2005). "The Spindle Checkpoint: Tension versus Attachment". In: *Trends in Cell Biology* 15.9, pp. 486–493. DOI: 10.1016/j.tcb.2005.07.005.

Poon, Randy Y. C. (2007). "Mitotic Phosphorylation: Breaking the Balance of Power by a Tactical Retreat". In: *Biochemical Journal* 403.2, e5. DOI: 10.1042/BJ20070290.

Potapova, Tamara A. et al. (2006). "The Reversibility of Mitotic Exit in Vertebrate Cells". In: *Nature* 440.7086, pp. 954–958. DOI: 10.1038/nature04652.

Qi, Guangying et al. (2007). "Aurora-B Expression and Its Correlation with Cell Proliferation and Metastasis in Oral Cancer". In: *Virchows Archiv* 450.3, pp. 297–302. DOI: 10.1007/s00428-006-0360-9.

Qian, Junbin et al. (2011). "PP1/Repo-man Dephosphorylates Mitotic Histone H3 at T3 and Regulates Chromosomal Aurora B Targeting." In: *Current biology : CB* 21.9, pp. 766–773. DOI: 10.1016/j.cub.2011.03.047.

Qian, Junbin et al. (2013). "Aurora B Defines Its Own Chromosomal Targeting by Opposing the Recruitment of the Phosphatase Scaffold Repo-Man". In: *Current Biology* 23.12, pp. 1136–1143. DOI: 10.1016/j.cub.2013.05.017.

Qian, Junbin et al. (2015). "Cdk1 Orders Mitotic Events through Coordination of a Chromosome-Associated Phosphatase Switch". In: *Nature Communications* 6. DOI: 10.1038/ncomms10215.

Qu, Qianhui et al. (2019). "SET Binding to Sgo1 Inhibits Sgo1–Cohesin Interactions and Promotes Chromosome Segregation". In: *Journal of Cell Biology* 218.8, pp. 2514–2528. DOI: 10.1083/jcb.201810096.

Ramos, Facundo et al. (2019). "Role of Protein Phosphatases PP1, PP2A, PP4 and Cdc14 in the DNA Damage Response". In: *Cell Stress* 3.3, pp. 70–85. DOI: 10.15698/cst2019.03.178.

Ravi, Maruthachalam and Simon W. L. Chan (2010). "Haploid Plants Produced by Centromere-Mediated Genome Elimination". In: *Nature* 464.7288, pp. 615–618. DOI: 10.1038/nature08842.

Rello-Varona, S et al. (2010). "An Automated Fluorescence Videomicroscopy Assay for the Detection of Mitotic Catastrophe". In: *Cell Death & Disease* 1.2, e25–e25. DOI: 10.1038/cddis.2010.6.

Reverón-Gómez, Nazaret et al. (2018). "Accurate Recycling of Parental Histones Reproduces the Histone Modification Landscape during DNA Replication". In: *Molecular Cell* 72.2, 239–249.e5. DOI: 10.1016/j.molcel.2018.08.010.

Rieder, C L et al. (1995). "The Checkpoint Delaying Anaphase in Response to Chromosome Monoorientation Is Mediated by an Inhibitory Signal Produced by Unattached Kinetochores." In: *The Journal of cell biology* 130.4, pp. 941–948. DOI: 10.1083/jcb.130.4.941.

Robbins, Elliott and Thaddeus W. Borun (1967). "The Cytoplasmic Synthesis of Histones in HeLa Cells and Its Temporal Relationship to DNA Replication". In: *Proceedings of the National Academy of Sciences* 57.2, pp. 409–416. DOI: 10.1073/pnas.57.2.409.

Rogakou, Emmy P. et al. (1998). "DNA Double-stranded Breaks Induce Histone H2AX Phosphorylation on Serine 139". In: *Journal of Biological Chemistry* 273.10, pp. 5858–5868. DOI: 10.1074/jbc.273.10.5858.

Romei, Matthew G. and Steven G. Boxer (2019). "Split Green Fluorescent Proteins: Scope, Limitations, and Outlook". In: *Annual Review of Biophysics* 48.1, pp. 19–44. DOI: 10.1146/annurev-biophys-051013-022846.

Saccani, Simona, Serafino Pantano, and Gioacchino Natoli (2002). "P38-Dependent Marking of Inflammatory Genes for Increased NF-κB Recruitment". In: *Nature Immunology* 3.1, pp. 69–75. DOI: 10.1038/ni748.

Sad, K et al. (2023). *Histone H3 E50K Mutation Confers Oncogenic Activity and Supports an EMT Phenotype*. DOI: 10.1101/2023.10.11.561775. preprint.

Sadelain, Michel, Eirini P. Papapetrou, and Frederic D. Bushman (2012). "Safe Harbours for the Integration of New DNA in the Human Genome". In: *Nature Reviews Cancer* 12.1, pp. 51–58. DOI: 10.1038/nrc3179.

Sankar, Aditya et al. (2022). "Histone Editing Elucidates the Functional Roles of H3K27 Methylation and Acetylation in Mammals". In: *Nature Genetics* 54.6 (6), pp. 754–760. DOI: 10.1038/s41588-022-01091-2.

Sanyal, Swastika, Ines Kovacikova, and Juraj Gregan (2013). "Chromosome Segregation: Disarming the Protector". In: *Current Biology* 23.6, R236–R239. DOI: 10.1016/j.cub.2013.02.028.

Saotome, K and H Morita (1989). “Cytotoxicity Test with Simplified Crystal Violet Staining Method Using Microtitre Plates and Its Application to Injection Drugs”. In: *Toxicology in Vitro* 3.4, pp. 317–321. DOI: 10.1016/0887-2333(89)90039-8.

Sauer, B and N Henderson (1988). “Site-Specific DNA Recombination in Mammalian Cells by the Cre Recombinase of Bacteriophage P1.” In: *Proceedings of the National Academy of Sciences* 85.14, pp. 5166–5170. DOI: 10.1073/pnas.85.14.5166.

Saurin, Adrian T. et al. (2011). “Aurora B Potentiates Mps1 Activation to Ensure Rapid Checkpoint Establishment at the Onset of Mitosis”. In: *Nature Communications* 2.1, p. 316. DOI: 10.1038/ncomms1319.

Schindelin, Johannes et al. (2012). “Fiji: An Open-Source Platform for Biological-Image Analysis”. In: *Nature Methods* 9.7 (7), pp. 676–682. DOI: 10.1038/nmeth.2019.

Schlake, Thomas and Juergen Bode (1994). “Use of Mutated FLP Recognition Target (FRT) Sites for the Exchange of Expression Cassettes at Defined Chromosomal Loci”. In: *Biochemistry* 33.43, pp. 12746–12751. DOI: 10.1021/bi00209a003.

Schmitz, M. Lienhard, Jonathan M. G. Higgins, and Markus Seibert (2020). “Priming Chromatin for Segregation: Functional Roles of Mitotic Histone Modifications”. In: *Cell Cycle* 19.6, pp. 625–641. DOI: 10.1080/15384101.2020.1719585.

Schneider, Caroline A., Wayne S. Rasband, and Kevin W. Eliceiri (2012). “NIH Image to ImageJ: 25 Years of Image Analysis”. In: *Nature Methods* 9.7 (7), pp. 671–675. DOI: 10.1038/nmeth.2089.

Schneider, Robert et al. (2004). “Direct Binding of INHAT to H3 Tails Disrupted by Modifications”. In: *Journal of Biological Chemistry* 279.23, pp. 23859–23862. DOI: 10.1074/jbc.C400151200.

Schuster, T (1986). “Yeast Histone H2A and H2B Amino Termini Have Interchangeable Functions”. In: *Cell* 45.3, pp. 445–451. DOI: 10.1016/0092-8674(86)90330-2.

Seibert, Markus (2016). “Characterization of histone H2B serine 6 phosphorylation”. Gießen: Justus-Liebig-Universität Gießen. 123 pp.

Seibert, Markus et al. (2019). “CDK1-mediated Phosphorylation at H2B Serine 6 Is Required for Mitotic Chromosome Segregation.” In: *The Journal of cell biology* 218.4, pp. 1164–1181. DOI: 10.1083/jcb.201806057.

Seo, Sang-beom et al. (2001). “Regulation of Histone Acetylation and Transcription by INHAT, a Human Cellular Complex Containing the Set Oncoprotein”. In: *Cell* 104.1, pp. 119–130. DOI: 10.1016/S0092-8674(01)00196-9.

Serena, Michela et al. (2020). “Molecular Basis of MKLP2-dependent Aurora B Transport from Chromatin to the Anaphase Central Spindle”. In: *Journal of Cell Biology* 219.7, e201910059. DOI: 10.1083/jcb.201910059.

Serpico, Angela Flavia, Caterina Pisauro, and Domenico Grieco (2023). “On the Assembly of the Mitotic Spindle, Bistability and Hysteresis”. In: *Cellular and Molecular Life Sciences* 80.4, p. 83. DOI: 10.1007/s00018-023-04727-6.

Shakhnovich, Eugene (2006). “Protein Folding Thermodynamics and Dynamics: Where Physics, Chemistry, and Biology Meet”. In: *Chemical Reviews* 106.5, pp. 1559–1588. DOI: 10.1021/cr040425u.

Sheng, Peike, Krystal A. Flood, and Mingyi Xie (2020). “Short Hairpin RNAs for Strand-Specific Small Interfering RNA Production”. In: *Frontiers in Bioengineering and Biotechnology* 8, p. 940. DOI: 10.3389/fbioe.2020.00940.

Shima, H. et al. (1993). “Identification of PP1 Catalytic Subunit Isotypes PP1γ1, Pp1δ and Pp1α in Various Rat Tissues”. In: *Biochemical and Biophysical Research Communications* 192.3, pp. 1289–1296. DOI: 10.1006/bbrc.1993.1556.

Shimada, Midori et al. (2010). “Protein Phosphatase 1γ Is Responsible for Dephosphorylation of Histone H3 at Thr 11 after DNA Damage”. In: *EMBO reports* 11.11, pp. 883–889. DOI: 10.1038/embor.2010.152.

Shimizu, Noriaki et al. (2005). “When, Where and How the Bridge Breaks: Anaphase Bridge Breakage Plays a Crucial Role in Gene Amplification and HSR Generation”. In: *Experimental Cell Research* 302.2, pp. 233–243. DOI: 10.1016/j.yexcr.2004.09.001.

Shindo, Norihisa, Kazuki Kumada, and Toru Hirota (2012). “Separase Sensor Reveals Dual Roles for Separase Coordinating Cohesin Cleavage and Cdk1 Inhibition”. In: *Developmental Cell* 23.1, pp. 112–123. DOI: 10.1016/j.devcel.2012.06.015.

Shogren-Knaak, Michael et al. (2006). “Histone H4-K16 Acetylation Controls Chromatin Structure and Protein Interactions”. In: *Science* 311.5762, pp. 844–847. DOI: 10.1126/science.1124000.

Shrestha, Roshan L. et al. (2017). “Mislocalization of Centromeric Histone H3 Variant CENP-A Contributes to Chromosomal Instability (CIN) in Human Cells”. In: *Oncotarget* 8.29, pp. 46781–46800. DOI: 10.18632/oncotarget.18108.

Shuaib, Muhammad et al. (2010). “HJURP Binds CENP-A via a Highly Conserved N-terminal Domain and Mediates Its Deposition at Centromeres”. In: *Proceedings of the National Academy of Sciences* 107.4, pp. 1349–1354. DOI: 10.1073/pnas.0913709107.

Siebenkotten, Gregor et al. (1997). “Employing Surface Markers for the Selection of Transfected Cells”. In: *Cell Separation Methods and Applications*. 1st ed. Boca Raton, Florida: CRC Press.

Singh, Rajbir et al. (2013). “Increasing the Complexity of Chromatin: Functionally Distinct Roles for Replication-Dependent Histone H2A Isoforms in Cell Proliferation and Carcinogenesis”. In: *Nucleic Acids Research* 41.20, pp. 9284–9295. DOI: 10.1093/nar/gkt736.

Singh, Rajbir et al. (2015). “Proteomic Profiling Identifies Specific Histone Species Associated with Leukemic and Cancer Cells”. In: *Clinical Proteomics* 12.1, p. 22. DOI: 10.1186/s12014-015-9095-4.

Singh, Rajbir et al. (2018). “Replication-Dependent Histone Isoforms: A New Source of Complexity in Chromatin Structure and Function”. In: *Nucleic Acids Research* 46.17, pp. 8665–8678. DOI: 10.1093/nar/gky768.

Singh, Rakesh Kumar et al. (2009). “Histone Levels Are Regulated by Phosphorylation and Ubiquitylation-Dependent Proteolysis”. In: *Nature Cell Biology* 11.8, pp. 925–933. DOI: 10.1038/ncb1903.

Singh, Rakesh Kumar et al. (2010). “Excess Histone Levels Mediate Cytotoxicity via Multiple Mechanisms”. In: *Cell Cycle* 9.20, p. 9. DOI: 10.4161/cc.9.20.13636.

Singh, Ritambhara et al. (2016). “DeepChrome: Deep-Learning for Predicting Gene Expression from Histone Modifications”. In: *Bioinformatics* 32.17, pp. i639–i648. DOI: 10.1093/bioinformatics/btw427.

Sinha, Joydeb et al. (2023). *The H3.3 K36M Oncohistone Disrupts the Establishment of Epigenetic Memory through Loss of DNA Methylation*. DOI: 10.1101/2023.10.13.562147. preprint.

Smith, P.K. et al. (1985). “Measurement of Protein Using Bicinchoninic Acid”. In: *Analytical Biochemistry* 150.1, pp. 76–85. DOI: 10.1016/0003-2697(85)90442-7.

Solomon, Mark J. et al. (1990). “Cyclin Activation of P34cdc2”. In: *Cell* 63.5, pp. 1013–1024. DOI: 10.1016/0092-8674(90)90504-8.

Son, Seung-Yeol (1999). “Role of the Promoter Region of a Chicken H3 Histone Gene in Its Cell Cycle Dependent Expression”. In: *BMB Reports* 32.

Spalding, J, K Kajiwara, and G C Mueller (1966). “The Metabolism of Basic Proteins in HeLa Cell Nuclei.” In: *Proceedings of the National Academy of Sciences* 56.5, pp. 1535–1542. DOI: 10.1073/pnas.56.5.1535.

Straathof, Karin C. et al. (2005). “An Inducible Caspase 9 Safety Switch for T-cell Therapy”. In: *Blood* 105.11, pp. 4247–4254. DOI: 10.1182/blood-2004-11-4564.

Strahl, Brian D. and C. David Allis (2000). “The Language of Covalent Histone Modifications”. In: *Nature* 403.6765, pp. 41–45. DOI: 10.1038/47412.

Sukackaite, Rasa et al. (2017). "Mouse Rif1 Is a Regulatory Subunit of Protein Phosphatase 1 (PP1)". In: *Scientific Reports* 7.1, p. 2119. DOI: 10.1038/s41598-017-01910-1.

Sullivan, Steven A. and David Landsman (2003). "Characterization of Sequence Variability in Nucleosome Core Histone Folds". In: *Proteins: Structure, Function, and Bioinformatics* 52.3, pp. 454–465. DOI: 10.1002/prot.10441.

Sun, Daqian et al. (2006). "Multi-miRNA Hairpin Method That Improves Gene Knockdown Efficiency and Provides Linked Multi-Gene Knockdown". In: *BioTechniques* 41.1, pp. 59–63. DOI: 10.2144/000112203.

Suntronpong, Aorarat et al. (2016). "CENP-B Box, a Nucleotide Motif Involved in Centromere Formation, Occurs in a New World Monkey". In: *Biology Letters* 12.3, p. 20150817. DOI: 10.1098/rsbl.2015.0817.

Swygert, Sarah G. and Craig L. Peterson (2014). "Chromatin Dynamics: Interplay between Remodeling Enzymes and Histone Modifications". In: *Biochimica et Biophysica Acta (BBA) - Gene Regulatory Mechanisms* 1839.8, pp. 728–736. DOI: 10.1016/j.bbagrm.2014.02.013.

Takami, Y. (1996). "Organization of the Chicken Histone Genes in a Major Gene Cluster and Generation of an Almost Complete Set of the Core Histone Protein Sequences". In: *DNA Research* 3.2, pp. 95–99. DOI: 10.1093/dnares/3.2.95.

Talbert, Paul B. and Steven Henikoff (2010). "Histone Variants — Ancient Wrap Artists of the Epigenome". In: *Nature Reviews Molecular Cell Biology* 11.4, pp. 264–275. DOI: 10.1038/nrm2861.

Tan, Minjia et al. (2011). "Identification of 67 Histone Marks and Histone Lysine Crotonylation as a New Type of Histone Modification". In: *Cell* 146.6, pp. 1016–1028. DOI: 10.1016/j.cell.2011.08.008.

Thompson, Sarah L., Samuel F. Bakhoum, and Duane A. Compton (2010). "Mechanisms of Chromosomal Instability". In: *Current Biology* 20.6, R285–R295. DOI: 10.1016/j.cub.2010.01.034.

Tiberghien, Pierre (1994). "Use of Suicide Genes in Gene Therapy". In: *Journal of Leukocyte Biology* 56.2, pp. 203–209. DOI: 10.1002/jlb.56.2.203.

Trinkle-Mulcahy, Laura, Judith E. Sleeman, and Angus I. Lamond (2001). "Dynamic Targeting of Protein Phosphatase 1 within the Nuclei of Living Mammalian Cells". In: *Journal of Cell Science* 114.23, pp. 4219–4228. DOI: 10.1242/jcs.114.23.4219.

Trinkle-Mulcahy, Laura et al. (1999). "Nuclear Organisation of NIPP1, a Regulatory Subunit of Protein Phosphatase 1 That Associates with Pre-mRNA Splicing Factors". In: *Journal of Cell Science* 112.2, pp. 157–168. DOI: 10.1242/jcs.112.2.157.

Trinkle-Mulcahy, Laura et al. (2003). "Time-Lapse Imaging Reveals Dynamic Relocalization of PP1γ throughout the Mammalian Cell Cycle". In: *Molecular Biology of the Cell* 14.1. Ed. by Joseph Gall, pp. 107–117. DOI: 10.1091/mbc.e02-07-0376.

Trinkle-Mulcahy, Laura et al. (2006). "Repo-Man Recruits PP1γ to Chromatin and Is Essential for Cell Viability". In: *Journal of Cell Biology* 172.5, pp. 679–692. DOI: 10.1083/jcb.200508154.

Trivedi, Prasad and P. Todd Stukenberg (2016). "A Centromere-Signaling Network Underlies the Coordination among Mitotic Events". In: *Trends in Biochemical Sciences* 41.2, pp. 160–174. DOI: 10.1016/j.tibs.2015.11.002.

Tropberger, Philipp and Robert Schneider (2013). "Scratching the (Lateral) Surface of Chromatin Regulation by Histone Modifications". In: *Nature Structural & Molecular Biology* 20.6, pp. 657–661. DOI: 10.1038/nsmb.2581.

Truong, David M. and Jef D. Boeke (2017). "Resetting the Yeast Epigenome with Human Nucleosomes". In: *Cell* 171.7, 1508–1519.e13. DOI: 10.1016/j.cell.2017.10.043.

Turan, Soeren et al. (2013). "Recombinase-Mediated Cassette Exchange (RMCE) — A Rapidly-Expanding Toolbox for Targeted Genomic Modifications". In: *Gene* 515.1, pp. 1–27. DOI: 10.1016/j.gene.2012.11.016.

Uhlmann, Frank and Kim Nasmyth (1998). "Cohesion between Sister Chromatids Must Be Established during DNA Replication". In: *Current Biology* 8.20, pp. 1095–1102. DOI: 10.1016/S0960-9822(98)70463-4.

Uy, Rosa and Finn Wold (1977). "Posttranslational Covalent Modification of Proteins: Only 20 Amino Acids Are Used in. Protein Synthesis, yet Some 140 "Amino Acids" Are Found in Various Proteins." In: *Science* 198.4320, pp. 890–896. DOI: 10.1126/science.337487.

Vagnarelli, Paola et al. (2011). "Repo-Man Coordinates Chromosomal Reorganization with Nuclear Envelope Reassembly during Mitotic Exit". In: *Developmental Cell* 21.2, pp. 328–342. DOI: 10.1016/j.devcel.2011.06.020.

Vanneste, David et al. (2009). "The Role of Hklp2 in the Stabilization and Maintenance of Spindle Bipolarity". In: *Current Biology* 19.20, pp. 1712–1717. DOI: 10.1016/j.cub.2009.09.019.

Varmark, Hanne et al. (2009). "DNA Damage-Induced Cell Death Is Enhanced by Progression through Mitosis". In: *Cell Cycle* 8.18, pp. 2952–2964. DOI: 10.4161/cc.8.18.9539.

Venkatesh, Swaminathan and Jerry L. Workman (2015). "Histone Exchange, Chromatin Structure and the Regulation of Transcription". In: *Nature Reviews Molecular Cell Biology* 16.3, pp. 178–189. DOI: 10.1038/nrm3941.

Vietri, Michele et al. (2006). "Direct Interaction between the Catalytic Subunit of Protein Phosphatase 1 and pRb". In: *Cancer Cell International* 6.1, p. 3. DOI: 10.1186/1475-2867-6-3.

Vogelstein, Bert and Kenneth W. Kinzler (1993). "The Multistep Nature of Cancer". In: *Trends in Genetics* 9.4, pp. 138–141. DOI: 10.1016/0168-9525(93)90209-Z.

Vukušić, Kruno and Iva M. Tolić (2021). "Anaphase B: Long-standing Models Meet New Concepts". In: *Seminars in Cell & Developmental Biology* 117, pp. 127–139. DOI: 10.1016/j.semcdb.2021.03.023.

Wächter, K., E. Kowarz, and R. Marschalek (2014). "Functional Characterisation of Different MLL Fusion Proteins by Using Inducible Sleeping Beauty Vectors". In: *Cancer Letters* 352.2, pp. 196–202. DOI: 10.1016/j.canlet.2014.06.016.

Waizenegger, Irene C et al. (2000). "Two Distinct Pathways Remove Mammalian Cohesin from Chromosome Arms in Prophase and from Centromeres in Anaphase". In: *Cell* 103.3, pp. 399–410. DOI: 10.1016/S0092-8674(00)00132-X.

Walter, Corvin et al. (2021). "Global Kinome Profiling Reveals DYRK1A as Critical Activator of the Human Mitochondrial Import Machinery". In: *Nature Communications* 12.1, p. 4284. DOI: 10.1038/s41467-021-24426-9.

Wang, Enxiu, Edward R. Ballister, and Michael A. Lampson (2011). "Aurora B Dynamics at Centromeres Create a Diffusion-Based Phosphorylation Gradient". In: *The Journal of Cell Biology* 194.4, pp. 539–549. DOI: 10.1083/jcb.201103044.

Wang, Fangwei et al. (2010). "Histone H3 Thr-3 Phosphorylation by Haspin Positions Aurora B at Centromeres in Mitosis". In: *Science* 330.6001, pp. 231–235. DOI: 10.1126/science.1189435.

Watrin, Erwan and Jan-Michael Peters (2006). "Cohesin and DNA Damage Repair". In: *Experimental Cell Research* 312.14, pp. 2687–2693. DOI: 10.1016/j.yexcr.2006.06.024.

Watson, Nikolaus A. et al. (2020). "Kinase Inhibition Profiles as a Tool to Identify Kinases for Specific Phosphorylation Sites". In: *Nature Communications* 11.1, pp. 1–16. DOI: 10.1038/s41467-020-15428-0.

Wei, Yi et al. (1998). "Phosphorylation of Histone H3 at Serine 10 Is Correlated with Chromosome Condensation during Mitosis and Meiosis in *Tetrahymena*". In: *Proceedings of the National Academy of Sciences* 95.13, pp. 7480–7484. DOI: 10.1073/pnas.95.13.7480.

Wen, Wen et al. (2024). *Discriminative Histone Imputation Using Chromatin Accessibility*. DOI: 10.1101/2024.01.11.575175. preprint.

Whitfield, M. L. (2004). "SLBP Is Associated with Histone mRNA on Polyribosomes as a Component of the Histone mRNP". In: *Nucleic Acids Research* 32.16, pp. 4833–4842. DOI: 10.1093/nar/gkh798.

Whitfield, Michael L. et al. (2000). "Stem-Loop Binding Protein, the Protein That Binds the 3' End of Histone mRNA, Is Cell Cycle Regulated by Both Translational and Posttranslational Mechanisms". In: *Molecular and Cellular Biology* 20.12, pp. 4188–4198. DOI: 10.1128/MCB.20.12.4188-4198.2000.

Wilkins, Bryan J. et al. (2014). "A Cascade of Histone Modifications Induces Chromatin Condensation in Mitosis". In: *Science* 343.6166, pp. 77–80. DOI: 10.1126/science.1244508.

Wolffe, A. (1998). *Chromatin: Structure and Function*. 3rd ed. San Diego: Academic Press. 447 pp.

Xia, Yongzhen et al. (2019). "T5 Exonuclease-Dependent Assembly Offers a Low-Cost Method for Efficient Cloning and Site-Directed Mutagenesis". In: *Nucleic Acids Research* 47.3, e15–e15. DOI: 10.1093/nar/gky1169.

Xie, Zhongyu et al. (2012). "Lysine Succinylation and Lysine Malonylation in Histones". In: *Molecular & Cellular Proteomics* 11.5, pp. 100–107. DOI: 10.1074/mcp.M111.015875.

Xin, Guangwei et al. (2020). "Aurora B Regulates PP1g–Repo-Man Interactions to Maintain the Chromosome Condensation State". In: p. 9.

Xu, Ming et al. (2009). "A Ubiquitin Replacement Strategy in Human Cells Reveals Distinct Mechanisms of IKK Activation by TNFα and IL-1β". In: *Molecular Cell* 36.2, pp. 302–314. DOI: 10.1016/j.molcel.2009.10.002.

Xu, Zhengyao et al. (2013). "Accuracy and Efficiency Define Bxb1 Integrase as the Best of Fifteen Candidate Serine Recombinases for the Integration of DNA into the Human Genome". In: *BMC Biotechnology* 13.1, p. 87. DOI: 10.1186/1472-6750-13-87.

Yaakov, Gilad, Kurt Thorn, and David O. Morgan (2012). "Separase Biosensor Reveals That Cohesin Cleavage Timing Depends on Phosphatase PP2ACdc55 Regulation". In: *Developmental Cell* 23.1, pp. 124–136. DOI: 10.1016/j.devcel.2012.06.007.

Yamagishi, Yuya et al. (2012). "MPS1/Mph1 Phosphorylates the Kinetochore Protein KNL1/Spc7 to Recruit SAC Components". In: *Nature Cell Biology* 14.7, pp. 746–752. DOI: 10.1038/ncb2515.

Yamamoto, Yumi et al. (2003). "Histone H3 Phosphorylation by IKK-α Is Critical for Cytokine-Induced Gene Expression". In: *Nature* 423.6940, pp. 655–659. DOI: 10.1038/nature01576.

Yanisch-Perron, Celeste, Jeffrey Vieira, and Joachim Messing (1985). "Improved M13 Phage Cloning Vectors and Host Strains: Nucleotide Sequences of the M13mpl8 and pUC19 Vectors". In: *Gene* 33.1, pp. 103–119. DOI: 10.1016/0378-1119(85)90120-9.

Yin, Qijin et al. (2019). "DeepHistone: A Deep Learning Approach to Predicting Histone Modifications". In: *BMC Genomics* 20.S2, p. 193. DOI: 10.1186/s12864-019-5489-4.

Yoshikawa, Genki et al. (2019). "Medusavirus, a Novel Large DNA Virus Discovered from Hot Spring Water". In: *Journal of Virology* 93.8. Ed. by Joanna L. Shisler, e02130–18. DOI: 10.1128/JVI.02130-18.

Zeng, Yan, Eric J Wagner, and Bryan R Cullen (2002). "Both Natural and Designed Micro RNAs Can Inhibit the Expression of Cognate mRNAs When Expressed in Human Cells". In: *Molecular Cell* 9.6, pp. 1327–1333. DOI: 10.1016/S1097-2765(02)00541-5.

Zhang, Hui, Zhiquan Wang, and Zhiguo Zhang (2013). "PP1α, PP1β and Wip-1 Regulate H4S47 Phosphorylation and Deposition of Histone H3 Variant H3.3". In: *Nucleic Acids Research* 41.17, pp. 8085–8093. DOI: 10.1093/nar/gkt583.

Zhang, Qian and Hong Liu (2020). "Functioning Mechanisms of Shugoshin-1 in Centromeric Cohesion during Mitosis". In: *Essays in Biochemistry*. DOI: 10.1042/ebc20190077.

Zhang, Qian et al. (2024). "CDK11 Facilitates Centromeric Transcription to Maintain Centromeric Cohesion during Mitosis". In: *Molecular Biology of the Cell* 35.2. Ed. by Rong Li, ar18. DOI: 10.1091/mbc.E23-08-0303.

Zhang, Weimin et al. (2019). "Probing the Function of Metazoan Histones with a Systematic Library of H3 and H4 Mutants". In: *Developmental Cell* 48.3, 406–419.e5. DOI: 10.1016/j.devcel.2018.11.047.

Zhang, Yanjun et al. (2021). “Overview of Histone Modification”. In: *Histone Mutations and Cancer*. Ed. by Dong Fang and Junhong Han. Vol. 1283. Singapore: Springer Singapore, pp. 1–16. DOI: 10.1007/978-981-15-8104-5_1.

Zheng, Lianxing et al. (2003). “Phosphorylation of Stem-Loop Binding Protein (SLBP) on Two Threonines Triggers Degradation of SLBP, the Sole Cell Cycle-Regulated Factor Required for Regulation of Histone mRNA Processing, at the End of S Phase”. In: *Molecular and Cellular Biology* 23.5, pp. 1590–1601. DOI: 10.1128/MCB.23.5.1590-1601.2003.

Zhou, Jian and Olga G Troyanskaya (2015). “Predicting Effects of Noncoding Variants with Deep Learning–Based Sequence Model”. In: *Nature Methods* 12.10, pp. 931–934. DOI: 10.1038/nmeth.3547.

Zhou, Jun, Joyce Yao, and Harish C. Joshi (2002). “Attachment and Tension in the Spindle Assembly Checkpoint”. In: *Journal of Cell Science* 115.18, pp. 3547–3555. DOI: 10.1242/jcs.00029.

Zhou, X et al. (2006). “Optimization of the Tet-On System for Regulated Gene Expression through Viral Evolution”. In: *Gene Therapy* 13.19, pp. 1382–1390. DOI: 10.1038/sj.gt.3302780.

Zickler, Denise and Nancy Kleckner (2015). “Recombination, Pairing, and Synapsis of Homologs during Meiosis”. In: *Cold Spring Harbor Perspectives in Biology* 7.6, a016626. DOI: 10.1101/cshperspect.a016626.

Zink, Lisa-Maria and Sandra B Hake (2016). “Histone Variants: Nuclear Function and Disease”. In: *Current Opinion in Genetics & Development* 37, pp. 82–89. DOI: 10.1016/j.gde.2015.12.002.

Zou, Hui et al. (1999). “Identification of a Vertebrate Sister-Chromatid Separation Inhibitor Involved in Transformation and Tumorigenesis”. In: *Science* 285.5426, pp. 418–422. DOI: 10.1126/science.285.5426.418.

Danksagung

Mein größter Dank gilt zuallererst Prof. Lienhard Schmitz. Zuerst einmal dafür, dass ich Teil deiner Arbeitsgruppe sein durfte und ich dieses großartige, spannende Projekt übernehmen durfte. Vor allem aber auch für die lehrreichen Diskussionen, die mich, auch wenn wir nicht immer einer Meinung waren, stets weitergebracht haben. Die Doktorarbeit war trotz mancher Frustration eine spannende und bewegende Zeit. Ich danke Dir, immer ein Wegweiser gewesen zu sein, mich auf meinem Weg unterstützt zu haben und nicht zuletzt auch zu meiner persönlichen Entwicklung beigetragen zu haben. Vielen Dank für Deine Betreuung!

Des Weiteren möchte ich mich bei Prof. Sandra Hake für die Erstbetreuung meiner Arbeit am Fachbereich Biologie sowie natürlich für die Begutachtung und Prüfung bedanken. Außerdem herzlichen Dank für die Möglichkeit, an Deinem Laborseminar teilzunehmen und für die stets bereichernden Diskussionen vor Ort.

Außerdem danke ich Prof. Tilman Borggrefe für das Interesse an meiner Arbeit, für all die Tipps und Ideen, die mir sehr weitergeholfen haben sowie die Bereitschaft mich und meine Arbeit zu prüfen. Ebenso danke ich Prof. Elena Evguenieva-Hackenberg, dass sie sich für die Prüfung von meiner Arbeit und mir zur Verfügung stellt.

Ich hatte das Privileg, während meiner Zeit als Doktorand mehrere medizinische Doktorarbeiten und eine Bachelorarbeit betreuen zu dürfen. Ich möchte euch, Roman Robert, Johanna Segbers, Amelie Pritz, Paulin Nikuradse und Henrik Senge herzlich dafür danken, mich bei meinen Projekten so tatkräftig unterstützt zu haben und immer wieder neuen Wind in unser Labor gebracht zu haben. Ihr habt einen erheblichen Anteil zu dieser Arbeit beigetragen. I also want to thank Anna Parry, whom I had the pleasure of supervising for a summer internship. Thank you for your contributions to my project and for bringing your energy into our group.

Meine lieben Kolleginnen und Kollegen, aktuell und ehemalig, haben mir immer unterstützend zur Seite gestanden, eine angenehme Arbeitsumgebung geschaffen und mir nicht zuletzt eine Menge beigebracht. Danke für eure wissenschaftliche, technische und persönliche Unterstützung: Murtaza Ali, Ratnal Belapurkar, David van den Borre, Martin Brockhaus, Shashi Chillappagari, Ines Höfliger, Yvonne Horn, Regina Jilg, Chloe Leff, Valeriia Leoshko, Lu Liu, Denis Maihöfer, Kai Müller, Kristin Ott, Sehar Qudsia, Olesja Ritter, Vera Saul, Lena Schmidt, Markus Schwinn, Markus Seibert, Maja Treusch, Hans-Günter Welker, Till Wöckener.

Von meinen Kolleginnen und Kollegen möchte ich Susanne Bacher hervorheben. Wir haben uns über die letzten Jahre ein Labor geteilt und das immer mit guter Laune, Musik und Kaffee. Vielen Dank dafür!

Besonders hervorheben möchte ich aber Jan Dreute. Du bist mit dafür verantwortlich, dass ich in diesem Labor gelandet bin aber vor allem auch mit verantwortlich, dass ich meine Arbeit in dieser Form machen konnte. Ich danke Dir für jede Diskussion, die wir geführt haben, jeden Rat den Du mir gegeben hast, für alles was Du mir beigebracht hast sowie für Deine Freundschaft!

Ich möchte meinen Eltern meinen unendlichen Dank aussprechen. Für alles, was ihr für mich getan habt, für die Unterstützung die ich immer bekommen habe und dafür, dass ihr mich zu der Person gemacht habt, die ich heute bin. Danke auch an meine Freunde, dass ihr mich auf jedem Abschnitt unterstützt habt!

Wie bei der Autorenliste einer Publikation, wer zum Schluss genannt wird, ist ebenso wichtig wie die erste Person. Mein unendlicher Dank gilt Dir Julia: Ohne Deine unermüdliche Unterstützung jeden Tag wäre diese Arbeit nicht zur Vollendung gekommen. Deine Anwesenheit hat nicht nur unser Labor, sondern auch mein gesamtes Leben bereichert. Danke, dass du immer an meiner Seite bist und mich auf meinem Weg begleitest.